



Brunel
University
London

**Involvement of Innate Immune Humoral Factors, CFHR5
and SP-D, in Glioblastoma Multiforme**

A thesis submitted for the degree of Doctor of Philosophy by

Syreeta De Cordova

Department of Life Sciences

College of Health and Life Sciences

Brunel University

London

April 2017

Declaration

I hereby declare that the research submitted in this thesis is my own work except where specified otherwise, and has not been submitted for any other degree.

Abstract

Glioblastoma Multiforme (GBM) is an extremely aggressive grade IV brain tumour that is highly infiltrative and can spread to other parts of the brain quickly. It is the most common primary brain tumour where patients have a median survival of 14.6 months. Symptoms vary depending upon the location of the tumour and include seizures, progressive headaches and focal neurological deficit. The poor prognosis is characterised by deregulation of many key signalling pathways involving survival, growth, apoptosis and evasion of immune surveillance.

In this study, we investigated whether complement factor H related protein 5 (CFHR5) from primary GBM cells direct from patients exhibited functional activity similar to factor H. The presence of CFHR5 was validated by western blot and ELISA technique from B30, B31 and B33 primary GBM cells. The functional capacity of CFHR5 was examined through the alternative pathway, co-factor, and decay acceleration assay. We demonstrated that CFHR5 was able to inhibit the alternative pathway through the same mechanism as factor H.

Emerging evidence had shown that the innate immune protein surfactant protein D (SP-D) and recombinant human SP-D (rhSP-D) were able to induce apoptosis in eosinophilic leukaemic cells. We studied the ability of rhSP-D to induce apoptosis in U87 GBM cells through apoptotic and viability assays. rhSP-D was unable to mediate cell death and instead increased cell viability. This led us to investigate the expression of SP-D in U87 and B30 GBM cells through western blot, ELISA and immunofluorescence detection. We demonstrated novel information about the production of SP-D by GBM cells. To extend our study, we investigated the interaction of THP-1 macrophage with rhSP-D bound U87 cells. We carried out live cell imaging, RT-qPCR, and cell viability assays, to study the changes in cytokine expression and viability of cells. THP-1 did not engulf U87 cells; however, it did reduce the number of cells and decrease the expression of pro-tumourigenic cytokines.

This study highlights the ability of primary GBM cells to evade innate immune detection by the secretion of functionally active CFHR5. It also demonstrated the ability of U87 to evade destruction by rhSP-D and THP-1 highlighting the extremely aggressive behaviour of the tumour and lack of new treatment to improve prognosis in over a decade.

Acknowledgements

I would like to thank:

Dr Kishore for his guidance and opportunity to undertake this study in his laboratory. I am grateful for the skills and knowledge I take away from it.

Dr Slijepcevic for his encouragement and support.

Dr Pathan for his help and support.

Dr Tsolaki for his help and supply of primers.

Dr Abdelgany for supplying primary GBM cells direct from patients.

My family for all they have done for me.

Table of content	Page
Title page	I
Declaration	II
Abstract	III
Acknowledgement	IV
Table of content	V
List of abbreviations	XII
List of figures	XVI
List of tables	XVIII
Chapter 1: Introduction	1
1.1. Tumourigenesis.....	2
1.2. Acquired capabilities.....	2
1.2.1. Self-sufficiency in growth signals.....	2
1.2.2. Insensitivity to anti-growth inhibitory signals.....	3
1.2.3. Evading Apoptosis.....	4
1.2.4. Limitless replicative potential.....	4
1.2.5. Inducing tumour angiogenesis.....	4
1.2.6. Activating tissue invasion and metastasis.....	5
1.3. Cancer stem cell hypothesis.....	5
1.4. Astrocytoma.....	6
1.5. GBM.....	7
1.6. CD133 ⁺ cancer stem cells in GBM.....	10
1.7. EGFR amplification pathway in GBM.....	11

1.8. p53 mutation in GBM.....	11
1.9. <i>PTEN</i> mutation in GBM.....	11
1.10. Astrocyte physiology and morphology.....	12
1.11. The immune system.....	13
1.12. Astrocytes innate immunity in the brain.....	14
1.13. Cytokines in GBM.....	17
1.13.1. The role of TNF- α in GBM.....	20
1.13.2. The role of IL-6 in GBM.....	20
1.13.3. The role of TGF- β in GBM.....	21
1.13.4. The role of IL-12 in GBM.....	22
1.14. Immune privilege of the brain.....	22
1.15. Cancer immuno-editing of GBM.....	23
1.16. The Complement system	24
1.16.1. The Alternative pathway.....	27
1.16.2. Factor H.....	28
1.16.3. CFHR5.....	29
1.17. Surfactant protein D expression.....	32
1.17.1. SP-D structure.....	35
1.17.2. Pathogen recognition and clearance.....	38
1.17.3. A recombinant form of truncated SP-D.....	40
1.17.4. SP-D in the brain.....	40
1.17.5. SP-D in cancer.....	40

1.18. Microglia.....	43
1.18.1 Microglia function.....	43
1.18.2. Microglia in GBM.....	44
1.19. Aims.....	45
2. Chapter 2: Materials and methods.....	46
2.1. Purification of factor H.....	47
2.2. Nanodrop.....	47
2.3. Preparation of 12% polyacrylamide gel.....	48
2.4. SDS polyacrylamide gel electrophoresis (SDS-PAGE) of cellular components.....	49
2.5. Western blot of factor H- Bio-Rad transblot.....	49
2.6. Cell culture for primary GBM cells.....	50
2.7. Extraction of cellular components.....	51
2.8. Dot Blot for factor H.....	52
2.9. Purification of factor H in primary GBM.....	52
2.10. Western blot of primary GBM for factor H.....	53
2.11. Enzyme linked immunosorbent assay (ELISA) for factor H.....	54
2.12. Alternative pathway assay.....	55
2.13. Co-factor assay.....	56
2.14. Decay acceleration assay.....	57
2.15. RT-qPCR of B30.....	57
2.16. Competent cells.....	60
2.17. Transformation of cells.....	61

2.18. Pilot scale protein expression of rhSP-D.....	61
2.19. Large scale protein expression of rhSP-D.....	62
2.20. Cell lysis and sonication of inclusion bodies.....	63
2.21. Dialysis to refold rhSP-D.....	63
2.22. Purification of rhSP-D.....	64
2.23. Lipopolysaccharide removal.....	64
2.24. Endotoxin quantitation.....	65
2.25. Western blot for rhSP-D.....	67
2.26. Cell culture for U87 cells.....	68
2.27. The binding of rhSP-D to U87 cells.....	68
2.28. Apoptosis assay.....	69
2.29. Analysis of cell viability.....	70
2.30. Agglutination.....	70
2.31. RT-qPCR for U87 and rhSP-D.....	71
2.32. Cell proliferation assay.....	72
2.33. Western blot for U87 supernatant.....	73
2.34. ELISA for U87 supernatant.....	74
2.35. RT-qPCR of U87.....	75
2.36. Intracellular detection of SP-D in U87 and B30 GBM cells.....	77
2.37. Cell culture for THP-1 cells.....	77
2.38. THP-1 differentiation.....	78
2.39. Dissociation of THP-1 with trypsin-EDTA.....	79
2.40. Cytokine gene expression of U87 cells in co-culture with THP-1 cells.....	79

2.41. Live imaging.....	81
2.42. Proliferation assay of U87 in co-culture.....	82
2.43. ELISA for co-culture.....	83
2.44 Statistical analysis.....	83
Chapter 3: Purification of CFHR5 and its functional activity.....	84
3.1. Abstract.....	85
3.2. Objectives.....	86
3.3. Results.....	87
3.3.1. Factor H purified from normal human serum.....	87
3.3.2. Factor H family protein is present in B30, B31 and B33.....	89
3.3.3. CFHR5 is present in B30, B31 and B33.....	92
3.3.4. Western blot analysis of CFHR5.....	95
3.3.5. Primary GBM cells secrete CFHR5.....	97
3.3.6. CFHR5 is an inhibitor of the alternative pathway.....	100
3.3.7. CFHR5 has co-factor activity for factor I mediated cleavage of C3b.....	105
3.3.8. CFHR5 has decay acceleration activity for C3 convertase.....	108
3.3.9. Cytokine gene expression within primary GBM.....	109
3.4. Discussion.....	113
Chapter 4: Purification of rhSP-D and its effect on U87 GBM cell line.....	117
4.1. Abstract.....	118
4.2. Objectives.....	119
4.3. Results.....	120
4.3.1. Pilot scale of rhSP-D.....	120

4.3.2. Large scale expression of rhSP-D.....	122
4.3.3. Purification of rhSP-D by affinity chromatography.....	123
4.3.4. Determination of rhSP-D endotoxin level.....	125
4.3.5. Detection of rhSP-D.....	127
4.3.6. rhSP-D is able to bind to U87 cells.....	128
4.3.7. rhSP-D does not induce apoptosis in U87 cells.....	131
4.3.8. rhSP-D does not affect U87 viability.....	136
4.3.9. rhSP-D does not facilitate agglutination of U87 cells.....	138
4.3.10. P53, TNF- α and IL-6 gene expression is reduced in rhSP-D treated cells.....	140
4.3.11. rhSP-D promotes U87 proliferation.....	143
4.4. Discussion.....	145
Chapter 5: The detection of SP-D in U87 and B30 cells.....	153
5.1 Abstract.....	154
5.2 Objectives.....	155
5.3. Results.....	156
5.3.1. Detection of SP-D in GBM supernatant.....	156
5.3.2. SP-D is secreted by GBM cells.....	158
5.3.3. Time dependent gene expression of SP-D in GBM.....	162
5.3.4. SP-D is present in GBM cells.....	165
5.3.5. TNF- α and IL-6 gene expression is upregulated in GBM.....	170
5.4. Discussion.....	175

Chapter 6: The effect of THP-1 in co-culture with U87	179
6.1 Abstract.....	180
6.2. Objective.....	181
6.3 Results.....	182
6.3.1. THP-1 cells are differentiated by rhSP-D.....	182
6.3.2. Trypsin-EDTA does not dissociate THP-1.....	184
6.3.3. THP-1 co-culture alters U87 cytokine gene expression.....	184
6.3.4. THP-1 do not engulf U87 cells.....	189
6.3.5. Reduced cell growth of U87 cells in co-culture.....	191
6.3.6. Co-culture reduces the secretion of factor H and SP-D.....	193
6.4. Discussion.....	198
7. General discussion	204
8. References	208

List of abbreviations

GBM	glioblastoma multiforme
PDGF	platelet derived growth factor
WHO	World Health Organisation
TGF- α	tumour growth factor alpha
pRB	retinoblastoma protein
CSC	cancer stem cell
HSC	haematopoietic stem cells
CNS	central nervous system
PRRs	pattern recognition receptors
TLR	Toll like receptor
BBB	blood brain barrier
MGMT	O ⁶ -methylguanine-DNA methyltransferase
EGFR	epidermal growth factor receptor
<i>PTEN</i>	<i>phosphate and tensin homolog</i>
NOD	nucleotide-binding domain
PAMP	produce pathogen associated molecular pattern
SR	Scavenger receptor
CTL	cytotoxic lymphocyte
IFN- γ	interferon gamma
NF- κ B	nuclear factor kappa B
MAPK	mitogen activated protein kinase
IL	interleukin
GM-CSF	granulocyte macrophage- colony stimulating factor
TNF- α	tumour necrosis factor alpha

DAF	decay accelerating factor
MCP	membrane co-factor protein
CaR	complement anaphylatoxin receptor
MARCO	macrophage receptor with collagenous structure
CL	C type lectin
TH	T helper
STAT	signal transducers and activators of transcription
JAK	Janus kinase
DC	dendritic cell
NK	natural killer cell
MBL	mannose binding lectin
MASP	mannan binding lectin serine protease
MAC	membrane attack complex
CR	complement receptor
MCP	membrane co-factor protein
Mg ²⁺	magnesium ion
SCR	short consensus repeat
CCP	complement control protein
DDD	dense deposit disease
RCA	regulators of complement activation
CFHL-1	complement factor H like protein 1
CFHR	complement factor H related protein
aHUS	atypical haemolytic uremic syndrome
AMD	Age related macular degeneration
SP-D	surfactant protein D

CRD	carbohydrate recognition domain
rhSP-D	recombinant human surfactant protein D
FBS	fetal bovine serum
DMEM/F12	Dulbecco's modified eagle medium-F12
RPMI	Roswell park memorial institute
CO ₂	carbon dioxide
PBS	phosphate buffer saline
EDTA	ethylenediaminetetraacetic acid
rpm	revolutions per minute
APS	ammonium persulphate
TEMED	tetramethylethylenediamine
NaCl	sodium chloride
PMSF	phenylmethylsulphonyl fluoride
SDS	sodium dodecyl sulphate
MgCl ₂ ,	magnesium chloride
KH ₂ PO ₄ ,	monopotassium phosphate
IgG-HRP	immunoglobulin g- horse radish peroxidase
DAB	3,3'diaminobenzidine
P	passage
CBC	carbonate bi-carbonate
OPD	o-Phenylenediamine
EGTA	ethylene glycol tetraacetic acid
β-ME	β-mercaptoethanol
A	absorbance
C _T	cycle threshold

RQ	relative quantity
<i>E.coli</i>	<i>Escherichia coli</i>
RQ	relative quantification
IPTG	isopropyl-1-thio- β -D-galactopyranoside
CaCl ₂	calcium chloride
LPS	lipopolysaccharide
LAL	limulus amoebocyte lysate
PA	protein A
FITC	Fluorescein isothiocyanate
DAPI	4',6-Diamidino-2-phenylindole dihydrochloride
GIM	Glioma infiltrating macrophages
PMA	phorbol 12-myristate 13-acetate
DMSO	dimethyl sulfoxide
si	small interference
MHC	major histocompatibility complex
ROS	reactive oxygen species
PAGE	polyacrylamide gel electrophoresis
BSA	bovine serum albumin
pNA	p-Nitroaniline
<i>S</i>	<i>Staphylococcus</i>
ROS	reactive oxygen species
SIRP- α	signal regulatory protein alpha
EMT	epithelial mesenchymal transition

List of figures	Page
Chapter 1	
Fig 1.1. The spread of GBM visualised on MRI scans.....	9
Fig 1.2. Complement system.....	26
Fig 1.3. Schematic representation of factor H, CFHL-1 and CFHR1-CFHR5.....	30
Fig 1.4. Nucleotide sequence of CFHR5 cDNA and amino acid sequence.....	30
Fig 1.5. Schematic diagram illustrating the organisation and assembly of SP-D.....	37
Fig 1.6. Immuno-histochemical staining of malignant and non-malignant prostate cells.....	42
Chapter 3	
Fig 3.1. Purification of full length factor H from normal human serum.....	87
Fig 3.2. SDS-PAGE and dot blot of primary B30, B31 and B33 supernatant, total cell extract and membrane fraction.....	90
Fig 3.3. Purification of CFHR5 from primary GBM.....	93
Fig 3.4. Detection of CFHR5 from primary GBM.....	95
Fig 3.5. Quantification of CFHR5 secreted by primary GBM cells.....	98
Fig 3.6. Inhibition of the alternative pathway by CFHR5.....	101
Fig 3.7. CFHR5 has co-factor activity.....	105
Fig 3.8. CFHR5 promotes decay acceleration activity on C3 convertase.....	108
Fig 3.9. A qPCR of cytokine gene expression from primary B30 cells.....	110
Chapter 4	
Fig 4.1. SDS-PAGE of rhSP-D pilot scale expression.....	120
Fig 4.2. SDS-PAGE of the large scale expression of rhSP-D.....	122
Fig 4.3. An SDS-PAGE of purified rhSP-D.....	123

Fig 4.4. A standard curve for the quantitation of endotoxin in a chromogenic assay.....	125
Fig 4.5. Western blot analysis of endotoxin free rhSP-D.....	127
Fig 4.6. Binding of rhSP-D to the membrane of U87 cells was dose responsive and calcium dependent	129
Fig 4.7. Fluorescent microscopy of the induction of apoptosis by rhSP-D.....	132
Fig 4.8. The effect of rhSP-D on the viability of U87 cells.....	136
Fig 4.9. Agglutination assay of U87 treated with rhSP-D.....	138
Fig 4.10. RT-qPCR of U87 treated and untreated cells.....	141
Fig 4.11. rhSP-D increased U87 proliferation.....	144
Chapter 5	
Fig 5.1. Western blot analysis of the secretion of SP-D by U87 and B30 cells.....	157
Fig 5.2. Quantification of SP-D in U87 and B30 cell by ELISA.....	159
Fig 5.3. RT-qPCR of SP-D gene expression in U87 and B30 cells.....	163
Fig 5.4. Detection of intracellular SP-D in U87 and B30 cells by immuno-Fluorescent microscopy	166
Fig 5.5. RT-qPCR analysis of cytokine gene expression in U87 and B30 cells.....	172
Chapter 6	
Fig 6.1. Differentiation of THP-1.....	182
Fig 6.2. Analysis of cytokine gene expression in U87 and THP-1 co-culture.....	186
Fig 6.3. Co-culture of U87 and THP-1.....	190
Fig 6.4. Co-culture reduced U87 proliferation.....	192
Fig 6.5. A co-culture of THP-1 and U87 cells reduced the production of SPD and factor H.....	195

List of Tables	Page
Table 1.1. PRR expressed by astrocytes.....	16
Table 1.2. cytokine function in non-tumourigenic brain and GBM.....	18
Table 1.3. Pulmonary and extra pulmonary sites of SP-D expression.....	33
Table 1.4. Summary of interaction with SP-D and pathogen.....	39
Table 1.5. Expression of SP-D in extrapulmonary cancers.....	41
Table 2.1. Composition for preparing 12% resolving gel.....	48
Table 2.2. Composition for preparing 5% of stacking gel.....	48
Table 2.3. Table of primers used for B30 RT-qPCR.....	59
Table 2.4 Primers used for RT-qPCR treated and untreated U87.....	72
Table 2.5. Primers used for RT-qPCR U87.....	76
Table 2.6. primers for RT-qPCR for co-culture.....	78

Chapter 1: Introduction

1.1. Tumourigenesis

The development of human tumour cells involves a complex succession of multistep processes including the transition and progression of a single or cluster of cells into a tumour (von Deimling *et al.*, 1992;Smith *et al.*, 1991). During this sequence of events the incipient tumour cells acquire mutation of genes which drives the transformation from normal into cancerous cells. These include the mutations of proto-oncogenes to form oncogenes, and loss of tumour suppressor function. These mutations violate tissue homeostasis and form a growth promoting environment (Schuurman *et al.*, 1997).

1.2. Acquired capabilities

The disruption of the cellular regulatory pathway of human cells is sufficient to impart tumorigenesis as genetic and cellular principles control cancer formation (Miller *et al.*, 1980). There are in excess of 100 distinct types of cancer and subtypes of tumours which can be located within specific organs. Most cancers acquire the same set of alterations in cell physiology of self-sufficiency in growth signals, insensitivity to growth suppressors, evasion of apoptosis, limitless replication, sustained angiogenesis, tissue invasion and metastasis to breach anti-cancer defence mechanism (Hanahan and Weinberg, 2000;Hirose *et al.*, 2003).

1.2.1. Self-sufficiency in growth signals

Cancer cells are able to activate growth signals and independently stimulate cellular proliferation. These cells deregulate growth signals from normal tissue which carefully control cell growth and division to maintain a homeostatic environment. Cancer cells do not rely upon exogenous growth stimulation factors and mitogenic growth signals to trigger mitosis. The activation of oncogenes contributes to tumourigenesis with some mimicking normal growth signalling to exert their effect (Hirose *et al.*, 2003). Cancer cells have the ability to synthesise growth factors creating autocrine stimulation

which is also referred to as positive feedback signalling loop. Tumours such as GBM and sarcomas frequently produce the growth factors platelet derived growth factor (PDGF) and tumour growth factor α (TGF- α) relinquishing their dependence on growth factors from other cells in the tissue (Fedi, Tronick and Aaronson, 1997). This ability for cancer cells to produce growth factor to which they can respond to creates autocrine proliferation. Cancer cells are also able to favour pro-growth signals by elevating the level of signalling receptors to render hyper-responsiveness to growth factors that normally would not trigger proliferation (Lukashev and Werb, 1998;Giancotti and Ruoslahti 1999).

1.2.2. Insensitivity to anti-growth signals

Incipient cancer cells avoid anti-proliferative signals which function to maintain cellular quiescence and tissue homeostasis. These signals compel cells into a quiescent state or force cells to abandon their proliferative potential. Tumour suppressors such as the retinoblastoma protein (pRB) and p53 protein play a crucial role in the negative control of the cell cycle and tumour progression. The pRB combine the intracellular and extracellular signals received and control whether or not a cell proceeds through its growth and division cycle. Loss of function through events such as mutations of its gene (*RBI*) permits persistent cell growth through the deregulation of the cell cycle in which the cell obtains a malignant phenotype (Weinberg, 1995;Moses, Yang and Pietsenpo, 1990). The p53 signalling pathway has the ability to prevent cell cycle progression and induce apoptosis in response to a variety of stress signals such as damage to DNA. A common feature of cancer is the mutation of *TP53* gene in which p53 lose their anti-tumourigenic activities and gain oncogenic functions that endow the cells with growth advantages (Muller and Vousden, 2013;Olivier, Hollstein and Hainaut, 2010).

1.2.3. Evading Apoptosis

The ability of tumour cells to evade apoptosis is significant in the increase of tumour cell proliferation. Programmed cell death of damaged cells beyond repair, hypoxic cells and cells affected by signalling balance provoked by oncogene activation is essential for the organisms' viability. The mutation of the pro-apoptotic regulator p53 is an acquired alteration in many types of cancer resistance to apoptosis. This aberration is present in more than 50% of human cancers and promotes tumourigenesis through the evasion of apoptosis (Harris, 1996).

1.2.4. Limitless replicative potential

Tumour cells have a profound characteristic in which they acquire the ability to escape the finite limit of the cell replicative life span (Corn and El-Deiry, 2002; Mathon and Lloyd, 2001). Normal cells evoke mortality after 60-70 doublings. With each doubling a progressive shortening of the telomeres is attributed to the end of chromosomes. After a finite number of replication, cells lacking telomerase enter senescence (Granger, Wright, and Shay, 2002). Telomere maintenance is a clear component of the capability of tumour limitless replicative potential (Jefford and Finger, 2006). Telomerase expression permits telomere maintenance and 85-90% of cancer cells have telomerase present whereas the majority of somatic cells do not. It is evident that telomerase has a key role in immortalising cells (Li *et al.*, 2005; Hiyama *et al.*, 1996).

1.2.5. Inducing tumour angiogenesis

Progressive tumour cells rapidly divide and outgrow the blood supply causing hypoxic conditions (Vaupel, 2004). The blood supply provides oxygen and nutrients essential for cell survival (Byrne, Bouchier-Hayes and Harmey, 2005). Tumour angiogenesis induction relies upon an increase of pro-angiogenic gene expression by physiological stimuli such as hypoxia, oncogene activation or mutations of tumour suppressors (Hirose *et al.*, 2003). Dependent upon the tumour type and microenvironment, the

angiogenesis switch is activated at different stages of the tumour progression. The aberrant vascular structure, abnormal blood flow, and haemorrhagic vascular network present in tumour angiogenesis as a result of the over expression of factors such as vascular endothelial growth factor (Bergers and Benjamin, 2003).

1.2.6. Activating tissue invasion and metastasis

Malignant tumours acquire characteristics allowing the cancerous cells to escape the primary tumour mass and invade adjacent tissue (Fidler, 1975). Carcinomas arising from epithelial tissue have an increased propensity to invade local tissue and metastasize distant. This progression involves a number of biological changes that start from local invasion to intravasation in which cancer cells spread to nearby blood and lymphatic vessels. The cancer cells then undergo extravasation as they invade the parenchyma of distant tissue, followed by the formation of small nodules of cancer cells. Macroscopic tumours are then formed in this final step known as colonisation from small nodules of cancer cells (Talmadge and Fidler, 2010;Fidler, 2003).

1.3. Cancer stem cell hypothesis

Recent evidence supports the concept that in several cancers, a phenotypically distinct subset of cancer cells with properties of stem cells is able to form tumours. These small numbers of cancer stem cells (CSC) are integral to the development and perpetuation of tumorigenesis. The majority of the tumour cells are non-tumorigenic cancer cells. CSC have been identified in tumours of the brain, hematopoietic system, breast, prostate and colon (Jordan, Guzman, and Noble, 2006;Bauman *et al.*, 1999;O'Brien *et al.*, 2006). These cells have the ability of self-renewal, the capability to differentiate into any cell within the tumour and to proliferate extensively (Jordan, Guzman, and Noble, 2006). The existence of CSC had been suggested in 1971 by Park et al and in 2002 by Ignatova et al as they described cells with stem cell properties in human cortical glial tumours (Ignatova *et al.*, 2002;Park, Bergsagel and McCulloch, 1971). It is likely that CSC originate from mutations of normal self-renewal stem cells or mutated progenitor

cells that have acquired the ability of self-renewal. Progenitor cells have the ability to differentiate into a specific type of cell but unlike stem cells lack the ability of self-renewal (Jordan, Guzman, and Noble, 2006). For many cancers, the origin of the cancer stem cells is unknown (Reya *et al.*, 2001). However, there is recent evidence that particular types of leukaemia occur from accumulating mutations in haematopoietic stem cells (HSC). Cancer stem cells unique ability of self-renewal allows tumour recurrence after treatment including chemotherapy despite the small number of cancer stem cells present. This relapse can occur many years after treatment (Tu, Lin, and Logothetis, 2002)

1.4. Astrocytoma

Astrocytomas are brain tumours which are divided into four histological gradings by the world health organisation (WHO) depending upon the invasiveness, atypia, mitotic activity, vascular proliferation and necrosis of the cancer . They are derived from astrocytes which are star shaped glial cells in the brain (Walker *et al.*, 2011). Generally, astrocytomas do not spread from the brain to other parts of the body, however there are extremely rare incidences of extracranial metastasis of grade IV astrocytoma (Robert and Wastie, 2008).

Pilocytic astrocytoma is the most common paediatric brain tumour. It is classified by the WHO as a grade I tumour and accounts for 20% of brain tumours in patients under the age of 20 (Goth and Rajewsky, 1974; Jones *et al.*, 2012). Pilocytic astrocytoma is a low-grade tumour usually benign or slow growing and has the potential to be completely removed by surgical resection. Survival rates are as high as 96% over a 10 year period and the majority of patients are cured of their tumour (Louis *et al.*, 2007; Ohgaki and Kleihues, 2005). Grade II (low grade) astrocytoma is a slow growing, diffusely infiltrating glioma with a tendency to progress to a high-grade astrocytoma. It is the most common form of low grade glioma with epileptic seizures as the most common symptom (van der Sanden, G.A.C *et al.*, 1998; Lote *et al.*, 1997). The mean age of diagnosis is between 35-40 years and only a small percentage of children and adults

older than 65 years of age are diagnosed (Shaw *et al.*, 1989). Anaplastic astrocytoma is a malignant tumour with an intrinsic predisposition to progress to GBM. According to the WHO 2007 grading system, histologically anaplastic astrocytoma displays cytological atypia, anaplastic features and mitotic activity (Louis *et al.*, 2007). A poor prognosis with a median survival of 2-3 years is associated and current treatment includes surgical resection and radiotherapy (Fritsche *et al.*, 2010).

1.5. GBM

GBM is the most common primary brain tumour with an incidence of 3.55 new cases per 100,000 per year (Ohgaki *et al.*, 2004). GBM is a grade IV astrocytoma, characterised by uncontrolled cellular proliferation, diffuse infiltration, extensive genomic instability, tendency for necrosis, angiogenesis, and resistance to apoptosis. The tumour is composed of high inter- and intra- morphological heterogeneity hence the term "multiforme" (Furnari *et al.*, 2007;Liu *et al.*, 2012). Despite aggressive treatment including surgical resection and radiotherapy with concomitant chemotherapy, prognosis remains poor due to GBM recurrence, with a median survival of 14.6 months. This poor prognosis is mostly characterised by deregulation of many key signalling pathways involving survival, growth, proliferation and apoptosis due to a highly-mutated genome (Furnari *et al.*, 2007).

GBM is a robust malignant tumour distinguished by its local invasion pattern (Gabrusiewicz *et al.*, 2014;Hermanson *et al.*, 1992). Generally, GBM do not metastasize extracranially, however there have been rare cases in which 0.44% of GBM have spread to other parts of the body (Robert and Wastie, 2008). These rare cases are often reported in patients who have undergone craniotomy which is the surgical removal of part of the bone from the skull to access the brain (Anzil, 1970). Metastasis is rare as the brain does not have a lymphatic system; the presence of the dura matter which is a thick membrane surrounding the brain would make penetration of GBM difficult; it is likely that the short life span of GBM patients does not allow the tumour long enough to metastasize (Newton, Rosenblum and Walker, 1992;Robert and Wastie, 2008).

There are also three prominent features that aid success of radio- and chemo-resistance in GBM patients. This includes the high tendency of tumour cells to spread to normal brain causing recurrences, the restriction imposed by the blood brain barrier (BBB) for drug distribution to the brain and the different cell population within the tumour with different drug sensitivities. The highly infiltrative manner of GBM entails maximal surgical resection of 78-98% to avoid neurological morbidity (Fritsche *et al.*, 2010;Lehtinen *et al.*, 2009).

The DNA repair pathways are crucial mechanism for resistance to treatment as they endeavour to prevent DNA damage caused by chemotherapy and radiotherapy in an attempt to destroy tumour cells thus counteracting the effect of treatment. Likewise, the DNA repair enzyme O⁶-methylguanine-DNA methyltransferase (MGMT) is able to reverse the cytotoxic effect implemented by GBM treatment including temozolomide (Minniti *et al.*, 2009). Survival rates show 42% after 6months of diagnosis, 18% at 1 year and 3% at 2 years. GBM are highly invasive and lack clear margins and therefore cannot be completely removed by surgical resection which increases the prospect for remission. Although there have been recent advances in cancer biology the treatment outcome has remained consistently poor in GBM (Friedman, Kerby and Calvert, 2000;Fujisawa *et al.*, 1999).

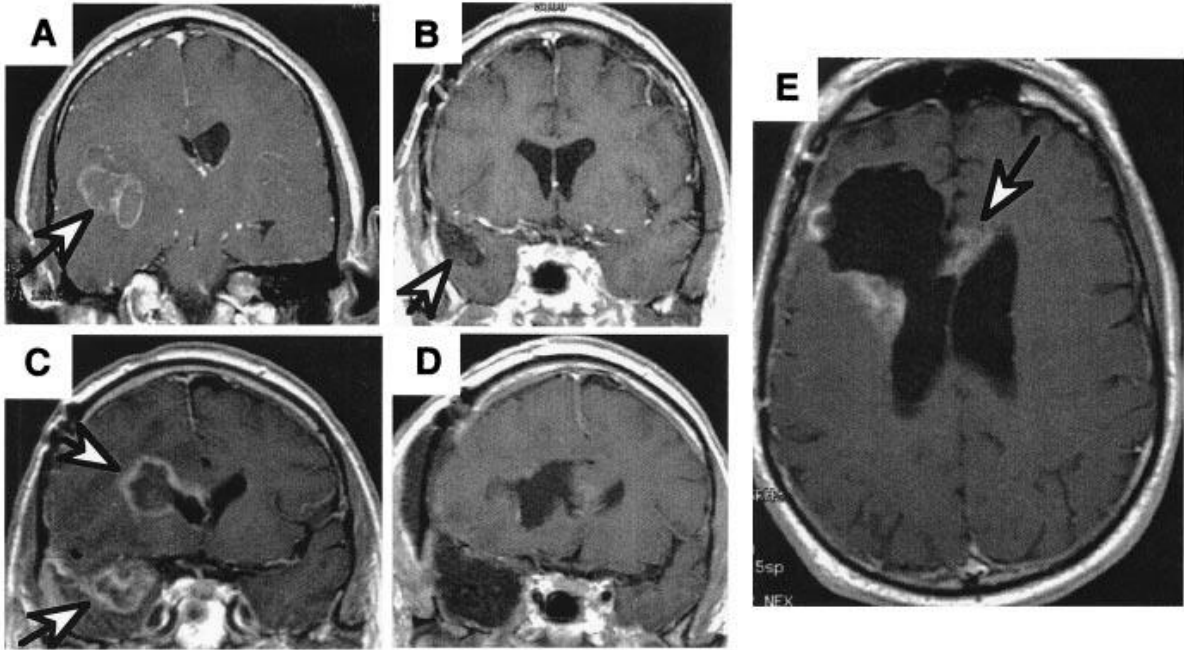


Fig 1.1. The spread of GBM visualised on MRI scans. A patient with the tumour predominately located on the right temporal. A) Presurgical scan of GBM surrounded by oedema (arrow). B) Gross total resection and clear resection cavity through surgery and radiotherapy. C) Scan 6 months later of GBM recurrence at the resection margin (arrow) and the spread across the Sylvian fissure in the frontal lobe. D) Scan after surgery of both tumours. E) Postsurgical scan after 3 months of GBM recurrence at the resection margin and the spread across the corpus callosum to the other hemisphere (Holland, 2000).

GBM are composed of three major populations: tumour cells, CSC and microglia infiltration (Fritsche *et al.*, 2010;Tada *et al.*, 2001). Clinical symptoms may include progressive headaches, seizures and focal neurological deficit (Oberndorfer *et al.*, 2008;Pace *et al.*, 2009;Faithfull, Cook and Lucas, 2005). The tumour is generally located in the frontal and temporal lobes of the brain (Fig 1.1.), but may also be present in the brainstem, cerebellum and spinal cord (Kanu *et al.*, 2009;Holland, 2000). GBM are most often *de novo* (primary GBM) which develop quickly and robustly with a three month period before the initial symptoms develop to indicate the onset of the tumour. Primary GBM accounts for approximately 90% of GBM cases and are predominately found within patients older than 45. This tumour may also develop from a lower grade tumour to a higher malignancy (secondary GBM) over a 5-10 year period and is primarily present in patients younger than 45. These subtypes have distinct genetic aberrations but are histologically indistinguishable (Furnari *et al.*, 2007;Maher *et al.*, 2006;Fujisawa *et al.*, 1999).

1.6. CD133⁺ CSC in GBM

CSC are proposed to extensively contribute to tumour progression and resistance to treatment. These cells have the same characteristics as normal stem cells as they are capable of self-renewal, the ability to differentiate into any cell within the tumour, proliferate extensively and are rare (Jordan, Guzman, and Noble, 2006). Normal neural stem cells express CD133 (Prominin-1) a 120 kDa five-transmembrane protein which are found in CSC in multiple brain tumour samples including GBM (Morse *et al.*, 2004;Samaras *et al.*, 2009). CD133⁺ cells have shown clonogenic, infinite growth and stem cell properties and are capable of forming original polyclonal tumours when xenografted onto nude mice. The xenograft consisted of approximately 20% CD133⁺ cells mimicking the unique low frequency of normal stem cells and 80% CD133⁻ cells. CSC are chemoresistant and radioresistant and therefore responsible for tumourigenesis and recurrence after conventional glioblastoma therapy (Zipfel *et al.*, 2002;Hao *et al.*, 2002;Tada *et al.*, 2001).

1.7. EGFR amplification pathway in GBM

The epidermal growth factor receptor (EGFR) gene is involved in the regulation of cellular proliferation and is amplified in 50% of GBM cases, half of which exhibit the most common mutant form EGFRvIII that has a deletion of exons 2-7 (Shinojima *et al.*, 2003). This variant is tumour-specific and has the ability to increase tumourigenesis in GBM by down-regulating apoptosis and enhancing proliferation (Nagane *et al.*, 1996; Narita *et al.*, 2002). The presence of EGFRvIII has shown to associate with a worse prognosis than EGFR alone. Amplification of EGFR is predominant in primary GBM as 60% of primary cases exhibit EGFR amplification whereas only 10% of secondary GBM patients have EGFR amplification (Shinojima *et al.*, 2003; Watanabe *et al.*, 1996).

1.8. p53 mutation in GBM

The p53 tumour suppressor responds to DNA damage, cytotoxic stress and prevents the initiation of cells with unstable genomes by inducing cell cycle arrest and apoptosis. p53 has the ability to have this regulatory effect as it is a transcription factor. More than 2500 genes many of which are involved in tumourigenesis are regulated by p53 (Hoh *et al.*, 2002; Vousden and Lu, 2002). Mutations of *TP53* gene are present in GBM and are unable to elicit tumour suppression. Secondary GBM have a considerably high incidence of *TP53* mutations (>65%), of which approximately 90% were previously present in the first biopsy with low grade or anaplastic astrocytoma, while *TP53* mutations are rare (<10) in primary GBM (Watanabe *et al.*, 1997; Ohgaki *et al.*, 2004; Watanabe *et al.*, 1996). It is evident that progression of low grade astrocytomas to GBM is associated with a clonal expansion of cells driven by successive p53 mutations that had been previously acquired, endowing them with a selective growth advantage (Sidransky *et al.*, 1992).

1.9. *PTEN* mutation in GBM

The tumour suppressor gene *phosphate and tensin homolog (PTEN)* at chromosome 10q23 is mutated in approximately 30% of GBM. *PTEN* mutations are enhanced in 30% of primary GBM but are rare in secondary GBM as only 4% is present in this subtype (Fujisawa *et al.*, 1999;Knobbe, Merlo and Reifengerger, 2002). The loss of *PTEN* tumour suppression function is triggered by *PTEN* homozygous deletion or *PTEN* methylation. *PTEN* mutations do not affect the outcome of GBM patients (Tohma *et al.*, 1998;Ohgaki *et al.*, 2004)

1.10. Astrocyte physiology and morphology

Astrocytes from which GBM are derived from are the most abundant cells in the central nervous system (CNS) and outnumber neurons by over 5 fold. Astrocytes are divided into two main subtypes based on their anatomical location and cellular morphologies (Rivest, 2009; Sofroniew and Vinters, 2010). *Fibrous astrocytes* are found mainly in white matter of the central nervous system and have many long cylindrical branching processes. *Protoplasmic astrocytes* are present throughout gray matter with shorter and fewer sheet-like processes, some of which fill the spaces between elements in the neutrophil (Miller and Raff, 1984;Sofroniew and Vinters, 2010).

The prevailing view for many years regarded astrocytes as passive elements in the brain providing support to neurons as well as development and maintenance of the BBB which protects neural tissue from circulating blood in the rest of the body (Sofroniew and Vinters, 2010;Kimelberg and Nedergaard, 2010;Markiewicz and Lukomska, 2006). It is now clear astrocytes play a vital role in maintaining homeostasis in the CNS especially in ionic homeostasis, energy metabolism, synaptic signalling between neurons and in the innate immune response. These neuroglia cells express receptors that enable them to respond to compounds such as neurotransmitters which transmit

signals from one neuron to another, growth factors and cytokines (Miller and Raff, 1984; Sofroniew and Vinters, 2010; Ransohoff and Brown, 2012).

1.11. The immune system

The mammalian immune system is designed for efficient detection and elimination of a variety of pathogens and modified host cells. The immune system can be classified as two interconnected subsystems of innate and adaptive immunity; both rely upon the ability of the immune system to distinguish between self and non-self molecules (Weller *et al.*, 1995). Innate immunity encompasses host defences that range from non-specific barrier function of epithelia to non-specific response using germ-line encoded pattern recognition receptor (PRR) for immediate recognition of microbial pathogens. The PRR that enable the prompt response include scavenger receptor (SR) and toll like receptor (TLR) (Getz, 2005; Clark and Kupper, 2005). The binding of pathogens to TLRs activate nuclear factor kappa B (NF- κ B) signalling which is a master switch for the induction of inflammation (Takeda, Kaisho and Akira, 2003). Microbes produce pathogen associated molecular patterns (PAMPs) which are essential for microbial survival and are detected by PRR. Cellular components include macrophage, dendritic cells (DC), natural killer (NK) cells, and granulocytes which destroy pathogens (Clark and Kupper, 2005). The principle functions of innate immunity include opsonisation, activation of complement and coagulation cascade which leads to activation of pro-inflammatory signalling pathways, phagocytosis and induction of apoptosis (Mogensen, 2009; Kumar, Kawai and Akira, 2011).

Activation of adaptive immune system is controlled by the induction of PRR signals (Weller *et al.*, 1995; Akira, Uematsu, Takeuchi, 2006). It is initiated by the innate immune DC presentation of the antigen to 'naïve' T lymphocytes. A direct adaptive immune response is generated against the antigen presented through destruction by cytotoxic T lymphocytes (CTL) and stimulation of B lymphocytes to produce antibodies against the antigen (Hansson *et al.*, 2002). This system has the advantage of immunologic memory to remember pathogens and tumour cells to mount an immunological

response of a greater magnitude upon re-encounter with fewer antigens (Clark and Kupper, 2005).

1.12. Astrocytes innate immunity in the brain

Over the past decade, research in the area of innate immunity within the brain has mainly focused upon microglial the resident immune cell. More recently astrocytes have been acknowledged for their ability to elicit an innate immune response as they express cytokines, complement proteins and a variety of PRRs (Rivest, 2009;Nair, Frederick and Miller, 2008) .

PRRs efficiently detect infectious agents or endogenous danger signals, and in-turn augment an inflammatory response. One of the main PRRs expressed by astrocytes is TLR3 which is essential for the recognition of TLR3 ligands such as mRNA from necrotic cells due to tissue damage (Table 1.1.). A local inflammatory reaction is then mediated as a result of the receptor-ligand binding (Jack *et al.*, 2005; Farina *et al.*, 2005). Unlike TLR that facilitate extracellular recognition of pathogens, nucleotide-binding domain (NOD) 1 and 2 sense intracellular microbes. Upon activation, an immune response is induced promoting the recruitment of interleukin-6 (IL-6), chemokines and activation of mitogen activated protein kinase (MAPK) and NF-kB pathway (Sterka, Rati and Marriott, 2006). A highly effective endocytic receptor termed mannose receptor is also a PRR located on the cell surface of astrocytes that enable the clearance of pathogens through internalisation (Burudi *et al.*, 1999;Liu *et al.*, 2004). Similarly, SR have the ability to internalise modified lipids and therefore may potentially provide a mechanism through which bacterial infections can be fought (Husemann *et al.*, 2002).

The complement system plays a crucial role the innate immune response in the brain. Components of the complement system including factor B and D as well as the complement inhibitors factor H and I, are expressed by astrocytes in normal and pathological conditions. The complement components expressed can initiate a pro-inflammatory response through the release of anaphylatoxins, pathogen cell lysis and opsonisation for pathogen clearance (Gasque *et al.*, 2000; Ohlsson *et al.*, 2003).

Several cytokines such as IL-6, granulocyte macrophage- colony stimulating factor (GM-CSF), IL-1 β , TGF- β and tumour necrosis factor alpha (TNF- α) are important mediators of astrocyte function, secreted succeeding a pathogen recognition trigger. The released cytokines have the ability to activate nearby cells, promote the innate immune response, and generate an immunosuppressive environment when needed. During brain trauma IL-6 and IL-1 β are crucial cytokines which repair lesions and restore the integrity of the BBB (Herx, Rivest and Yong, 2000 ;Swartz *et al.*, 2001). Chemokines are also expressed by astrocytes and these chemotactic cytokines including CCL2 and CXCL12 promote the recruitment of inflammatory immune cells (Tran and Miller, 2003).

Table 1.1 PRR expressed by astrocytes

PRR	Astrocytes	References
TLR	TLR2, TLR3, TLR4, TLR5, TLR9	(Park <i>et al.</i> , 2006) (Carpentier <i>et al.</i> , 2005) (Bsibsi <i>et al.</i> , 2002) (Bowman <i>et al.</i> , 2003)
NOD	NOD1, NOD2	(Sterka, Rati and Marriott, 2006b)
SR	SR-B1, SR-macrophage receptor with collagenous structure (MARCO), SR C type lectin (CL)	(Alarcon <i>et al.</i> , 2005) (Nakamura <i>et al.</i> , 2006) (Husemann and Silverstein, 2001) (Sasaki <i>et al.</i> , 2001)
Mannose receptor	Mannose receptor	(Liu <i>et al.</i> , 2004b)
Complement factors	C1q, C1r, C1s, C4, C2, C3, factor B, factor D, C5, C6, C7, C8, C9	(Gasque <i>et al.</i> , 2000)
Complement receptors (CR)	CR1, CR2, complement anaphylatoxin receptor (CaR); C3aR, C5aR	(Gasque <i>et al.</i> , 2000)
Complement inhibitors	C1-INH, decay accelerating factor (DAF)/CD55, membrane co-factor protein	(Gasque <i>et al.</i> , 2000)

(MCP)/CD46, CD59, factor H, factor I	
---	--

1.13. Cytokines in Glioblastoma

Cytokines are small multifunctional pleiotropic proteins composed of glycoproteins and polypeptides. The dual function of some cytokines enables the same protein to support tumour growth or inhibit it (Table 1.2.). Functionally cytokines exert pro-inflammatory T helper 1 (Th1) response, anti-inflammatory (Th-2) and immunosuppressive effects. Glioma cells secrete cytokines which influence proliferation, immune cell infiltration, migration and tumour cell infiltration on GBM microenvironment (Curtin *et al.*, 2005; Fenstermaker and Ciesielski, 2004).

Table 1.2. Cytokine function in non-tumourigenic brain and GBM

CYTOKINE	Role in immunity	Role in GBM	References
Pro-inflammatory cytokine			
TNF-α	-Promotes monocytes, granulocytes and NK cells cytotoxicity. -Induces the expression of IL-6	-Enhances tumour growth through promoting glioma cell invasion and angiogenesis	(Chen <i>et al.</i> , 1993) (Roth and Weller, 1999)(Yarlagadda, Alfson and Clayton, 2009)
IL-6	-Promotes B-cell differentiation into antibody producing cells	-Increases tumour progression by enhancing glioma invasion, angiogenesis and inhibition of apoptosis.	(Erta, Quintana and Hidalgo, 2012) (Weissenberger <i>et al.</i> , 2004) (Yarlagadda, Alfson and Clayton, 2009)
Interferon (IFN)-γ	-Increased antigen processing and presentation through up-regulating MHC class I and II expression to enable recognition by T-cells.	-Inhibits GBM growth.	(Fabry, Raine and Hart, 1994) (Kominsky <i>et al.</i> , 1998) (Natsume <i>et al.</i> , 2000)
IL-12	-Increases the cytotoxicity of NK cells and DC.	-decreased expression. -reduces tumour growth.	(Roy <i>et al.</i> , 2000) (Tugues <i>et al.</i> , 2015) (Wang <i>et al.</i> , 2015)

Anti-inflammatory cytokine	IL-8	-A chemoattractant that activates neutrophils.	-Enhances tumour growth through angiogenesis and invasion. -Aberrantly highly expressed.	(Bickel, 1993) (Brat, Bellail and Van Meir, 2005)
	TGF-β	-Regulate migration. -Prevents B and T cell proliferation. -Inhibits DC maturation.	-Promotes tumour growth through stimulating GBM migration and angiogenesis.	(Barcellos-Hoff <i>et al.</i> , 2009) (Lu <i>et al.</i> , 2011)
	IL-10	-Down-regulates T-helper cell cytokines.	-Enhances tumour growth by preventing T-cell proliferation.	(Huettner <i>et al.</i> , 1997) (Yarlagadda, Alfson and Clayton, 2009)
	IL-4	-Regulates maturation of B cells, T cells and mast cells.	-Inhibits tumourigenesis.	(Yarlagadda, Alfson and Clayton, 2009) (Yu <i>et al.</i> , 1993)
	IL-13	-Down regulate T helper cell cytokines.	-Over expression in GBM. -Cytotoxic activity.	(Husain and Puri, 2003) (Mori, Maher and Conti, 2016)

1.13.1. The role of TNF- α in GBM

TNF- α is a pro-inflammatory cytokine that plays a crucial role in cellular events including differentiation, proliferation, cell survival, and death (Parameswaran and Patial, 2010). The pro-inflammatory cytokine has the ability to activate the NF-KB signalling pathway to elicit its inflammatory function. TNF- α has the ability to induce activation of NF-KB pathway by enabling the activation of the inhibitor KB kinase (IKK) to phosphorylate the inhibitor of KB (IKB). This in turn allows the translocation of NF-KB from the cytoplasm into the nucleus to promote the transcription of target genes that have anti-apoptotic properties. Activation of the pathway induces anti-apoptotic signals to maintain cell viability (Kwon *et al.*, 2004;Hoesel and Schmid, 2013). NF-KB can act as an activator or inhibitor of apoptosis depending upon the apoptotic stimuli (Kaltschmidt *et al.*, 2000). There is growing evidence that increased concentrations of endogenous TNF- α in cancer are linked to tumour progression. In GBM, the expression of TNF- α is associated with inflammation driven carcinogenesis. Endogenous TNF- α actively promotes tumour growth through the enhancement of tumour proliferation angiogenesis (Nabors *et al.*, 2003;Grivennikov, Greten and Karin, 2010). The expression of TNF- α is high in GBM and contributes to the chronic inflammatory environment that enhances tumour growth. TNF- α has the ability to induce the expression of downstream cytokines including IL-6 which contributes to glioma progression (Tanabe *et al.*, 2010).

1.13.2. The role of IL-6 in GBM

IL-6 is a pro-inflammatory cytokine that is highly expressed in many malignant tumours including GBM as it plays an important role in maintaining growth and survival (Sikora, Chlebna-Sokol and Krzyzanska-Oberbek, 2001;Liu *et al.*, 2010). It promotes cell invasion and migration through auto- and paracrine signals that induce the phosphorylation of signal transducers and activators of transcription (STAT) by Janus kinases (JAK). It is known that after IL-6 activation of the cytoplasmic transcription factors they are translocated to the nucleus and trigger transcription of

targeted genes (Goswami, Gupta and Sharma, 1998; Liu *et al.*, 2010; Sansone and Bromberg, 2012; Sansone and Bromberg, 2012). Mice models have previously shown that IL-6 contributes to tumour progression and growth by activation of STAT3 through mediating cell growth and differentiation (Weissenberger *et al.*, 2004). The expression of IL-6 is also related to the grade of the astrocytoma as previous studies had found that the concentration of IL-6 increased in a positively correlation to an increased malignancy of different grade gliomas, as the more aggressive tumours had greater IL-6 production (Shan *et al.*, 2015; Weissenberger *et al.*, 2004).

1.13.3. The role of TGF- β in GBM

TGF- β production is known to be enhanced in glioma tissue as this ability of tumour cells to generate their own growth factors reduces their dependency on stimulation from normal tissue microenvironment (Olofsson *et al.*, 1992; Joseph *et al.*, 2013). TGF- β stimulation is also associated with the mutation of the gene regulator c-myc and the activation of platelet derived growth factors (PDGF) signalling events. Upregulation of TGF- β enables the cytokine to prevent proliferation of normal human astrocytes by interfering with growth factors including epidermal growth factor (EGF). TGF- β is an immunosuppressive cytokine which can elicit a cascade of events allowing GBM to evade the host immune system (Barcellos-Hoff *et al.*, 2009; Grauer *et al.*, 2007).

These events include the ability to suppress tumour infiltrating T cells, DC maturation and reduce major histocompatibility complex (MHC) class II expression of CD4+ T cells. The inhibition of dendritic cells reduces the production of IL-12 which is involved in T cell proliferation and thus contributes to GBM avoiding an immune response (Llopiz *et al.*, 2009; Joseph *et al.*, 2013). It is known that within the early stages of tumourigenesis TGF- β has the capacity to induce tumour regression by inhibition of tumour cell proliferation in comparison to the later stages of tumour development (Drabsch and ten Dijke, 2012). Cui *et al.* demonstrated that within low grade tumours the cytokine contributed to tumour inhibition whereas in higher grade glioma it contributed to tumour progression. As over 90% of GBM cases are primary tumours in

which the disease develops rapidly with no early precursor signs this anti-tumour characteristic is rarely seen (Cui *et al.*, 1996; Furnari *et al.*, 2007).

1.13.4. The role of IL-12 in GBM

IL-12 is secreted by mature DC and macrophages to increase the presence of cytotoxic immune cells including CTL, NK cells, DC and the production of B lymphocyte (Morse *et al.*, 2004; Okada *et al.*, 2007). Within GBM, the ability of IL-12 to facilitate the production of CTLs permits an induction of pro-inflammatory cytokine release. In turn apoptosis is induced and a TH1 response mediated by the differentiation of naïve T cells to eliminate tumours is triggered. Preliminary data obtained from clinical trials of the use of IL-12 in GBM therapy indicated a reduction in tumour size of approximately 50%. In addition, administration of IL-12 to C57BL/6 mice with GBM demonstrated a decrease in tumour growth. IL-12 expression is reduced in GBM to allow the tumour to invade neighbouring tissue (Vom Berg *et al.*, 2013; Liu *et al.*, 2002)

1.14. Immune privilege of the brain

Immune privilege had previously been defined as the absence of immune cells in the CNS including the brain. In light of recent data, the characteristics of immune privilege has been redefined and is no longer considered absolute. It is now acknowledged that immune privilege varies between region and age. There had been a general misconception spanning decades that had attributed immune privilege entirely to the BBB (Carson *et al.*, 2006). The concept of immune privilege had stemmed from the ability of antigens within the brain to avoid systemic immunological recognition. It is now evident that immune privilege is specific to brain parenchyma and the peripheral immune system. The immune privilege of the brain is imperative for damage limitation during inflammation as it is an extremely sensitive organ with poor regenerative capacity (Cosacak, Papadimitriou and Kizil, 2015; Hong and Van Kaer, 1999; Shrestha *et al.*, 2013).

Microglia are resident macrophages of the brain and are known to be the main innate immune cells within the brain. They are derived from monocytic lineage and originate from the bone marrow. Due to the brain micro-environment the phenotype of microglia is reduced compared to other tissue macrophages. Once there is an onset of injury or pathogen invasion the microglia are able to upregulate immune-phenotype characteristics (Chan, Kohsaka and Rezaie, 2007;Lull and Block, 2010). Inflammation in the brain is minimised to prevent brain damage through the secretion of anti-inflammatory cytokines such as TGF- β or IL-10 which suppress microglia activity. Once inflammation has been established within the brain the immune privilege concept is undermined which may be a result of blood brain barrier damage and the upregulation of cytokine expression including IL-6 and IL-12 (Boche *et al.*, 2006; Hagberg *et al.*, 2015).

1.15. Cancer immuno-editing of GBM

Cancer immuno-editing is comprised of 3 phases in which the innate and adaptive immunity shape the fate of tumour development. Elimination also known as immune surveillance is the first phase characterised by the ability of the immune system to destroy transformed cells before they are clinically detectable (Mittal *et al.*, 2014). Theories of the immune system scanning for and eradicating early tumour cells was first proposed in the early 1900s by Ehrlich (Ehrlich, 1909). 50 years later this theory was developed and the concept of immune surveillance was proposed by Burnet and Thomas (Burnet, 1957; Thomas, 1959).

In the brain, early transformed cells are detected by innate immune cells such as DC, macrophages, the complement system and NK cells to facilitate elimination through destruction of tumour cells, phagocytosis, cell lysis and presentation to T cells (Friese, Steinle and Weller, 2004). As the brain is known to be an immuno-privileged site protected by BBB, it lacks lymphatics (Galea *et al.*, 2007). To overcome this hurdle dendritic cells, have the ability to pass through the perivascular space and cerebral spinal space to present the antigen to T cells in the lymph node. The activated T cells

undergo clonal expansion and migrate from the cervical lymph node to the brain tumour. CD8⁺ CTL are able to recognise the tumour and induce killing through the release of cytotoxic effector molecules such as perforin and IFN- γ (Pellegatta, Cuppini and Finocchiaro, 2011; Ransohoff, Kivisakk and Kidd, 2003).

The next step in cancer immuno-editing is the equilibrium phase in which the tumour cells are in a state of functional dormancy. During this phase the cells are in constant interaction with the immune system and some of the cells undergo changes and become resistant to immune recognition and elimination (Dunn, Old and Schreiber, 2004). The final phase is the escape phase commonly recognised as the 7th hallmark of cancer in which the tumour cells are immuno-edited and escape elimination (Hanahan and Weinberg, 2011). Brain tumour cells enter the escape phase through changes to the cell or microenvironment. This ultimately reduces the immunogenicity of tumour cells and lowers immune recognition. Brain tumours are able to escape elimination from the immune system and develop into clinically detectable gliomas through several mechanisms including the release of immuno-suppressive cytokines such as TGF- β and IL-10. The release of these cytokines suppress the proliferation of T-cells, NK cells, and macrophage to evade immune destruction (Pellegatta, Cuppini and Finocchiaro, 2011; Weller and Fontana, 1995; Huettner *et al.*, 1997). In addition, glioma cells are able to disguise themselves as normal cells and escape immune detection. This occurs through a variety of mechanisms including expressing complement protein factor H to prevent complement activation (Gasque *et al.*, 2000; Ferreira, Pangburn and Cortes, 2010).

1.16. The Complement system

The complement system is one of the first line of defence mechanisms in innate immunity for the brain. Activation of complement opsonises the pathogen or altered self-cells for phagocytic uptake, induces an inflammatory response and also enables cell lysis. Complement is activated through 3 different pathways which are the alternative, classical and lectin pathway (Fig 1.2.) (Dunkelberger and Song, 2010). The

alternative pathway is triggered by the spontaneous hydrolysis of C3 in which 2 cleaved products are formed. The cleaved anaphylatoxin C3a elicits inflammation whereas C3b opsonises pathogens and also bind to C3 convertase (C3bBb) to form C5 convertase (C3bBbC3b) (Thurman and Holers, 2006). The activation of the classical pathway is through the binding of C1q directly to pathogens, altered self-cells or to antibody antigen complexes. This triggers the C1r to activate C1s which cleaves C4 and C2 to generate C4a anaphylatoxin, C4b opsonin, C2a and C2b. C4b and C2b bind to form C3 convertase (C4b2b) (Celik *et al.*, 2001). Similarly, in the lectin pathway both C4 and C2 are also cleaved producing the same products and generate C3 convertase (C4b2b). The lectin pathway is activated by mannose binding lectin (MBL) binding to oligosaccharides on pathogens. The associated enzyme mannan binding lectin serine protease (MASP) 1 and 2 are responsible for the cleavage of C4 and C2 (Ali *et al.*, 2012).

All 3 pathways converge at C3 convertase enabling the cleavage of the central complement component C3 to form C3a and C3b (Fig 1.2.). The opsonin C3b binds to C3 convertase and generate C5 convertase (C3bBbC3b) (C4b2Bc3b), which enables the cleavage of C5 to form anaphylatoxin C5a, and opsonin C5b. C5b binds to the pathogen and also to C6, C7, C8, and C9, and produce a membrane attack complex (MAC) which generates pores on the cell leading to osmotic cell lysis (Dunkelberger and Song, 2010).

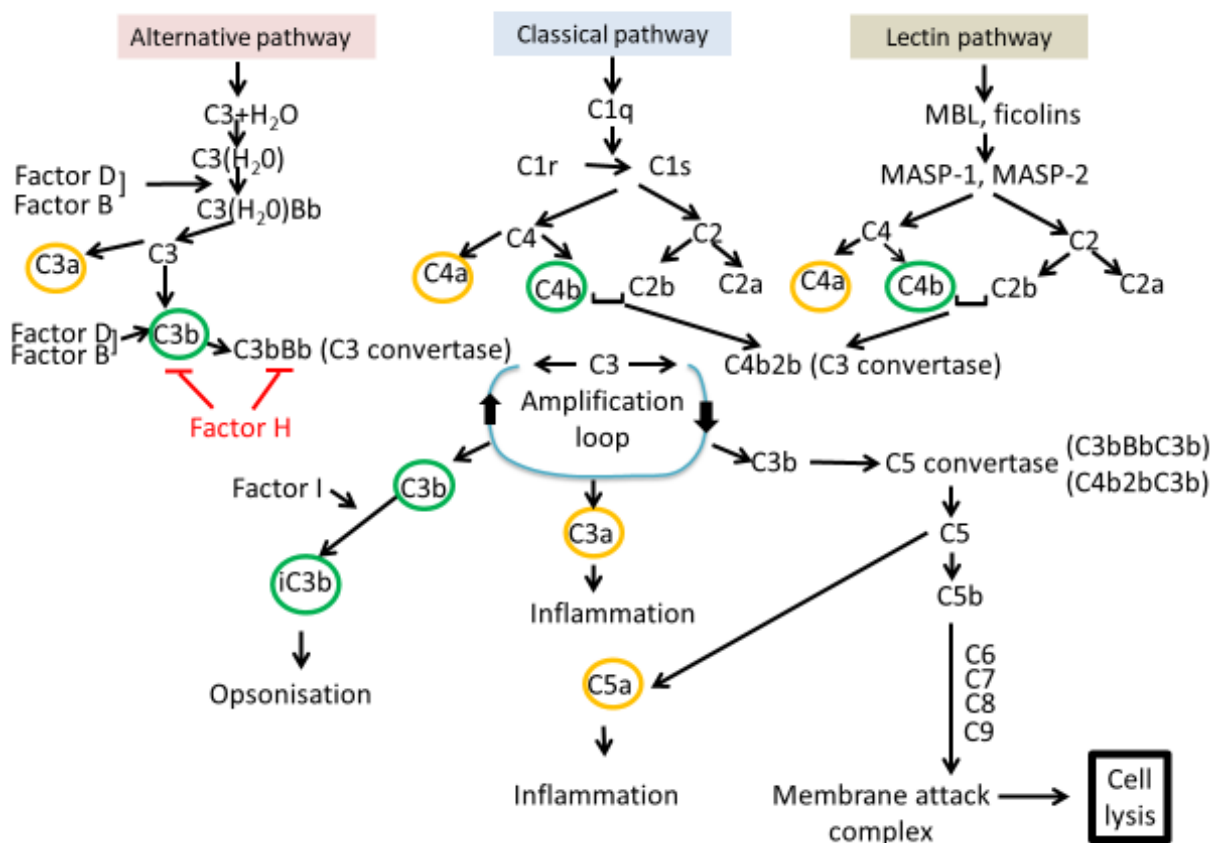


Fig 1.2. Complement system. Complement activity is initiated by 3 main pathways, the alternative pathway, classical pathway and lectin pathway. Opsonins generated are circled green and anaphylatoxins are circled yellow. The activated cascade of complement leads to the formation of C3 convertase. An amplification loop is generated as the cleavage of C3 forms C3b and C3a. C3a is an anaphylatoxin which elicits inflammation. The opsonin C3b is either inactivated or binds to C3 convertase to form C5 convertase that cleaves C5 to generate C5b or anaphylatoxin C5a. The terminal stages of complement include C5b bound to C6, C7, C8 and C9 to form MAC which allows cell lysis (Adapted from; Rus, Cudrici and Niculescu, 2005)

1.16.1. The Alternative pathway

The alternative pathway is an antibody independent system, capable of differentiating between self and non-self through the strict control of the host's soluble and membrane bound complement regulatory components. Soluble factor H and properdin regulate activation of the alternative pathway. Factor H enhances the protection of host surfaces from complement activation through its ability to bind to sialic acid exhibited on host cells when C3b is present. In contrast properdin is important for the stabilisation of C3 convertase (Rodriguez de Cordoba *et al.*, 2004;Hourcade, 2006). The majority of Pathogens do not exhibit complement regulators or sialic acids on their surface and therefore do not attract factor H. Membrane bound self-cell regulators CD35 (complement receptor type 1, CR1), CD46 (membrane cofactor protein, MCP), and CD55 (decay accelerating factor, DAF) are essential to the prevention of an autoimmune response by initiating the inactivation of C3b whereas CD59 prevents the formation of MAC (Dinasarapu *et al.*, 2012).

The ability of auto-activation by the alternative pathway is a unique characteristic originating in the fluid phase in plasma. Low level spontaneous conformational change of C3 is termed tickover which enables this abundant protein to be constantly hydrolysed as the internal thioester bonds bind with water at a rate of 1% per total C3 generated per hour. C3(H₂O) evokes a C3b like function in the ability to recruit factor B in the presence of Magnesium ion (Mg²⁺) permitting its cleavage by the serum protease factor D to generate Ba and Bb fragments (Thurman and Holers, 2006;Harris *et al.*, 2007). The active Bb fragment remains bound to C3(H₂O) which is integral for the formation of the initial C3 convertase. This molecule elicits the cleavage of C3, triggering the formation of C3a and C3b. In turn C3b binds to the cleaved Bb fragment generating C3 convertase (C3bBb) which initiates a positive feedback amplification loop. The released C3a is an anaphylatoxin with chemotactic functions. C3b is deposited in an indiscriminately manner onto self and pathogenic surfaces, if left

uncontrolled opsonisation and the assembly of the membrane attack complex will occur on self-cells (Thurman and Holers, 2006; Pangburn *et al.*, 2000).

1.16.2. Factor H

Factor H (150 kDa) is an important soluble regulator of the alternative pathway. It is composed of 20 short consensus repeats (SCRs) also known as complement control proteins (CCPs). Each unit is highly conserved and is composed of 60 amino acids. This complement inhibitor is a single chain glycoprotein which is present in plasma at a concentration between 110-615 $\mu\text{g}/\text{mL}$. It is mainly secreted by the liver and has the appearance of 'flexible beads' on a string (Ripoche *et al.*, 1988; Rodríguez de Córdoba *et al.*, 2004). Factor H gene is located on chromosome 1q32 in the regulators of complement activation (RCA) gene cluster which include, complement factor H like protein 1 (CFHL-1) Complement factor H related protein (CFHR) 1-5, the regulators C4 binding proteins, CR type 1, DAF, and MCF (Ferluga *et al.*, 2017). Factor H has the ability to elicit a complement inhibitor effect through its ability to compete with factor B for C3b binding, preventing the formation of C3 convertase; accelerate the decay of C3 convertase (C3bBb) by displacing factor Bb to disassemble the enzyme; act as a co-factor for factor I to inactivate C3b by cleaving the α -C3b chain into 2 fragments of 68 and 43 kDa. The functional activity of factor H is facilitated through the N-terminal SCRs 1-4 (Rodríguez de Córdoba *et al.*, 2004)

In the presence of glycosaminoglycans and sialic acid (polyanionic molecules) the affinity of factor H increases for surface bound C3b. Factor H has 3 binding sites for C3b at SCRs 1-4, 7-15, and 19-20. Once bound it then has ability to form dimers and tetramers at the C-terminus through SCRs 19-20 (Ferreira, Pangburn and Cortes, 2010). The C-terminus 19-20 SCRs represents the central binding and recognition domain of the protein. Factor H is able to bind to cell membrane and differentiate between self and non-self surfaces through its C-terminal. Some multicellular pathogens have remained undetected for destruction by the complement system as they are able recruit host factor H to their surface (Kopp *et al.*, 2012).

Factor H deficiencies and mutations are associated with the onset of diseases such as; dense deposit disease (DDD) which is caused by uncontrolled activation of the alternative pathway. It is generated through deposition of activated C3 fragments into the kidney glomeruli in which end-stage renal failure can develop (Appel *et al.*, 2005). Mutations in the C-terminus of factor H at SCR 19-20 lead to defective recognition and the onset of atypical haemolytic uremic syndrome (aHUS). This rare kidney disease is characterised by haemolytic anaemia, low platelet count, and acute renal failure in which end stage renal failure can develop through uncontrolled activation of the alternative pathway (Jozsi *et al.*, 2006). Age related macular degeneration (AMD) is the leading cause of blindness in the elderly due to uncontrolled activation of the alternative pathway and factor H polymorphism (Klein *et al.*, 2005).

1.16.3. CFHR5

CFHR5 is the longest human CFHR protein at 65 kDa composed of 9 SCRs. This protein is unique in comparison to CFHR 1-4 as it contains 5 SCR domains that share sequence homology (46%, 75%, 57%, 48% and 71%) to SCRs 10-14 of factor H (Fig 1.3.). This particular domain of factor H has been attributed to C3b, heparin and C-reactive protein binding. CFHR5 is a glycosylated protein associated with lipoprotein particles with an unknown plasma concentration. The N-terminal shares 89% and 84% sequence identity with SCRs 1-2 of CFHR 1-2 and the C-terminal shares a sequence homology of 64% with SCR 19 and 42% with SCR 20 of factor H deduced from the cDNA sequence (Fig 1.4) (McRae *et al.*, 2002). This protein has the ability to bind to C3b, heparin, C-reactive protein, and iC3b the cleavage product of C3b. Weak co-factor activity in cleaving C3b by factor I and competing with factor B for C3b binding has been attributed to CFHR5 (McRae *et al.*, 2005;McRae *et al.*, 2001).

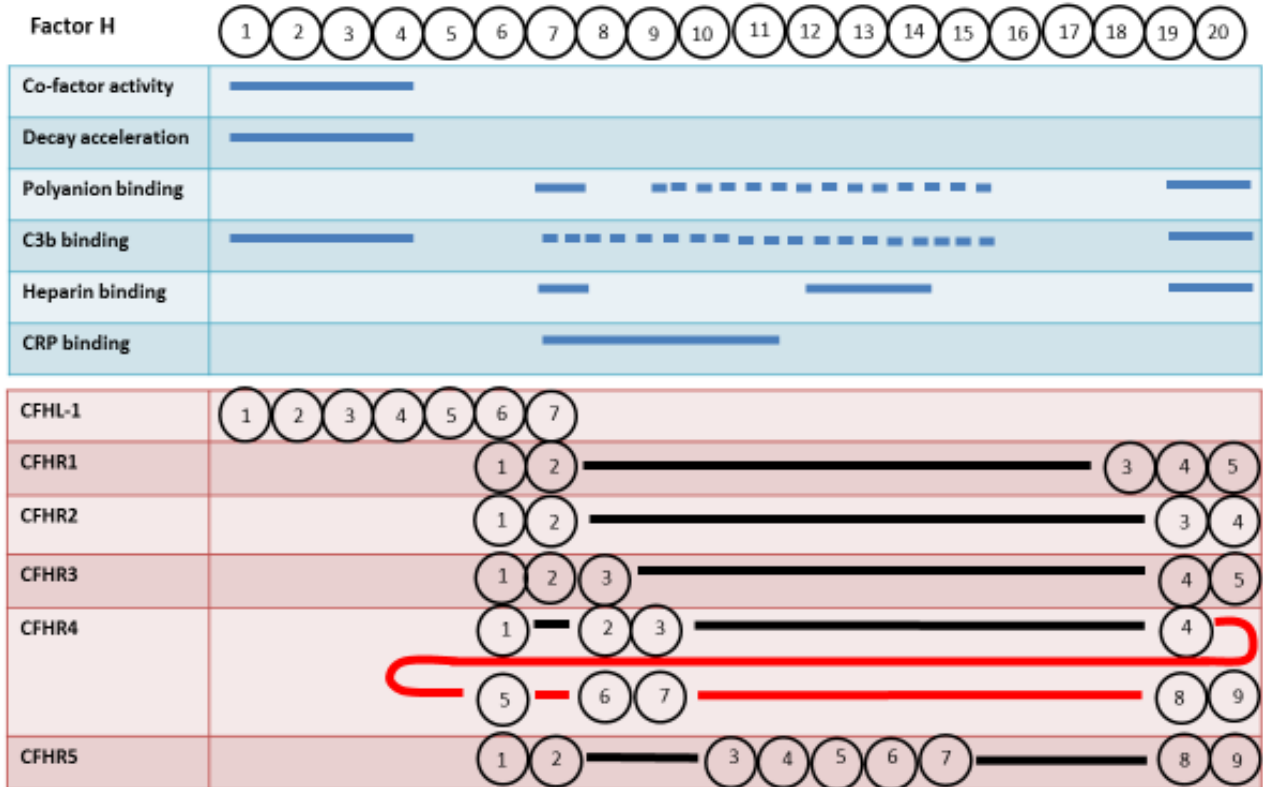


Fig 1.3. Schematic representation of factor H, CFHL-1 and CFHR1-CFHR5. Each circle represents a SCR and is aligned on the basis of amino acid sequence homology with factor H. It includes a summary of the SCRs involved in protein binding, decay acceleration and co-factor activity which is represented by a solid blue. The dotted lines indicate SCRs where binding sites or function remain uncertain (Adapted from; Skerka *et al.*, 2013).

```

1   GGCAGGTGCTTGTACTGTTAATGAAAGCAGATTTAAAGCAACACCACCATCTCGGAGT
61  ATTTTGTATATACGATTGAGACTACCAAGCATGTGCTCTTATTCAGTGTAAATCCTA
      M L L L F S V I L
121 ATCTCATGGGTATCCACTGTTGGGGGAGAAGGAACACTTTGTGATTTTCCAAAAATACAC
      I S W V S T V G G E G T L C D F P K I H
181 CATGGATTCTGTATGATGAGAAGATTATAACCTTTTCCCAAGTCTACAGGGGAA
      H G F L Y D E E D Y N P F S Q V P T G E
241 GTTTCTATTACTCCTGTGAATATAATTTGTGTCCTTCAAAATCCTTTGGACTCGC
      V F Y Y S C E Y N F V S P S K S F W T R
301 ATAACATGCACAGAAGAAGGATGGTACCAACACCGAAGTGTCTCAGAATGTGTCCTT
      I T C T E E G W S P T P K C L R M C S F
361 CCTTTGTGAAAAATGGTCAITCTGAATCTCAGGACTAATACATCTGGAAGGTGATACT
      F V K N G H S E S S G L I H L E G D T
421 GTACAATATTGTCAACACAGGATACAGCCTTCAAAACATGAGAAAAACATTTCTGTG
      V Q I I C N T G Y S L Q N N E K N I S C
481 GTAGAACGGGGCTGGTCCACTCCTCCATATGCAGCTTCACTAAAGGAGAATGTCATGT
      V E R G W S T P P I C S P T K G E C H V
541 CCAATTTTAGAAGCAATGTAGATGCTCAGCCAAAAAAGAAAGCTACAAGTTGGAGAC
      P I L E A N V D A Q P K K E S Y K V G D
601 GTGTGAAATCTCCTGCAGAAAAATCTTATAAGAGTTGGATCAGACTCAGTCAATGT
      V L K F S C R K N L I R V G S D S V Q C
661 TACCAATTTGGGTGGTACCTAATTTCCAACATGCAAGGACAAGTACGATCATGTGT
      Y Q F G W S P N F P T C K G Q V R S C G
721 CCACCTCCTCAACTCTCCAATGGTGAAGTTAAGGAGATAAGAAAAAGGAATATGGACAC
      P P P Q L S N G E V K E I R K E E Y G H
781 AATGAAGTAGTGGAAATGATGCAATCTCAATTTATAAATAAACGGCCCTAAGAAAAA
      N E V V E Y D C N P N F I I N G P K K I
841 CAATGTGTGATGGAGAATGGACAATTTACCCACTTGTGTGACAAGTGAACAAATGT
      Q C V D G E W T T L P T C V E Q V K T C
901 GGATACATACCTGAACCTGAGTACGGTTATGTTACAGCCGCTGTGCCCTCCCTATCAACAT
      G Y I P E L E Y G Y V Q P S V P P Y Q H
961 GGAGTTTCAGTCGAGTGAATTCAGAAATGAATATGCAATGATTGGAATAACATGATT
      G V S V E V N C R N E Y A H I G N N H I

1021 ACCTGTATTAATGGAAATGGACAGAGCTTCTATGTGTGTCACACACCAACTTAAG
      T C I N G I W T E L P H C V A T H Q L K
1081 AGGTGCAAAATAGCAGGATTAATATAAAAACATCTCAAGCTATCTGGGAAAGAAATTT
      R C K I A G V N I K T L L K L S G K E F
1141 AATCATAATCTAGAAATACGTTACAGATGTTACAGACATCTCAGATACAGGCACCTCAGTC
      N H N S R I R Y R C S D I F R Y R H S V
1201 TGTATAAACGGGAAATGGAAATCTGGAAGTACTGCACAGAAAAAGGAAACAATCTGTC
      C I N G K W N P E V D C T E K R E Q F C
1261 CCACCGCCACTCAGATACCTAATGCTCAGAAATGACAACCCAGTGAATATCAGGAT
      P P P P Q I P N A Q N M T T T V N Y Q D
1321 GGAGAAAAGTAGCTGTTCTCTGTAAGAAAAATCTACTTCCAGAAGCAAAAGAAAT
      G E K V A V L C K E N Y L L P E A K E I
1381 GTATGTAAGATGGACGATGGCAATCATTACCACGCTGTGTTGAGTCTACTGCATATGT
      V C K D G R W Q S L P R C V E S T A Y C
1441 GGGCCCCCTCCATCTATTAACAATGGAGATACCACCTCATCCCATTTATCAGTATATCCT
      G P P P S I N N G D T T S F P L S V Y P
1501 CCAGGTCACAGTACGTAACCGTTGCCAGTCTCTATAAACTCCAGGGCTCTGTAAC
      P G S T V T Y R C Q S F Y K L Q G S V T
1561 GTAACATGCAGAAATAAACAGTGGTCAGAACCAACCAAGATGCTAGATCCATGTGGTA
      V T C R N K Q W S E P P R C L D P C V V
1621 TCTGAAGAAAATGAAACAAAATAACATACAGTTAAAATGGAGAACGATGAAAAC
      S E E N M N K N N I Q L K W R N D G K L
1681 TATGCAAAAACAGGGGATGCTGTGAAATCCAGTGTAAATCCCACATAAGCGATGATA
      Y A K T G D A V E F Q C K F P H K A H I
1741 TCATCACCACCATTTGAGCAATCTGTCAGGAAGGAAATTTGAATATCCTATATGTGAA
      S S P P P R A I C Q E G K F E Y P I C E

1801 TGAAGCAAGCATAATTTCTGAAATATTTTCAAAACATCCATCTACGCTAAAAGTAGC
1861 CATATGTAGCCAATCTGTAGTACTCTTTTATCTTTTCAGGTGTGTTAACTCAGT
1921 TTTATTTAGAACTCTGGATTTTGTAGCTTTTGAAGATTTGTAAGCTGAGAGAACAATGTT
1981 TCACITTAATAGGAGGGTCTTAGTCCATATTACATTTGTTATAACAGAGATACAGACT
2041 GGATACTTCAACCAATAGTTTATTTGTTTATAAATCTAAAAGCTGAGAGTCAAGA
2101 TGGTGGGGCTGCCCTGTTGAGGGTCTTCTCGAAGCATCATAATATGCTGGAAGGCATCA
2161 CAACATGGTGAAGGATCAGGTGGCAAAAGGACATGTACATGGGAGTGAGAGAAAAAGA
2221 GAGAGAGAGACAGAGTGGCGGGGCGGGGAGGAGCGCAACTCATCTTTATAAGACA
2281 CCATCTCGAGATAACAACTCAATCCATGATATGACATTAATCCATCAAGAGATAG
2341 AGCTCTCGTACTTAATCACCTTCTAAAGATCTCACCTGACAACACTGTTGCAATGGCAG
2401 TTAAGTTTCACGTAACCTTTCGGGGACACATTCAAAACACAGGAGAACTCAAATGTT
2461 CCTGGGCAATCAACATGGGAAATTTTATCATAAATGTCACAGAAACAGTAAATGT
2521 TCTCGCTCAGAACCTAATTCATCTAATCCCTCCTGTTGTCTCAAAATATAGGATAACT
2581 TTGAACTTCTGAATTAACGTTATTTAAAAGGAAATGTAGATGTTATTTAGTCTCAT
2641 CTCAGGTTATATCACTTAAAACCTCGCAAGCTGCAACTTTTGTGGTTGTAGCAAG
2701 TATTAATAAATATTTATAAATCCTCAATGTAAGTCTAGCTACCTATCCCAATCTAAAA
2761 CCCCTTAAAGTATTAATGCACTATCTGCTGTAACCGAAAAAAGAAAAAAGAAAAA
2821 AAA

```

Fig 1.4. Nucleotide sequence of CFHR5 cDNA and amino acid sequence. Numbering of the nucleotide acid sequence is indicated on the left and the mature amino acid sequence on the right (McRae *et al.*, 2001).

1.17. Surfactant protein D expression

Surfactant protein D (SP-D) is a collagen containing C-type lectin, termed collectin which is capable of providing innate immuno-protection at pulmonary as well as extra pulmonary sites. In serum SP-D concentration is present at 48.7 ng/mL. SP-D is predominantly synthesised and secreted into the lung airspace by alveolar and bronchiolar epithelial cells. It is constitutively secreted by alveolar type II cells at the alveolar level and more proximally by non-ciliated Clara cells (Crouch, 2000;Kuroki *et al.*, 1998;Lemos, McKinney and Rhee, 2011;Madsen *et al.*, 2000). Extra pulmonary detection of SP-D has increasingly become more common and has been shown to be secreted by ductal epithelial cells in salivary glands, glandular epithelial cells in the stomach, mucosal epithelial cells in the small intestine, mammary epithelial cells in the breast and is present in human amniotic fluid as early as 26 weeks gestation (Table 1.3.) (Miyamura *et al.*, 1994;Crouch, 2000;Madsen *et al.*, 2000). Recently SP-D has also been detected within the brain but the source from which the collectin has been secreted from is yet to be confirmed (Schob *et al.*, 2013).

Table 1.3. Pulmonary and extra pulmonary sites of SP-D expression

Anatomical site	Organ	Cellular source	References
Respiratory tract/oropharynx/nasopharynx			
	Lacrimal glands	Ductal epithelial cells	(Brauer <i>et al.</i> , 2007)
	Lung	Alveolar type II cell, non-ciliated bronchiolar cells	(Voorhout <i>et al.</i> , 1992)
	Salivary gland	Ductal epithelial cells	(Crouch, 2000)
	Trachea and bronchi	Submucosal glands and respiratory epithelial cells	(Wong <i>et al.</i> , 1996)
Gastrointestinal tract			
	Biliary tract	Intrahepatic ductal epithelial cells	(Madsen <i>et al.</i> , 2000)
	Oesophagus	Squamous epithelium	(Madsen <i>et al.</i> , 2000)
	Pancreas (exocrine)	Ductal epithelial cells (and islets)	(Crouch, 2000)
	Small intestine	Mucosal epithelial cells	(Reid, 1998)
	Stomach	Glandular epithelial cells	(Reid, 1998)
Genitourinary tract			
	Kidney	Collecting duct epithelium	(Madsen <i>et al.</i> , 2000)
	Prostate	Glandular epithelium	(Herias <i>et al.</i> , 2007)
Skin and soft tissue			
	Breast	Mammary epithelium	(Crouch, 2000)
	Sweat glands	Ductal epithelium	(Crouch, 2000)

Other

Brain	?	(Schob <i>et al.</i> , 2013)
Heart	?	(Reid, 1998)
Pancreas (endocrine)	Islets	(Herias <i>et al.</i> , 2007)
Placenta	?	(Leth-Larsen <i>et al.</i> , 2004)
Testis	Leydig cells	(Crouch, 2000)

1.17.1. SP-D structure

SP-D is composed of four main regions that include an N-terminal, collagenous region, α -helical neck and carbohydrate recognition domain (CRD) located on chromosome 10q 22-23 (Fig 1.5.). The cysteine rich N-terminal region is required for disulphide dependent crosslinking to stabilise the 130 kDa trimer comprised of 3 identical 43 kDa polypeptide chains. A 520 kDa dodecamer structure is regularly assembled from 4 homotrimeric subunits at the N-terminal and a maximum of 8 dodecamers are able to assemble to form a large oligomeric structure (Holmskov, Thiel and Jensenius, 2003; Kolble *et al.*, 1993; Madhukaran *et al.*, 2015).

The triple helical collagen region is highly conserved and lacks interruption in the gly-x-y repeats where x and y can be any amino acid. Each SP-D monomeric structure has 59 gly-x-y repeats which are intertwined with 2 additional chains and form a right handed super helix with a 4 nm diameter. The conserved gly-x-y repeats reveal the importance of the conserved regions ability to control the spacial separation of CRDs which is critical for normal SP-D function (Kishore *et al.*, 2005). Maintenance of the shape and stability of the protein is provided by interchain hydrogen bonds between the C-terminus of amino acids at position x and the N-terminus of the glycine residue which face into the centre of the helix. The collagen region is rich in hydroxylated proline and lysine residues which are commonly at position x and contribute to stabilise the domain (Crouch *et al.*, 1994; Ogasawara and Voelker, 1995).

The trimerising coiled coil neck region is composed of 33 amino acid residues and connects the globular CRDs with the collagen domain. The neck consists of 8 α -helical turns which are formed upon the parallel arrangement of the polypeptide chains. In addition, this region acts as an initiation point for the trimerisation and nucleate the formation of the collagen triple helix (Hoppe and Reid, 1994; Kovacs *et al.*, 2002; Zhang *et al.*, 2001). The neck also maintains and supports the organisation of CRDs within a trimer which is a crucial feature for ligand recognition. The globular CRDs are located

at the C-terminus and have the ability to recognise carbohydrates and PAMPS on the surface of pathogens in a calcium dependent manner (Zhang *et al.*, 2001).

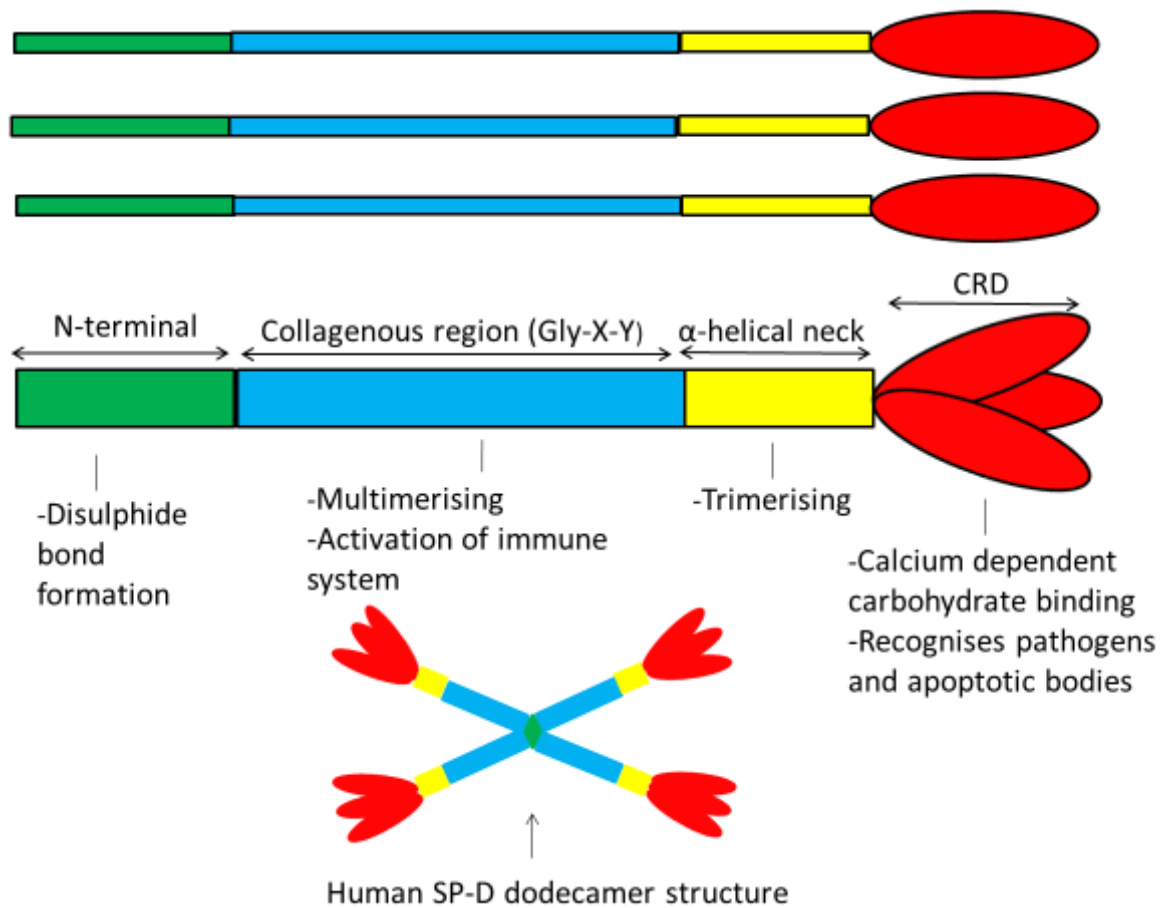


Fig 1.5. Schematic diagram illustrating the organisation and assembly of SP-D.

The primary structure of SP-D is composed of a cysteine rich N-terminal (green), a collagen gly-x-y domain (blue), an α -helical coiled coil neck (yellow) and a CRD region (red). SP-D is a large dodecamer structure comprised of four trimeric subunits and has a cruciform like appearance in electron microscopy in which the subunits are of equal lengths and end in globular heads (Adapted from Nayak *et al.*, 2012).

1.17.2. Pathogen recognition and clearance

SP-D via its CRD region has the ability to recognise and interact with viruses, bacteria, yeast, fungi and dying cells to elicit an immune response through agglutination and opsonisation which renders the microbes susceptible to macrophage and neutrophil killing (Table 1.4.). The CRD region can recognise repetitive carbohydrate moieties conserved within all pathogens, which in turn elicits agglutination, and enhance phagocytosis (Haczku, 2008;Kishore *et al.*, 2006). Interaction between the gly-x-y collagenous domain and immune cell receptors promote a clearance of apoptotic cells, necrotic cells, allergens and pathogens through a variety of mechanisms that involve phagocytosis, chemotaxis, viral neutralisation, oxidative and antigen presenting properties. Enhanced phagocytosis is a crucial step in pathogen clearance as it is likely to take place by regulating the expression of pattern recognition receptors, opsonisation of pathogens and acting as an activation ligand (Nayak *et al.*, 2012;Wright, 2005).

Table 1.4. Summary of interaction with SP-D and pathogen

Microbe	Effect of SP-D	Reference
Gram negative bacteria		
<i>E.coli</i>	Agglutination, enhanced uptake and growth inhibition	(Wu <i>et al.</i> , 2003)
<i>Enterobacter aerogenes</i>	Growth inhibition	(Wu <i>et al.</i> , 2003)
<i>Klebsiella pneumoniae</i>	Growth inhibition	(Wu <i>et al.</i> , 2003)
<i>Legionella pneumophila</i>	Growth inhibition	(Sawada <i>et al.</i> , 2010)
<i>Pseudomonas aeruginosa</i>	Enhanced uptake by phagocytosis	(Lim <i>et al.</i> , 1994)
Gram positive bacteria		
<i>Staphylococcus aureus</i>	Enhanced uptake	(Hartshorn <i>et al.</i> , 1994)
<i>Streptococcus pneumoniae</i>	Agglutination and enhanced uptake	(Hartshorn <i>et al.</i> , 1998)
<i>Mycobacterium avium</i>	Enhanced uptake by macrophages	(Kudo <i>et al.</i> , 2004)
Virus		
Influenza A virus	Agglutination, neutralisation, enhanced phagocytosis	(Hartshorn <i>et al.</i> , 1994)
Human Immunodeficiency virus	Neutralisation	(Meschi <i>et al.</i> , 2005)
Respiratory syncytial virus	Neutralisation	(Hickling <i>et al.</i> , 1999)
Fungi		
<i>Aspergillus fumigatus</i>	Agglutination and enhanced uptake	(Madan <i>et al.</i> , 1997)
<i>Candida albicans</i>	Agglutination, growth inhibition, and inhibition of phagocytosis	(van Rozendaal <i>et al.</i> , 2000)
<i>Cryptococcus neoformans</i>	Agglutination	(Schelenz <i>et al.</i> , 1995)

1.17.3. A recombinant form of truncated SP-D

A recombinant truncated form of human SP-D (rhSP-D) was produced containing 8 gly-X-Y repeats, α -helical trimerising neck region, and CRD. The absence of the oligomerising N-terminal was to prevent formation of a larger SP-D structure. The rhSP-D expressed represented a 60 kDa homotrimeric subunit when analysed by gel filtration chromatography and chemical crosslinking. This relatively small structure of the native 520 kDa dodecamer is a 20 kDa monomeric protein under reduced electrophoresis conditions. It is apparent that the trimer formed is not a result of aberrant linking between CRDs as no higher oligomers were observed. The recombinant protein has the ability to bind to carbohydrates through the 3 CRDs held together by the trimerising neck which is stabilised by the 8 gly-x-y collagen region. The α -helical neck is essential for CRDs to bind to carbohydrates as without it the recombinant protein has a weak affinity for sugars (Singh *et al.*, 2003).

1.17.4. SP-D in the brain

The presence of SP-D has also been detected in extra pulmonary sites including the brain (Madsen *et al.*, 2000; Akiyama *et al.*, 2002). The expression was detected at the microvascular levels of the brain parenchyma, choroid plexus stroma and pineal gland. In patients who have an autoimmune disease, CNS infection or cerebral infarction SP-D levels are reduced compared to those who are healthy. SP-D is abundant at the limitan astrocytic feet and immunological perivascular space. The location of such abundancy is of great importance as both play an vital role in the immunological response, therefore the function of SP-D in the brain is considered to resemble its pathogen elimination role in the brain (Schob *et al.*, 2013).

1.17.5. SP-D in cancer

Little attention has been placed upon the expression of SP-D in cancer and more research is needed in order to understand the implications this protein has in tumours. SP-D is expressed in mice with lung cancer and can potentially be used as a biomarker

for the disease as it can distinguish normal mice from mice with lung adenocarcinoma. Tumour bearing mice have a significant increased serum level of SP-D compared to mice that do not have tumours and the size of the tumour correlates with SP-D level (Lin *et al.*, 2007;Zhang *et al.*, 2003). The enhanced SP-D level is present whether the lung cancer is induced chemically or genetically or conditionally regulated mutant *k-ras* induced tumours. Type II cells which surround the tumour also have an elevated level of SP-D expression however the cause for this is unknown. It is suggested that the enhanced SP-D secretion from the tumour cells within the lung trigger a response by the surrounding type II cells too also enhance SP-D production. After the SP-D is secreted by lung tumours into the extracellular space it is assumed that the collectin will reach the systemic circulation through lymphatic drainage (Zhang *et al.*, 2003).

Gene expression of the SP-D is also present in mammary, prostatic, colonic, gastric and pancreatic carcinomas obtained from lymph node metastatic non-pulmonary adenocarcinoma (Table 1.5.) (Betz *et al.*, 1995). The expression of SP-D was revealed in prostate adenocarcinomas through positive immunostaining for malignant prostate (Fig 1.6.).

Table 1.5. Expression of SP-D in extrapulmonary cancers

SP-D expression in extrapulmonary tumours
Location
Breast
Colon
Lymph node
Pancreas
Prostate
Stomach

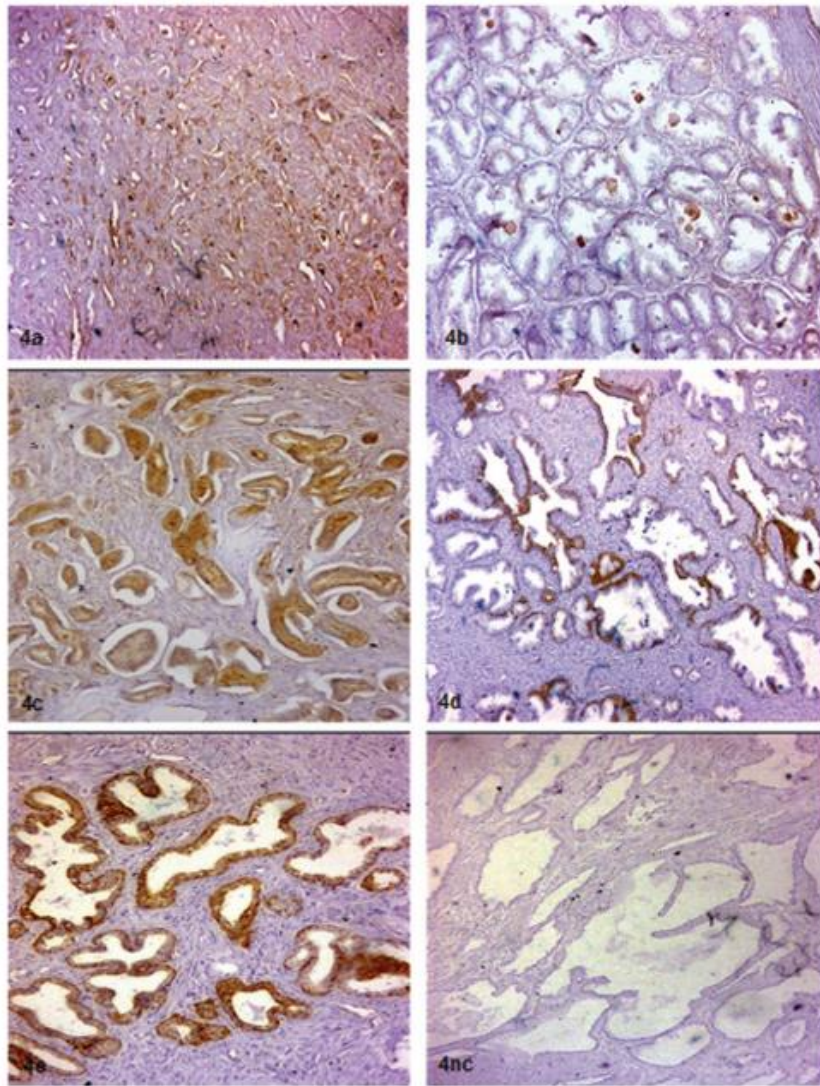


Fig 1.6. Immuno-histochemical staining of malignant and non-malignant prostate cells. 4a, 4c= prostate adenocarcinoma; 4b, 4d, 4e= non-malignant prostate tissue; 4nc= negative control staining (Kankavi *et al.*, 2014) .

There is a greater concentration of SP-D at the inflammatory sites of non-malignant prostate tissue with an immunoreactivity of 91% for SP-D and 82% in malignant prostate. Kankavi et al, suggested that the decreased expression in malignant prostate may be due to the malignant transformation of cells which may impair their capacity to produce SP-D. The reduced SP-D expression in prostate adenocarcinoma can influence the progression of the tumour. Interestingly high grade prostatic intraepithelial neoplasia had strong SP-D staining (Kankavi *et al.*, 2014).

1.18. Microglia

Microglia are the main immune cells of the brain and are the resident macrophage located within the brain parenchyma behind the BBB. They are mononuclear cells derived from monocytic lineage and originate in the bone marrow. Within the adult brain these cells are slowly turned over and replenished by proliferation and constitute between 5%-20% of total glia cells in the brain (Benveniste, 1997;Greter, Lelios and Croxford, 2015;Pivneva, 2008;Saijo and Glass, 2011). In the healthy brain microglia are described as resting and adopt a ramified morphology in which they function as supportive glial cells. In response to brain injury or pathogen invasion microglia are activated and their cellular processes undergo contraction. The organ specific macrophage is transformed into a amoeboid morphology to render the cell competent to elicit an innate immune response or tissue repair (Saijo and Glass, 2011). They serve as the first line of defence and function similarly to tissue macrophage in other organs and migrate towards the site of injury. Prolonged microglia activation has the ability to sustain chronic inflammation of the brain and can lead to neuronal dysfunction and cell death through the release of toxic reactive oxygen species (ROS) (Rock *et al.*, 2004).

1.18.1. Microglia function

Microglia are stimulated by macrophage colony stimulating factor (M-CSF) and granulocyte M-CSF (GM-CSF). M-CSF deficient mice that experience injury or pathogen infiltration do not have normal microglia proliferation and have a down

regulated complement response. In the developing brain microglia phagocytose cells undergoing apoptosis whereas in the adult brain, the phagocytic function is downregulated in resting ramified microglia (Fischer and Reichmann, 2001; Santambrogio *et al.*, 2001). Upon activation by pathological endogenous signals such as neuronal dysfunction or exogenous infection the phagocytic function is upregulated and microglia respond appropriately. The cells acquire the ability to undergo proliferation, migration towards the affected site, phagocytosis and generate ROS (Pivneva, 2008). They also enhance innate immune cell surface receptors including pattern recognition and complement as well as the secretion of pro-inflammatory cytokines such as TNF- α and IL-6 and IL-12. The expression of pro-inflammatory cytokines is one of the main defence mechanisms implemented by microglia. They also express the cytokine receptors and can react or be activated by the pro-inflammatory cytokines thus extending the inflammatory response (Lawson, Perry and Gordon, 1992; Lee, Nagai and Kim, 2002)

1.18.2. Microglia in GBM

GBM is the most common and deadliest primary intracranial brain tumour characterised by a high degree of microglia and macrophage infiltration. The Glioma infiltrating macrophages (GIM) comprise up to 40% of the total GBM tumour mass (Gabrusiewicz *et al.*, 2011). The origin of GIM are mainly resident microglia, and can also contain monocyte derived from circulating blood if the integrity of the BBB has been compromised. Recent evidence has revealed that these innate immune cells have a potent pro-tumour function in GBM (Watters, Schartner and Badie, 2005). GIM contribute to the mediation of GBM growth and infiltration into normal brain as they acquire the ability to enhance tumour proliferation, survival and immune-suppression (Tran Thang *et al.*, 2010). The recruitment of GIM is induced by a variety of factors including GBM secreted cytokines such as TGF- β which is known to promote tumour growth. The ability of the infiltrating resident macrophage to mediate GBM invasion is unique as other endogenous cells such as oligodendrocytes and endothelial cells do not influence GBM motility (Markovic *et al.*, 2009; Coniglio and Segall, 2013).

1.19. Aims

GBM is the most aggressive primary brain tumour and is resistant to current treatment. This report describes studies aimed at understanding the involvement of the innate immune proteins factor H and SP-D in GBM. The main aims are to:

- To analyse the functional activity of CFHR5 derived from primary GBM cells including; inhibiting activation of the alternative pathway; acting as a co-factor for factor I mediated cleavage of C3b; accelerating the decay of C3 convertase.
- To investigate the effects of rhSP-D on U87 cells to reduce cell viability through inducing apoptosis, and altering tumour suppressor and cytokine gene expression.
- To study the expression of SP-D in GBM.
- To investigate the effects of a co-culture with THP-1 and U87

2: Chapter 2- Materials and Methods

2.1. Purification of factor H

50 mL of filtered normal human serum (TCS biosciences) was dialysed overnight against wash buffer I (25 mM Tris (sigma-Aldrich) pH 7.5, 140 mM sodium chloride (NaCl) (sigma-Aldrich), 0.5 mM ethylenediaminetetraacetic acid (EDTA) (sigma-Aldrich) with a magnetic stir bar on a stirrer at 4 °C. A CnBr-activated sepharose column coupled with anti-factor H antibody (MRC immuno-chemistry unit, Oxford) was equilibrated to room temperature for 15 min.

The column was washed with distilled water and wash buffer I. The serum was passed through the column which was then washed to remove impurities. Factor H elution buffer (3 M magnesium chloride ($MgCl_2$) (sigma-Aldrich), 25 mM Tris pH 8.0, 140 mM NaCl, 0.5 mM EDTA) was added to the column and the protein was collected in 1 mL fractions then neutralised with 1 M Tris pH 7.5. A spectrophotometer was used to measure the absorbance (A) 280 and the fractions of a similar reading were dialysed together overnight against 1 L of distilled water and then against dialysis buffer I (10 mM monopotassium phosphate (KH_2PO_4) (sigma-Aldrich), 140 mM NaCl, 0.5 mM EDTA, pH 7.5) for 4 h. The concentration was measured using a nanodrop.

2.2. Nanodrop

A nanodrop spectrophotometer was used to measure the concentration of purified Factor H. 3 μ L of distilled water was pipetted onto the bottom pedestal of the nanodrop. The upper pedestal was lowered onto the bottom pedestal and left to rest for 1 min. The water was wiped away with dry lint free lab wipe to ensure both pedestals were clean. 1 μ L of factor H elution buffer was pipetted onto the bottom pedestal. The arm was then closed and the solution was used as a blank to calibrate the nanodrop. The solution was removed with a lab wipe and cleaned with 1 μ L of distilled water. 1 μ L from each 1 mL factor H aliquot was pipetted onto the lower pedestal and the arm was lowered. The absorbance was measured at A280 and the

concentration was measured in $\mu\text{L}/\text{mL}$. After each reading the upper and lower pedestals were cleaned with 1 μL of water and a lab wipe.

2.3. Preparation of 12% polyacrylamide gel

Table 2.1.- Composition for preparing 12% resolving gel

Components	Volume (μL)
Distilled water	1600
30% Acrylamide (sigma-Aldrich)	2000
1.5 M Tris (pH 8.8)	1300
10% SDS	50
10% ammonium persulphate (APS) (sigma-Aldrich)	50
tetramethylethylenediamine (TEMED) (sigma-Aldrich)	10

Table 2.2.- Composition for preparing 5% of stacking gel

Components	Volume (μL)
Distilled water	1400
30% acrylamide	330
1.0 M Tris-HCL (pH 6.8)	250
10% SDS	20
10% APS	20
TEMED	5

A 12% poly-acrylamide gel was prepared using the components in Table 2.1. and 2.2. Two glass plates were placed into a casting frame and transferred onto a casting stand. The resolving solution using the components in Table 2.1 was prepared. TEMED and APS were added last to catalyse the acrylamide polymerisation. The solution was

pipetted in-between the glass plates and left to polymerise for 10 min at room temperature. After this period the stacking solution in Table 2.2 was prepared and TEMED and APS were added last. The solution was pipetted on top of the resolving gel and a gel comb was inserted and left for 10 min for the gel to polymerise. The plates were then transferred into an electrophoresis chamber and placed into a gel tank which was then filled with 1X running buffer (2.5 mM Tris, 19.2 mM glycine (sigma-Aldrich), 0.01% SDS) and the gel comb was then removed.

2.4. SDS polyacrylamide gel electrophoresis (SDS-PAGE) of cellular components

200 µg/mL of factor H was added in a 1:1 ratio with 2X sample buffer (sigma-Aldrich) and placed on a heating block at 100 °C. It was denatured for 10 min and vortexed for 10 s to mix the sample. Protein marker (thermo-scientific) and denatured factor H were loaded onto the gel and separated according to size by electrophoresis for 90 min at 120 V. The gel was removed from the apparatus and stained with coomassie blue stain solution (0.1% coomassie blue (sigma-Aldrich), 10% acetic acid (sigma-Aldrich), 20% methanol (sigma-Aldrich)) over night at room temperature. The following day the staining solution was removed and the gel was de-stained with de-stain solution (10% acetic acid, 20% methanol) for 3 h to allow the bands to be visualised. An image was taken of the gel with a Bio-Rad imager.

2.5. Western blot of factor H– Bio-Rad transblot

A 12% gel was composed using the components in table 2.1 and 2.2. 200 µg/mL of factor H in a 1:1 ratio with 2X sample buffer was heated to 100 °C and an SDS-PAGE was run to separate the protein according to size. The gel was placed onto a premade turbo sandwich containing filter paper and nitrocellulose membrane soaked in buffer (Bio-Rad). Bubbles between the membrane and gel were removed with a blot roller. The stack was placed onto the transfer cassette (Bio-Rad) and the transfer was run for 7 min at 25 V. Nitrocellulose membrane was blocked overnight with 2% bovine serum albumin (BSA) (sigma-Aldrich) at 4 °C to enable the agent to bind to all the unoccupied

sites on the membrane to prevent antibody non-specific binding. The following day the membrane was washed in 1X PBS with 0.05% tween-20 (sigma-Aldrich).

Primary monoclonal anti-human, mouse, anti-factor H (MRCOX23) antibody (MRC immune-chemistry unit, Oxford) in a 1:1000 ratio with 1X PBS was added to the membrane as the antibody is able to recognise epitopes on factor H. The membrane was incubated for 1 h at room temperature on a shaker to allow the antibody to bind. The membrane was washed to prevent background and remove unbound antibodies. It was then probed with the secondary antibody anti-mouse, rabbit immunoglobulin G- horse radish peroxidase (IgG-HRP) (sigma-Aldrich) in a 1:1000 ratio with 1X PBS for 1 h at room temperature on a shaker. The membrane was washed and 3,3'-diaminobenzidine (DAB) (sigma-Aldrich) was added for 5 min as the substrate is able to bind to the enzyme HRP and form an insoluble brown product where the protein is positioned. An image was taken with a Bio-Rad imager.

2.6. Cell culture for primary GBM cells

Ethical approval was obtained from Brunel University and John Radcliffe hospital. All patients consented to obtaining GBM cells during surgical resection.

Primary GBM cells B30, B31, B33 (John Radcliffe hospital), were grown in Dulbecco's modified eagle medium-F12 (DMEM/F12) (thermo-fisher life technologies), supplemented with 10% v/v heat inactivated fetal bovine serum (FBS) (thermo-fisher life technologies) v/v and 1% penicillin streptomycin (thermo-fisher life technologies).

The cells were placed into a 75 cm³ culture flask (nunc) and incubated for 48 h in a humidified 5% carbon dioxide (CO₂) atmosphere at 37 °C. The media was discarded and the cells were washed with 1X PBS. 3 mL of 1X trypsin- EDTA (thermo-fisher life technologies) was added to the flask and incubated for 2 min at 37 °C with 5% CO₂ to dissociate the adherent cells from the flask. 1X PBS was added to neutralise the cells and the entire content was centrifuged at 2000 revolutions per minute (rpm) for 5 min and the pellet was re-suspended in 1 mL of DMEM/F12.

2.7. Extraction of cellular components

Removal of supernatant

0.2 x10⁶ B30, B31 and B33 passage (P) 2 cells were re-suspended in 1 mL of DMEM-F12 with 1% penicillin streptomycin in replicates. The cells were dispensed into 12 well plates (nunc) and incubated for 48 h at 37 °C with 5% CO₂. After this period the supernatant was centrifuged for 5 min at 10,000 rpm to remove any cells in suspension. The pellet was discarded and the supernatant was stored at 4 °C.

Total cell extract

The wells were washed with 1X PBS and 250 µL of 1X trypsin-EDTA was added to the adherent cells. The plate was placed into the incubator for 3 min under normal growth conditions and 1X PBS was added to the wells to neutralise the effect. The cells were then centrifuged for 5 min at 10,000 rpm and the pellet was re-suspended in 500 µL of lysis buffer I (150 mM Tris Ph 7.5, 150 mM NaCl, 1 mM EDTA, 1% Triton x-100 (sigma-Aldrich), 0.1 SDS, 1% sodium deoxycholate (sigma-Aldrich), 1 mM phenylmethylsulfonyl fluoride (PMSF) (sigma-Aldrich)) to lyse the cell and release the intracellular content.

Membrane fraction

Replicates of the total cell extract were placed on ice for 25 min with regular vortexing every 5 min for 10 s. The cells were then centrifuged at 10,000 rpm for 20 min. The pellet was discarded and the supernatant containing the membrane was stored at 4 °C. An SDS-PAGE was run with the supernatant, membrane fraction and total cell extract of primary GBM cells.

2.8. Dot Blot for factor H

10 μ L of B30 P2, B31 P2, B33 P2 supernatant, membrane fraction, total cell extract, 200 μ g/mL of purified full length factor H (positive control) and 10 μ L of 2% BSA (negative control) was added to nitrocellulose membrane (thermo-fisher scientific). The samples were incubated at room temperature for 30 min and were blocked with 2% BSA on a shaker for 45 min at room temperature. The membrane was washed with 1X PBS-0.05% tween20. A 1:1000 ratio of primary antibody mouse anti-factor H with 1X PBS was added to the nitrocellulose membrane and incubated at room temperature for 45 min on a shaker. The membrane was then washed and probed with the antibody rabbit IgG-HRP and 1X PBS (1:1000) for 45 min at room temperature. The nitrocellulose membrane was washed again and the colour was developed with DAB.

2.9. Purification of factor H in primary GBM

2 X10⁶ B30 P3, B31 P3, B33 P3, and B30 P30 cells were grown in 75 cm³ culture flask in serum free DMEM/F12 until the cells were 80% confluent. The growth media was centrifuged for 5 min at 2000 rpm to remove cells in suspension. The pellets were discarded and the supernatants were dialysed overnight against wash buffer I and then passed through the CnBr activated sepharose column coupled to anti-factor H antibody. The column was washed and the protein was eluted and dialysed overnight against distilled water followed by dialysis buffer. The concentration was measured with a nanodrop.

A 12% acrylamide gel was run with 50 μ g/mL of eluted protein and 200 μ g/mL of factor H in 1 X running buffer. A dot blot was then performed using the primary antibody anti-factor H and secondary antibody IgG-HRP with 45 min incubation period. The colour was then developed with DAB.

2.10. Western blot of primary GBM for factor H

A 12% SDS-PAGE was prepared using the components in table 2.1 and 2.2. 200 µg/mL of factor H, 5 µL of supernatant and 15 µL of membrane fraction from primary GBM cells were added in a 1:1 ratio with 2X sample buffer and denatured at 100 °C for 10 min. The samples were vortexed and loaded into the wells of the gel along with 5 µL of protein marker. The gel was run at 120 V with 1X running buffer for 90 min.

Once the run was complete the gel was placed in 1X transfer buffer (25 mM Tris, 190 mM glycine (sigma-Aldrich), pH 8.3) with 2 fibre pads, 6 pieces of whatman filter paper (thermo fisher scientific), and a nitrocellulose membrane for 5 min to ensure the gel was equilibrated by the removal of contaminating electrophoresis buffer salts. A transfer sandwich was assembled with whatman filter paper, fibre pads, nitrocellulose membrane and the gel. Air bubbles were removed with a blot roller to allow efficient transfer to take place. The sandwich was fastened into a western blot cassette and transferred into an electrode assembly chamber. An ice pack and the assembly chamber were placed into a gel tank and filled with 1X transfer buffer and left to run at 70 V for 2 h at 4 °C to mitigate the heat produced.

After this period the nitrocellulose membrane was blocked overnight with 2% BSA at 4 °C on a shaker. The blocking agent was discarded and the membrane was rinsed in 1X PBS with 0.05% tween20. Primary anti-factor H antibody in a 1:1000 ratio with 1X PBS was added to the membrane for 1 h at room temperature on a shaker and was then washed. The secondary antibody IgG-HRP with 1X PBS in a 1:1000 ratio was incubated with the nitrocellulose membrane on a shaker at room temperature for 1 h. The membrane was then washed and the bands were visualised by the addition of DAB.

2.11. Enzyme linked immunosorbent assay (ELISA) for factor H

0.2 X10⁶ B30 P3, B31 P3, and B33 P3 cells were re-suspended in 1 mL of serum free DMEM/F12 in a 12 well plate, which was then incubated in a humidified 5% CO₂ atmosphere at 37 °C. At 6 h, 12 h, 24 h, and 48 h, 100 µL of the growth medium was centrifuged for 5 min at 10,000 rpm. The pellet was discarded and the supernatant was added to 100 µL 50 mM carbonate bi-carbonate buffer (CBC) (Ph 9.6) (sigma-Aldrich) in a microtiter plate (nunc). 100 µL of CBC buffer was added to separate wells in replicates. 20 µg/100 µL of human factor H was added to the first well and underwent a 2 fold serial dilution with the neighbouring wells which contained CBC buffer creating a serial dilution from 10 µg/100 µL to 0.075 µg/100 µL. The microtiter plate was incubated overnight at 4 °C to immobilise the protein to the well in the presence of CBC.

The following morning the samples were decanted and the wells were washed with 1X PBS-0.05% tween 20. 2% BSA was added to each well and the plate was incubated for 2 h at 37 °C. The blocking solution was removed and the wells were washed thoroughly. Primary anti-factor H antibody was added to each well in a 1.5000 ratio with 1X PBS for 1 h at 37 °C. The antibody was removed and the wells were washed. The wells were then probed with secondary antibody IgG-HRP with 1X PBS in a 1.5000 ratio for 1 h at 37 °C. After this period the wells were washed and the colour was developed with o-Phenylenediamine (OPD) (sigma-Aldrich) in the dark. The plate was then placed into a microtiter plate reader and the A450 was measured.

A linear graph was then plotted of the absorbance reading against the concentration of human factor H was then used to calculate the concentration of protein secreted from GBM cells. An unpaired T-test statistical analysis was performed with the 6 h time point against 12 h, 24 h, and 48 h.

2.12. Alternative pathway assay

10⁹ rabbit blood cells

2 mL of rabbit red blood cells in alsevers (tcs bioscience) was washed with 1X PBS with 55 mM EDTA. The samples were centrifuged for 5 min at 2000 rpm (4°C). The supernatant was then removed and the pellet was re-suspended and washed with DGVB buffer ((2.1 mM sodium barbital (sigma-Aldrich), 59 mM NaCl, 0.08% gelatine (sigma-Aldrich) ,7 mM MgCL₂, 10 mM ethylene glycol tetraacetic acid (EGTA) (sigma-Aldrich)) and centrifuged for 5 min at 2000 rpm. The pellet was re-suspended in 4 mL of DGVB buffer and 100 µl was added to 1.4 mL of distilled water. The A541 was measured until a value of 0.7 was obtained which is equivalent to, 10⁹cells/mL.

AH50

100 µL of DGVB buffer was added to wells in replicates on a microtiter plate. 40 µL of normal human serum with 160 µL of DGVB buffer was added to a separate well. The serum underwent a 2 fold serial dilution with the neighbouring wells that contained 100 µL of DGVB buffer. The plate was incubated for 1 h at 37°C followed by the addition of 100 µL of 10⁹ rabbit blood cells to each well. 100 µL of 10⁹ rabbit blood cells and 100 µL of distilled water were added to a separate well for 100% lysis and 200 µL of distilled water was added to a different well for 0% lysis. The plate was incubated for 1 h at 37°C and then centrifuged for 5 min at 2000 rpm. 150 µL of supernatant was transferred to a new microtiter plate and the A541 was measured. The percentage of haemolysis was calculated using the formula; $(\text{measured OD}) - (\text{OD } 0\% \text{ lysis}) / (\text{OD } 100\% \text{ lysis}) - (\text{OD } 0\% \text{ lysis}) * 100$. A graph was plotted and the serial dilution at which 50% haemolysis (AH50) occurred was noted.

Factor H depleted serum

The same serum used to calculate the AH50 was passed through the factor H column. The flow through of factor H depleted serum was stored at 4 °C. A dot blot of factor H

deficient serum, factor H (positive control) and 2% BSA (negative control) was performed with primary anti-factor H antibody and secondary IgG-HRP antibody.

Alternative pathway assay for purified factor H related protein

100 μL DGVB buffer was added in replicates to wells on a microtiter plate. 200 $\mu\text{g}/\text{mL}$ of purified protein from B30 P3, B31 P3, and B33 P3 were added to wells with 40 μL of AH50 factor H deficient serum. DGVB buffer was added to a total volume of 200 μL . A 2X fold serial dilution of the purified protein was carried out with the neighbouring cells that contained 100 μL DGVB buffer. The samples were incubated for 1 hour at 37 $^{\circ}\text{C}$. After this period 100 μL of 10^9 rabbit blood was added to each sample; 100 μL of 10^9 rabbit blood cells and 100 μL of distilled water were added to a separate well for 100% lysis; and 200 μL of distilled water was added to a separate well for 0% lysis. The microtiter plate was returned to the 37 $^{\circ}\text{C}$ incubator for 1 h and then centrifuged for 5 min at 2000 rpm. 150 μL of supernatant was removed and transferred from each well to a new microtiter plate. The A541 was measured with an ELISA plate reader and the percentage of haemolysis was calculated using the formula; $(\text{measured OD}) - (\text{OD } 0\% \text{ lysis}) / (\text{OD } 100\% \text{ lysis}) - (\text{OD } 0\% \text{ lysis}) * 100$. A graph was then produced.

2.13. Co-factor assay

200 and 100 $\mu\text{g}/\text{mL}$ of purified protein from B30, B31, B33, factor H (positive control) and 0 $\mu\text{g}/\text{mL}$ of factor H (negative control) were incubated with 3 μg of C3b (comp tech), 500 ng of factor I (comp tech), 10 mM sodium phosphate (pH 7.2) (sigma-Aldrich), and 1X PBS to a final volume of 30 μL . The samples were incubated at 37 $^{\circ}\text{C}$ for 30 min and were then heated for 15 min at 60 $^{\circ}\text{C}$. The samples were separated under reduced conditions through SDS-PAGE. The bands were stained overnight in staining solution and were then de-stained for 4 h with de-staining solution. An image was taken with a Bio-Rad imager of the gel.

2.14. Decay acceleration assay

A microtiter plate was coated with 250 ng of C3b in replicates and immobilised in a 96 well plate in 50 mM CBC buffer (pH 9.6) overnight at 4 °C. The wells were then washed with 1X PBS. 400 ng of factor B (comp tech), 25 ng of factor D (comp tech), 2 mM of nickel chloride (sigma-Aldrich) and 4% BSA were added to each well for 2 h at 37 °C for the formation of nickel chloride stabilised C3 convertase. The wells were then washed with 1X PBS. 0, 10, 50, 100, 150, 200 µg/mL of factor H and CFHR5 were added to each well. The plate was incubated for 30 min at 37 °C. After the incubation period the plate was washed and, goat polyclonal antibody to human factor B (comp-tech) with 1X PBS (1:2000) was added to detect intact C3 convertase complexes. The plate was incubated for 1 h at 37 °C and was then washed extensively. Anti-goat IgG-HRP (comp-tech) with 1X PBS (1:2000) was added to each well and incubated for 1 h at 37 °C. The wells were then washed and OPD was added for 5 min in the dark. The A450 was measured with an ELISA plate reader, and a graph was produced.

2.15. RT-qPCR of B30

Cell preparation

0.5 X10⁶ B30 P3 cells were re-suspended in 2 mL of serum free media, in replicates and placed into a 6 well plate at 37 °C with 5% CO₂. At each time point of 1 h, 6 h, 12 h, 24 h and 48 h. The wells were washed with 1X PBS and 500 µL of 1% trypsin-EDTA was added to the adherent cells and incubated for 2 min at 37 °C with 5% CO₂. The cells were transferred to room temperature conditions and 1.5 mL of 1X PBS was added to the cells in suspension and centrifuged for 5 min at 10,000 rpm. The supernatant was decanted and the pellet was stored at -80 °C.

RNA extraction

An RNA extraction kit (sigma-Aldrich) was used to extract RNA from B30 cells. 10 μ L of β -mercaptoethanol (β -ME) was added to the ready-made lysis solution (10 μ L β -ME/1 mL lysis solution). The pelleted cells were lysed with 250 μ L of lysis solution and vortexed for 10 s. 250 μ L of 70% ethanol (sigma-Aldrich) was added to the lysate and the entire content was transferred to a binding column. The samples were centrifuged at 13,000 rpm for 15 s and the flow through was discarded. 500 μ L of ready-made wash solution I was added to the column and centrifuged for 15 s at 13,000 rpm. The column was transferred to a new collection tube and 500 μ L of wash solution II was added. The sample was centrifuged for 15 s at 13,000 rpm and the flow through was discarded. 500 μ L of wash solution II was added and centrifuged for 2 min at 13,000 rpm. The flow through was discarded and a dry spin took place for 1 min. The column was transferred to a new collection tube and 50 μ L of ready-made elution buffer was added. The sample was centrifuged for 1 min at 13,000 rpm and the eluted RNA was stored at 4 °C.

DNase treatment

To prevent DNA contamination of RNA sample a DNase kit (qiagen) was used. 5 μ L of 10X reaction buffer and 5 μ L of DNase 1 enzyme were added to the eluted RNA and incubated for 15 min at room temperature. 5 μ L of stop solution was added and the samples were incubated at 70 °C for 10 min. The concentration (ng/ μ L) and purity 260/280 of RNA were measured using nanodrop. A reading of the ratio at ~2.0 was accepted as pure RNA.

cDNA synthesis

A high capacity RNA- cDNA kit (thermo-fisher scientific) was used to synthesise cDNA from the eluted RNA. 10 μ L of 2X RT buffer and 1 μ L of 20X RT enzyme mix were added to 9 μ L of RNA. The samples were transferred into a PCR machine to commence the

reverse transcription reaction. The mixtures were incubated at 37 °C for 60 min and the reaction was then stopped automatically by the change in temperature to 95 °C for 5 min. The cDNA formed was stored at 4 °C.

qPCR

A master mix for each gene to be detected was formed which included 5 µL of power SYBR green master mix (thermo-fisher scientific), 75 nM of forward primer (Dr Tsolaki, Brunel University), 75 nM of reverse primer (Dr Tsolaki, Brunel University), and 100 ng of B30 cDNA template of 1 h, 6 h, 12 h, 24 h or 48 h. The following forward and reverse primers were used (Table 2.3.)

Table 2.3. Table of primers used for B30 RT-qPCR

<u>Primer</u>	<u>Forward primer sequence</u> <u>(5'-3')</u>	<u>Reverse primer sequence</u> <u>(5'-3')</u>
18S	ATGGCCGTTCTTAGTTGGTG	CGCTGAGCCAGTCAGTGTAG
TNF-α	AGCCCATGTTGTAGCAAACC	TGAGGTACAGGCCCTCTGAT
TGF-β	GTACCTGAACCCGTGTTGCT	GTATCGCCAGGAATTGTTGC
IL-6	GAAAGCAGCAAAGAGGCACT	TTTACCAGGCAAGTCTCCT
IL-12	AACTTGCAGCTGAAGCCATT	GACCTGAACGCAGAATGTCA

1 µL of cDNA were pipetted into separate wells in replicates on a 96 well Micro Amp plate. 9 µL of master mix in Table 2.3. were also added to the same wells at each time point. The plate was sealed and centrifuged for 2 min at 2000 rpm to eliminate air bubbles. The plate was then placed into the qPCR machine to undergo 40 cycles at which the samples were heated to 95 °C to break double stranded DNA into single strands, 55 °C to allow annealing of primers to single stranded DNA template, and 72

°C for the formation of cDNA. During the process the wells were illuminated and SYBR green that had bound to newly formed double stranded DNA were excited at 497 nm and emitted fluorescence at 520 nm. Once enough amplicons had been produced the fluorescent signal rose above the baseline and crossed the threshold during the exponential phase.

Data analysis

Data was analysed by relative quantification (RQ) which is the fold change between the sample and calibrator. The following equations below were used:

$$\Delta Ct = Ct (\text{gene of interest}) - Ct (\text{housekeeping gene})$$

$$\Delta\Delta Ct = \Delta Ct (\text{sample}) - \Delta Ct (\text{calibrator})$$

$$\text{Relative quantity (RQ)} = 2^{-\Delta\Delta Ct}$$

Data was represented in log₁₀ scale as qPCR results are highly skewed in the linear phase. The statistical analysis unpaired T-test was carried out to deduce the significance of the results.

2.16. Competent cells

A single colony of *Escherichia coli* (*E.coli*) BL21 (λDE3) pLysS was inoculated in 5 mL of nutrient rich Luria Broth (LB) (10 g tryptone (sigma-Aldrich), 5 g yeast extract (sigma-Aldrich), 10 g NaCl, pH 7.5) to maintain bacterial growth. 5 µL of chloramphenicol (34 µg/mL, dissolved in ethanol) was also added in a 1:1000 ratio of LB as this *E.coli* strain is resistant to this antibiotic. A single colony was also inoculated without chloramphenicol as a control. The cells were grown overnight in a 37 °C shaking incubator. 500 µL of the overnight culture was added to 30 mL of LB and 30 µL of chloramphenicol (1:1000) to ensure only the desired *E.coli* pLysS strain would grow. The cells were grown until an A₆₀₀ of 0.3- 0.4 which is when the *E.coli* cells are in the early log phase and are at their optimum state to produce protein. The culture was then centrifuged at 3,500 rpm for 10 min and the supernatant was discarded. 12 mL of ice cold 0.1 M calcium chloride (CaCl₂) (sigma-Aldrich) was added to the pellet and the

cells were placed on ice for 1 h. After this period the cells were centrifuged at 3,500 rpm for 10 min and the supernatant was removed. The pellet was re-suspended in 2 mL of 0.1 M CaCl₂ to improve the competence of the cells as the positively charged calcium ions, is able to neutralise the effect of the negatively charged outer membrane.

2.17. Transformation of cells

1 µL of plasmid pUK-D1 containing cDNA for the 8 gly-x-y collagen domain, α-helical neck region and CRD of SP-D (Dr Kishore, Brunel University, Singh *et al.*, 2003).was added to 100 µL of competent cells which contained CaCl₂ to enable the negatively charged plasmid DNA and competent cells to get into close proximity. The cells were left on ice for 1 h to decrease the temperature. Afterwards, the cells underwent heat shock as they were suddenly placed into a 42 °C water bath for 90 s to enable the plasmid DNA to pass into the cell. Immediately after, the cells were placed on ice for 5 min. 800 µL of LB was added to the cells and incubated at 37 °C for 45 min to allow the cells to recover. After incubation, the cells were streaked onto LB agar (LB, 15g/L agar) petri dishes one of which contained ampicillin (100 µL/mL) as the plasmid is resistant to this antibiotic and chloramphenicol in a 1.1000 ratio. The cells were grown overnight at 37 °C and the LB agar plate was stored at 4 °C the following morning.

2.18. Pilot scale protein expression of rhSP-D

A single colony of transformed competent cells was inoculated and grown in 5 mL LB, in a 1.1000 ratio with ampicillin and chloramphenicol overnight within a shaking incubator at 37 °C. Cells from the overnight culture were streaked onto LB agar petri dishes which contained ampicillin and chloramphenicol in a 1.1000 ratio. The petri dishes were incubated overnight at 37 °C. 500 µL of overnight culture were added to 10 mL of LB with ampicillin and chloramphenicol (1.1000). The cells were placed in a 37 °C shaking incubator and were grown for approximately 3 h until the cells were in log phase represented by A600 0.6- 0.8. This is when the number of cells continue to double at a constant rate every 20 min. Once the required absorbance was reached 1

mL of the cells were transferred to a separate culture tube and left in the 37 °C shaking incubator for 3 h to represent an uninduced control to observe expression efficiency. The remaining cells were induced with 0.5 mM isopropyl-1-thio- β -D-galactopyranoside (IPTG) (sigma-Aldrich) for 3 h at 37 °C. 1 mL of induced and uninduced samples were centrifuged for 2 min at 13,000 rpm. The supernatant was decanted and the pellets were re-suspended in 100 μ L of 2X sample buffer.

A 12% acrylamide gel was composed with the components in Table 2.1. and 2.2. The induced and un-induced samples were denatured at 100 °C for 10 min and were then loaded into the wells of the gel. The SDS-PAGE was run with 1X running buffer for 90 min at 120 V. The gel was stained overnight and de-stained the following morning for 3 h. An image was then taken with a Bio-Rad imager to visualise the induced band at 20 kDa.

2.19. Large scale protein expression of rhSP-D

A single colony from the pilot scale expression was inoculated in 30 mL of LB supplemented with ampicillin and chloramphenicol (1.1000), in a 37 °C shaking incubator overnight. 25 mL of overnight culture was added to 500 mL of LB (ampicillin and chloramphenicol 1.1000) until A600 0.6- 0.8 was reached which indicate that the cells were in log phase which is when the number of cells increase exponentially. After this period 1 mL of the cells were transferred to a separate culture tube and left in the 37 °C shaking incubator for 3 h to be used as an un-induced control. The remaining cells were induced with 0.5 mM (IPTG) for 3 h in the 37 °C shaking incubator. 1 mL of induced and uninduced cells were centrifuged for 2 min at 13,000 rpm and the pellets were re-suspended in 100 μ L of 2X sample buffer.

The samples were denatured for 10 min at 100 °C and were then briefly vortexed before loaded onto an acrylamide gel. An SDS-PAGE was run for 90 min at 120 V. The gel was stained overnight and destined the following morning to observe if the protein had been expressed at 20 kDa. The remaining cells were harvested by centrifugation

at 10,000 rpm for 10 min and the pellet containing insoluble inclusion bodies were stored at -20 °C.

2.20. Cell lysis and sonication of inclusion bodies

The cell pellet containing inclusion bodies was re-suspended in lysis buffer (50 mM Tris pH7.5, 200 mM NaCl, 5 mM EDTA, 0.1% v/v Triton X-100, 0.1 mM PMSF) to agitate the cells and rupture the cell membrane. A magnetic stir bar was added to the cells and left spinning on a magnetic stirrer at 4 °C for 1h. The cells were placed on ice and had 10 cycle of sonication, in which sound waves of ultrasonic frequencies >20 kHz was applied for 30 s with 2 min interval periods to further disrupt the cell membrane and release cellular content. The cells were then centrifuged for 30 min at 10,000 rpm after which the supernatant was discarded and the pellet was stored at -20 °C.

2.21. Dialysis to refold rhSP-D

The rhSP-D was recovered in an inactive state in inclusion bodies within the pellet. 50 mL of buffer I (50 mM Tris-HCl pH7.5, 100 mM NaCl, 5 mM EDTA, 6 M urea and 10 mM β -ME) which contained the denaturants urea and β -ME was added to solubilise the sample as part of the process to obtain active rhSP-D. A magnetic stir bar was added to the cells and left spinning on a magnetic stirrer at 4 °C for 1h. The resolubilised material was dialysed against buffer I containing 4 M urea, followed by 2 M urea, then 1 M urea at 2 hour intervals to slowly decrease the concentration of the solubilisation agent buffer I to allow the protein to refold optimally. Buffer I with no urea was dialysed against the dialysate overnight to remove urea. The following day the dialysate was dialysed against affinity calcium buffer (50 mM Tris pH7.5, 100 mM NaCl, 5 mM CaCl_2 , 0.05% sodium azide) for 4 h to remove EDTA and calcify the protein in preparation for affinity chromatography. The dialysate was centrifuged at 10,000 rpm for 15 min and the supernatant was stored at 4 °C.

2.22. Purification of rhSP-D

The refolded rhSP-D was purified via affinity chromatography containing a maltose agarose matrix within a column. The maltose-agarose column was washed with distilled water and affinity calcium buffer (50 mM Tris pH7.5, 100 mM NaCl, 5 mM CaCl₂, 0.05% sodium azide) to remove any contaminants and equilibrate the column. The dialysate was passed through the maltose agarose column as rh-SPD is able to bind to carbohydrates such as maltose in the presence of calcium. The column was then washed with 1 M salt buffer (50 mM Tris pH7.5, 1 M NaCl, 5 mM CaCl₂, sodium azide 0.01%) to remove impurities such as non-specific complexes. 30 mL of affinity calcium buffer (50 mM Tris-HCL, 100 mM NaCl, 5 mM CaCl₂, 0.05% sodium azide) was then passed through the column to remove the salt.

The bound protein was then eluted with SP-D elution buffer (50 mM Tris pH 7.5, 100 mM NaCl, 5 mM EDTA, 10 mM β-ME) and collected in 1 mL fractions. The protein A280 and concentration in µg/mL was measured on a nanodrop and stored at -20 °C. 15 µL from each 1 mL fraction was added to 2X sample buffer in a 1.1 ratio. The samples were heated to 100 °C for 10 min and an SDS-PAGE was run to deduce if purified rhSP-D at 20 kDa had been obtained. The gel was stained and de-stained to visualise the band of purified rhSP-D.

2.23. Lipopolysaccharide removal

During pilot and large scale, endotoxin is released from the outer membrane of *E.coli* and contaminates the recombinant protein. A Pierce high capacity endotoxin removal column (thermo-fisher scientific) was used to remove endotoxins from rhSP-D which are able to elicit endotoxin shock, tissue injury, death in host organisms and interfere in cell culture techniques. The column contained resin with porous cellular beads attached to ε-poly-L-lysine which has a high affinity for lipopolysaccharide (LPS) as it has a binding capacity of 2 million EU/ mL and is capable of removing up to 99% of endotoxin. Use of the column was followed as instructed by the manufacturer's

guidelines. The column was equilibrated at room temperature and then placed into a collection tube. It was centrifuged for 1 min at 2000 rpm and the storage solution was removed.

To regenerate the column 0.2 N sodium hydroxide in 95% ethanol was added and the resin was suspended in the solution. The column was incubated at room temperature for 2 h on a shaker. The column was placed into a collection tube and centrifuged for 1 min at 2000 rpm. The solution was discarded and 2 M NaCl was added to the column then removed via centrifugation at 2000 rpm for 1 min into a collection tube. Endotoxin free ultra-pure water was added to the column which was then placed within a collection tube; centrifuged for 1 min at 2000 rpm and the solution was then discarded. This step was repeated 3 times. Purified rhSP-D was added to the column and incubated for 1 h at 4 °C on a shaker. The column was placed within a new collection tube and centrifuged for 1 min at 2000 rpm. The protein was collected and stored at -20 °C.

2.24. Endotoxin quantitation

The Pierce limulus amoebocyte lysate (LAL) Chromogenic Endotoxin Quantitation Kit (thermo-fisher scientific) was used to detect gram negative bacterial endotoxin within purified rhSP-D. Firstly, the endotoxin standard stock solutions were prepared in sterile endotoxin free Eppendorf tubes. A 1.0 EU/mL endotoxin standard solution was prepared using the equation $[(X-1)/20]$ mL of endotoxin-free water where X represents the endotoxin concentration on the vial. Therefore 50 μ L of endotoxin stock was added to 1.25 mL of endotoxin free water to obtain the stock concentration of 1.0 EU/mL. The solution was vortexed for 1 min and 250 μ L was removed and added to 250 μ L of endotoxin free water to form 0.5 EU/mL. 250 μ L of 1.0 EU/mL stock was transferred to 750 μ L of endotoxin free water within to form 0.25 EU/mL stock. 100 μ L of 1.0 EU/mL was then added to 900 μ L of endotoxin free water to form 0.1 EU/mL.

1.4 mL of endotoxin free water was added to a LAL reagent composed of the pro-enzymes lyophilised lysate from amebocytes of a horse shoe crab that are catalysed by bacterial endotoxins. The lyophilised LAL was stored on ice in the dark. A vial containing 7 mg of lyophilized chromogenic substrate was then reconstituted with 6.5 mL of endotoxin free water to yield a concentration of 2 mM. In the presence of endotoxin, the colourless chromogenic substrate is cleaved and a yellow chromophore p-Nitroaniline (pNA) is released.

A 96 well microtiter plate was equilibrated on a heating block at 37 °C for 10 min. 50 µL of rhSP-D, endotoxin free water, and stock solutions of 1.0, 0.5, 0.25 and 0.1 EU/ mL were added in replicates to separate wells on the plate and then covered with a lid. The plate was incubated at 37 °C for 5 min, followed by the addition of 50 µL of reconstituted LAL to each sample to enable any endotoxin present to catalyse the pro-enzyme. The plate was placed on a shaker for 10 s and then incubated for 10 min at 37 °C. 100 µL of substrate solution was pipetted into each well at a regular speed in the same order that the LAL was added. The plate was transferred onto a shaker for 10 s and then incubated at 37 °C for 6 min. 50 µL of stop reagent (25 % acetic acid) was added to each well and the plate was placed on a shaker for 10 s. The absorbance at 450 nm was measured on a spectrophotometer plate reader and the values obtained for endotoxin free water was subtracted from rhSP-D and endotoxin stock absorbance readings. A standard curve was plotted as the absorbance is directionally proportional to the endotoxin level and can therefore be used to determine the concentration of endotoxin. The coefficient of determination (r^2) was also calculated to establish the accuracy of the regression curve. Endotoxin free rhSP-D was then divided into 1 mL aliquots and stored at -20 ° C. The concentration of each aliquot was then measured on a nanodrop.

2.25. Western blot for rhSP-D

A 12% SDS-PAGE was prepared using the components in table 2.1 and 2.2. The polymerised gel was placed into an electrophoresis cassette and then transferred into a gel tank, filled with 1 X running buffer. 200 µg/mL of rhSP-D and 2% BSA (negative control) were added to 2X sample buffer in a 1:1 ratio. The samples were placed onto a 100 °C heating block for 10 min. The samples were vortexed for a 10 s and loaded into the wells of the gel along with 5 µL of protein marker. The gel was run in an electrophoresis tank for 90 min at 120 V. Once the run was complete the gel was placed in 1X transfer buffer with fibre pads, whatman filter paper, and nitrocellulose membrane for 5 min. The sandwich was placed into the gel tank and the transfer took place for 2 h at 4 °C.

After this period the nitrocellulose membrane was blocked overnight with 2% BSA at 4 °C. The blocking agent was discarded and the membrane was rinsed in 1X PBS-0.05% tween20. Primary polyclonal anti-human, rabbit anti-SPD antibody (Dr Kishore, Brunel University Singh *et al.*, 2003), in 1:1000 ratio with 1X PBS was added to the nitrocellulose membrane as the antibody is able to recognise epitopes on SP-D. The membrane and antibody were incubated for 1 h at room temperature on a shaker. The membrane was washed with 1X PBS-0.05% tween-20.

Staphylococcus (S).aureus Protein A (PA) -HRP (sigma-Aldrich) antibody with 1X (1:1000) was incubated with the nitrocellulose membrane on a shaker at room temperature for 1 h to bind to the primary antibody. The membrane was then washed. To visualise the protein band, DAB was added to the membrane for 5 min and an Image was taken with a Bio-Rad imager.

2.26. Cell culture for U87 cells

U87 cells (Sappo Meri, Haartman Institute, Helsinki) are grown in DMEM/F12 with 10% FCS and 1% penicillin streptomycin at 37 °C in 5% CO₂. The adherent cells are dissociated from the flask with 1X trypsin-EDTA and were washed with 1X PBS.

2.27. The binding of rhSP-D to U87 cells

0.1 X10⁶ U87 cells were re-suspended in 500 µL of serum free media and placed in replicates onto coverslips in a 24 well plate. The cells were incubated overnight at 37 °C with 5% CO₂. The media was removed and the cells were washed with 1X PBS. 4% para-formaldehyde (sigma-Aldrich) was added to the cells and fixed for 10 min at room temperature to immobilise cellular structures to prevent the degeneration process in order to preserve the cell in a life like state.

The cells were then washed thoroughly with 1X PBS and 0, 5, 10 and 15 µg/mL of rhSP-D were then added to separate wells in replicates. 5 mM CaCl₂ was added to each well as rhSP-D binds to carbohydrates in a calcium dependent manner. The plate was incubated for 2 h at 4 °C on a shaker to allow the protein to bind to U87 cells without becoming internalised. The wells were washed thoroughly with 1X PBS to remove any unbound rhSP-D. 2% BSA was added to each well at room temperature for 1 h to block the remaining surfaces to prevent non-specific binding.

A 1:1000 dilution of primary anti-SP-D antibody with 1X PBS was added to each well to allow the antibody to bind rhSP-D. 1X PBS alone was added to the control replicates. The plate was then incubated at room temperature for 1 h and was then washed with 1X PBS to remove unbound antibodies. A 1:500 dilution of the secondary conjugate antibody PA- Fluorescein isothiocyanate (FITC) (sigma-Aldrich) with 1X PBS was added to all the cells for 1 h at room temperature in the dark.

The cells were then washed with 1X PBS and 1:1000 dilution of the fluorescent nuclear stain 4',6-Diamidino-2-phenylindole dihydrochloride (DAPI) (sigma-Aldrich) with 1X PBS (1:1000) was added to each well at room temperature for 10 min in the dark to allow the stain to bind to double stranded DNA. The cover slips were washed with 1X PBS to remove excess unbound stains and were then mounted onto microscope slides. One drop of antifade (sigma-Aldrich) was added to each cover slip to prevent photobleaching and preserve fluorescent signals. A new cover slip was placed on top and the results were analysed using a Leica fluorescent microscope at 40X magnification to detect the blue nucleic stain DAPI and the green fluorescent signals emitted by the conjugate FITC. 100 cells were counted and the number of cells labelled with FITC was recorded and this was repeated 10X to calculate the percentage of bound protein.

2.28. Apoptosis assay

0.1×10^6 U87 cells were resuspended in 1 mL of serum free media. The cells were incubated with 0, 10, 15, or 20 $\mu\text{g}/\text{mL}$ of rhSP-D and 5 mM CaCl_2 for 2 h at 4 °C to allow the protein to bind to the membrane. The cells were centrifuged for 5 min at 10,000 rpm to remove unbound rhSP-D. The pellet was re-suspended in 1 mL of serum free media and dispensed onto cover slips for 6, 12, 24 and 48 h at 37 °C with 5% CO_2 .

An apoptosis assay was carried out with an annexin V-FITC apoptosis detection kit (sigma-Aldrich) to observe apoptosis induced by membrane bound rhSP-D. 1 μL of ready-made 10 X binding buffer stock solution (100 mM HEPES/sodium hydroxide, 1.4 M sodium chloride, 25 mM CaCl_2 , pH 7.5) was added to 1 mL of distilled water and vortexed for 10 s to form 1 X binding solution of which 200 μL was added to each well. 5 μL of annexin V FITC (50 $\mu\text{g}/\text{mL}$) was added to each well to allow the protein conjugate to label phosphatidylserine sites on the membrane surface of U87 cells. 10 μL of propidium iodide (100 $\mu\text{g}/\text{mL}$) which was used to label necrotic cells and 10 μL of the nucleic stain DAPI in 1X PBS (1:1000) were both added to all the cells. The plate was then incubated at room temperature, for 10 min in the dark to allow binding to

take place. The cover slips were washed with 1X PBS to remove any unbound stains and were then placed onto microscope slides. 1 drop of antifade was added to each cover slip to prevent photobleaching of the fluorescent dyes. A new cover slip was placed over the cells and the results were analysed immediately with a Leica fluorescent microscope to detect any fluorescent signals present at 40X magnification.

2.29. Analysis of cell viability

0.25×10^6 U87 cells were counted and re-suspended in 1 mL of serum free media. The cells were dispensed into a 12 well plate and were incubated for 24 h at 37 °C with 5 % CO₂. The following day the cells were washed with 1X PBS and 0, 10, 15, or 20 µg/mL of rhSP-D were added in replicates to the cells with 5 mM CaCl₂. The wells at different concentrations of rhSP-D were incubated for 6 h, 12 h, and 24 h.

At each time point the cells were washed with 1X PBS and dissociated with 1X trypsin-EDTA was added for 2 min at 37 °C with 5 % CO₂. The cells were centrifuged for 5 min at 10,000 rpm and the pellet was re-suspended in 1 mL of serum free media. 30 µL of re-suspended cells were mixed with trypan blue in a 1:1 ratio and vortexed for 10 s. The mixture was pipetted onto a haemocytometer and viewed under a microscope at 10X magnification. The total number of cells and total number of cells stained blue per 4X4 quadrant were counted with a microscope. The formula ((viable cell number/total cell)X100) was used to calculate the percentage of death caused by the addition of rhSP-D.

2.30. Agglutination

0.1×10^6 U87 cells were re-suspended in 1 mL DMEM-F12 including 1% penicillin streptomycin and 5 mM of CaCl₂. 0, 10, or 15 µg/mL of rhSP-D was added to the re-suspended cells at 4 °C for 2 h on a shaker to allow rhSP-D to bind. The cells were then centrifuged for 5 min at 10,000 rpm and the pellet was re-suspended in 1 mL of serum free media. The cells were transferred onto a cover slip within a 24 well plate for 24 h

at 37 °C with 5% CO₂. 1X PBS was then used to wash the cells. 500 µL of 4% para-formaldehyde was added to each well for 10 min at room temperature. The cells were washed thoroughly with 1X PBS and the cover slip was placed onto a slide. A drop of anti-fade was added and a new cover slip was placed on top. A Leica microscope was used to take a phase contrast image of the cells at 10X magnification.

2.31. RT-qPCR for U87 and rhSP-D

Cell preparation

0.5 X10⁶ U87 cells were re-suspended in 2 mL of DMEM-F12 and 1% penicillin streptomycin in replicates with 0 or 20 µg/mL of rhSP-D and 5 mM CaCl₂. The cells were incubated for 2 h at 4°C to allow rhSP-D to bind and were then centrifuged at 10,000 rpm for 5 min. The supernatant was discarded and each pellet was re-suspended in 2 mL of serum free media. The cells were transferred into a 6 well plate at 37 °C with 5% CO₂. At each time point of 1 h, 6 h, 12 h, 24 h and 48 h the supernatant was discarded and the cells were washed with 1X PBS. 500 µL of 1X trypsin-EDTA was added to the adherent cells and incubated for 2 min under normal growth conditions. The cells were transferred to room temperature conditions and 1.5 mL of 1X PBS was added to the cells in suspension. The cells were centrifuged for 5 min at 10,000 rpm and the pellet was stored at -80 °C.

RT-qPCR

RNA was extracted from the cells at each time point using an RNA extraction kit in which the cells were lysed and passed through a binding column. The eluted RNA was treated with DNase to remove contaminating DNA. RNA was then converted into cDNA as the sample were heated to 37 °C for 60 min and 95 °C for 5 min to stop the reaction. A master mix for each target gene was composed containing SYBR green, forward primer, reverse primer and cDNA. The following primers were used (Table 2.4.).

Table 2.4. Primers used for RT-qPCR treated and untreated U87

Primer	Forward primer sequence (5'-3')	Reverse primer sequence (5'-3')
18S	ATGGCCGTTCTTAGTTGGTG	CGCTGAGCCAGTCAGTGTAG
TNF-α	AGCCCATGTTGTAGCAAACC	TGAGGTACAGGCCCTCTGAT
P53	AGCACTGTCCAACAACACCA	CTTCAGGTGGCTGGAGTGAG
IL-6	GAAAGCAGCAAAGAGGCACT	TTTCACCAGGCAAGTCTCCT

1 μ L of cDNA from treated and untreated cells were pipetted into separate wells on a 96 well Micro Amp plate in replicates. 9 μ L of master mix P53, TNF- α , IL-6 and 18s RNA were added to the wells at each time point. The plate was then placed into a qPCR machine to undergo 40 cycles at which the samples were heated to 95 $^{\circ}$ C, 55 $^{\circ}$ C and 72 $^{\circ}$ C. A statistical analysis paired T-test were carried out to deduce the significance of the results.

The following equations were used:

$$\Delta\text{Ct} = \text{Ct (gene of interest)} - \text{Ct (housekeeping gene)}$$

$$\Delta\Delta\text{Ct} = \Delta\text{Ct (sample)} - \Delta\text{Ct (calibrator)}$$

$$\text{Relative quantity (RQ)} = 2^{-\Delta\Delta\text{Ct}}$$

2.32. Cell proliferation assay

0.25 $\times 10^6$ U87 cells were counted and re-suspended in serum free media. 0, 10 and 15 μ g/mL of rhSP-D with 5 mM CaCl_2 . The cells were placed on a shaker at 4 $^{\circ}$ C to allow the protein to bind to the cells. After this period the cells were centrifuged for 5 min at 10,000 rpm and the pellet was re-suspended in 1X PBS to wash away un-bound protein. The cells were centrifuged for 5 min at 10,000 rpm and the supernatant was

discarded. The pellet was re-suspended in DMEM-F12 with 1% penicillin streptomycin and dispensed into 6 well plates along with the untreated cells in replicates. The plate was incubated for 48 h at 37 ° C with 5% CO₂.

After 48 h the media was removed and the cells were washed. The cells were dissociated with 1X trypsin-EDTA and centrifuged for 5 min at 10,000 rpm. The supernatant was decanted and the pellet was re-suspended in 1 mL of media. 30 µL of treated and untreated cells were mixed with trypan blue and vortexed for 10 s to ensure the samples were mixed together. A cover slip was placed onto a haemocytometer and the cells were pipetted underneath and viewed under a microscope at 10X magnification. 4 quadrants were counted and the number of cells in each quadrant were added together and divided by 4 to obtain the average cell count. The cells were then divided by 2 which is the dilution factor and then multiplied by 10⁴ in order to calculate the number of cells per mL. The formula used was shown below:

$$\text{Total cells/mL} = ((\text{Total cells counted}/\text{number of quadrants})/\text{dilution factor}) \times 10^4$$

2.33. Western blot for U87 supernatant

Cell preparation

0.25 X10⁶ U87 and B30 cells were re-suspended in 1 mL of DMEM-F12 with 1 % penicillin streptomycin and dispensed into a 12 well plate. The cells were incubated for 48 h at 37 °C with 5% CO₂. The growth media was centrifuged for 5 min at 10,000 rpm to remove non adherent cells that were in suspension. The supernatant was added to 2X sample buffer in a 1.1 ratio and placed onto a heating block at 100 °C for 10 min to denature the protein.

Transfer

A 12 % acrylamide gel was prepared using the components in table 2.1 and 2.2. The samples were denatured for 10 min, vortexed for 10 s, and loaded onto the wells of the gel along with 5 μ L of protein marker and a negative control of 2% BSA. The gel was run in an electrophoresis tank for 2h at 120V in 1X running buffer. After the cells, had been separated on the gel according to their size, the gel and western blot materials were soaked in 1X transfer buffer, for 5 min. They were then fastened into a sandwich and placed into an electrode assembly. The tank was filled with 1X transfer buffer and left to run for at 70 V for 2 h at 4 °C.

Blotting

The nitrocellulose membrane was blocked overnight with 2% BSA at 4 °C on a shaker and was then washed in 1X PBS- 0.05% tween20. Primary, rabbit, anti-SP-D antibody and 1X PBS were added in a 1.1000 ratio onto the nitrocellulose membrane and incubated for 1 h at room temperature on a shaker. The membrane was again washed and then incubated with secondary *S.aureus* PA-HRP antibody with 1X PBS in a 1.1000 ratio for 1 h at room temperature on a shaker. The membrane was washed and DAB was added for 5 min. An image was then taken on a Bio-Rad imager.

2.34. ELISA for U87 supernatant

0.25 X10⁶ U87 and B30 cells were re-suspended in 1 mL of DMEM-F12 with 1% penicillin streptomycin and added to a 12 well plate which was then incubated in a humidified 5% CO₂ atmosphere at 37 °C. At 1 h, 6 h, 12 h, 24 h, and 48 h, the growth media was removed and centrifuged for 5 min at 10,000 rpm to separate non-adherent cells from the media. 100 μ L of supernatant was added to 100 μ L of 0.05 M CBC (pH 6.9) in a well of a microtiter plate. 100 μ L of 0.05 M CBC was added to separate wells in replicates. 20 μ g/100 μ L of rhSP-D was added to the first well that contained CBC and was mixed thoroughly. A 2 fold serial dilution took place with the neighbouring

CBC wells creating a serial dilution from 10 µg/100 µL to 0.075 µg/100 µL. The microtiter plate was incubated overnight at 4 °C.

The following morning the samples were decanted and the wells were washed with 1X PBS-0.05% tween-20. 2% BSA was added to each well and incubated for 2 h at 37 °C. The wells were washed and primary antibody, rabbit, anti-human, SP-D with 1X PBS (1.5000) was added to each well for 1 h at 37 °C. After this incubation period the wells were washed and secondary antibody *S.aureus* PA-HRP in 1X PBS (1.5000) was added to each well for 1 h at 37 °C. Washing with 1X PBS-0.05% tween-20 then took place followed by the addition of OPD in the dark for 5 min. The plate was then placed into a microtiter plate reader and the absorbance was read at an OD of 450 nm.

A linear graph was then plotted of the absorbance reading against the concentration of rhSP-D which was then used to calculate the concentration of SP-D secreted from U87 and B30 cells.

2.35. RT-qPCR of U87

Cell preparation

0.5 X10⁶ U87 and B30 cells were re-suspended in 2 mL of DMEM-F12, with 1% penicillin streptomycin and transferred into a 6 well plate in replicates. The plates were incubated at 37 °C with 5% CO₂. At each time point of 1 h, 6 h, 12 h, 24 h, 48 h the supernatant was discarded and the wells were washed with 1X PBS. The cells were dissociated with 1X trypsin EDTA and were centrifuged for 5 min at 10,000 rpm. The supernatant was discarded and the pellet was stored at -80 °C.

qPCR

An RNA extraction kit was used to lyse the pellets and pass the samples through a binding column. The column was washed extensively and RNA was eluted in 50 µL fractions. Contaminating DNA was removed from the eluted RNA using a DNase kit. The RNA was converted into cDNA with an RNA to cDNA conversion kit in which the sample was heated at 37 °C for 1 h and 95 °C for 5 min. A master mix for each gene to be detected was formed using the forward and reverse primers in Table 2.5. (SP-D primer- Dr Sotiriadis, Brunel University)

Table 2.5. Primers used for RT-qPCR U87

<u>Primer</u>	<u>Forward primer sequence</u> <u>(5'-3')</u>	<u>Reverse primer sequence</u> <u>(5'-3')</u>
18S	ATGGCCGTTCTTAGTTGGTG	CGCTGAGCCAGTCAGTGTAG
SPD	AATGGCAAGTGGAAATGACAG	GCACCCCAGTTGGCTCAGAA
TNF-α	AGCCCATGTTGTAGCAAACC	TGAGGTACAGGCCCTCTGAT
IL-6	GAAAGCAGCAAAGAGGCACT	TTTACCAGGCAAGTCTCCT

10 µL of master mix were added to separate wells on a 96 well Micro Amp plate. The plate underwent 40 cycles at which it was heated to 95 °C, 55 °C and 72 °C during qPCR. The comparative C_T method ($\Delta\Delta C_T$) was used for data analysis which involved calculating the ΔC_T and $\Delta\Delta C_T$ value. A statistical analysis unpaired T-test test were carried out to deduce the significance of the results.

The following equations were used:

$$\Delta C_T = C_T (\text{gene of interest}) - C_T (\text{housekeeping gene})$$

$$\Delta\Delta C_T = \Delta C_T (\text{sample}) - \Delta C_T (\text{calibrator})$$

$$\text{Relative quantity (RQ)} = 2^{-\Delta\Delta C_T \#}$$

2.36. Intracellular detection of SP-D in U87 and B30 GBM cells

0.1 X10⁶ U87 and B30 cells were re-suspended in 1 mL of DMEM-F12 with 1% penicillin streptomycin and were cultured on to coverslips in a 24 well plate in replicates. The cells were incubated for 6 h, 12 h, 24 h, and 48 h at 37 °C with 5% CO₂. At each time point the cells were washed with 1X PBS and fixed with 4% paraformaldehyde for 10 min at room temperature. The solution was removed and the cells were washed thoroughly with 1X PBS. 1 mL of 100% methanol was added to each well for 10 min at -20 °C to permeabilise the membrane of the adherent cells to ensure access of the antibody to the antigens. The methanol was removed and the cells were washed with 1X PBS. The cells were fixed with 4 % para-formaldehyde to immobilise the antigens whilst maintaining the authentic cellular structure.

2% BSA was added to each well for 1 h at room temperature and the cells were then washed with 1X PBS. Primary antibody anti-SP-D with 1X PBS (1.1000) and 1X PBS alone (negative control) were both added to the permeabilised cells in replicates. The plates were then incubated at room temperature for 1 h. After this period the wells were washed and *S.aureus* PA-FITC with 1X PBS in a 1.500 ratio was added to all the wells for 1 h at room temperature in the dark. The cells were then washed with 1X PBS and then 1X DAPI was added to each well at room temperature for 10 min in the dark. The cells were washed thoroughly and the cover slips were then mounted onto microscope slides. Anti-fade was added to the cover slips and new coverslips was placed over the adherent cells. The results were analysed using a Leica fluorescent microscope at 20X magnification.

2.37. Cell culture for primary THP-1 cells

THP-1 (Dr Pathan, Brunel University) cells were grown in Roswell Park Memorial Institute (RPMI) (thermo-fisher life technologies), supplemented with 10% v/v heat inactivated FBS v/v and 1% penicillin streptomycin. The cells were placed into a 75 cm³ culture flask and incubated for 48 h with CO₂ at 37 °C. The growth media containing

the cells in suspension were centrifuged at 2000 rpm for 5 min and the pellet was re-suspended in 1 mL of RPMI.

2.38. THP-1 differentiation

0.5×10^6 THP-1 cells were counted and re-suspended in serum free RPMI. The cells were placed into a 6 well plate and 25 ng/mL of phorbol 12-myristate 13-acetate (PMA), or 15 μ g/mL of rhSP-D with 5 mM of CaCl_2 were added to the cells in replicates. Untreated THP-1 cells were included as a negative control and all the cells were incubated for 24 h at 37 °C with 5% CO_2 . The following day the cells in suspension were centrifuged for 5 min at 10,000 rpm. The supernatant was discarded and the pellet was re-suspended in 1 mL and a cell count was taken with a haemocytometer. 1X PBS was added used to wash the cells to ensure all the cells in suspension were removed and an image was taken of the differentiated cells. A sterile cell scarper was then used to remove the adherent cells. 1 mL of 1X PBS were added to the wells and the cells were removed and centrifuged for 5 min at 10,000 rpm. The supernatant was discarded and the pellet was re-suspended in 1 mL of RPMI.

The cells were mixed in a 1:1 ratio with trypan blue and the cell count was taken with a haemocytometer viewed under a microscope with a 10X magnification. The number of cells in 4 quadrants were counted and this was repeated for each sample.

Equation used to calculate cell number: $\text{total cells/mL} = ((\text{Total cells counted}/\text{number of quadrants})/\text{dilution factor}) \times 10^4$.

To calculate the average % of differentiated THP-1 cells into macrophage the following calculation was used: $(\text{adherent cell count}/\text{total well cell count}) \times 100$.

2.39. Dissociation of THP-1 with trypsin-EDTA

0.5 X10⁶ THP-1 cells were re-suspended in 2 mL of RPMI with 1% penicillin streptomycin and were then placed into 6 well plates with 25 ng/mL of PMA. The plates were incubated for 24 h at 37 °C with 5% CO₂ and the following day the wells were washed with 1X PBS. Serum free media was added to the wells and placed back into the same incubator for 24 h to allow the cells to rest. The wells were washed thoroughly and 500 µL of 1X trypsin-EDTA was added for 2 min at 37 °C with 5% CO₂. After this time period 1.5 mL of 1X PBS was added to the wells to neutralise the effect. The solution was centrifuged for 5 min at 10,000 rpm. The supernatant was discarded and the pellet was re-suspended in media. The cells were added to trypan blue and the cell count was taken with a haemocytometer.

2.40. Cytokine gene expression of U87 cells in co-culture with THP-1 cells

Cell preparation

0.5 X10⁶ THP-1 cells were re-suspended in 2 mL of RPMI with 1% penicillin-streptomycin and pipetted into 6 well plates in replicates. 25 ng/mL of PMA was added to each well and the plate was then incubated for 24 h at 37 °C with 5% CO₂. The following morning after the cells had differentiated and adhered to the wells, the media was removed. 1X PBS was used to wash the cells which were then replenished with RPMI for 24 h under normal growth conditions to allow the cells to rest. The following day the media was removed and the cells were washed. 1 X10⁶ U87 cells were counted and 15 µg of rhSP-D and 5 mM of CaCl₂ were added to for 2 h at 4 °C on a shaker to allow the collectin to bind.

After this period the cells were centrifuged for 5 min at 10,000 rpm and the pellet was re-suspended in 1 mL of 1X PBS to remove any unbound protein. The cells were then centrifuged for 5 min at 10,000 rpm and the pellet was re-suspended in 2 mL of DMEM-F12. These cells were then placed into the same well as the THP-1 cells. U87 cells with

no protein bound were also pipetted in replicates into wells with THP-1 cells and wells without THP-1. The cells were placed into an incubator at 37 °C with 5% CO₂ for 1 h, 2 h, and 6 h. At each time point the media was discarded from the wells and the cells were washed to remove any non-adherent cells. 500 µL of 1X trypsin-EDTA was added to the wells for 2 min at 37 °C with 5% CO₂. 1.5 mL of 1X PBS was then added to the wells and the U87 cells in suspension were centrifuged for 5 min at 10,000 rpm after which the supernatant was discarded and the pellet was stored at -80 °C.

RT-qPCR

An RT-qPCR was then carried out on with U87 cells alone, U87 cells in co-culture with THP-1 and rhSP-D bound U87 cells in co-culture with THP-1. The primers in Table 2.6. were used.

Table 2.6. primers for RT-qPCR for co-culture

<u>Primer</u>	<u>Forward primer sequence</u> <u>(5'-3')</u>	<u>Reverse primer sequence</u> <u>(5'-3')</u>
18S	ATGGCCGTTCTTAGTTGGTG	CGCTGAGCCAGTCAGTGTAG
TNF-α	AGCCCATGTTGTAGCAAACC	TGAGGTACAGGCCCTCTGAT
TGF-β	GTACCTGAACCCGTGTTGCT	GTATCGCCAGGAATTGTTGC
IL-6	GAAAGCAGCAAAGAGGCACT	TTTCACCAGGCAAGTCTCCT
IL-12	AACTTGCAGCTGAAGCCATT	GACCTGAACGCAGAATGTCA

The comparative C_T method ($\Delta\Delta C_T$) was used for data analysis which involved calculating the ΔC_T and $\Delta\Delta C_T$ value. A statistical analysis unpaired T-test and paired T-test were carried out to deduce the significance of the results.

The following equations were used:

$\Delta Ct = Ct(\text{gene of interest}) - Ct(\text{housekeeping gene})$

$\Delta\Delta Ct = \Delta Ct(\text{sample}) - \Delta Ct(\text{calibrator})$

Relative quantity (RQ) = $2^{-\Delta\Delta Ct}$

2.41. Live imaging

0.5×10^6 THP-1 cells were counted and re-suspended in 2 mL of RPMI with 1% penicillin streptomycin and placed into 6 well plates in replicates. 25 ng/mL of PMA was added to each well for 24 h and the plates were incubated at 37 °C with 5% CO₂. The following day the wells were washed with 1X PBS and 2 mL of RPMI with 1% penicillin streptomycin for 24 h. The media was then discarded and the wells were washed with 1X PBS. 1×10^6 U87 cells were counted and 15 µg/mL of rhSP-D and 5 mM CaCl₂ were added for 2 h on a shaker at 4 °C. After this incubation period the cells were centrifuged for 5 min at 10,000 rpm and the pellet was resuspended in 1 mL of 1X PBS to remove to remove any unbound protein. The samples were again centrifuged for 5 min at 10,000 rpm and the pellets was re-suspended in 2 mL of serum free media. 1 µM of deep red dye (sigma Aldrich) in anhydrous dimethyl sulfoxide (DMSO) (sigma-Aldrich) was added to the rhSP-D bound and unbound U87 cells. The cells were incubated for 45 min at 37 °C with 5% CO₂ and was then centrifuged for 5 min at 10,000 rpm. The pellet was washed with 1X PBS to remove excess dye. The cells were centrifuged for 5 min at 10,000 rpm and the pellet was re-suspended in serum free DMEM-F12.

rhSP-D bound and unbound U87 cells were added to separate wells with differentiated THP-1 cells in a 2:1 ratio. The co-culture was observed for 6h on a live imaging microscope, Carl Zeiss Axiovert 200M microscope (Zeiss) whilst the cells were incubated at 37 °C with 5% CO₂. An image was taken every 10 min to analyse cell movement at 20X magnification. The stained U87 cells were excited at 630 nm and emitted fluorescence at 660 nm. The images were viewed as a merged image of phase contrast and cy5.

2.42. Proliferation assay of U87 in co-culture

0.1 X10⁶ THP-1 cells were placed in a 12 well plate with 25 ng/mL of PMA for 24 h at 37 °C with 5% CO₂ to activate the cells. The next day the media was removed and the cells were washed. 1 mL of RPMI was added to the wells and left for 24h under normal growth conditions. The cells were then washed with 1X PBS. 0.2 X10⁶ U87 cells were counted and 15 µg/ml of rhSP-D was added. The cells were incubated for 2 h at 4°C to allow rhSP-D to bind to the membrane of the cell. After this time period U87 were centrifuged for 5 min at 10,000 rpm to remove unbound protein. The cells were then washed by re-suspending the pellet in 1 mL of 1X PBS and the cells were centrifuged under the same conditions. rhSP-D bound U87 pellets were re-suspended in serum free media and dispensed into the same well as differentiated THP-1 in replicates. U87 cells without bound rhSP-D were placed in replicates into separate wells and wells with THP-1.

The co-cultures and U87 cells alone were left to grow for 6 h, 12 h, 24 h and 48 h. At each time point the wells were washed. The cells were dissociated with 1X trypsin-EDTA and were then centrifuged for 5 min at 10,000 rpm to remove trypsin-EDTA from the cells. The pellets were then re-suspended in media and a cell count was taken. The number of cells in 4 quadrants were recorded and a formula was used to calculate the average number of cells per mL; $\text{Total cells/mL} = ((\text{Total cells counted}/\text{number of quadrants})/\text{dilution factor}) \times 10^4$. A 2-tailed paired T-test was then carried out in Prism between the paired observation of U87 alone and U87 from co-culture and rhSP-D U87 from co-culture.

2.43. ELISA for co-culture

1 mL of 0.1×10^6 THP-1 cells were added to a 12 well plate and 25 ng/mL of PMA were added to each well to differentiate the cells. The plate was incubated for 24 h at 37 °C with a humidified 5% CO₂ atmosphere. The following day the media was discarded and the wells were washed and replenished with 1 mL of RPMI with 1% penicillin streptomycin and left to rest for 24 h at 37 °C with 5% CO₂. After this period, the cells were washed and 0.2×10^6 U87 cells were counted then placed in replicates with THP-1 to form a co-culture. The 12 well plate was transferred to the incubator for 6 h, 12 h, 24 h, and 48 h. At each time point the growth media was centrifuged for 5 min at 10,000 rpm to separate non-adherent cells from the growth media. The supernatant was stored at 4 °C.

An ELISA was carried out with the supernatant obtained from the co-culture and U87 cells grown alone for 6 h, 12, 24 h, and 48 h. A 2 fold serial dilution was carried out for factor H and rhSP-D. All samples were incubated overnight in a microtiter plate with CBC at 4 °C. The following day the wells were blocked with 2 % BSA and then probed with primary antibodies anti-factor H and anti-SP-D in a 1:5000 ratio of 1X PBS for 1 h at 37 °C. The wells were washed and probed with secondary antibodies IgG-HRP and PA-HRP. OPD was added and the A450 was measured with an ELISA plate reader. A calibration curve was formed with the 2 fold serial dilution absorbance readings and were then used to measure the concentration of protein.

The statistical analysis 2 tailed paired t-test in prism was used to analyse the significance of protein concentration between U87 and co-culture.

2.44 Statistical analysis

Paired and unpaired T-test, with error bars for standard deviation using Prism software.

Chapter 3: Purification of CFHR5 and its functional activity

3.1. Abstract

There are earlier reports that suggest that GBM cell lines secrete factor H, as a strategy to dampen the complement activation. Factor H-mediated resistance to complement attack is considered to work to the advantage of the GBM. We investigated this aspect by using primary GBM cells derived from GBM patients' post-surgery. Three primary cells, designated B30, B31 and B33, appear to secrete a related protein to factor H termed CFHR5. GBM cell-secreted CFHR5 was recognised by the monoclonal antibody MRCOX23 which is originally raised against human factor H. We also show that GBM CFHR5 is biologically active, as evident from its ability to inhibit the alternative pathway *in vitro*. Furthermore, we found that GBM CFHR5 had co-factor activity for factor I mediated cleavage of C3b. It also demonstrated its ability of decay acceleration on C3 convertase. qPCR analysis of the GBM primary cells revealed that their pro-inflammatory cytokine response peaked at 48 h. Thus, the ability of primary GBM cells to dampen complement activation via CFHR5 secretion, together with creating a pro-inflammatory milieu in the GBM microenvironment, highlights two of the important mechanisms that contribute towards GBM aggression and invasion.

3.2. Objectives

It has previously been reported that H2 GBM cells are resistant to complement mediated killing as they express factor H, whereas U251 cells do not (Junnikkala *et al.*, 2000). We hypothesised that primary GBM cells derived direct from patients would produce functionally active factor H. The main objectives of this study were:

- To purify factor H from normal human serum and primary GBM cells.
- To assess if purified factor H was functionally active.
- To detect the presence of factor H in different cellular components of primary GBM cells.
- To investigate the mechanisms used by factor H to elicit its functional activity.
- To study the expression of cytokines in primary GBM.

3.3 Results

3.3.1. Factor H purified from normal human serum

The purification process of passing normal human serum through a CnBr-activated sepharose column which was coupled to anti factor H antibody (MRCOX23) was successful in producing full length factor H to be used as a positive control in subsequent experiments. The eluted fractions yielded a recovery of 10 mg in 10 mL of factor H. The purity and molecular weight of factor H was analysed with SDS-PAGE under reduced conditions (Fig 3.1.A). A band was observed at 150 kDa which corresponds to the known molecular weight of full length factor H. There were no other bands present which indicated that there were no impurities. The identity of the band was confirmed by western blotting using anti-factor H and IgG-HRP monoclonal antibodies, as a brown precipitate at 150 kDa was present (Fig 3.1.B).

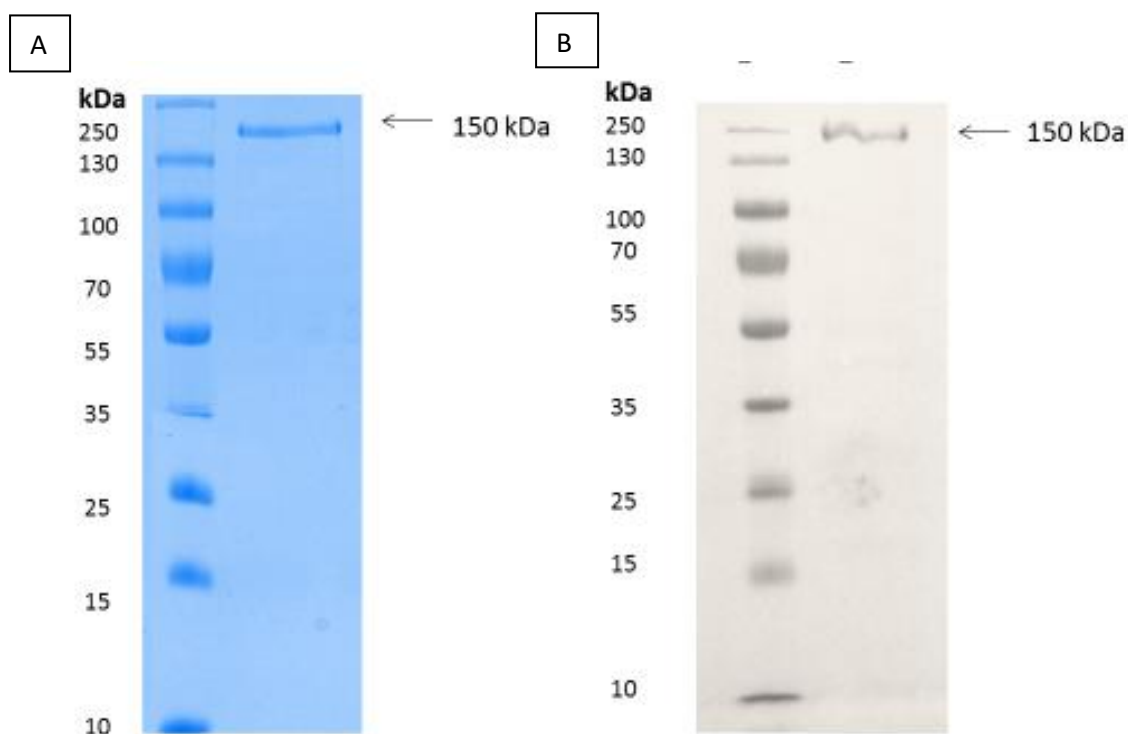


Fig 3.1. Purification of full length factor H from normal human serum. Normal human serum was dialysed over night against wash buffer I. The serum was then passed through a CnBr activated sepharose column coupled to anti-factor H antibody. The protein was eluted and neutralised by Tris pH 7.5. Factor H fractions were dialysed

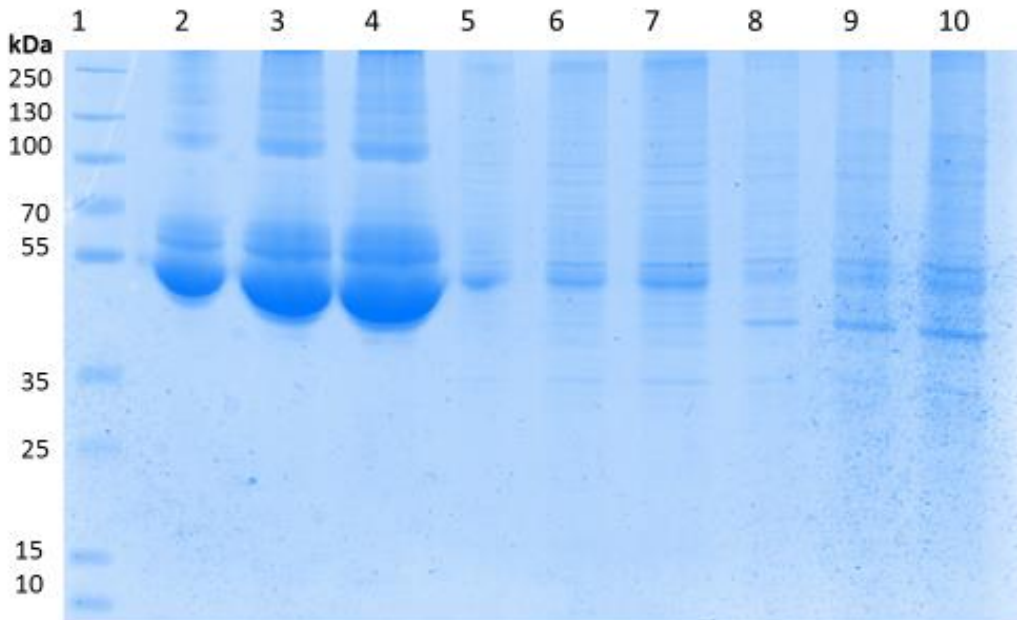
against distilled water and dialysis buffer I. The purity of the eluted protein was analysed by SDS-PAGE (A). The detection was confirmed by western blot with antibodies anti-factor H (1.1000) and IgG-HRP (1.1000) and the band was visualised with DAB (B). (Lane 1. Protein marker, 2. Factor H).

3.3.2. Factor H family protein is present in B30, B31 and B33

To detect the presence of factor H family protein in primary GBM supernatant, membrane and total cell extract, a preliminary dot blot procedure was carried out. B30, B31 and B33 P2 cells were grown for 48 h at 37 °C with 5% CO₂. The supernatants were stored at 4 °C and the adherent cells were trypsinised and pelleted down. To obtain total cell extract the pellets were resuspended in lysis buffer I. This was followed by incubation on ice and high speed centrifugation to obtain the cell membrane in the supernatant. An SDS-PAGE was run to visualise the separation of the samples on a gel (Fig 3.2.A). Membrane fraction was successful as there was a clear difference between the bands for membrane (Lane 5-7) and total cell extract, which had a prominent band at 40 KDa which is not present for membrane fraction (Lane 8-10). It is clear that B30 cells secreted a higher concentration of protein into the supernatant as the bands are thicker (Lane 3) than B31 (Lane 2) and B33 (Lane 1) despite the same number of cells incubated.

Immunoblotting with primary antibody anti-factor H and secondary antibody IgG-HRP, had shown primary GBM cells B30, B31, and B33 contained a factor H family protein in the cytoplasm and on the cell membrane. It also revealed that the protein was secreted into the supernatant as a brown insoluble precipitate had formed. Semi quantitative analysis revealed that the total cell extract in B30 (Fig 3.2.B, lane 3) had an intense DAB staining greater than membrane fraction and supernatant as the concentration of the protein was highest within the cell. The intensity of B30 cell extract staining, was also greater than the factor H control of 200 µg/ mL. The membrane fraction and supernatant from B30 as well as all cellular components and supernatant from B31 and B33 had very similar intensities of brown stain which was less than the factor H control.

A



B

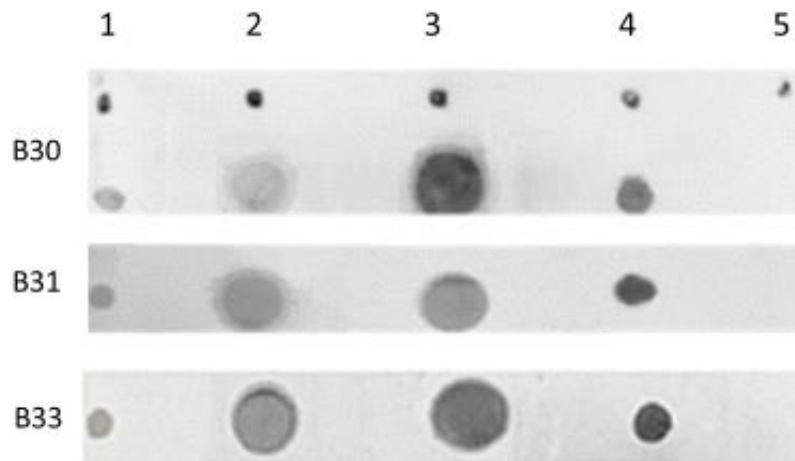


Fig 3.2. SDS-PAGE and dot blot of primary B30, B31 and B33 supernatant, total cell extract and membrane fraction. 0.2×10^6 B30, B31 and B33 P2 cells were grown for 48 h at 37 °C with 5% CO₂. The supernatant was removed and the adherent cells were dissociated. The cells were lysed with lysis buffer I to obtain total cell extract. Membrane fraction was employed to isolate the membrane, by lysing the cells with lysis buffer I, incubating the cells on ice for 20 min, and high speed centrifugation for

20 min at 10,000 rpm. A) SDS-PAGE of the supernatant, membrane fraction and total cell extract of B30, B31 and B33 P2, (Lane 1. protein marker, 2. B33 supernatant, 3. B31 supernatant, 4. B30 supernatant, 5. B33 membrane fraction, 6. B31 membrane fraction, 7. B30 membrane fraction, 8. B33 total cell extract, 9. B31 total cell extract, 10. B30 total cell extract. B) Dot blot of the presence of factor H in different cellular components and supernatant in B30, B31 and B33. The primary antibody anti-human, mouse, anti-factor H and secondary antibody anti-mouse, rabbit, IgG-HRP were used to detect the presence of the protein. (Lane 1. supernatant, 2. membrane fraction, 3. total cell extract, 4. human factor H (positive control) 5. 2% BSA (negative control))

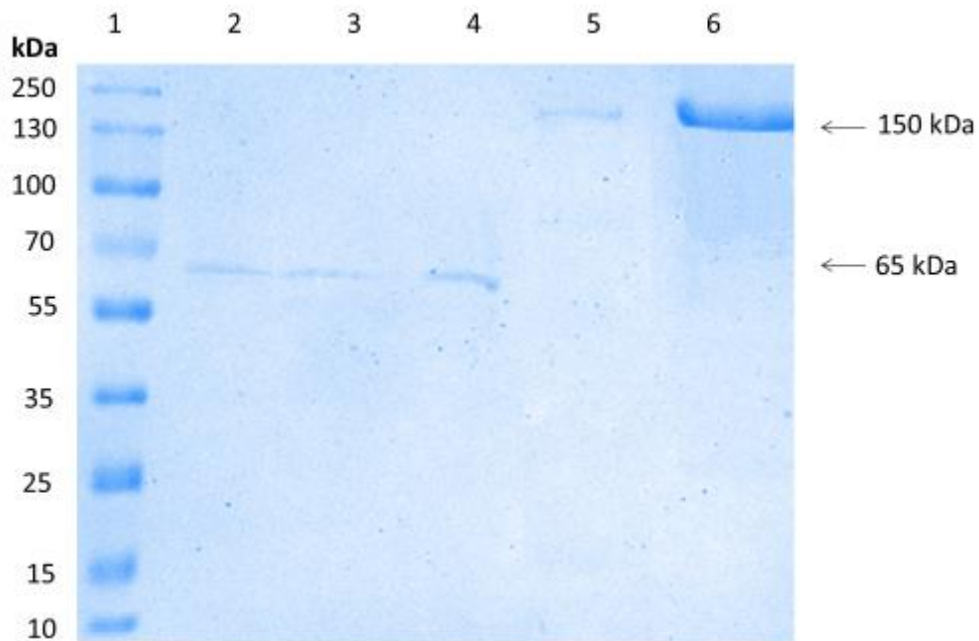
3.3.3. CFHR5 is present in B30, B31 and B33

In order to purify factor H from GBM cells the supernatant of primary GBM B30, B31 and B33 P3 and cell line B30 P30 were stored after the cells were 80% confluent. The supernatant from each cell was passed separately through a CnBr-activated sepharose column coupled to anti-factor H antibody (MRCOX23). The eluted fractions were collected, the concentration of the protein was measured using nanodrop and the purity and size of the eluted samples was assessed by a reduced SDS-PAGE.

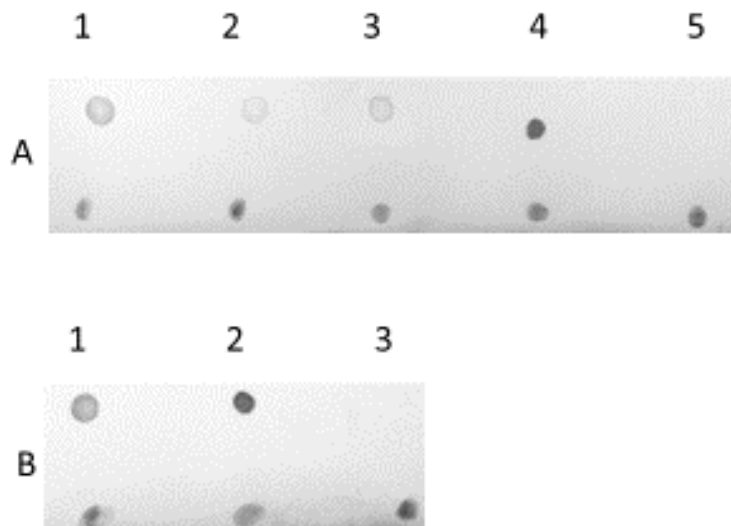
A protein yield of 8 mL of 4 mg for B30 P3, 8 mL of 3 mg for B31 P3, 8 mL of 3 mg for B33 P3, and 8 ml of 4 mg for B30 P30 was obtained. A band at 65 kDa was present on the gel for primary GBM cells, which corresponds for CFHR5 (Fig 3.3.A) No higher or lower bands were present, indicating that there were no impurities or other factor H family proteins eluted. B30 P30 cell produced a band at 150 kDa corresponding to full length factor H, with no other bands observed.

Having demonstrated after factor H purification, bands at 65 kDa for primary GBM and 150 kDa for B30 cell line, a preliminary dot blot procedure was carried out to confirm the presence of CFHR5 and factor H. Immunoblotting with primary anti-factor H antibody and secondary IgG-HRP antibody, produced insoluble brown precipitates after treatment with DAB confirming that the proteins eluted were from the factor H family (Fig 3.3.B) The precipitate intensities of staining for GBM purified proteins were less intense than the factor H control of 200 µg/mL.

A



B



3.3. Purification of CFHR5 from primary GBM. The supernatant from B30, B31, B33 P3, and B30 P30 was dialysed against wash buffer I overnight. The dialysate was passed through the CnBr activated sepharose column coupled to anti-factor H antibody. The bound protein was eluted and dialysed against distilled water over night and dialysis buffer I for 4 h. A) A reduced SDS-PAGE was run for the purified protein. (Lane 1.

protein marker, 2. CFHR5 B30, 3. CFHR5 B31, 4. CRHR5 B33, 5. factor H B30, 6. factor H). B) Dot blot analysis of purified factor H family protein. 10 μ L of purified protein from B30 P3, B31 P3, B33 P3 and B30 P30, were pipetted onto nitrocellulose membrane. Proteins of the factor H family were detected with primary anti-factor H and secondary IgG-HRP antibodies. The colour was developed with DAB. Full length factor H served as a positive control and 2% BSA as a negative control (A= Lane 1. B30 P3 CFHR5, 2. B31 P3 CFHR5, 3. B33 P3 CFHR5, 4. Factor H, 5. 2% BSA) (B= Lane 1. B30 P30 factor H, 2. factor H, 3. 2% BSA).

3.3.4. Western blot analysis of CFHR5

To confirm the identity and size of the factor H family protein produced by primary GBM cells a western blot was performed. The supernatant and membrane fraction were separated by size by SDS-PAGE, transferred to a nitrocellulose membrane and targeted with primary anti factor-H and secondary IgG-HRP antibodies. Unbound antibodies were washed away and the bands were visualised with DAB.

Prominent bands were observed at 65 kDa for the supernatant and membrane fraction of all primary GBM cells. As the primary antibody used only binds to factor H family proteins, the visualised bands confirmed the presence of CFHR5 (Fig 3.4.). The thickness of the 65 kDa bands were relatively similar to that of factor H (200 µg/mL) positive control which indicated that there was a similar concentration of protein present in the supernatant and membrane fraction used for the blot.

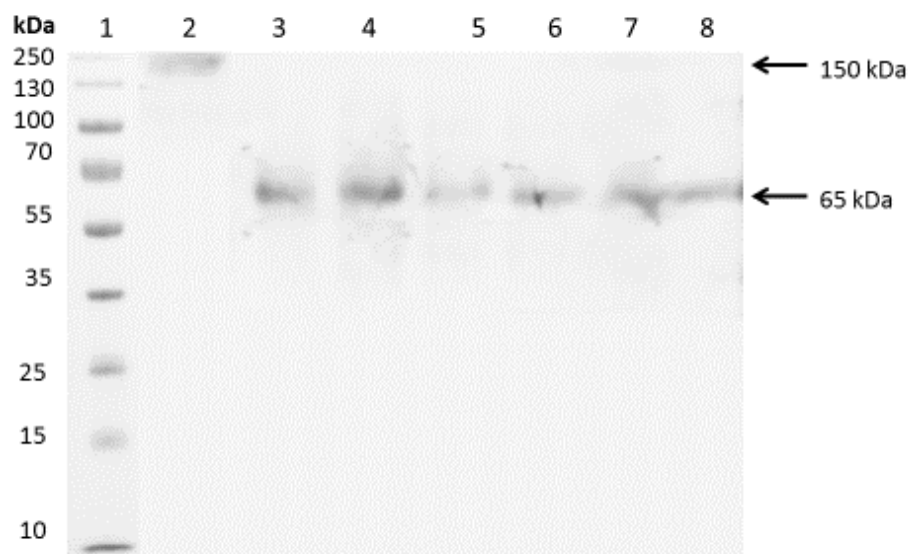


Fig 3.4. Detection of CFHR5 from primary GBM. An SDS-PAGE was run with 200 µg/mL of factor H, supernatant from P2 primary GBM cells and membrane fraction from P2 primary GBM cells. The protein was transferred to nitrocellulose membrane and probed with primary antibody anti-factor H and secondary antibody IgG-HRP. The

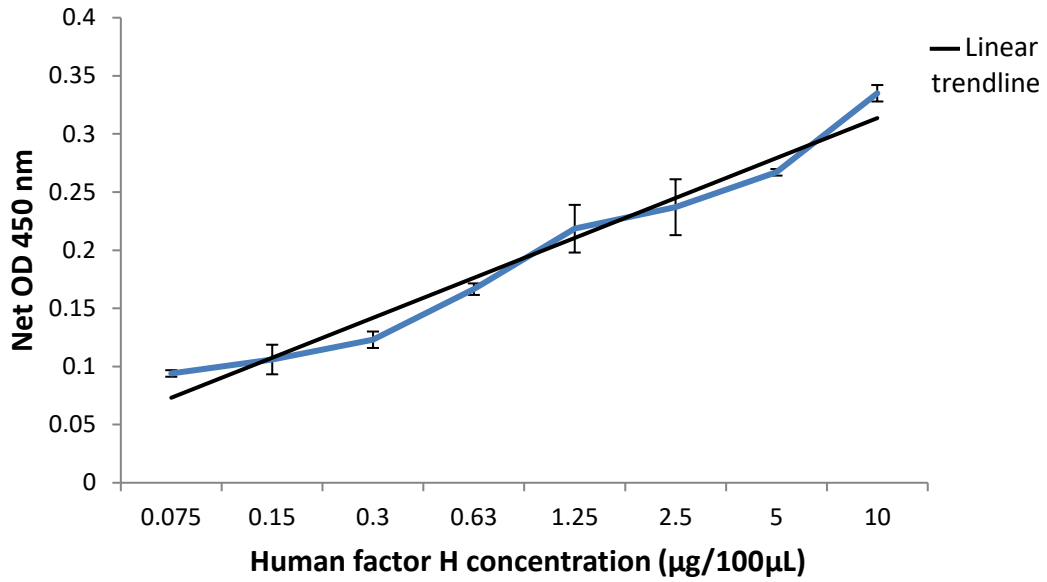
bands for the protein of interest were developed with DAB. (Lane 1. protein marker, 2. Factor H (positive control), 3. B30 supernatant, 4. B30 membrane fraction, 5. B31 supernatant, 6. B31 membrane fraction, 7. B33 supernatant, 8. B33 membrane fraction.

3.3.5. Primary GBM cells secrete CFHR5

In order to analyse the protein expression of CFHR5 by primary GBM cells, an ELISA was performed. The cells were grown without FCS at different incubation periods and the growth supernatant was used to detect the presence of CFHR5 with anti-factor H and IgG-HRP antibodies. A calibration curve of 2X serial dilution of 10 µg/100 µL of human factor H was used as a standard to calibrate the concentration of protein secreted by GBM cells (Fig 3.5.A). Primary GBM cells were found to secrete CFHR5 (Fig 3.5.B,C,D) into the growth supernatant as early as 6 h at < 10 µg/mL. Between 6-12 h the quantity of secreted CFHR5 was not significantly different as minimal change in concentration was detected. An extremely significant difference (***) with a P value <0.0001 was present at 24 h and 48 h when compared with the CFHR5 concentration at 6 h. The statistical analysis unpaired T-test was used to determine the level of significant difference of the concentration at 6 h compared to the other time points for each primary cell. It was clear that the most CFHR5 was produced at 48 h as B30 secreted 55 µg/mL, B31 secreted 37 µg/mL and B33 secreted 32 µg/mL. At each time point the concentration of CFHR5 increased in a dose dependent manner.

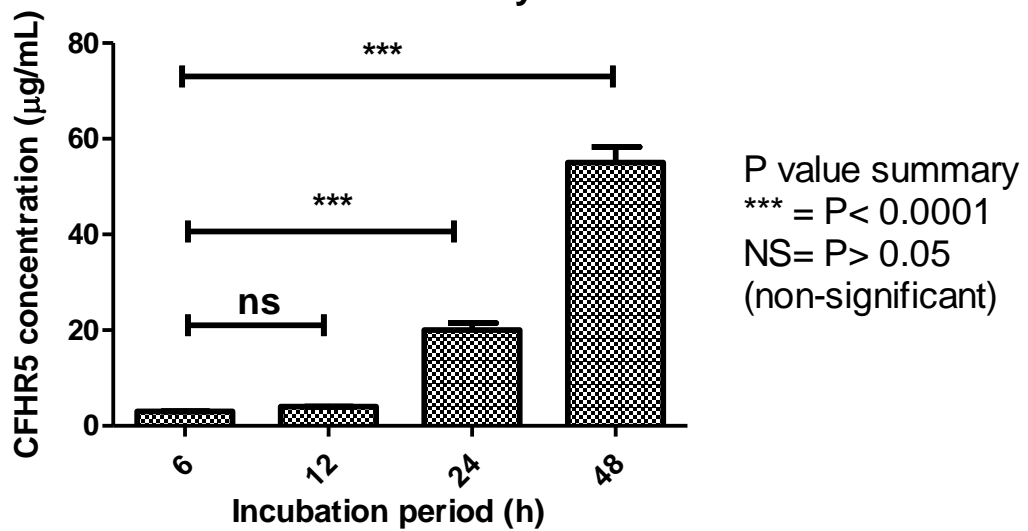
A

ELISA to detect factor H at different concentrations

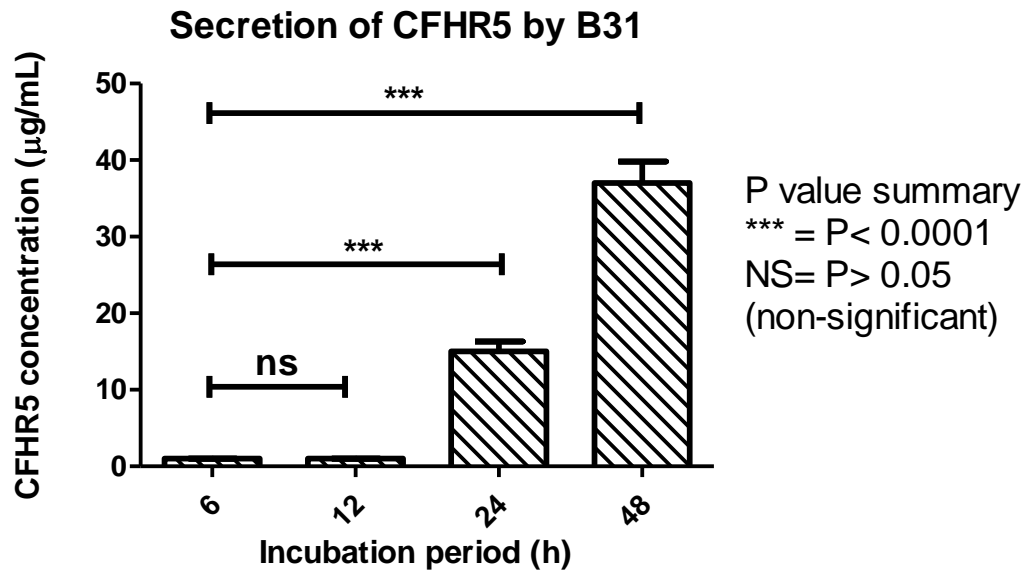


B

Secretion of CFHR5 by B30



C



D

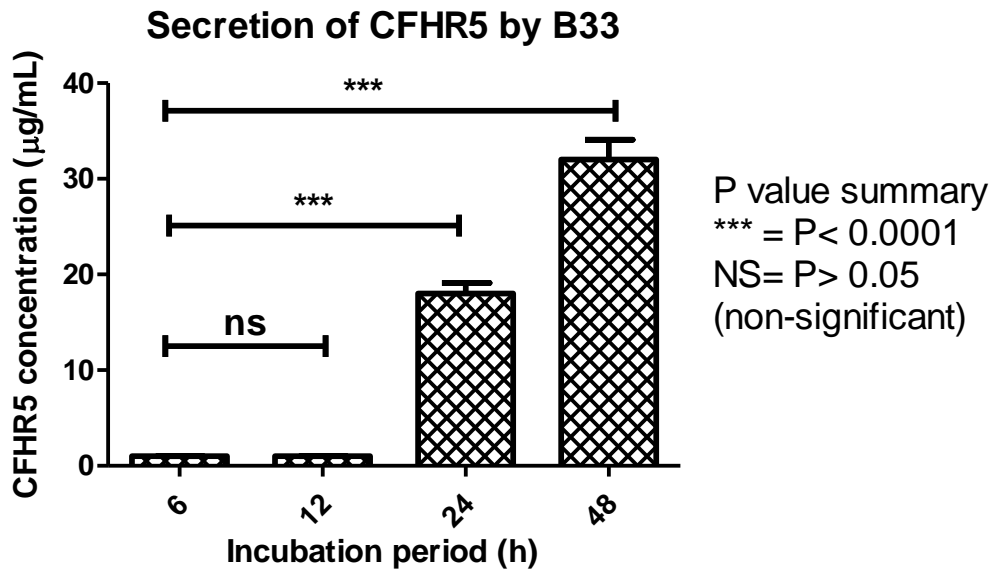


Fig 3.5. Quantification of CFHR5 secreted by primary GBM cells. 0.2×10^6 primary GBM cells were grown for 48 h in the absence of FCS. The growth supernatants were collected at different time points for ELISA and probed with primary anti-factor H antibody and IgG-HRP secondary antibody. A) A 2 fold serial dilution of 100 µg/mL of factor H. B, C, D) Growth supernatant at 6 h, 12 h, 24 h and 48 h for B30, B31 and B33 were collected and incubated with 0.05 M CBC, blocked with 2% BSA and probed with anti-factor H and IgG-HRP antibodies. The colour was developed with OPD and the OD 450 nm was read using a microtiter plate reader. An unpaired T-test was performed between the quantity of CFHR5 at 6 h with the concentration at 12 h, 24 h, and 48 h. Error bars represent standard deviation.

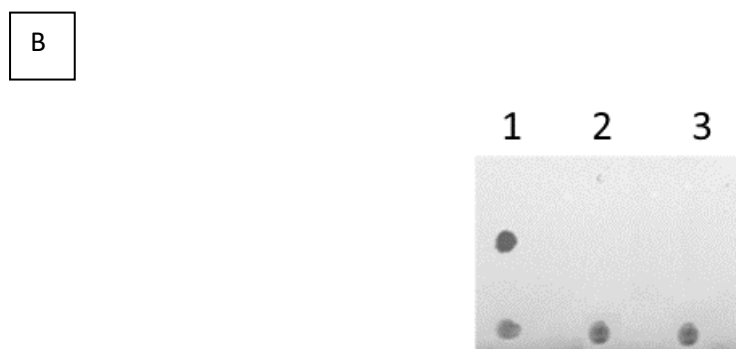
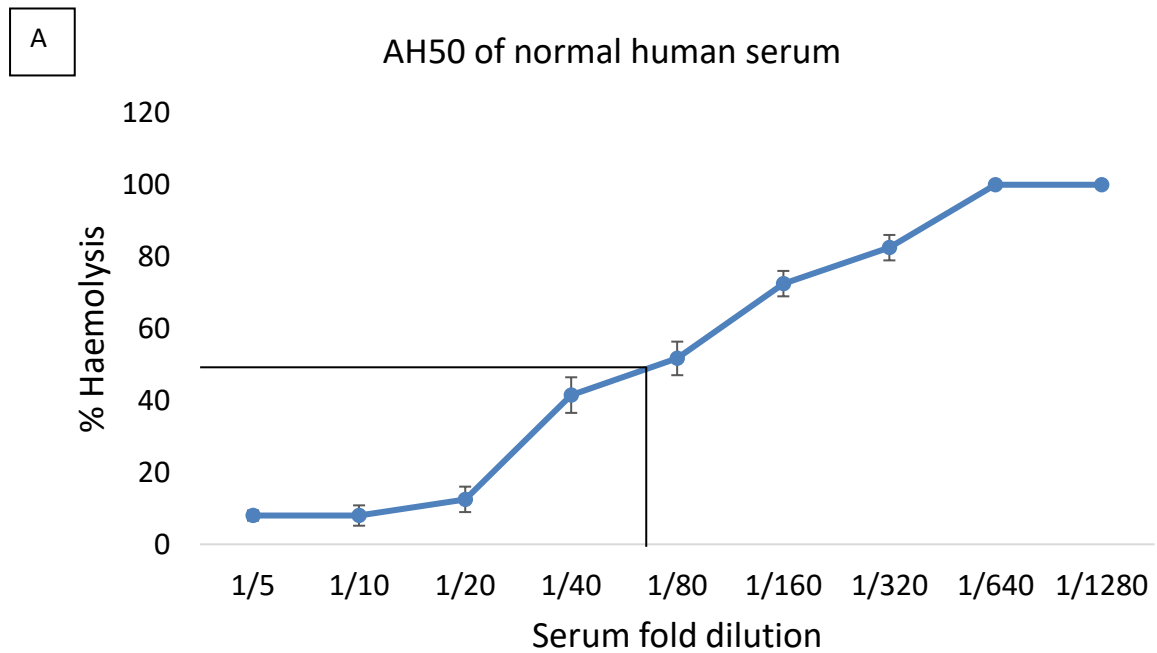
3.3.6. CFHR5 is an inhibitor of the alternative pathway

In order to determine the functional activity of CFHR5 an alternative pathway assay was performed. The fold dilution of AH50 was established to ensure at least 50% haemolysis could be detected from the assay. Factor H deficient serum was then obtained by passing the serum through the factor H column as any factor H present would bind to the resin. A dot blot was then carried out on the factor H deficient serum with anti-factor H primary antibody and IgG-HRP secondary antibody. The serum was reconstituted with factor H and CFHR5 and the percentage of rabbit blood cell haemolysis was recorded. A paired T-test was performed to assess the significant difference between the paired observation of non-reconstituted and reconstituted serum % haemolysis.

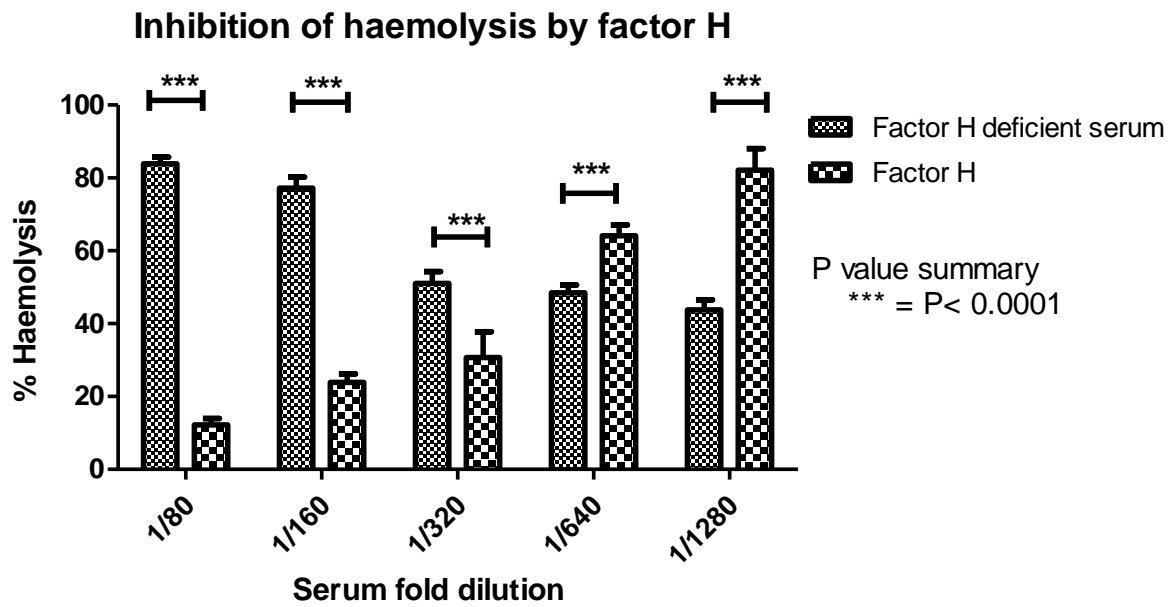
The AH50 curve (Fig 3.6.A) revealed that the normal human serum had haemolytic activity as there was a gradual increase in percentage haemolysis in correlation with reduced quantity of serum. Less than 10% haemolysis was detected at the fold dilution 1/5 and 1/10. The graph plateaued at complete cell lysis of 100% at serum dilution 1/640 and 1/1280. The AH50 of fold dilution 1/80 was depicted by the graph as the concentration of serum needed to yield 50% haemolysis. This dilution value was used to assess the functional activity of CFHR5 as at least 50% haemolysis was known to occur. The same serum was depleted of factor H and its absence was confirmed by dot blot as the primary antibody anti-factor H and secondary antibody IgG-HRP did not detect factor H family proteins (Fig 3.6.B).

It was clear that after the depleted serum was reconstituted with factor H (positive control) and CFHR5, the activity of the alternative pathway was inhibited in a dose dependent manner demonstrated by reduced haemolytic activity (Fig 3.6.C-F). Factor H deficient serum was included as a negative control and exhibited high percentage of haemolysis at 80% in the absence of factor H. A paired T-test with the depleted and reconstituted serum revealed that there was an extremely significant difference of % haemolysis represented by ***= $P < 0.0001$. At serum dilution 1/320 for CFHR5 a non-

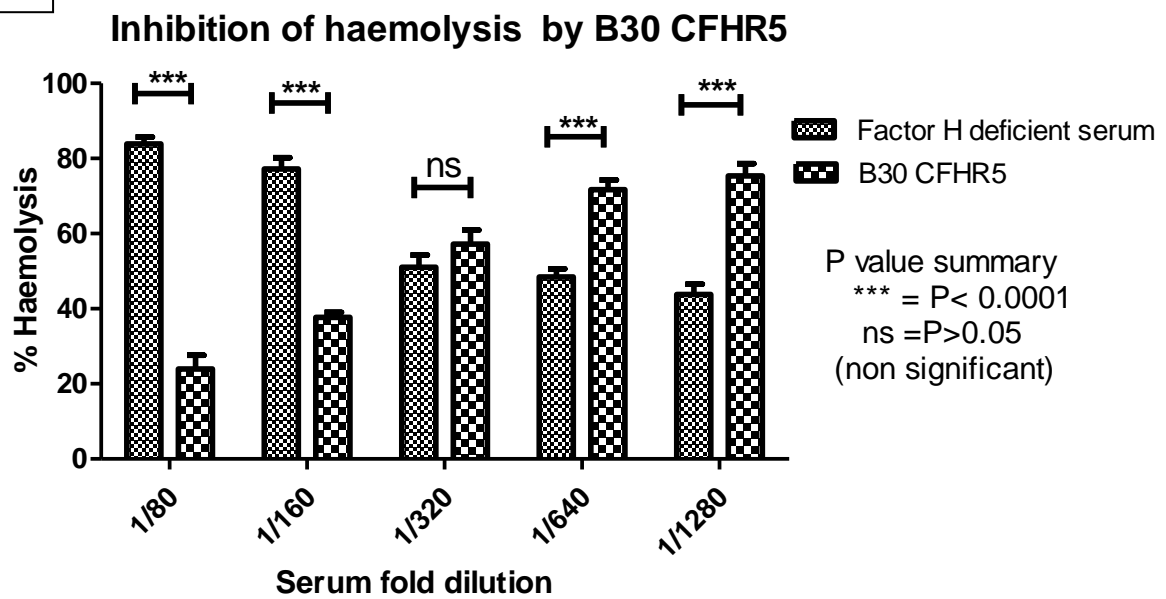
significant difference was observed as this was the point at which the depleted and reconstituted serum cross each other. In the presence of 200 $\mu\text{g}/\text{mL}$ of CFHR5 less than 30% of haemolysis was detected in rabbit blood cells whereas 80% of haemolysis was detected at 12.5 $\mu\text{g}/\text{mL}$ concentration.



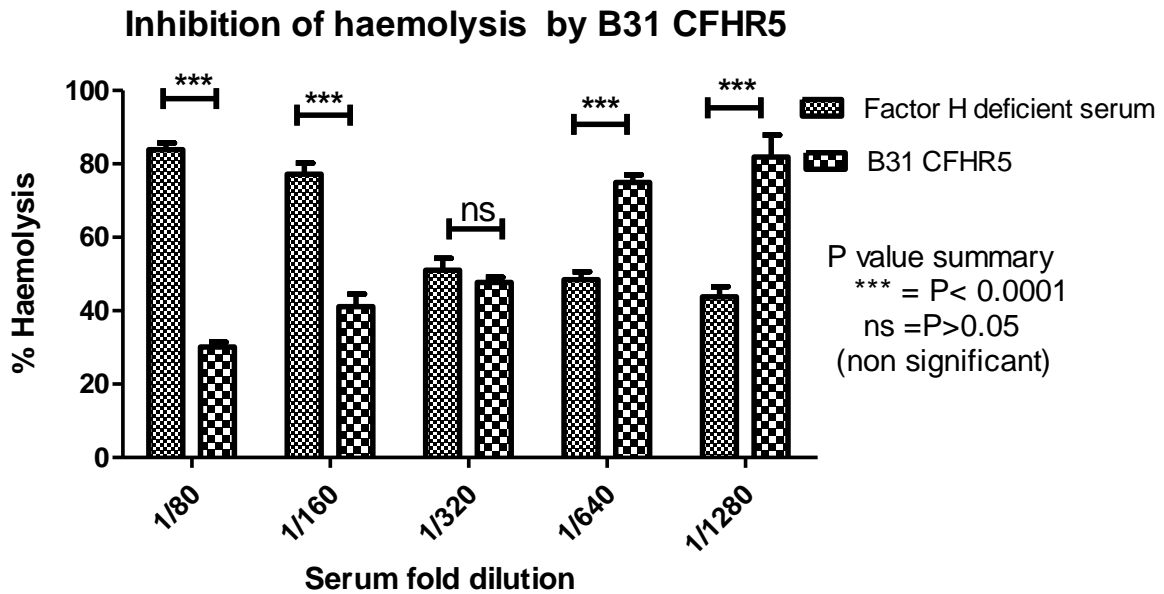
C



D



E



F

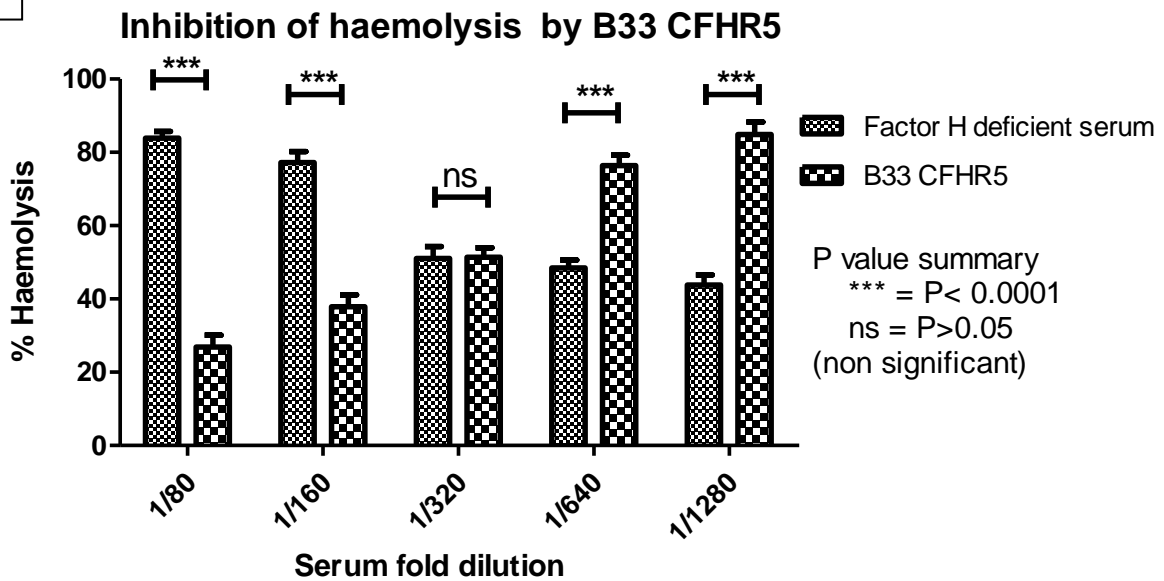


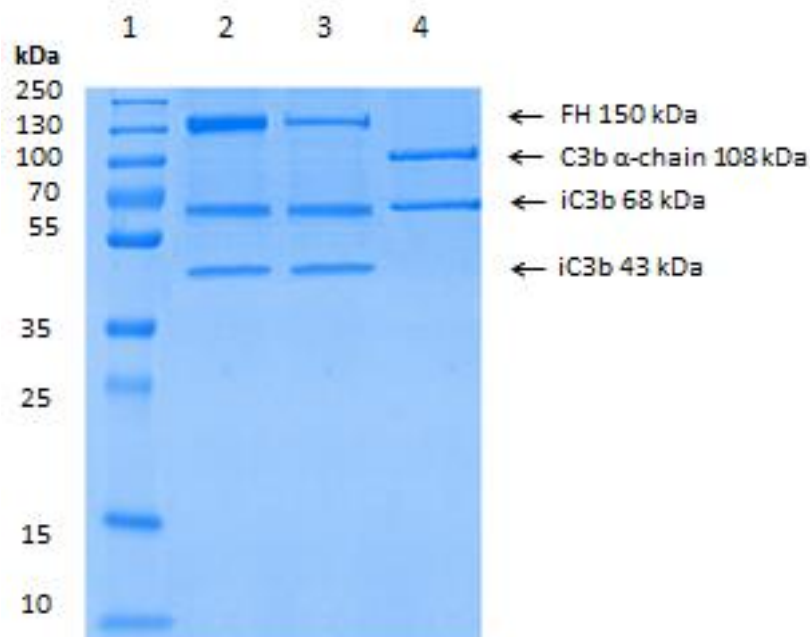
Fig 3.6. Inhibition of the alternative pathway by CFHR5. A 2 fold serial dilution of normal human serum in DGVB buffer was incubated with 10^9 rabbit blood cells. The AH50 was detected and the serum was depleted of factor H. Factor H deficient serum was reconstituted with CFHR5 and factor H (positive control). The reconstituted serum was incubated with rabbit blood cells and the % of haemolysis was calculated using the formula; $(\text{measured OD}) - (\text{OD } 0\% \text{ lysis}) / (\text{OD } 100\% \text{ lysis}) - (\text{OD } 0\% \text{ lysis}) * 100$. A paired T-test was carried out between factor H deficient serum and reconstituted serum A) AH50 of normal human serum. B) Dot blot of factor H deficient serum with primary

antibody anti-factor H and secondary antibody IgG-HRP (Lane 1. factor H (positive control) 2. 2% BSA (negative control) 3. factor H deficient serum. C) Haemolytic assay with factor H, D) Haemolytic assay with B30 CFHR5, E) Haemolytic assay with B31 CFHR5, F) Haemolytic assay with B33 CFHR5. A paired T-test was carried out between non-reconstituted and CFHR5 or factor H reconstituted haemolytic results. Error bars represent standard deviation

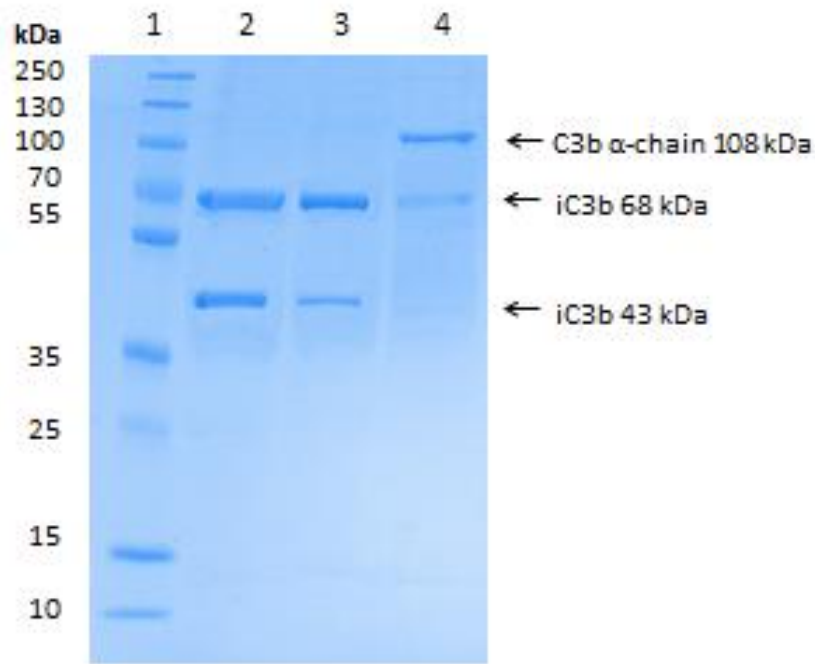
3.3.7. CFHR5 has co-factor activity for factor I mediated cleavage of C3b

To determine the mechanism through which CFHR5 inhibits the alternative pathway a co-factor assay was performed. The fluid phase assay measured the ability of CFHR5 obtained from the primary GBM cells to act as a co-factor for factor I mediated cleavage of C3b. Factor I, C3b and CFHR5 (200 $\mu\text{g}/\text{mL}$) or factor H (200 $\mu\text{g}/\text{mL}$) were incubated, to allow CFHR5 or factor H to bind to C3b and enable factor I mediated cleavage. Factor H and CFHR5 exhibited co-factor activity for factor I visualised through the loss of C3b alpha chain and the formation of 2 cleaved inactivated C3b (iC3b) fragments at 68 and 43 kDa (Fig 3.7.A,B,C,D). 200 and 100 $\mu\text{g}/\text{mL}$ of CFHR5 and factor H was sufficient for factor I mediated cleavage (Lane 2,3). In the absence of CFHR5 and factor H, factor I was unable to cleave C3b (Lane 4).

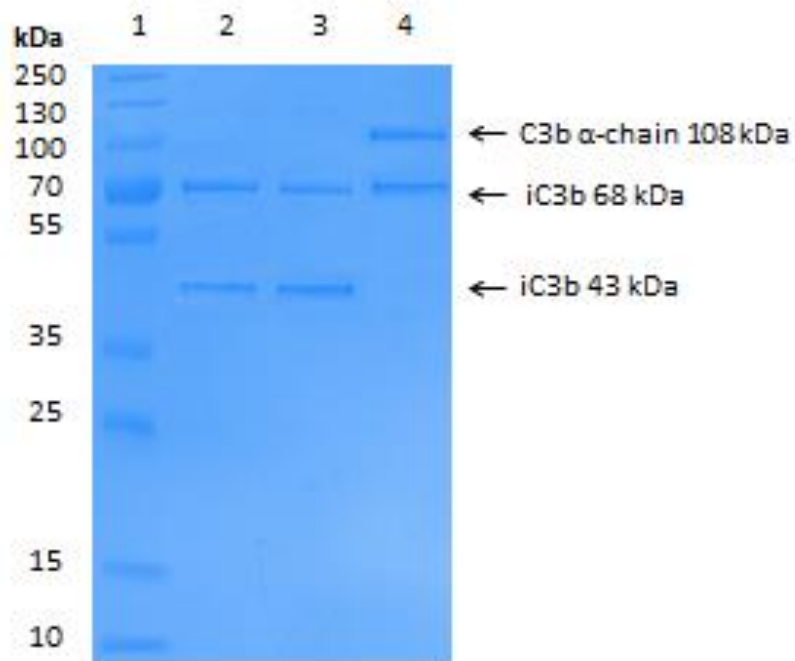
A



B



C



D

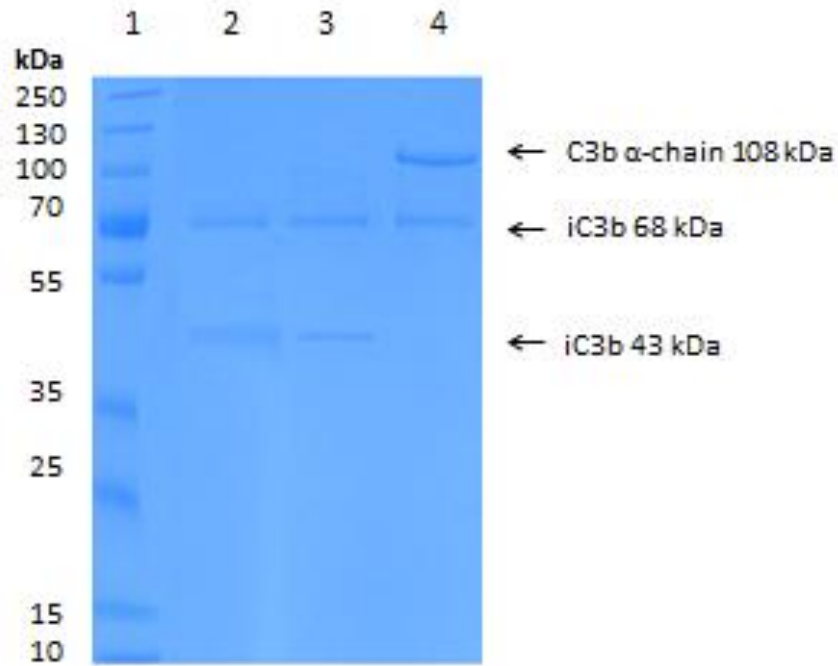


Fig 3.7. CFHR5 has co-factor activity. CFHR5 and factor H were incubated with 3 μ g of C3b, 500 ng of factor I, 10 mM sodium phosphate (pH 7.2), and 1X PBS to a final volume of 30 μ L. Samples were incubated at 37 $^{\circ}$ C for 30 min and then at 60 $^{\circ}$ C for 15 min. An SDS-PAGE was run under reduced conditions. A) Lane 1. protein marker, 2. 200 μ g/mL of factor H, 3. 100 μ g/mL of factor H, 4. 0 μ g/mL of factor H. B) Lane 1. protein marker, 2. 200 μ g/mL of B30 CFHR5, 3. 100 μ g/mL of B30 CFHR5, 4. 0 μ g/mL of B30 CFHR5. C) Lane 1. protein marker, 2. 200 μ g/mL of B31 CFHR5, 3. 100 μ g/mL of B31 CFHR5, 4. 0 μ g/mL of B31 CFHR5. D) Lane 1. protein marker, 2. 200 μ g/mL of B33 CFHR5, 3. 100 μ g/mL of B33 CFHR5, 4. 0 μ g/mL of B33 CFHR5.

3.3.8. CFHR5 has decay acceleration activity for C3 convertase

To establish whether CFHR5 had decay acceleration activity as a mechanism to inhibit the alternative pathway a dissociation assay was implemented. A modified ELISA technique was used to determine the ability of CFHR5 to exert decay acceleration activity on C3 convertase. Factor B (400 ng), factor D (25 ng) 2 mM of nickel chloride and 4% BSA were incubated at 37 °C with C3b to form nickel chloride stabilised C3 convertase. The addition of CFHR5 and factor H (positive control) was successful in dissociating Bb fragment from C3bBb in a dose dependent manner (Fig 3.8.). An inverse correlation was present between CFHR5 concentration and intact C3 convertase. It was clear that between 100-200 µg/mL of protein, factor H was able to decay a greater quantity of C3 convertase compared to CFHR5.

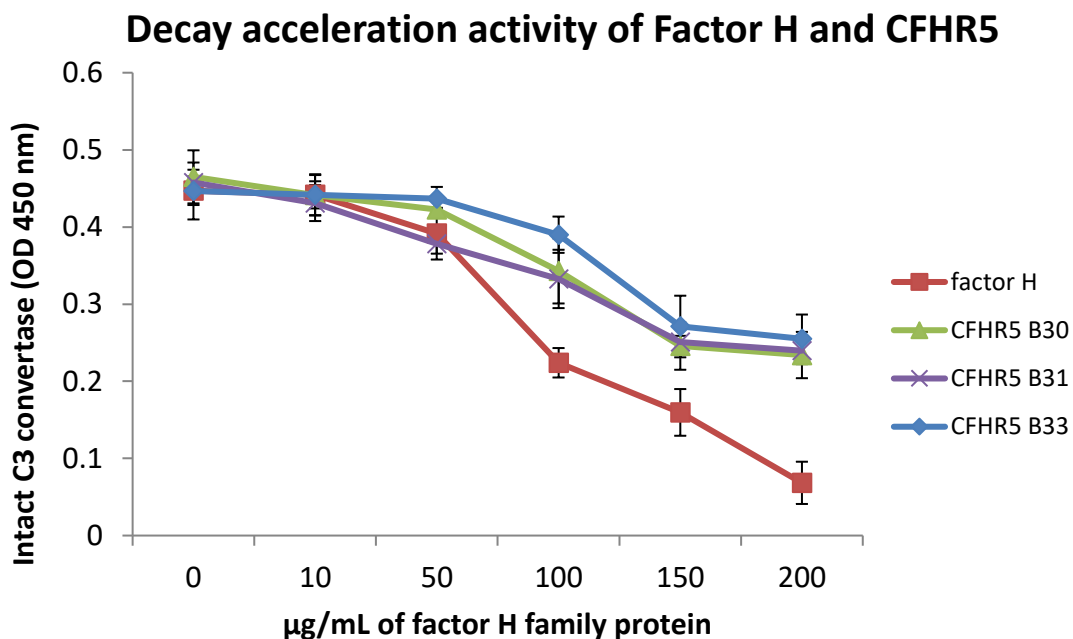


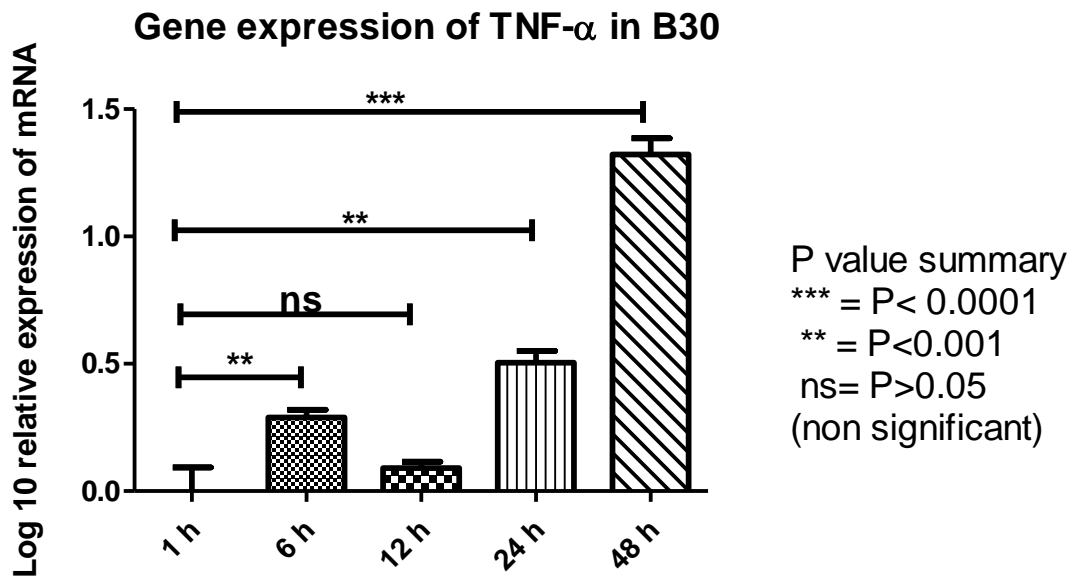
Fig 3.8. CFHR5 promotes decay acceleration activity on C3 convertase. C3 convertase was generated in microtiter plates from 250 ng of C3b, 400 ng of factor B, 25 ng of factor D, 2 mM of nickel chloride and 4% BSA for 2 h at 37 °C. Varying concentrations of CFHR5 and human factor H were added and incubated for 30 min at 37 °C. Intact C3 convertase was detected by primary antibody factor B and secondary antibody IgG-HRP. The colour was developed with OPD. Error represent standard deviation.

3.3.9. Cytokine gene expression within primary GBM

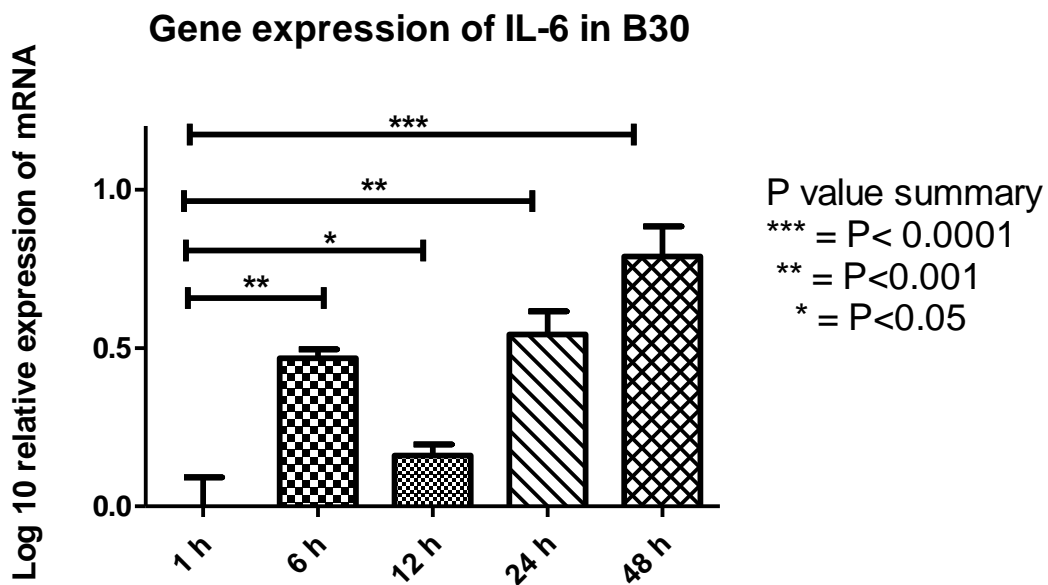
The change in gene expression of pro- and anti-inflammatory cytokines TNF- α , TGF- β , IL-6, and IL-12 in primary B30 was investigated over 48 h. qPCR was performed to amplify the cDNA samples collected at different time points to determine the presence and RQ of the different cytokines in each cDNA sample. The results obtained were normalised against the stably expressed 18S gene and calibrated against the 1 h time point. The unpaired T-test statistical analysis showed that all the time points displayed significant differences in cytokine expression, $P \leq 0.05$ except where ns is shown.

TNF- α which is predominately reported to be a pro inflammatory cytokine showed a biphasic pattern as there was an increase at each time point except for 12 h where the expression was less than 6 h and was deemed non-significant with a P value >0.05 (Fig 3.9.A). At 48 h there was a sharp increase in TNF- α expression and the upregulation was shown to be extremely significant ($P < 0.0001$). At 6 h and 12 h the increased expression was very significant ($P < 0.001$). The gene expression of pro-inflammatory IL-6 (Fig 3.9.B) was also significantly up regulated. At 6 h and 12 h the increased gene expression was extremely significant with a P value < 0.0001 . Similarly to TNF- α expression a biphasic trend was present as the gene expression at 12 h was less than 6 h. Despite this the upregulated expression was significant. Pro-inflammatory IL-12 gene expression was markedly downregulated over the 48 h period (Fig 3.9.C). The reduced gene expression was extremely significant between 12-48 h indicated by $P < 0.0001$. At 6 h the down-regulated expression was not significant. TGF- β gene expression which is mainly referred to as an anti-inflammatory cytokine was upregulated over the 48 h incubation period. Between 12-48 h the increased expression was very significant with minimal change observed between 24-48 h. At 6 h the change in expression was not significant (Fig 3.9.D).

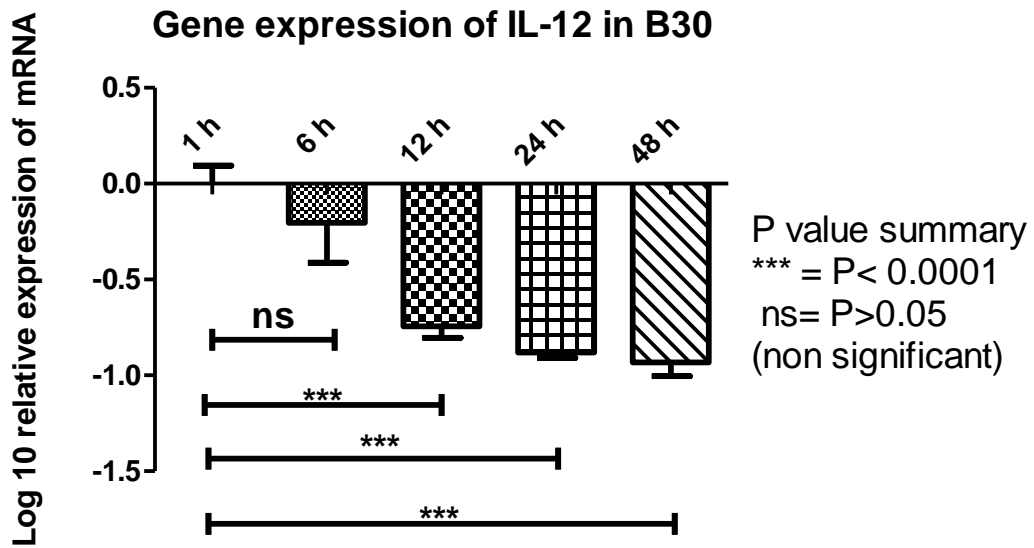
A



B



C



D

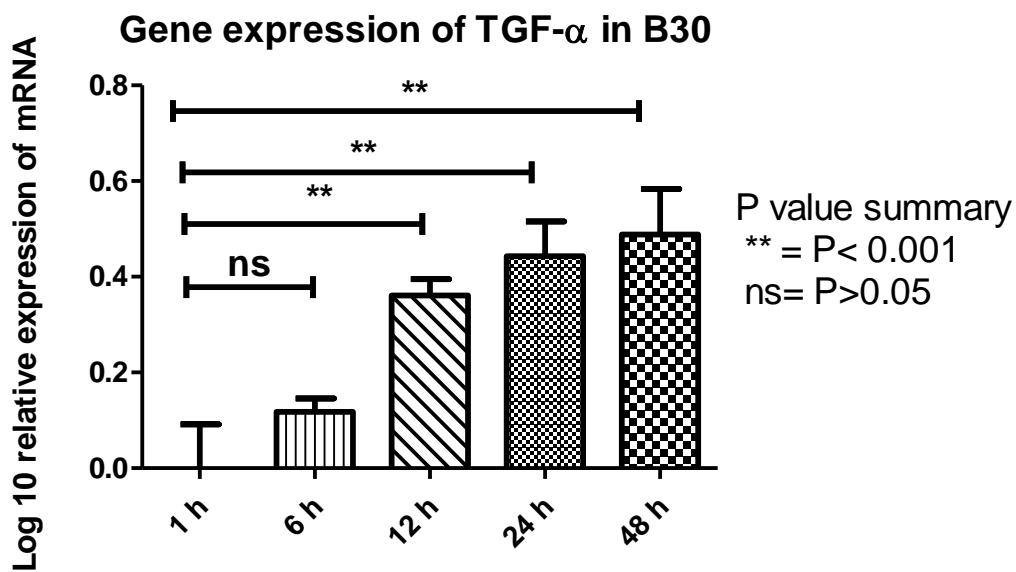


Fig 3.9. A qPCR of cytokine gene expression from B30 P3 cells. RNA was extracted from primary B30 at different time points of 12 h, 24 h, 48 h. The RNA was converted into cDNA as described in materials and methods and analysed in qPCR using TNF- α (A), IL-6 (B), IL-12 (C) and TGF- β (D) primers. The data was normalised against 18S endogenous control. Error bars represent $\log_{10} \pm$ standard error of mean. RQ was

calculated by using the comparative Ct method with the 12 h time point as the calibrator using the formula: $RQ = 2^{-\Delta\Delta C_t}$ and the 12 h time point was used as the calibrator. An unpaired 2-sided T-test were conducted.

3.4. Discussion

Malignant tumours have been shown to express Factor H. Recently Junnikkala et al demonstrated that this expression was also present in GBM cell line (Junnikkala *et al*, 2000). We decided to investigate if this expression was present in primary GBM cells direct from patients. It was clear that primary GBM did not produce factor H but instead CFHR5. There is currently limited data available for the function of complement factor H related proteins. Given the short consensus repeats similarities between CFHR proteins with factor H, it is expected that overlaps in function are present. Currently similarities have been identified with some of the CFHR proteins ability to bind to C3b. CFHR5 is unique in comparison to the remaining four CFHR proteins as it is the only CFHR protein to share homology with SCR 10-14 of factor H. The total cell extract, membrane fraction and factor H purification process from supernatant of primary GBM cells B30, B31 and B33 produced CFHR5. This revealed that CFHR5 was the only factor H family member to be secreted by primary GBM cells. Normal human serum studies reveal factor H is the most abundant factor H family member. Interestingly although no factor H was secreted in primary GBM cells, at B30 P30 a protein band at 150 kDa was visible after the factor H purification process. The size of this band corresponded to factor H. This suggests that between P2 to P 30 the presence of CFHR5 is reduced until it can no longer be detected. In contrast it appears that during this period B30 began to secrete factor H. This shows that at a higher passage, B30 cells experience a change in protein secretion from CFHR5 to factor H.

The quantification of protein from the factor H family secreted by B30, B31 and B33 over a 48 h period showed a dramatic increase between 24 h and 48 h as the ELISA demonstrated an active secretion of protein. It is likely that the dramatic increase between 24 -48 h is due to the greater presence GBM cells as the cells divide and multiply. This rapid increase of secreted protein from the factor H family can result in a greater inhibitory affect and resistance to complement mediated lysis, which in turn would drive the progression of the tumour. The presence of CFHR5 on the membrane

fraction is interesting as it is likely that the protein is bound to the membrane thus anchored to the cell providing an escape mechanism for GBM cells to avoid complement.

The functional activity of the purified CFHR5 derived from the supernatant of primary GBM cells, B30, B31 and B33 was assessed using the alternative pathway experiment. The experiments revealed that within all 3 purified CFHR5 a dose dependent response is observed as the inhibition of cell lysis was upregulated as the concentration of CFHR5 was increased. This shows B30, B31 and B33 CFHR5 are able to downregulate the alternative pathway and decrease the % of haemolysis of rabbit red blood cells . This indicates that the CFHR5 purified from primary GBM cells has the ability to inhibit the alternative pathway and ultimately suppress the capability for the alternative pathway to elicit cell lysis to destroy the targeted cell. This inhibitory effect is likely to contribute to GBM resistance to the immune systems attempt to cause cell death.

As we had shown that CFRH5 was functionally active we wanted to investigate the mechanism through which this inhibitory effect was delivered. The co-factor experiments revealed that CFHR5 were able to inhibit the alternative pathway by acting as a co- factor for factor I mediated cleavage. It was clear from SDS-PAGE analysis that the presence of CFHR5 had enabled factor I to cleave C3b into inactive C3b fragments of 68 and 43 kDa. The gel revealed that during the reaction CFHR5 is consumed as the band it is no longer present after the reaction.

It is known that factor H is able to display decay accelerating activity as a mechanism to inhibit activation of the alternative pathway. The inverse correlation depicted on the graph between CFHR5 concentration and intact C3 convertase showed that the eluted protein was able to degrade C3 convertase. This indicates that the ability of CFHR5 to degrade C3 convertase would prevent the enzyme from binding to C5 and eliciting the final stages of alternative pathway cell lysis via formation of the MAC. It is of significant interest that CFHR5 were able to act as a co-factor for factor I mediated cleavage and induce degradation of C3 convertase as these functions had been attributed to SCR 1-

4 of factor H. Therefore, as only factor H and CFHL-1 share SCR 1-4 it was believed that only these 2 proteins of the family were functionally active. However, our results show that CFHR5 are also functionally active and can elicit the same inhibitory actions through the same mechanisms as factor H. This eludes that the functional activity of factor H family is not solely encompassed within SCR 1-4. It is a possibility that as CFHR5 is the longest and the only CFHR to share homology with SCR 10-14 of factor H, we speculate that it is this feature which give CFHR5 is functional ability.

TNF- α is a pro-inflammatory cytokine often associated with causing cellular apoptosis. However, in GBM it has been reported in many cases to increase tumourigenesis. The qPCR results indicated a significant increase in the gene expression of TNF- α during 48 h of incubation. This suggested that this cytokine was highly expressed within B30 and contributed to the progression of the tumour. As the expression is high within the tumour it infers that this cytokine is aberrantly expressed and unable to destroy altered self-cells. This loss on innate immune function to destroy altered self-cells which are detected by the body as 'foreign' eludes the severity of the tumour and unregulated expression of TNF- α .

It was interesting that the gene expression of IL-6 was similar to that of TNF- α as both were significantly upregulated and had a biphasic pattern due to the 12 h time point. It has been previously reported that TNF- α influences the gene expression of IL-6. Our findings also support this view as the similarities in gene expression indicate that IL-6 expression is influenced by TNF- α . IL-6 is also a pro-inflammatory cytokine that has been attributed to contributing to gliomagenesis. The significant upregulation of gene expression infers that the cytokine is unable to elicit an immune response to remove the altered self-cells. Instead it appears that as these cytokines are from GBM cells their innate immune response will not be the same as expected had they of been expressed from non-tumourigenic cells. Therefore, it is likely that this cytokine is highly expressed to support the tumour environment and encourage GBM invasion.

TGF- β is an anti-inflammatory cytokine associated with regulating cell division. The cytokine gene expression revealed that the expression significantly increased at each time point. As this primary cell is derived from a highly malignant grade IV glioma it demonstrates that this cytokine is unable to carry out its anti-inflammatory function successfully as the pro-inflammatory cytokine IL-6 and IL-12 are highly expressed. The increased expression pattern eludes that within B30 TGF- β promotes tumour growth. This ultimately is likely to render the cytokine redundant in cell regulation thus allowing transformed cells to escape cell death and instead proliferate and invade neighbouring tissue promoting tumourigenesis.

It was interesting to detect a significant downregulation of IL-12 expression in B30 cells over 48 h of incubation. IL-12 has been commonly reported to provide potential therapeutic effects in regards to reducing tumour growth. Our finding support this view as the reduced expression over time indicates that this cytokine does not support tumour growth. Therefore, its expression is continuously downregulated as the expression of the pro-tumourigenic cytokines are up regulated. Reduced IL-12 expression is likely to provide a mechanism through which altered self-cells are able to escape death via innate immune responses.

It is evident that the early passage GBM cells direct from patients and the CFHR5 purified protein appear to be useful tools to study alternative pathway and cytokine regulation. The CFHR5 purified from GBM supernatant is free from impurities and is biologically active elucidating that the purification technique is effective.

Chapter 4: Purification of rhSP-D and its effect on U87

4.1. Abstract

It has been previously reported that using a recombinant fragment of human SP-D (rhSP-D) composed of homotrimeric neck and lectin domains, a role for SP-D in immune surveillance and homeostasis has been considered. rhSP-D has been shown to induce apoptosis in a leukemic cell line via p53 pathway, as it does to activated eosinophils derived from allergic patients. Although rhSP-D binds healthy as well as sensitised eosinophils, it appears to induce apoptosis only in sensitised cells (Mahajan *et al.*, 2008). Given the emerging role of rhSP-D in immune surveillance against tumours, we wanted to examine if rhSP-D is capable of inducing apoptosis in GBM cell lines and thus affect their viability. We first expressed the protein in *E. coli* and purified rhSP-D via denaturation-renaturation of inclusion bodies, followed by affinity purification and LPS removal. Here, we report that rhSP-D binds GBM cells in a dose- and calcium-dependent manner; however, it fails to induce apoptosis and reduce cell viability. This appears to suggest that the pro-apoptotic potency of rhSP-D is negated by GBM cells. In fact, treatment of GBM cells with rhSP-D increased the proliferative capacity of the GBM cells. The rhSP-D treatment also up-regulated the transcriptional level of pro-inflammatory cytokines TNF- α and IL-6. Our results suggest that rhSP-D promotes tumour growth in the case of GBM and thus may be an important constituent of the microenvironment.

4.2. Objectives

In previous reports rhSP-D had been found to bind to eosinophils and reduce the cell viability. Recently studies have shown that rhSP-D has the ability to induce apoptosis in tumours, including leukaemic eosinophils, and breast cancer cells (Mahajan *et al.*, 2013). We hypothesised that rhSP-D would reduce the viability of U87 which is a widely used GBM cell line. The main objectives were:

- To induce the expression of rhSP-D and remove endotoxins from the purified protein.
- To assess the ability of rhSP-D to bind to U87 cell.
- To investigate the induction of apoptosis by rhSP-D on U87 cells.
- To study the ability of rhSP-D to agglutinate U87.
- To study the change in gene expression of rhSP-D treated and untreated cells

4.3. Results

4.3.1. Pilot scale of rhSP-D

Plasmid pUK-D1 containing the neck and CRDs with 8 gly-x-y repeats of SP-D were expressed under the T7 promoter system in *E.coli* BL21 (λ DE3) pLysS. The pilot scale expression of rhSP-D was successfully induced at log phase by the addition of IPTG to the cell culture which contained transformed rhSP-D competent cells. The induced culture expressed rh-SPD in insoluble inclusion bodies which appeared as a prominent band at 20 kDa in lane 2 within the small scale preliminary study (Fig 4.1.). The 20 kDa band was absent in the cultures shown in lane 3, 4 and 5 which did not contain either IPTG which is important for the initiation of induction, or the antibiotics ampicillin and chloramphenicol which only enable the growth of cells that contain the resistant gene for that particular antibiotic.

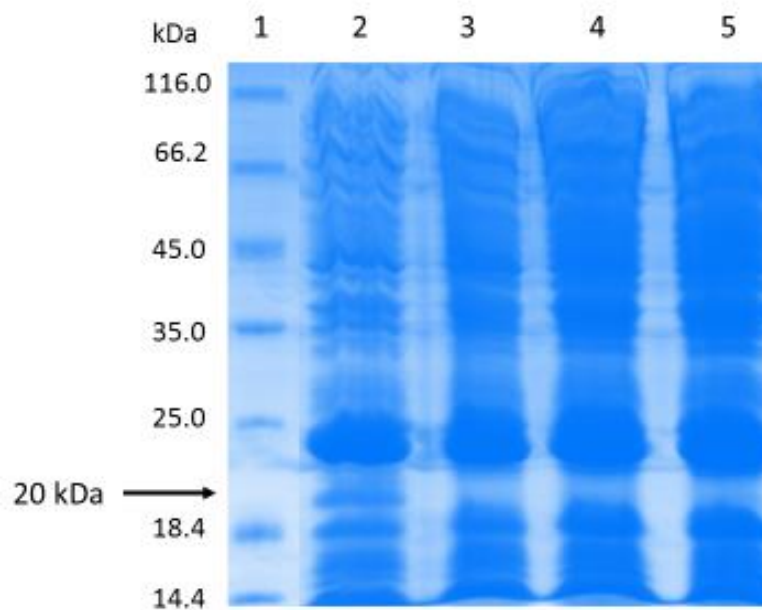


Fig 4.1. SDS-PAGE of rhSP-D pilot scale expression. Pilot scale expression of rhSP-D inclusion bodies using the *E.coli* host BL21 (λ DE3) pLysS and expression vector pUKD1 with an IPTG inducible T7 promoter. A single colony of transformed competent

cells containing rhSP-D DNA was expressed under T7 promoter of *E.coli* BL21 (λ DE3) pLysS. The cells were grown in LB in a 1:1000 ratio with ampicillin and chloramphenicol until log phase A600 0.6-0.8. The culture was induced with 0.5 mM IPTG for 3 h and an SDS-PAGE was run. The band corresponding to the expressed protein is indicated by the arrow. (Lane 1. protein marker, 2. rhSP-D +ampicillin+ chloramphenicol+ IPTG, 3. rhSP-D+ ampicillin+ chloramphenicol, 4. rhSP-D+ ampicillin+ IPTG, 5. rhSP-D+ chloramphenicol+ IPTG).

4.3.2. Large scale expression of rhSP-D

The successful expression of rhSP-D within the pilot scale experiment gave way to perform the induction of rhSP-D on a large scale to produce a greater quantity for in-vitro experiments. The recombinant protein was expressed by the addition of 0.5 mM IPTG during log phase at A600 0.6-0.8 and the results were analysed by SDS-PAGE. It was clear from the acrylamide gel that the induced culture expressed rhSP-D in insoluble inclusion bodies at 20 kDa whereas the uninduced sample did not produce a 20 kDa band (Fig 4.2.).

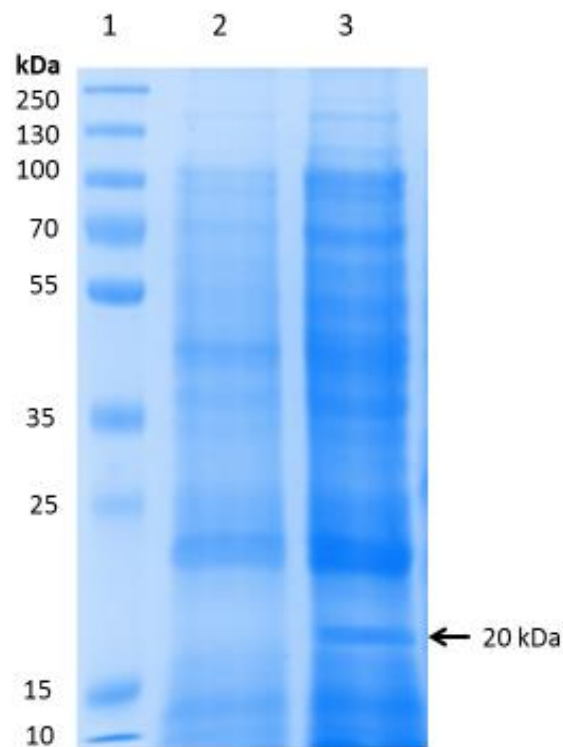


Fig 4.2. SDS-PAGE of the large scale expression of rhSP-D. A single colony from the pilot scale experiment was inoculated in LB with ampicillin and chloramphenicol in a 1:1000 ratio. The overnight culture was added to fresh LB with ampicillin and chloramphenicol (1:1000) and grown to A600 0.6- 0.8. The cells were then induced with IPTG for 3 h and a reduced SDS-PAGE was run and stained overnight and destained for 3 h. A 20 kDa band representing rhSP-D was visualised in the induced rhSP-D sample. The band corresponding to the expressed protein is indicated by an arrow. (Lane 1. protein marker, 2. rhSP-D+ ampicillin+ chloramphenicol+ IPTG, 3. rhSP-D+ ampicillin+ chloramphenicol).

4.3.3. Purification of rhSP-D by affinity chromatography

Insoluble rhSP-D in inclusion bodies were lysed and sonicated which resulted in the release of the recombinant protein from the inclusion bodies. The cells were denatured with 6 M urea and β -ME and were refolded by a gradual decrease of urea concentration by stepwise dialysis. Affinity chromatography on a maltose agarose column in the presence of CaCl_2 was successful in producing rhSP-D. The recombinant protein was visualised as a 20 kDa monomer confirming that rhSP-D is able to bind to maltose in a calcium dependent manner (Fig 4.3.). No higher or lower bands were observed on the gel which demonstrate that no impurities were present or higher oligomers were formed. The eluted fractions yielded an average recovery of 400 $\mu\text{g}/\text{mL}$ and in total produced 3.0 mg of rhSP-D.

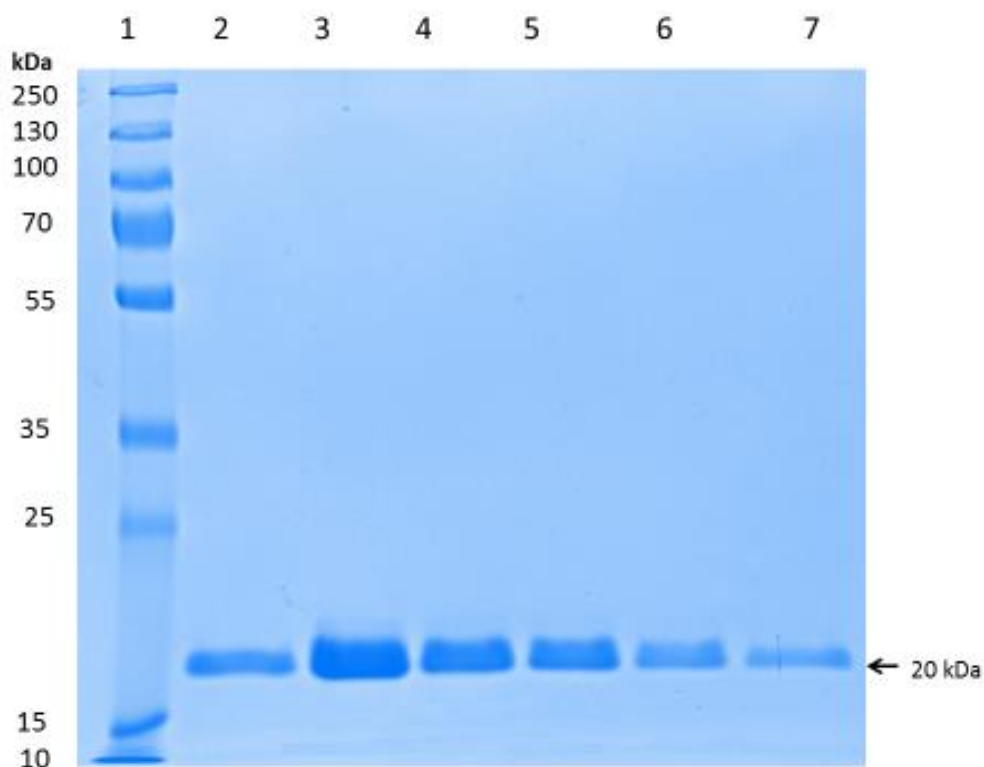


Fig 4.3. An SDS-PAGE of purified rhSP-D. The induced bacterial cells containing rhSP-D in insoluble inclusion bodies were lysed and sonicated. The cells were solubilised and refolded by step wise dialysis and a gradual decrease in the concentration of urea. The dialysate was passed through a maltose agarose column

and 1 mL of eluted fractions were obtained. An SDS-PAGE was run and purified rhSP-D was visualised at 20 kDa on an acrylamide gel (Lane 1. protein marker, 2. 2-6. rhSP-D). The arrow indicates the purified rhSP-D.

4.3.4. Determination of rhSP-D endotoxin level

An endotoxin removal method was successfully implemented to eliminate newly adhered LPS from rhSP-D that had been released from *E.coli* BL21 (λ DE3) pLysS during cell growth. The endotoxin stock solutions produced a linear regression curve as the A450 readings were proportional to the endotoxin level present in each standard (Fig 4.4). The coefficient of determination (r^2) for the graph was ≥ 0.98 and demonstrated that the graph had a 99% accuracy when used to predict future outcomes therefore indicating that the curve is extremely reliable to predict the endotoxin concentration from rhSP-D. Endotoxin levels of 0.12 EU/mL were measured for rhSP-D using the regression curve, and was considered safe for the recombinant protein to be used in vitro. The concentration of the endotoxin free rhSP-D was measured with a nanodrop and a total of 2.8 mg was obtained demonstrating that column was efficient in retaining purified protein.

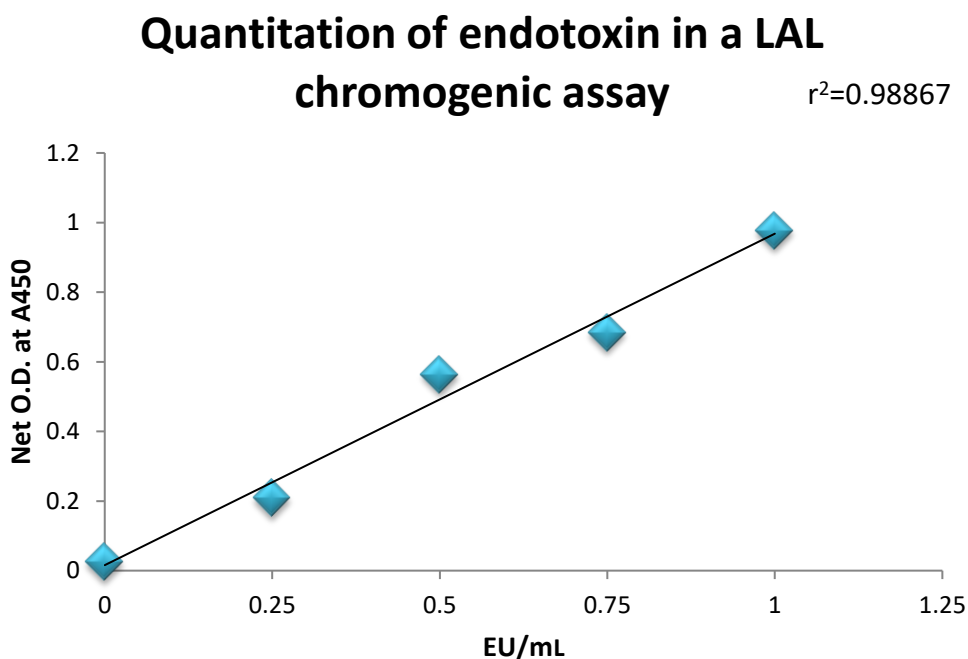


Fig 4.4. A standard curve for the quantitation of endotoxin in a chromogenic assay. Endotoxin stock concentrations of 1, 0.75, 0.5, 0.25 and 0.1 EU/mL were prepared and incubated with LAL for 10 min and a chromogenic substrate for 6 min at

37 °C. A stop solution was added to the samples and an A450 was measured. The statistical analysis coefficient of determination (r^2) for the graph was calculated.

4.3.5. Detection of rhSP-D

The identity of rhSP-D was confirmed by western blot detection method in which 20 µg/mL of rhSP-D was transferred to a nitrocellulose membrane and probed with primary anti-SP-D and secondary PA-HRP antibodies. It is clear that a brown insoluble precipitate is visualised at 20 kDa after treatment with DAB (Fig 4.5.) corresponding to the molecular weight of monomeric rhSP-D. No higher bands were observed demonstrating that oligomers were not formed. 2% BSA used as a negative control did not produce any bands indicating that the results are reliable as non-specific binding did not occur.

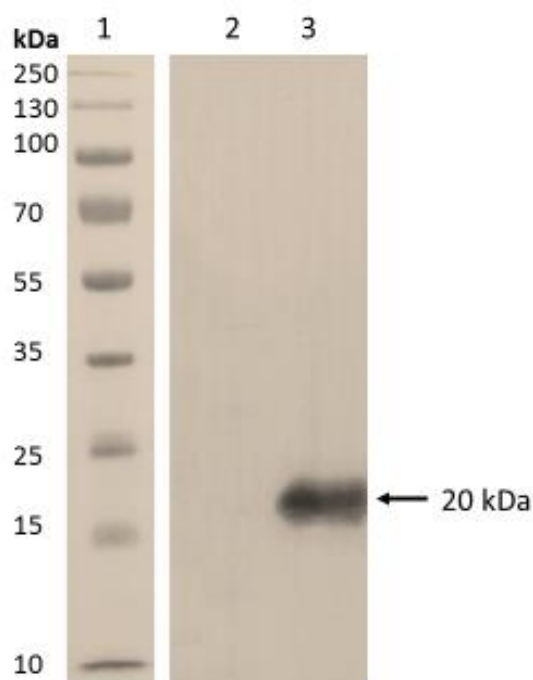


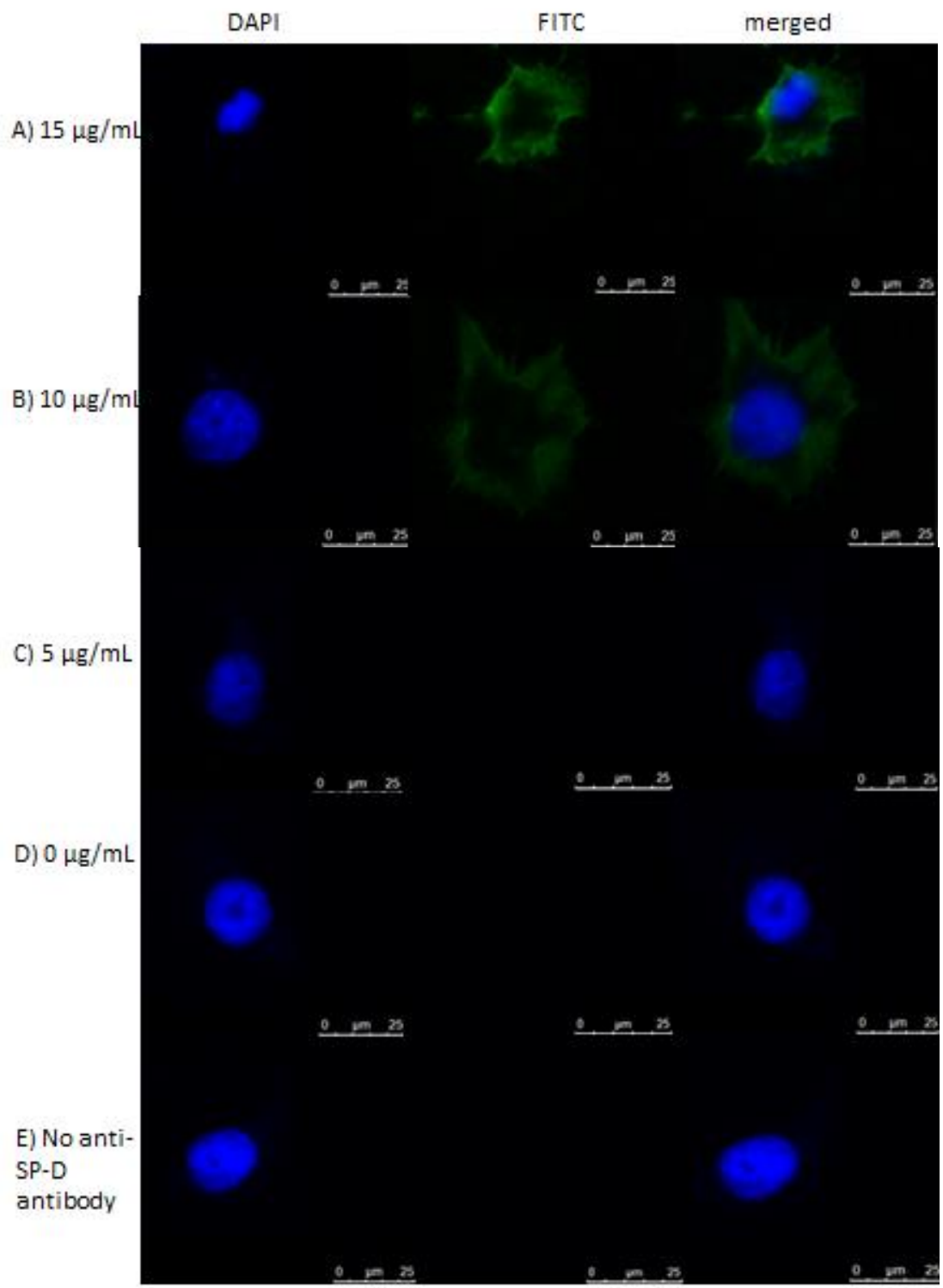
Fig 4.5. Western blot analysis of endotoxin free rhSP-D. rhSP-D and 2% BSA were denatured in 2X sample buffer and separated under reduced conditions on 12% acrylamide gel. The recombinant protein was transferred to a nitrocellulose membrane by wet tank transfer with 1X transfer buffer at 4 °C. The membrane was blocked with 2% BSA and the protein was detected by primary antibody anti-SP-D and secondary antibody PA-HRP antibodies (1:1000). The colour was developed with DAB and a 20 kDa band is observed. (Lane 1. protein marker, 2. 2% BSA, 3. 20 µg/mL of rhSP-D). The band corresponding to the expressed protein is indicated by the arrow.

4.3.6. rhSP-D is able to bind to U87 cells

An indirect fluorescent ligand binding assay was implemented to detect whether rhSP-D was able to bind to the membrane of U87 cells. The cells were fixed with 4% para-formaldehyde and incubated with 0, 5, 10 or 15 µg/mL of rhSP-D, and CaCl₂ for 2 h at 4 °C to prevent the protein from being internalised. Primary anti-SP-D and secondary PA-FITC antibodies were used to detect the presence of rhSP-D bound to the membrane and the nuclei were stained with DAPI.

The location of rhSP-D was visualised with conjugated FITC around the membrane of U87 cells when treated with 15 (Fig 4.6.A) and 10 (Fig 4.6.B) µg/ mL of rhSP-D. It demonstrated that the protein was able to bind to the membrane of the tumour cells in the presence of calcium without becoming internalised. Fluorescence was not observed at 5 µg/mL (Fig 4.6.C) of rhSP-D which indicated that insufficient binding occurred and could not be detected. There was no fluorescence present with U87 cells that had not been treated with rhSP-D (Fig 4.6.D) or in cells that had not been probed with the primary antibody anti-SP-D (Fig 4.6.E). This showed that non-specific binding did not occur and only specific antibody binding took place.

In order to establish the percentage of membrane bound rhSP-D the number of FITC labelled cells per 100 cells was recorded. It was evident that cells which were treated with 15 µg/mL of rhSP-D had 78% of protein bound whereas 30% of cells treated with 10 µg/mL of rhSP-D were bound by the recombinant protein. Fluorescence was not detected with cells treated with 5 µg/mL of rhSP-D, 0 µg/mL of rhSP-D and cells which had no primary antibody added. A dose dependent response was observed as the higher the concentration administered the greater the binding (Fig 4.6.e).



F

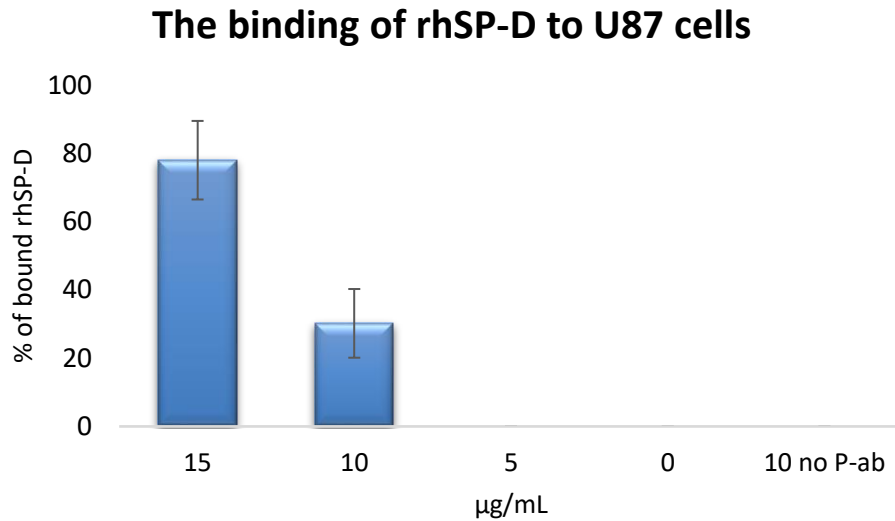


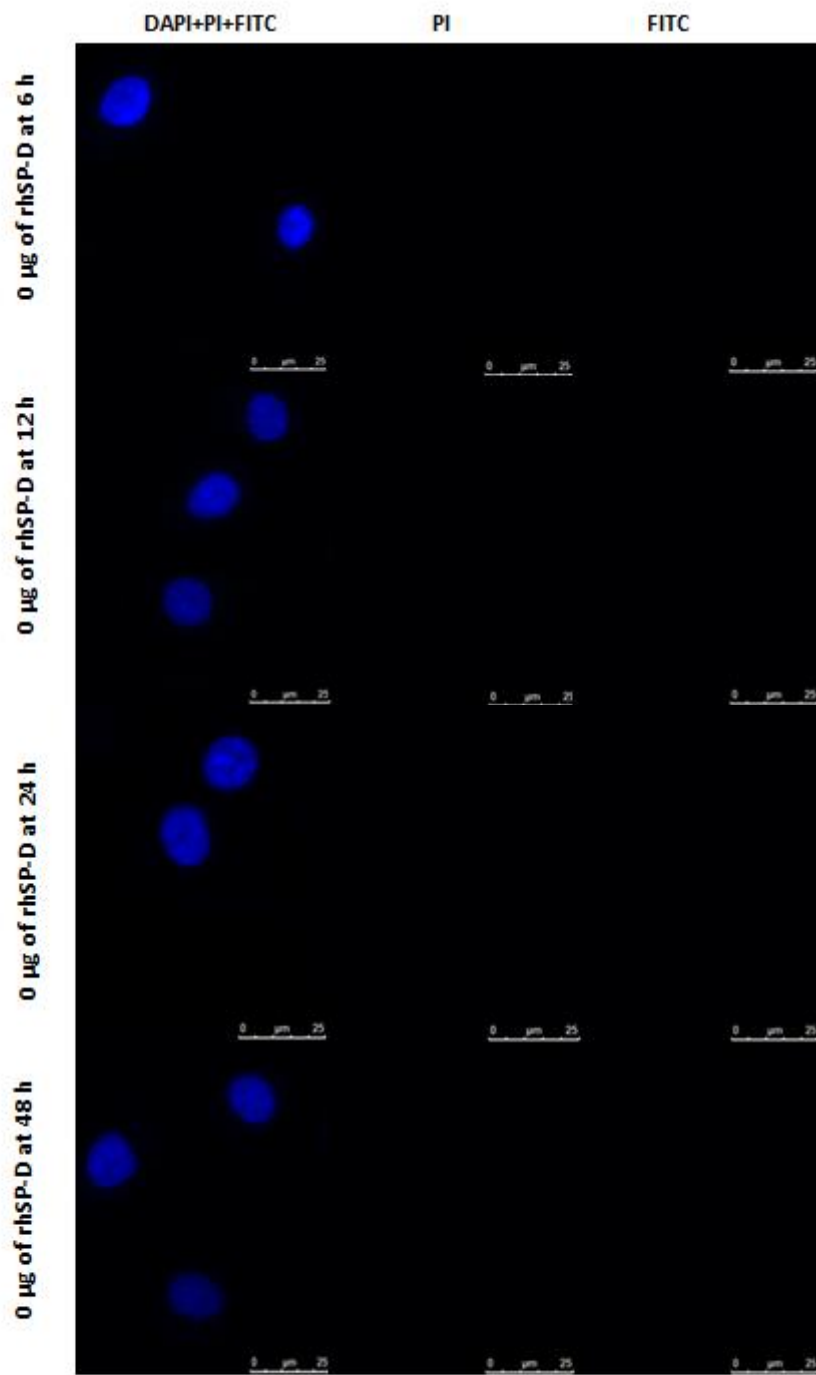
Fig 4.6. Binding of rhSP-D to the membrane of U87 cells was dose responsive and calcium dependent. U87 cells were grown for 24 h under normal growth conditions. The cells were incubated with A)15 µg/mL, B) 10 µg/ mL, C) 5 µg/ mL, D) 0 µg/ mL (control), E) no primary antibody (control) for 2 h at 4 °C. The cells were blocked with 2 % BSA and probed with anti-SPD and PA-FITC antibodies. DAPI was used to stain the nuclei and the fluorescence signals were observed with a Leica fluorescent microscope at 40X magnification. F) Graph of the % bound rhSP-D to U87. Error bars represent standard deviation.

4.3.7. rhSP-D does not induce apoptosis in U87 cells

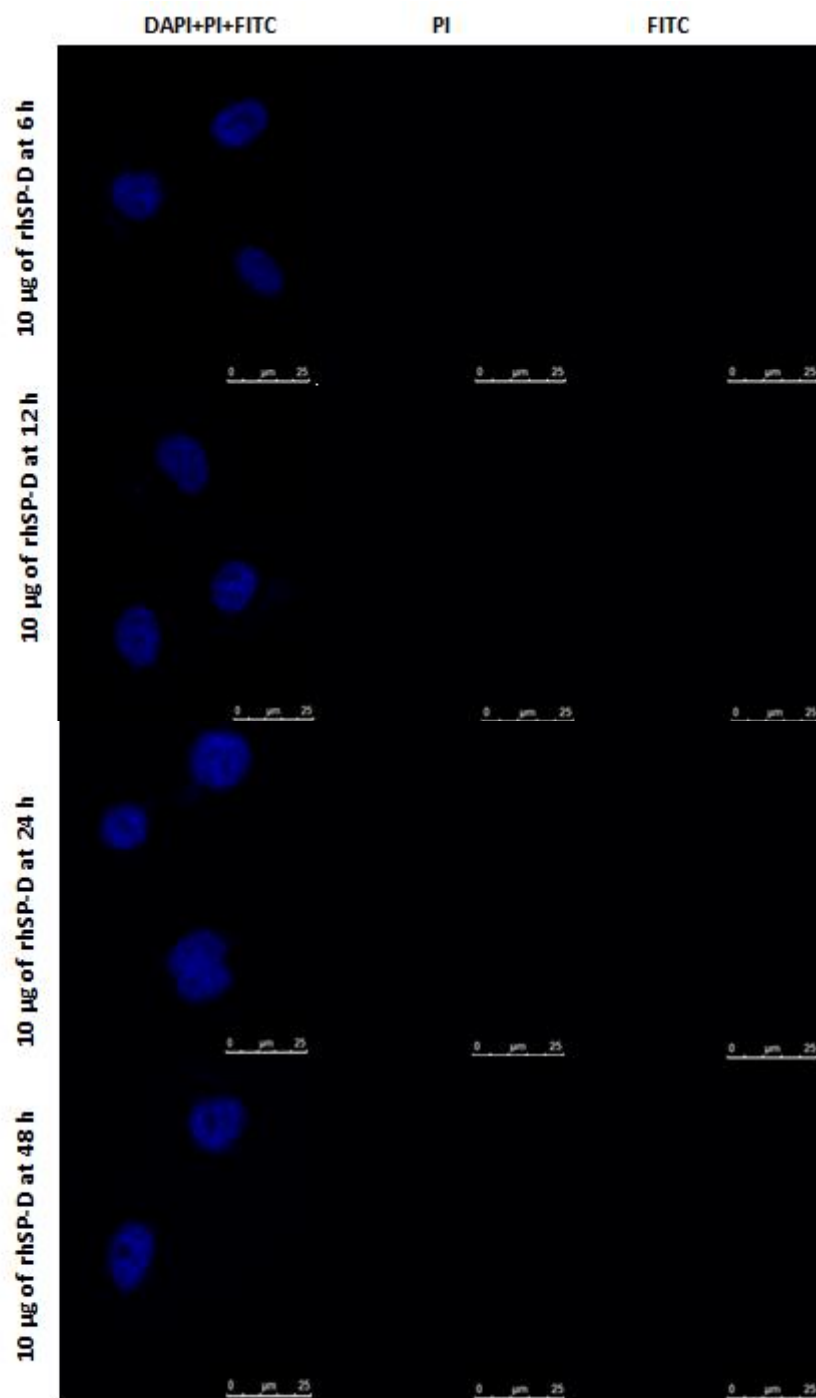
To determine the ability of rhSP-D to induce apoptosis in U87 cells an annexin V FITC apoptotic kit was used. Varying concentrations of rhSP-D were added to re-suspended U87 cells in the presence of CaCl_2 . The rhSP-D bound U87 cells were then grown for 6, 12, 24 and 48 h. Annexin V FITC was added to detect apoptotic cells as it has a high affinity for phosphatidylserine which are translocated to the outer membrane during early apoptosis. Propidium iodide was also added as it is permeable to damaged cells and allows a difference to be observed between cells destroyed due to apoptosis or necrosis. At each time point an image was taken with a Leica fluorescent microscope.

No green (FITC) or red (propidium iodide) staining was observed on the cell surface indicating that apoptosis nor necrosis had taken place (Fig 4.7. A-D). Despite increased concentrations of rhSP-D or longer incubation periods, U87 cells remained resistant to rhSP-D mediated killing.

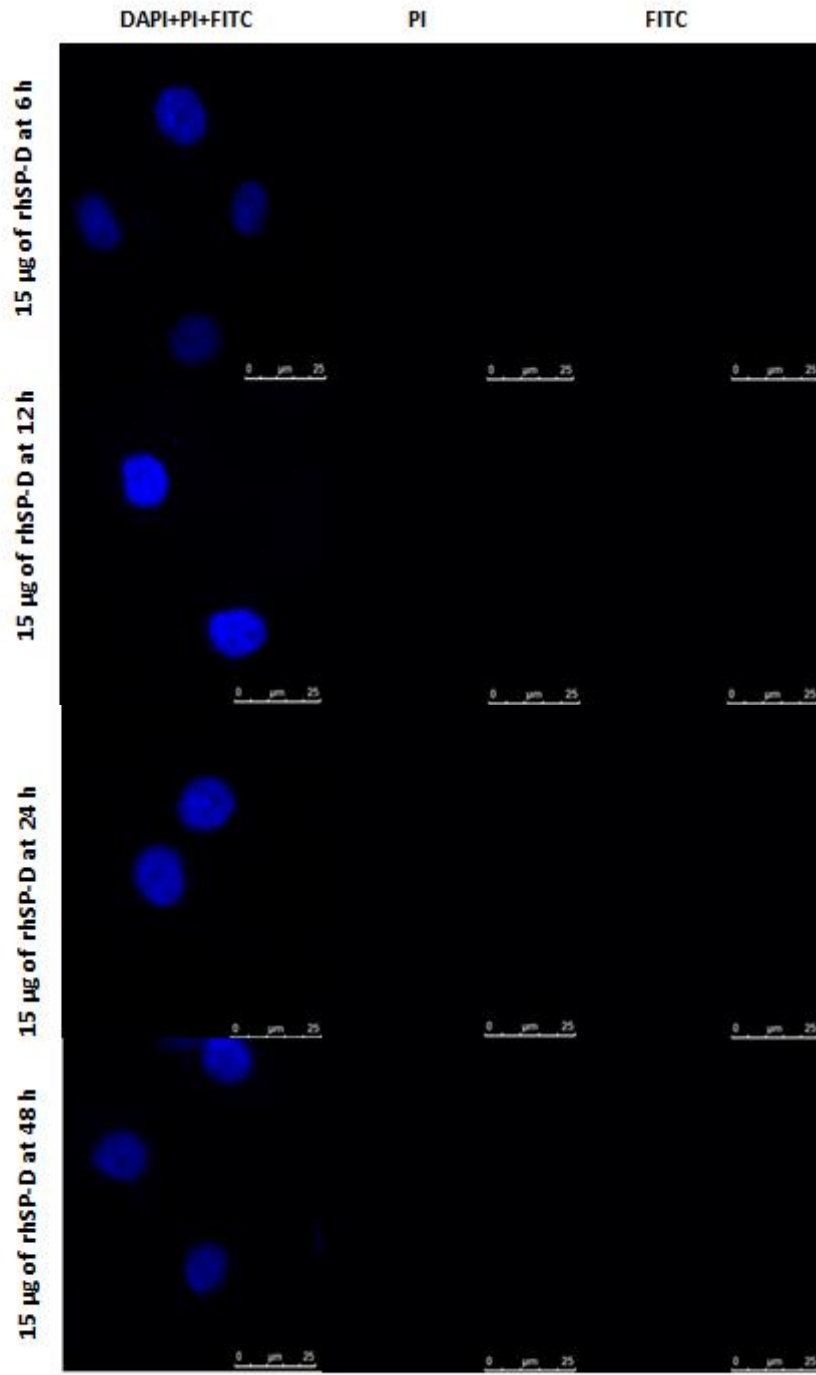
A



B



C



D

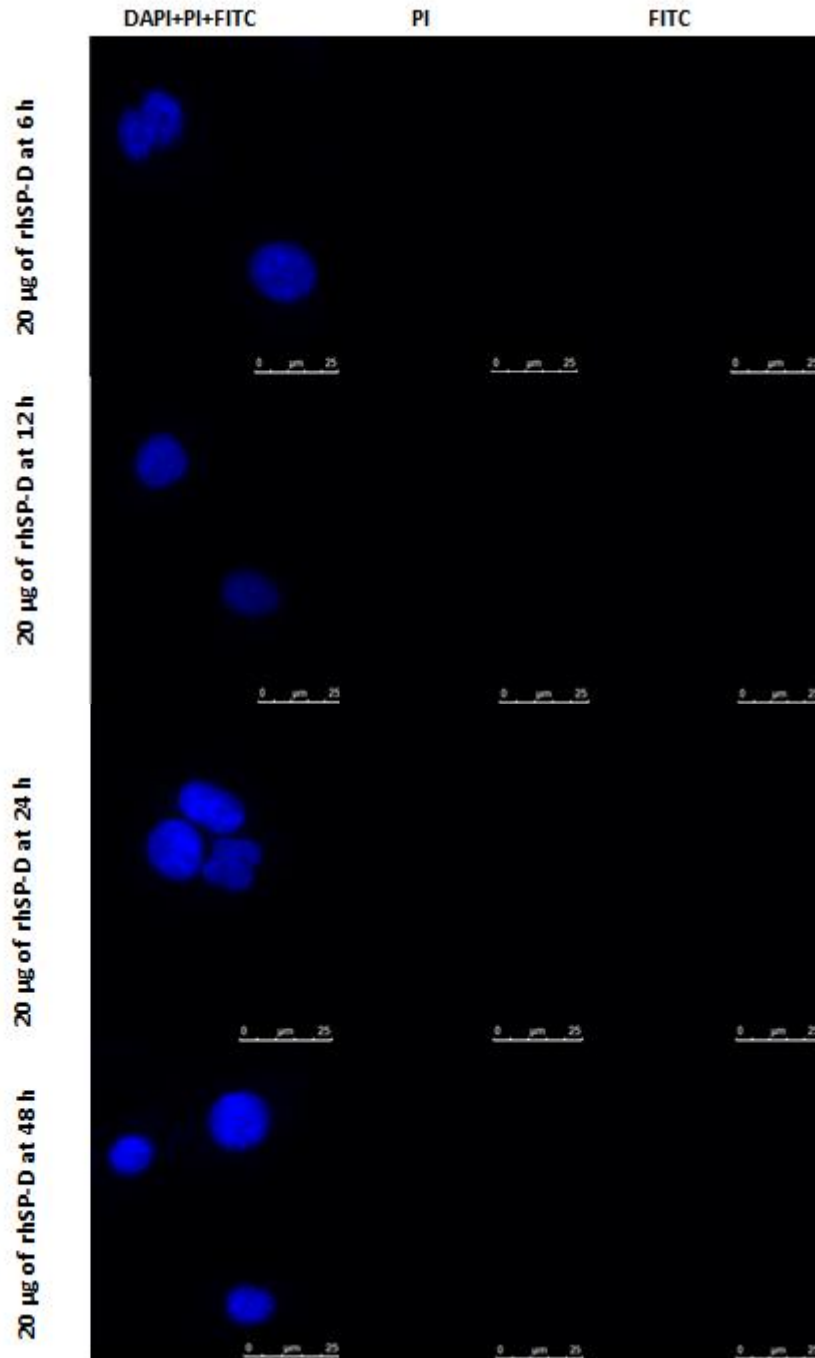
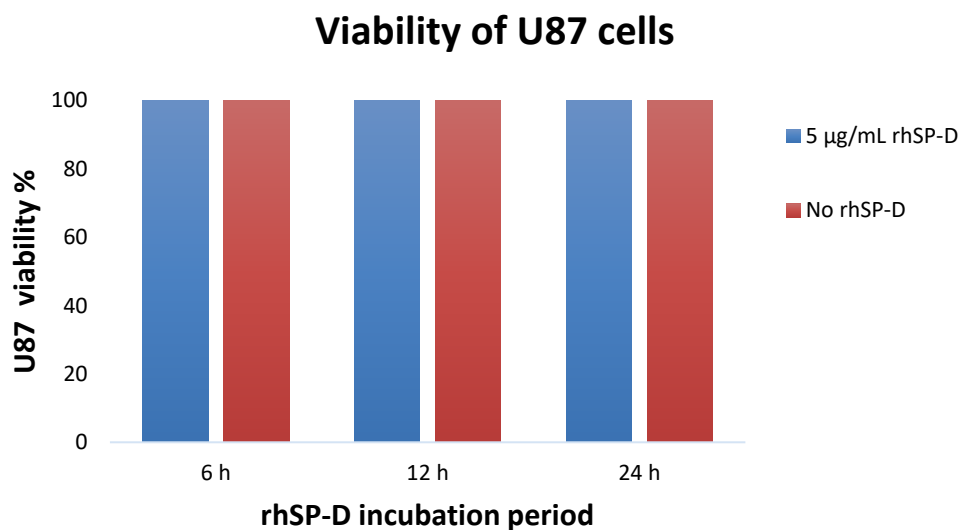


Fig 4.7. Fluorescent microscopy of the induction of apoptosis by rhSP-D. U87 cell were incubated with A) 0, B) 10, C) 15, and D) 20 µg/ mL or rhSP-D with 5 mM CaCl₂ for 2 h at 4 °C. The cells were grown for 6 h, 12 h, 24 h and 48 h. At each time point the cells were treated with Annexin V FITC and Propidium iodide. A Leica fluorescent microscope at 40X magnification was used immediately to view the results.

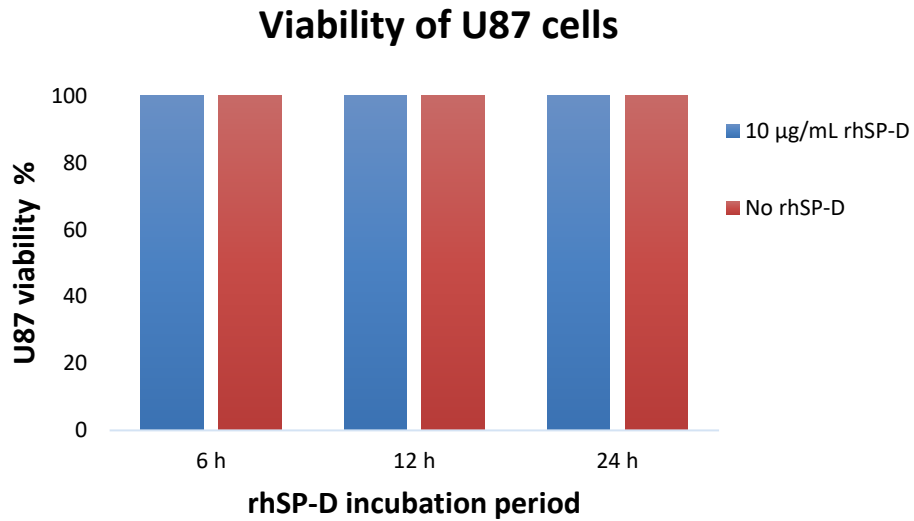
4.3.8. rhSP-D does not affect U87 viability

Cell viability and anti-proliferative effects of rhSP-D on U87 cells were evaluated by trypan blue assay. After the cells had been treated with varying concentrations of rhSP-D and viewed under a microscope, it was evident that trypan blue had not been taken up by any of the cells as they had not stained blue. Treated U87 cells showed 100% viability as the cell membrane integrity had not been lost (Fig 4.8. A-C). This indicated that rhSP-D did not have the capability to induce cell death despite the addition of increased rhSP-D concentration over a longer duration.

A



B



C

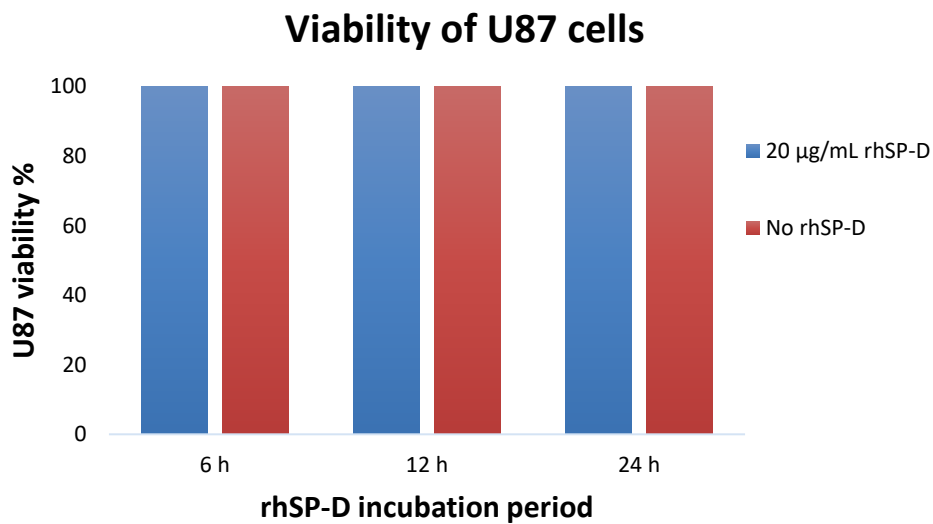


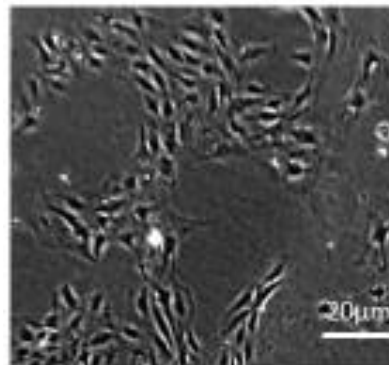
Fig 4.8. The effect of rhSP-D on the viability of U87 cells. Cell death was not induced in U87 cells when A) 5, B) 10, and C) 20 µg/mL of rhSP-D in the presence of 5 mM CaCl₂ was added to U87 cells. The cells had been cultured in DMEM-F12 for 24 h at 37 °C with 5% CO₂. Varying concentrations of rhSP-D were added for 6 h, 12 h, and 24 h. The adherent cells were dissociated and centrifuged. Cell pellets were re-suspended in 1 mL of DMEM-F12 and trypan blue was added in a 1.1 ratio. The number of viable and dead cells were counted using a haemocytometer and the % of cell viability was calculated with the formula (viable cell number/total cell)X100.

4.3.9. rhSP-D does not facilitate agglutination of U87 cells

To establish the physical effect of bound rhSP-D to U87 cells an agglutination assay was carried out. U87 cells bound to 10 μg and 15 μg of rhSP-D after 2 h of incubation at 4 $^{\circ}\text{C}$ in the presence of 5 mM CaCl_2 . The cells were grown overnight at 37 $^{\circ}\text{C}$ with 5% CO_2 for 24 h on a cover slip and the presence of agglutination was observed with a Leica microscope. There was no observation of U87 cells that had undergone agglutination and an increased concentration from 10 μg to 15 μg of rhSP-D did not induce clumping of the cells (Fig 4.9 A-C). There was no physical difference observed between the control group which did not have bound rhSP-D compared to the treated samples.

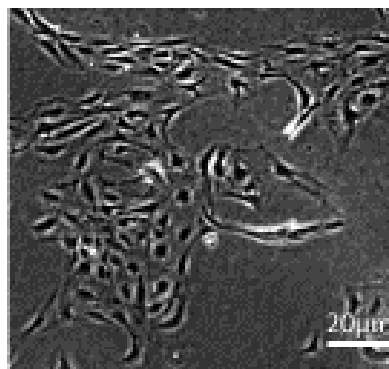
A

0 μg of rhSP-D



B

10 μg of rhSP-D



c

15 μg of rhSP-D

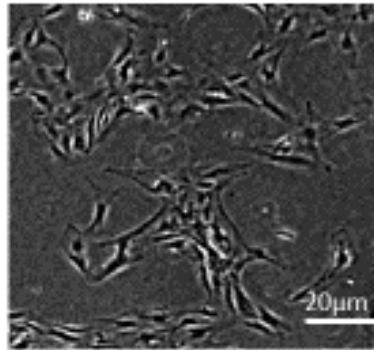


Fig 4.9. Agglutination assay of U87 treated with rhSP-D. U87 cells were incubated with 10 and 15 $\mu\text{g}/\text{mL}$ of rhSP-D with 5 mM CaCl_2 on a shaker at 4 $^\circ\text{C}$ for 2 h. The cells were transferred to a 24 well plate on top of a cover slip for 24 h at 37 $^\circ\text{C}$ with 5% CO_2 . The cells were fixed with 4% paraformaldehyde and viewed with a Leica microscope with phase contrast at a magnification of 10X. A) 0 μg of rhSP-D, B) 10 μg of rhSP-D, C) 15 μg of rhSP-D.

4.3.10. p53, TNF- α and IL-6 gene expression is reduced in rhSP-D treated cells

Gene expression RQ on rhSP-D treated and untreated U87 cells was performed with RT-qPCR. Specific p53, TNF- α , and IL-6 primers were used to produce the target gene in a thermal cycler machine. With each cycle number the amount of target DNA produced was increased and detected by SYBR green. The cycle number at which the fluorescent signal crossed the threshold (Ct) was used to calculate the RQ value. The RQs were converted into log 10 as gene expression levels were heavily skewed in linear scale. The results obtained were normalised against the stably expressed 18S gene and calibrated against the untreated samples.

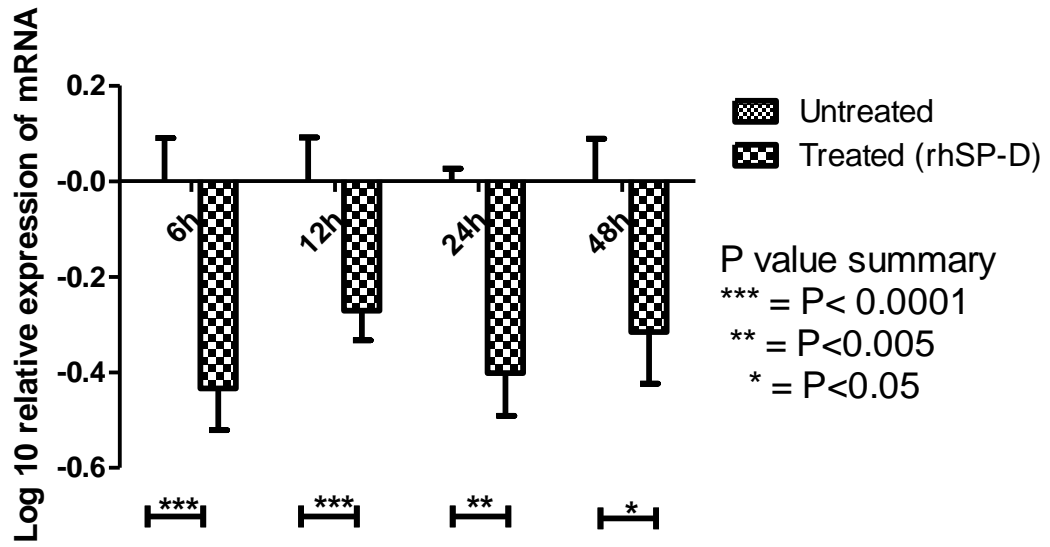
In order to statistically analyse 2 groups with paired observations a paired T-test was carried out in prism to analyse the difference in gene expression of p53 and TNF- α between treated and un-treated samples. At 6 and 12 h there is an extremely significant down regulation of p53 gene expression from U87 treated cells compared to untreated cells ($***=p<0.0001$). At 24 h a very significant decrease represented by $**=p<0.001$ in p53 expression was observed in treated cells and at 48 h a significant decrease ($=p<0.05$) was present. Overall there was a significant downregulation of p53 expression in U87 cells treated with rhSP-D compared to untreated cells (Fig 4.10. A)

An overall increase in the gene expression of TNF- α was observed between rhSP-D treated and untreated cells. At 6 h a significant upregulation of TNF- α expression occurred in treated cells ($=p<0.05$). An extremely significant upregulation ($***=p<0.0001$) took place at 12 and 48 h of rhSP-D treated U87 cells compared to untreated cells. Although there was also an increase of TNF- α gene expression at 24 h, the difference between both means was not significant (Fig. 4.10. B)

An extremely significant upregulation of IL-6 ($***=p<0.0001$) occurred during 6 - 48 h of growth between rhSP-D treated and untreated cells (Fig 4.10. C). A large surge in IL-6 expression is present at 6 h followed by a relatively consistent increased gene expression between 12 - 48 h.

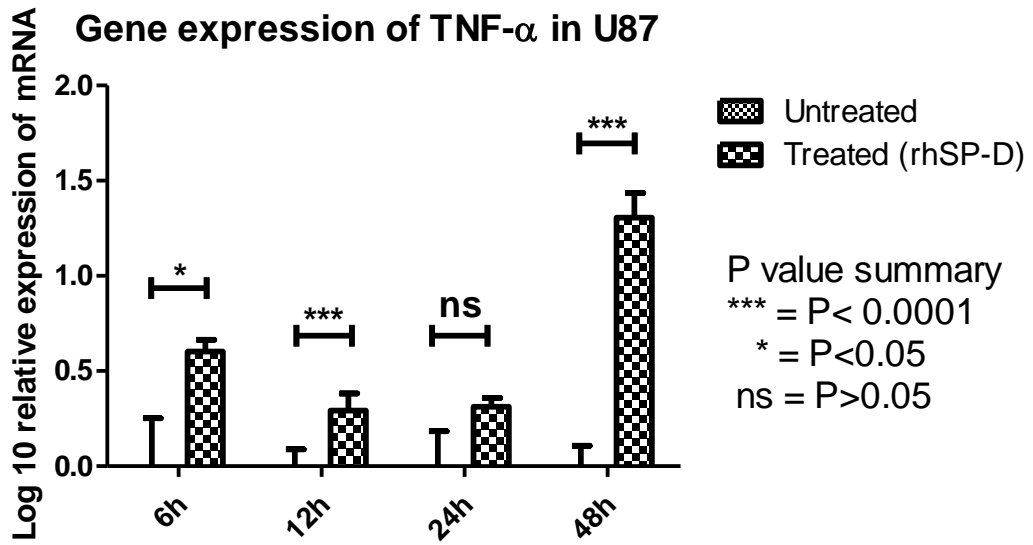
A

Gene expression of p53 in U87



B

Gene expression of TNF- α in U87



C

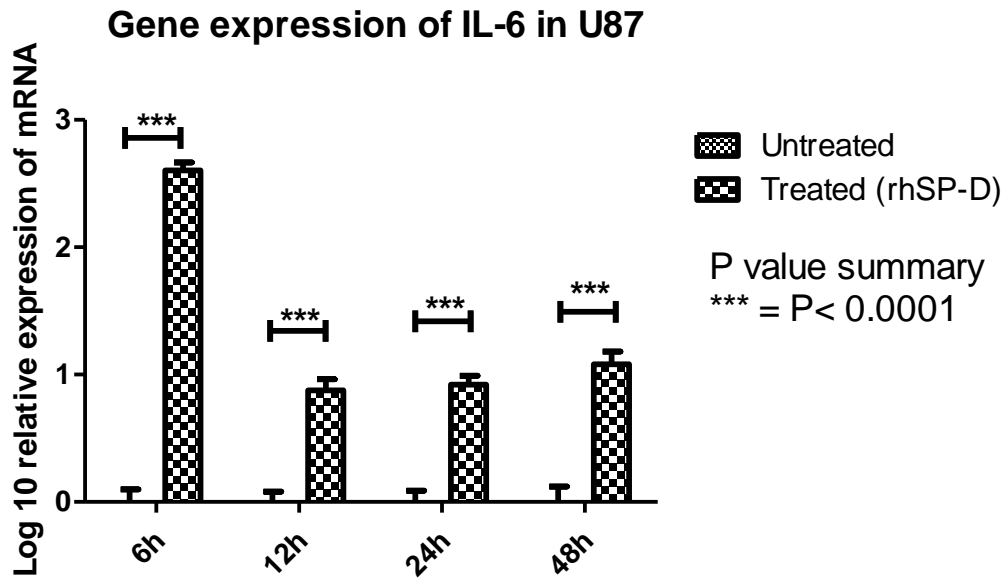


Fig 4.10. RT-qPCR of U87 treated and untreated cells. U87 cells were treated with 0 or 20 $\mu\text{g}/\text{mL}$ of rhSP-D for 2 h at 4 $^{\circ}\text{C}$ with 5 mM of CaCl_2 . The cells were grown for 1 h, 6 h, 12 h, 24 h and 48 h, at 37 $^{\circ}\text{C}$ with 5% CO_2 . At each time point the adherent cells were dissociated and pelleted down. RNA was extracted from the cells, followed by the synthesis of cDNA as described in materials and methods and analysed using qPCR using (A) p53, (B) TNF- α (C) IL-6 primers. The data was normalised against 18S endogenous control. Error bars represent standard deviation. RQ was calculated by using the comparative Ct method using the formula: $\text{RQ} = 2^{-\Delta\Delta\text{Ct}}$. A paired 2-sided T-test were conducted.

4.3.11. rhSP-D promotes U87 proliferation

A cell proliferation assay was performed in order to deduce if there was a difference in U87 cell proliferation between untreated and rhSP-D treated cells. To perform this experiment 10 and 15 µg of rhSP-D were bound to U87 cells in the presence of CaCl₂. The cells were grown in DMEM-F12 with 1% penicillin streptomycin for 48h. After which the adherent cells were dissociated and pelleted down. The cells were re-suspended in 1 mL of media and were added to trypan blue in a 1:1 ratio. To calculate the number of cells/mL. A haemocytometer was used along with the formula $\text{Total cells/mL} = (\text{Total cells counted}/\text{number of quadrants})/\text{dilution factor} \times 10^4$.

After 48 h incubation of U87 cells bound to 10 µg/mL of rhSP-D an increase in cell proliferation was detected in comparison to untreated cells. Within 48 h U87 treated cells had surpassed their doubling time as the average number of cells counted was 71000 compared to the control in which 52000 cells were present (Fig 4.11.). Likewise an increased proliferation of U87 cells that had bound 15 µg of rhSP-D was also observed with an average cell count of 77000 compared to 51000 cells counted for the control group. To establish the significance of the results a paired 2-sided T-test was conducted between treated and untreated cells. A significant increase in U87 cells treated with 10 µg of rhSP-D was observed (*= $p < 0.05$) and a very significant increase (**= $P < 0.001$) was also detected with cells treated with 15 µg.

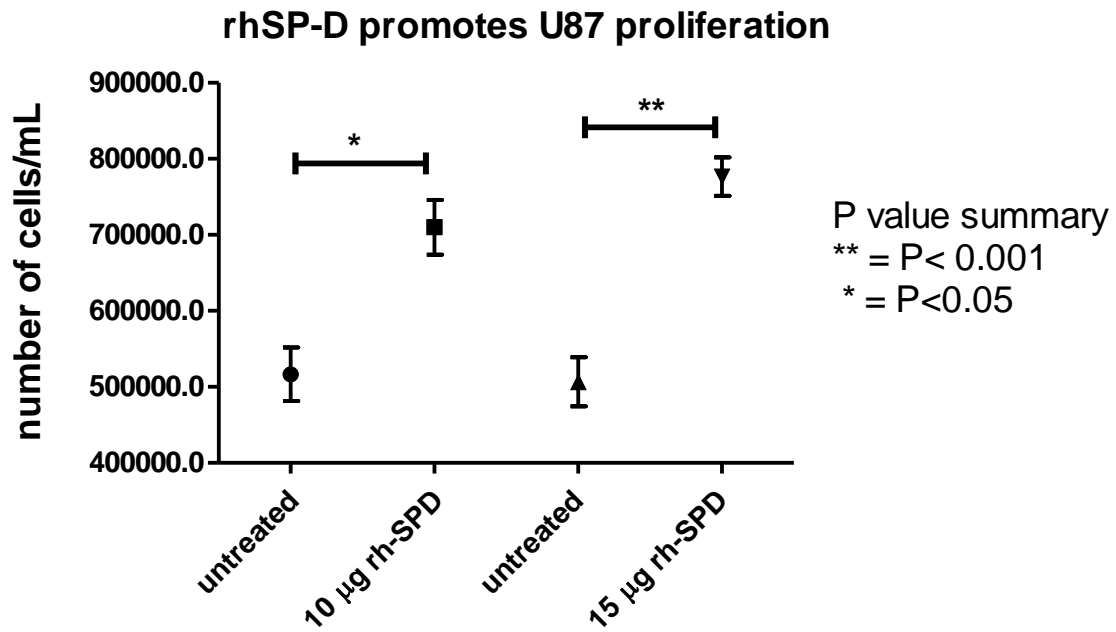


Fig 4.11. rhSP-D increased U87 proliferation. 0.25×10^6 U87 cells were incubated with 10 and 15 µg/mL of rhSP-D with 5 mM CaCl₂ were incubated for 2 h on a shaker at 4°C. The cells were grown for 48 h at 37 °C with 5% CO₂. The cells were centrifuged and the pellet was re-suspended in media. The cells were added in a 1:1 ratio with trypan blue and the number of cells per mL was calculated using the formula: Total cells/mL = ((Total cells counted/number of quadrants)/dilution factor) $\times 10^4$. A paired 2-sided T-test was conducted. Error bars represent standard deviation.

4.4. Discussion

In this chapter, we were able to successfully express plasmid pUK-D1 containing 8 glyx-y repeats, trimerising neck and CRDs in *E.coli* BL21(Δ DE3) pLysS upon induction with IPTG. Extensive processing of the inclusion bodies including isolation of cells, solubilisation, refolding and purification through affinity chromatography gave high yields of functional rhSP-D to be used in assays as a potential immunotherapy for GBM. Attention has been placed upon immunotherapy as a promising approach to treat various cancers, however such results are yet to be reflected in brain tumours as the immune privilege site the cells have originated from has curbed the expected response.

A major hurdle had to be overcome in the initial purification steps as the induced protein was frequently lost between large scale IPTG induction of transformed cells and purification of rhSP-D on a maltose agarose column. Clear induced bands could be visualised at 20 kDa via Coomassie blue staining of an SDS-PAGE large scale gel. However, after cell lysis, solubilisation of inclusion bodies and refolding the protein into its native form, rhSP-D was not successfully eluted. The addition of 50 μ g/mL of lysozyme to the lysis buffer did not result in a difference of rhSP-D recovery yield and therefore was not included in repeated purification attempts. A lower urea concentration from 8 M to 6 M was used in the solubilisation buffer and was found to enable a more efficient denaturation and smoother transition to the refolding of rhSP-D to produce high refolded yields of up to 700 μ g/mL. It is suspected that the reduction of concentration difference of urea between the solubilisation buffer and dialysing buffers allowed the protein to refold optimally without aggregation.

The high yield of rhSP-D obtained through affinity chromatography with a maltose agarose column confirmed that the CRDs of the recombinant protein have a high affinity for the carbohydrate in the presence of calcium. Coomassie blue staining of the SDS-PAGE gel for the eluted rhSP-D only produced a single band at 20 kDa. The absence of higher bands revealed no contaminants or higher oligomers were present

which rendered the protein to be pure therefore no additional purification steps such as ion exchange or gel filtration were needed. This eliminated the potential for protein to be lost during those purification steps. Western blot analysis confirmed that the eluted protein was rhSP-D and thus supported the result visualised by the gel for rhSP-D as the antibodies were able to detect the target protein.

Although there were no contaminants or higher oligomers observed on the SDS-PAGE for eluted rhSP-D it is known that upon incubation with *E.coli* BL21(Δ DE3) pLysS, LPS is released from the outer membrane and binds to the recombinant protein when the cells multiply. It was demonstrated that the pierce endotoxin removal column which contained ϵ -poly-L-lysine was effective in removing LPS from rhSP-D as the level of endotoxin measured was approved safe by European Pharmacopoeia and therefore would not interfere with in-vitro experiments by causing false readings. The final endotoxin levels obtained were also sufficient for rhSP-D to be used in-vivo as administration of the recombinant protein would not induce inflammation and septic shock therefore eliminating its potential to affect experimental results. It was evident through the high protein recovery of 87.5% revealed that rhSP-D had not aggregated with LPS or been removed with the endotoxin nor had it non-specifically bound to the column.

We decided to investigate the binding ability of rhSP-D to the membrane of U87 cells through indirect antibody immunofluorescent microscopy. It was important to demonstrate that the protein was able to bind in order to proceed with investigating the effect of bound rhSP-D to GBM cells (Mahajan *et al.*, 2008). Fluorescent microscopy was chosen as opposed to ELISA based binding assays as it enables a visual image of whether or not the protein had bound to the membrane or had become internalised. The Fluorescent ligand binding assay had initially shown the presence of rhSP-D throughout the entire U87 cell when the recombinant collectin was incubated with the cells at 37 °C for 2 h. The image indicated that rhSP-D had become internalised therefore the method was optimised through changing the incubation temperature

from 37 °C to 4°C. This adjustment had successfully shown that rhSP-D was able to bind to U87 without becoming internalised.

The visualised fluorescence image revealed that the CRDs of the purified protein were able to bind to carbohydrates on the cell membrane in the presence of calcium. This interaction was of great significance as it is vital for future analysis of the effects bound rhSP-D elicits. It is suspected that the homo-trimeric structure of rhSP-D which is held in place by the trimerising neck region is a crucial part of its binding ability as it is known to help maintain the orientation of CRDs (Hoppe and Reid, 1994) . As the N-terminal is not part of the recombinant protein, oligomerisation will not occur between membrane bound and free rhSP-D (Holmskov, Thiel and Jensenius, 2003). The dose dependent binding observed supports the notion that with a higher concentration of rhSP-D, the greater the percentage of bound protein to the cell membrane. The lack of binding visualised at 5 µg/ mL of rhSP-D indicates that at the reduced concentration the protein and cell membrane do not appear to come into close proximity which is essential for the protein to bind.

The ability of rhSP-D to induce apoptosis in U87 cells was investigated to establish whether this protein would have the same effect as those observed by Mahajan et al in 2013 and therefore could be considered as a potential immunotherapy for GBM. It was essential that the results of the apoptotic assay were viewed immediately by fluorescent microscopy as the cells could not undergo fixation. This procedure would have inactivated many functional abilities of the cell which would have ultimately effected the ability of rhSP-D to induce apoptotic pathways in the cells. The study provides evidence that despite rhSP-Ds ability to successfully bind to the membrane of U87 cells, the protein was unable to induce apoptosis. Treatment with higher doses of rhSP-D did not influence the outcome. These results opposed the findings previously obtained from Mahajan et al 2008 and 2013 in which it was demonstrated that rhSP-D was able to induce apoptosis in eosinophils from asthmatic patients,

leukaemic eosinophils and breast cancer cells (Mahajan *et al.*, 2013; Mahajan *et al.*, 2008).

In 2013, Mahajan *et al.*; 2013 revealed that the induction of apoptosis within leukaemic eosinophils and breast cancer cells were due to the activation of the p53 pathway (Mahajan *et al.*, 2013). This led us to investigate the gene expression of p53 upon administration with rhSP-D as it was likely to hold the crucial reasoning to the failure of apoptosis induction. P53 is a tumour suppressor protein which plays an important role during stressful conditions to regulate the cell cycle and trigger apoptosis. It is one of the most commonly mutated genes in human malignancies. However, in primary GBM which accounts for 90% of all GBM cases only approximately 20% of p53 is aberrant whereas more than 80% are mutated in secondary GBM (Nagpal *et al.*, 2006; Zilfou and Lowe, 2009).

The expression of p53 was investigated with RT-qPCR in order to gain a greater understanding of the expression levels at each time point. It was interesting to see that the results showed a significant downregulation of p53 expression which also contrasted with the results Mahajan obtained. It was clear that the addition of rhSP-D had the opposite effect to the one which was expected as upon administration the protein led to greater suppression of p53 expression and ultimately contributed to the prevention of apoptosis. None the less the decreased p53 gene expression did support the observed outcome of failure to induce apoptosis. The fact that the decline in p53 gene expression did not induce apoptosis indicates that the majority of these proteins are not mutated and suggests this particular cell line is derived from primary GBM. Aberrant p53 expression enhances tumorigenesis therefore it is likely that a decline in expression would have contributed to a reduction in tumourigenesis (Mao *et al.*, 2012). Therefore, had rhSP-D increased the accumulation of p53 of which the majority are wild type in primary GBM then it is very likely that anti-tumour conditions would have been promoted. This suggests that that U87 cells are derived from a patient whose

tumour did not escape destruction through the aberration of the tumour suppressor protein p53 and may therefore be a primary GBM.

Mahajan had previously shown that the ability of rhSP-D to induce oxidative stress which is an imbalance between free radical production and elimination had contributed to p53 accumulation which led to apoptosis. The induction of oxidative stress often requires the involvement of pro-inflammatory cytokines such as TNF- α which lead to elevated levels of reactive oxygen species (ROS) such as hydroxyl radicals. High concentrations of ROS damage DNA and protein which can lead to activation of the p53 signalling pathway and result in apoptosis (Salazar-Ramiro *et al.*, 2016). Therefore, we investigated the gene expression of TNF- α in U87 treated cells and the results showed an overall significant increase in gene expression. This finding eludes that the administration of rhSP-D to U87 cells up-regulated the gene expression of TNF- α which, in turn, would have contributed to the induction of oxidative stress. The enhanced generation of ROS as a result of oxidative stress is likely to have induced DNA damage and ultimately facilitate tumourigenesis instead of cell death (Landskron *et al.*, 2014) as neither p53 accumulation or apoptosis occurred.

In many cancers including GBM over expression of aberrant TNF- α is present and contributes to the enhancement of tumour progression (Smyth *et al.*, 2004). This makes known that in order for a tumour to progress successfully, aberration of TNF- α is essential as it prevents its ability to inhibit tumour growth through p53 activation therefore allowing the tumour to continue to spread. With this in mind it is suspected that the negative correlation between the increased TNF- α expression and reduced p53 expression after rhSP-D treatment indicate that TNF- α is involved. In cancers such as colorectal and ovarian TNF- α is known to upregulate p53 in order to induce apoptosis (Gotlieb *et al.*, 1994; Pastor, Irby and Poritz, 2010). However, it is clear that this was not the case with U87 treated cells which demonstrated that a tumour inhibitory environment was not present.

TNF- α is also known to induce the expression of the pro-inflammatory cytokine IL-6 which participates in the activation of oxidative stress (Landskron *et al.*, 2014; Sawada, Suzumura and Marunouchi, 1992; Tanabe *et al.*, 2010). We therefore investigated the change in gene expression of IL-6 in U87 cells before and after rhSP-D treatment in which a significant increase of IL-6 expression was detected in rhSP-D treated cells. This indicated that the treatment promoted tumour growth over a 48 h period as over expression of IL-6 is commonly detected in GBM and often contributes to glioma progression (Chang *et al.*, 2005). Reduced IL-6 expression would have likely suppressed tumour growth as previously demonstrated in a mouse model in which lost IL-6 signalling prevented the development of the tumour (Weissenberger *et al.*, 2004).

It is clear that rhSP-D administration is able to cause a pro-inflammatory response in U87 cells as demonstrated by the upregulation of TNF- α and IL-6. Under normal condition such a response would have elicited destruction of pathogens or altered cells in an attempt to maintain homeostasis. This shows that the current attempt to use rhSP-D as a potential immunotherapy to treat GBM directly reveals that due to the highly mutated and aggressive nature of the grade IV tumour that this form of treatment will not inhibit tumourigenesis. The stimulation of endogenous immune cells to induce apoptosis may have the opposite effect as many of the immune cells that are able to do this are aberrant and therefore can no longer elicit apoptotic effects when required. U87 cells were able to elicit a robust defence mechanism against the potential therapeutic effects of rhSP-D which had been demonstrated in leukaemic and breast cancer cells. Therefore, this gives greater understanding as to why the prognosis of GBM patients is extremely poor and why no major breakthrough in potential immunotherapies to treat GBM have occurred. It is highly likely that the immune surveillance ability of GBM cells is severely aberrant, thus stimulation of immune cells will not inhibit tumour progression.

The failure to induce apoptosis led us to investigate the effect rhSP-D had on U87 proliferation. We therefore carried out a proliferation assay which revealed that U87

proliferation significantly increased with increasing rhSP-D concentration over 48 h. It is suspected that the ability of rhSP-D to enhance proliferation of U87 cells is due to the upregulation of TNF- α and IL-6 and the down regulation of p53. This shows that rhSP-D induces tumorigenesis and suggests that IL-6 was able to play a key role in promoting proliferation as it is likely that the cytokine was able to bind to its receptors IL-6 R and co-receptor gp130. This would have activated the (JAK/STAT) pathway which lead to enhanced tumour progression (Landskron *et al.*, 2014).

The recombinant protein is also known to induce agglutination as demonstrated by Madan et al in which they revealed that as little as 1 μ g of rhSP-D was able to induce agglutination in the fungus *Aspergillus Fumigatus* (Madan *et al.*, 1997). They also demonstrated that the size of the clump formed is dose dependent. However, it was evident from my results that agglutination did not occur despite increased rhSP-D concentrations used. Agglutination by SP-D is followed by phagocytosis in-vivo which insinuates that the failure to induce agglutination in U87 is a mechanism through which cells avoid destruction and continue to proliferate. It is also likely that rhSP-D is unable to induce agglutination in tumours as it has only been shown in pathogens such as bacteria and fungi and not tumours.

We decided to conclude our experiments with a proliferation assay to establish if the addition of rhSP-D would affect the 48 h doubling time of U87 cells as although apoptosis was not induced the change in gene expression of p53 and cytokines eluded that a pro-tumourigenic environment was formed. Interestingly there was a significant increase between untreated cells and cells treated with 10 μ g of rhSP-D and a very significant increase when cells were treated with 15 μ g of rhSP-D compared to untreated cells. This reveals that the administration of rhSP-D to U87 cells accelerates proliferation which infers that the collectin promotes tumourigenesis.

These findings confirmed that not only does rhSP-D inhibit apoptosis but reduces the gene expression of the tumour suppressor p53 whilst simultaneously increasing the expression of pro-inflammatory cytokine IL-6 and TNF- α which are known to be pro-

tumourigenic in cancer. This ultimately lead to a significant increase of cell number in treated cells and demonstrated that rhSP-D enhanced a pro-tumourigenic environment and eventually cause the tumour to spread quicker. Therefore, our results show that rhSP-D administered alone cannot be used as a potential immunotherapy to treat GBM as it is associated with the development of an invasive glioma phenotype.

Chapter 5: The detection of SP-D in U87 and B30 cells

5.1 Abstract

For a long time, SP-D was considered to be a lung specific protein. In the last decade, a number of studies have reported extra-pulmonary existence of SP-D. We set out to examine if GBM cells themselves produced SP-D which can be exploited by tumour cells to induce proliferation in an autocrine manner, and at the same time, promote pro-inflammatory milieu for infiltrating microglia that form a major part of GBM tumour. Here, we report that GBM cells secrete full-length SP-D molecule which is antigenically similar to native human SP-D. Microscopy revealed their cytoplasmic presence. The secretion of SP-D by GBM cells increased exponentially in a time-dependent manner. Thus, this is the first study showing the competence of GBM cells to secrete SP-D which can have profound effect in the pathogenesis of GBM.

5.2 Objectives

SP-D has been studied intensively in the respiratory system and it is now widely acknowledged that the protein is expressed in extra pulmonary sites and has also been detected in extra-pulmonary tumours (Betz *et al.*, 1995). Recently it was reported that SP-D is present in the brain (Schob *et al.*, 2013). We hypothesised that SP-D is present in GBM. The aims of the study were:

- To detect SP-D in GBM cells
- To quantify secreted SP-D from GBM cells.
- To detect the intracellular presence of SP-D in GBM.
- To investigate the gene expression of SP-D in GBM cells

5.3. Results

5.3.1. Detection of SP-D in GBM supernatant

A western blot was performed to determine if U87 and B30 cells secreted SP-D which involved retaining supernatant from confluent cells that had grown for 48 h. The supernatant and the negative control of 2% BSA was separated on a SDS-PAGE gel and transferred onto nitrocellulose membrane for 2 h with 70 V at 4 °C. The membrane was blocked with 2% BSA and probed with anti-human, rabbit SP-D in a 1:1000 ratio with 1X PBS. The primary antibody was detected with *S.auerus* PA-HRP antibody to locate the position of the protein.

A distinct band was visualised at 43 kDa after the membrane was incubated with DAB for 5 min. The brown insoluble band was the same molecular weight as one of the monomeric structures that make up the homotrimeric subunit of SP-D. No band was observed in the negative control (Fig 5.1.) which indicates that nonspecific binding did not occur. The thickness of the band indicated that SP-D is strongly expressed by U87 cells. No higher or lower band were detected on the membrane which revealed that dimers and trimers of SP-D were not present after the sample was denatured at 100 °C.

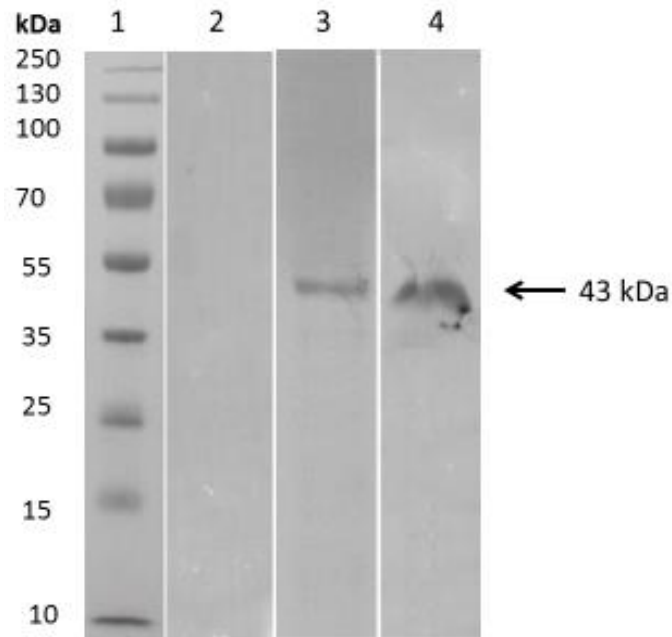


Fig 5.1. Western blot analysis of the secretion of SP-D by U87 and B30 cells. U87 and B30 cells were cultured for 48 h in serum free DMEM-F12 with 1% penicillin streptomycin. The supernatant and negative control 2% BSA were separated under reduced conditions on 12 % acrylamide gel and transferred onto a nitrocellulose membrane. The membrane was blocked with 2% BSA and probed with anti-SP-D and PA-HRP antibodies in a 1:1000 ratio with 1X PBS. DAB was added to the membrane and an image of the band was taken with a Bio-Rad imager. Lane 1. Protein marker, 2. 2% BSA, 3. B30 supernatant, 4. U87 supernatant.

5.3.2. SP-D is secreted by U87 and B30 cells

SP-D secretion from U87 and B30 cells was quantified by ELISA. The supernatant was removed at specific time points of 1 h, 6 h, 12 h, 24 h and 48 h to establish the change of SP-D secreted over a 48 h cell doubling period. The cells were immobilised onto the wells of a microtiter plate in the presence of CBC. A 2X serial dilution of 20 µg/100 µL of rhSP-D in the presence of CBC was carried out and used as a standard to form a calibration curve to calibrate the concentration of secreted SP-D. The wells were blocked with 2% BSA and probed with rabbit anti-SP-D and *S.auerus* PA-HRP antibodies in a 1:5000 ratio with 1X PBS to detect SP-D.

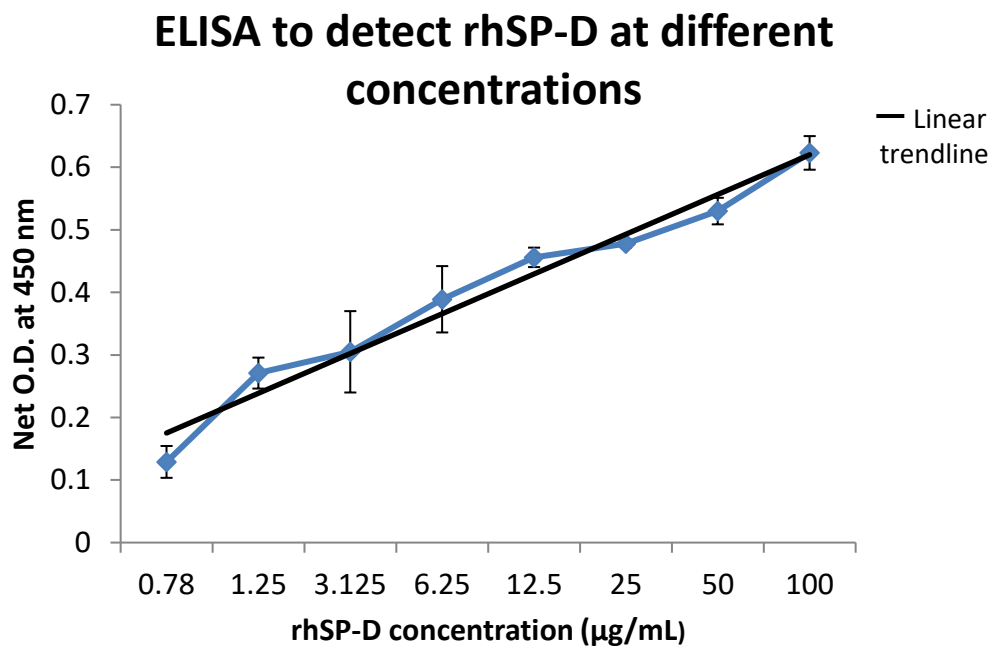
The linear calibration curve plotted demonstrated a positive correlation between concentration of rhSP-D and the 450 nm absorbance reading. The linear trend line passed through the majority of the points and was deemed reliable to be used to quantify SP-D secreted from U87 and B30 cells (Fig 5.2. A). The concentration of SP-D released from U87 and B30 cells increased in a time dependent manner (Fig 5.2. B,C) in positive correlation to the incubation time of GBM cells.

An unpaired t-test was used to establish if there was a statistically significant difference between the means of the 1 h time point against the 6 h-48 h time points. The test revealed that there was an extremely significant increase with a P-value of less than 0.0001 between the concentration of secreted SP-D at each time point compared to 1 h for both U87 and B30 cells. However, at 12 h of growth for B30, a significant increase with a P-value of less than 0.05 was obtained but none the less the value was still significantly different compared to 1 h. At 6 h and 12 h, U87 cells had secreted an average concentration of 2.2 and 2.7 (µg/mL) followed by a large surge of a 9 fold increase of secreted rhSP-D at 23.5 (µg/mL) for 24 h of growth. After 48 h of growth U87 had secreted an average of 72.0 (µg/mL) which is a 3 fold increase from 24 h.

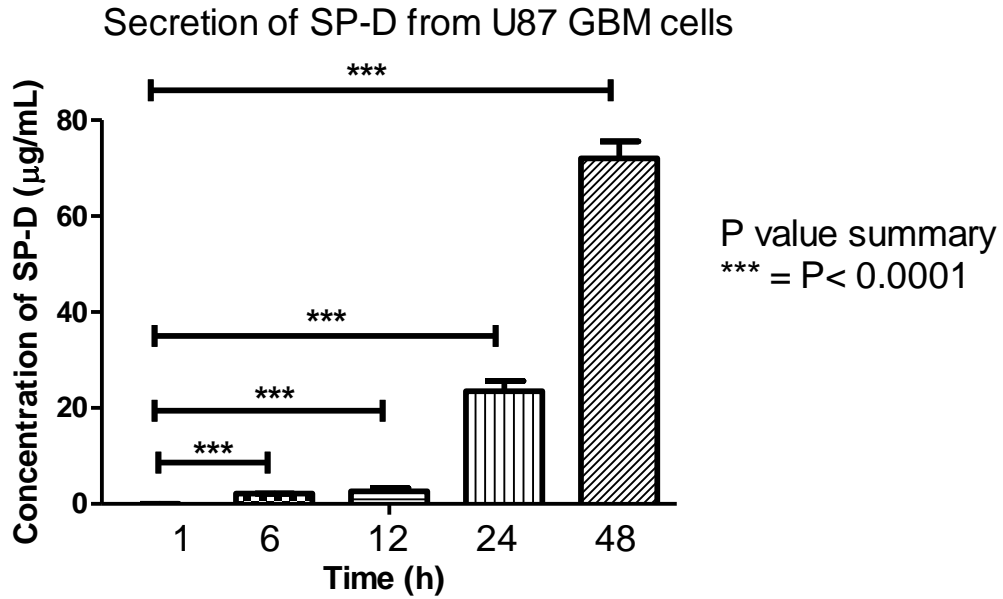
A similar trend was also observed for B30 cells as at 6 h and 12 h as there was an increase from 2.4 to 4.2 (µg/mL). Again, this was followed by a sharp 9 fold increase at

24 h of 35.5 ($\mu\text{g/mL}$) of secreted SP-D. There was then a 1.5 fold increase of secreted SP-D at 48 h of 56.5 ($\mu\text{g/mL}$).

A



B



C

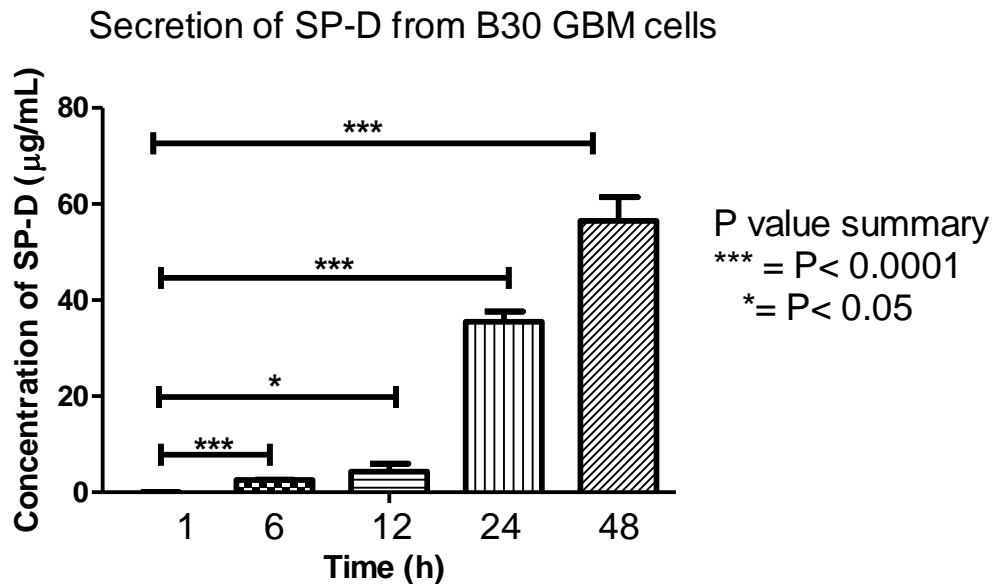


Fig 5.2. Quantification of SP-D in U87 and B30 cell by ELISA. U87 and B30 cells were grown in serum free media under normal growth condition for 1 h, 6 h, 12 h, 24 h and 48 h. At each time point the supernatant was removed and immobilised onto a 96 well microtiter plate with 0.5 M CBC. A 2 fold serial dilution of rhSP-D at 20 $\mu\text{g}/100 \mu\text{L}$ with CBC was carried out. The wells were then blocked with 2% BSA and probed with primary antibody, anti-SP-D and secondary antibody PA-HRP. OPD was added and the absorbance was measured at 450 nm. A 2 tailed unpaired t-test was performed. A) 2X serial dilution of rh-SPD 20 $\mu\text{g}/100 \mu\text{L}$ against 450 nm absorbance

reading. B) The concentration of SP-D ($\mu\text{g}/\text{mL}$) secreted at different time points for U87 cells. C) The concentration of SP-D ($\mu\text{g}/\text{mL}$) secreted at different time points for B30 cells.

5.3.3. Time dependent gene expression of SP-D in GBM

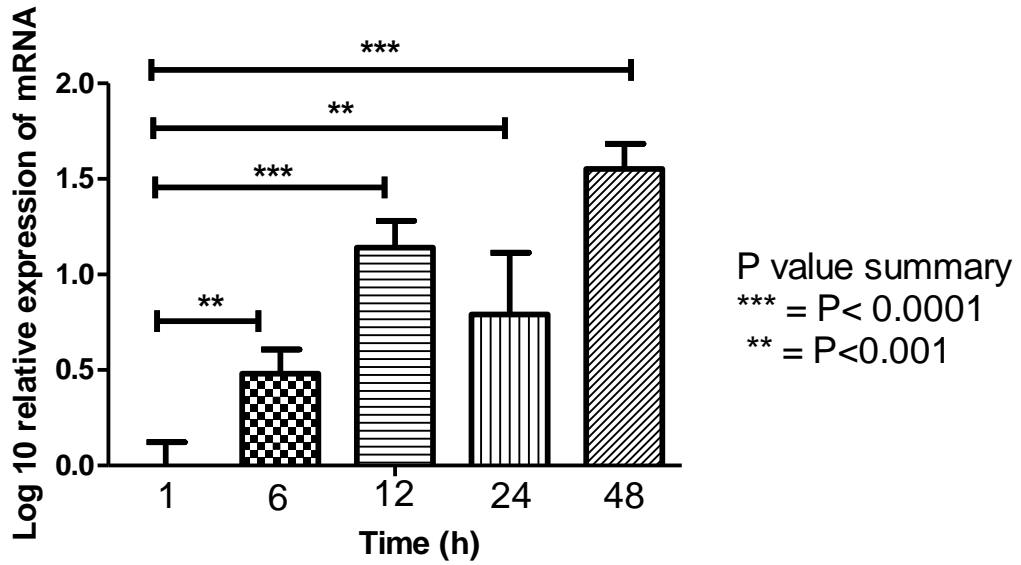
Having identified an increase in SP-D protein secretion over a 48 h period from U87 and B30 cells, the change of SP-D gene expression over the same 48 h time period was investigated. U87 and B30 cells were grown for 1 h, 6 h, 12 h, 24 h, and 48 h, after which the adherent cells were dissociated and pelleted down. RNA was extracted from the pelleted cells using a RNA extraction kit and then converted into cDNA using a RNA-cDNA kit. qPCR was performed to amplify the cDNA samples collected at different time points to determine the presence and RQ of the expression of SP-D gene in each sample with the use of specific primers.

The results obtained were normalised against the stably expressed 18S gene and calibrated against the 1 h time point. The data is expressed as (RQ) where the change in GBM gene expression is relative to the reference 1 h and a log₁₀ scale was used as results are highly skewed in a linear scale. An unpaired t-test was carried out to determine if the differences in the mean gene expression of the 2 samples and their relative standard deviation was due to chance.

All the time points displayed an increase of SP-D expression in a time dependent manner which were statistically significant. Data is expressed as log₁₀ of RQ and an unpaired T test was performed. There was a very significant increase at 6 h and 24 h represented by **= $P < 0.001$ and an extremely significant increase (***)= $P < 0.0001$ at 12 h and 48 h of U87 SP-D gene expression (Fig 5.3.A). At each time point, there was an upregulation of gene expression. At 24 h a biphasic pattern was observed as the concentration of protein was less than that at 12 h, none the less the expression was significant *= $P < 0.05$. A time dependent increase of SP-D gene expression for B30 cells was observed. There was also an extremely significant upregulation at 6 h, 24 h and 48 h represented by ***= $P < 0.0001$ and a significant increase of gene expression at 12 h (*= $P < 0.05$) (Fig 5.3.B).

A

Gene expression of SP-D in human U87 GBM



B

Gene expression of SP-D in human B30 GBM

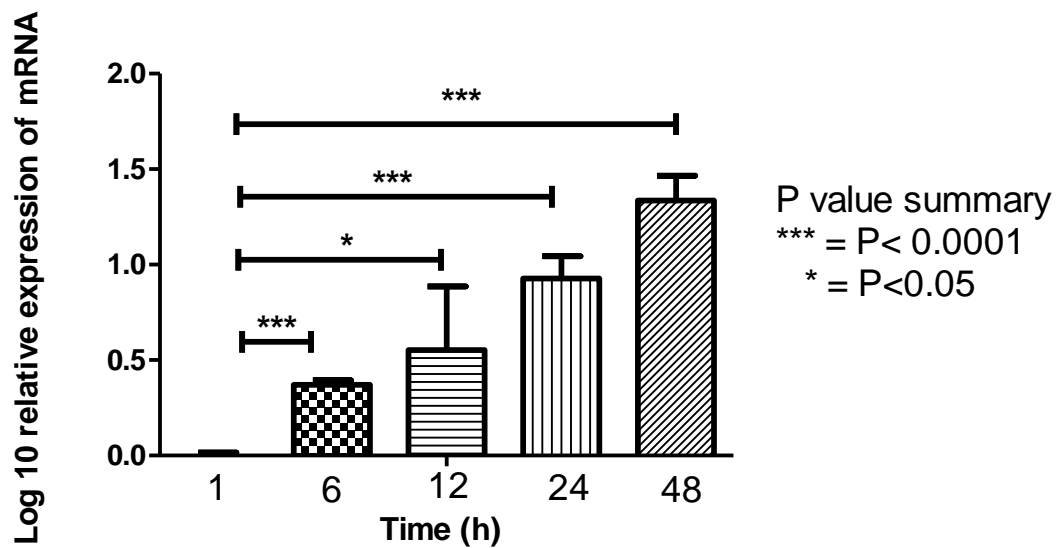


Fig 5.3. RT-qPCR of SP-D gene expression in U87 and B30 cells. GBM cells were grown for 1 h, 6 h, 12 h, 24 h, and 48 h at 37 °C with 5% CO₂. At each time point the

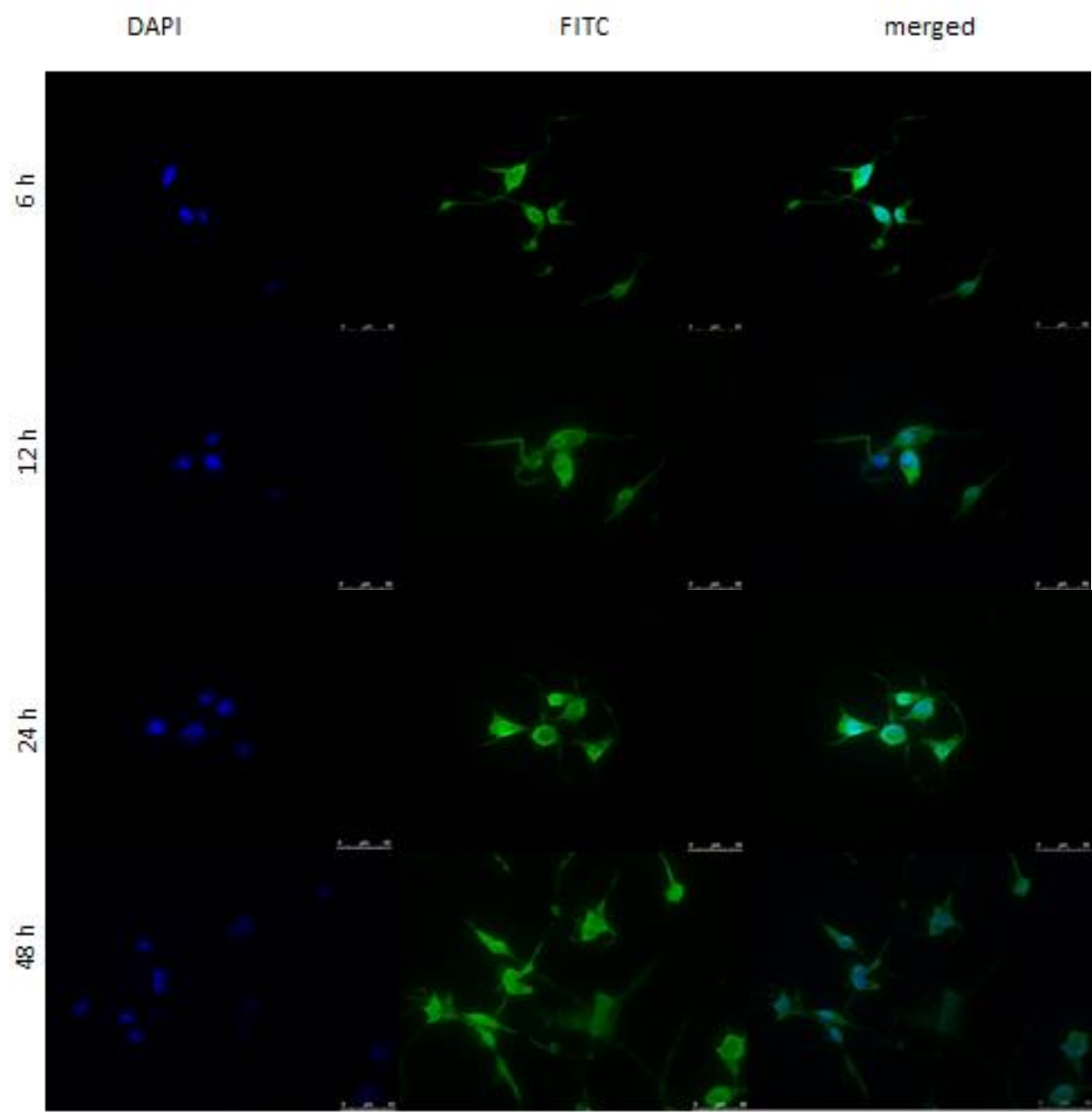
adherent cells were dissociated and pelleted down by centrifugation. RNA was extracted from the pellets in which the cells were lysed, then passed through an RNA binding column and RNA was then eluted. RNA was converted into cDNA using 2X RT buffer and 20X enzyme mix in which the samples were heated to 37 °C for 1 h and 95 °C for 5 min. A master mix for qPCR was made with distilled water, SYBR green, forward and reverse SP-D or 18S primers and cDNA. The samples underwent 40 cycles of the plate heated to 95 °C, 55 °C, and 72 °C at each cycle. The data was normalised against 18S endogenous control and calibrated against the reference of 1 h. Error bars represent $\log_{10} \pm$ standard deviation of the mean. The RQ value was calculated with the comparative Ct method using the formula: $RQ = 2^{-\Delta\Delta C_t}$. An unpaired 2-sided T-test were conducted.

5.3.4. SP-D is present in GBM cells

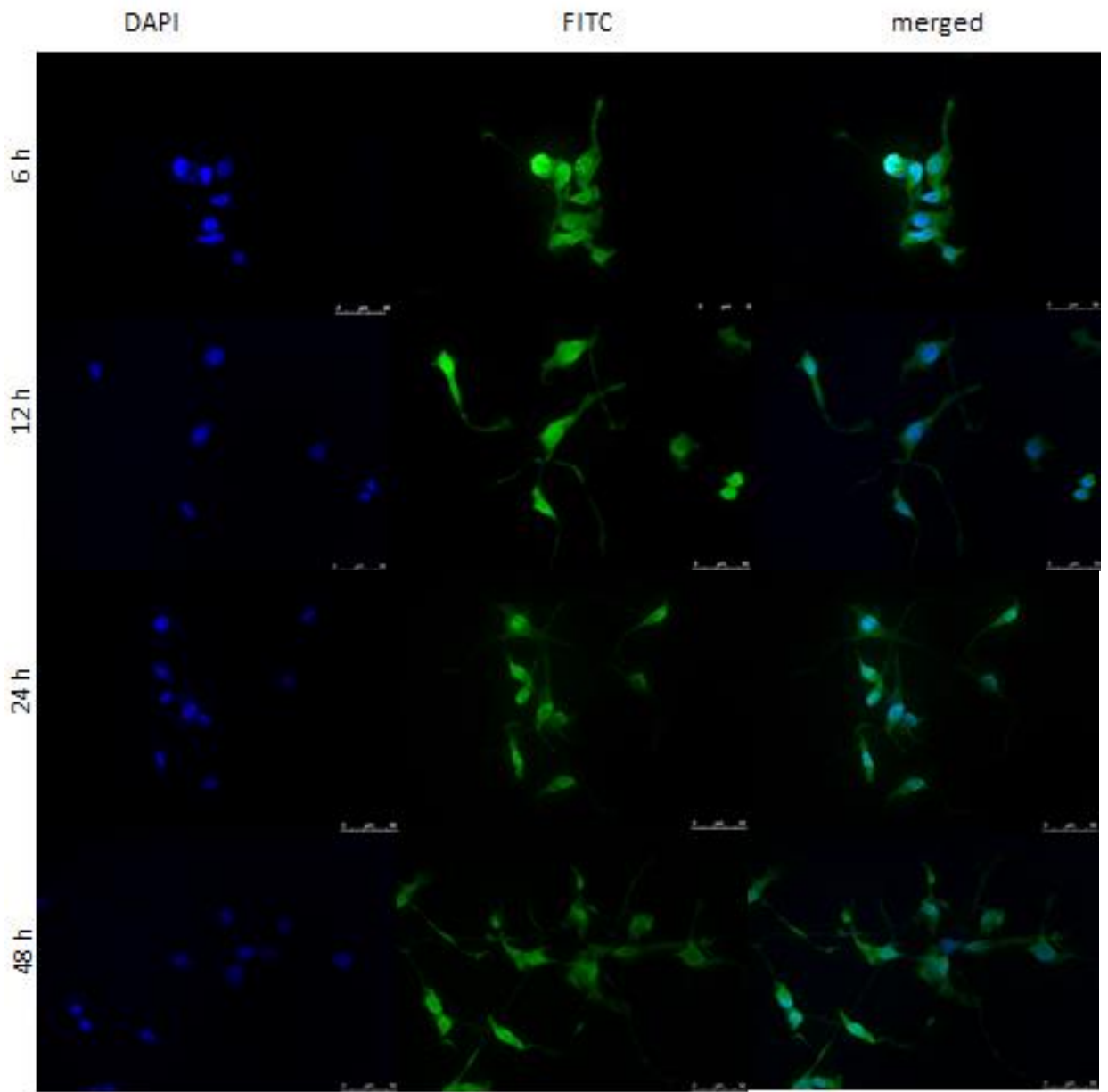
To confirm the intracellular presence of SP-D within U87 and B30 cells an indirect immunofluorescence technique was used. The cells were grown in serum free media for 6 h, 12 h, 24 h, and 48 h at 37 °C with 5% CO₂. The cells were fixed, permeabilised and then blocked with 2% BSA. The primary antibody anti-SP-D was added to detect SP-D within the cell. This was followed by the addition of the fluorescently labelled secondary antibody PA-FITC. DAPI was added to stain the nucleus and the slides were viewed under a Leica Fluorescent microscope at X20 objective.

The fluorophore DAPI was visible under the microscope for U87 and B30 cells including the controls. An intense FITC fluorescent staining was detected throughout the entire cytoplasm and nucleus of U87 (Fig 5.4.A) and B30 cell (Fig 5.4.B). No fluorescence was detected in the control (Fig 5.4.C,D). The FITC fluorescent dye was visible on U87 and B30 cells at each time point. There was also no difference in the intensity of the FITC dye observed for each time point. For both U87 and B30 cells between 6-48 h. The FITC stain was most intense at the nucleus and centre of the cells for both cell lines.

A



B



C

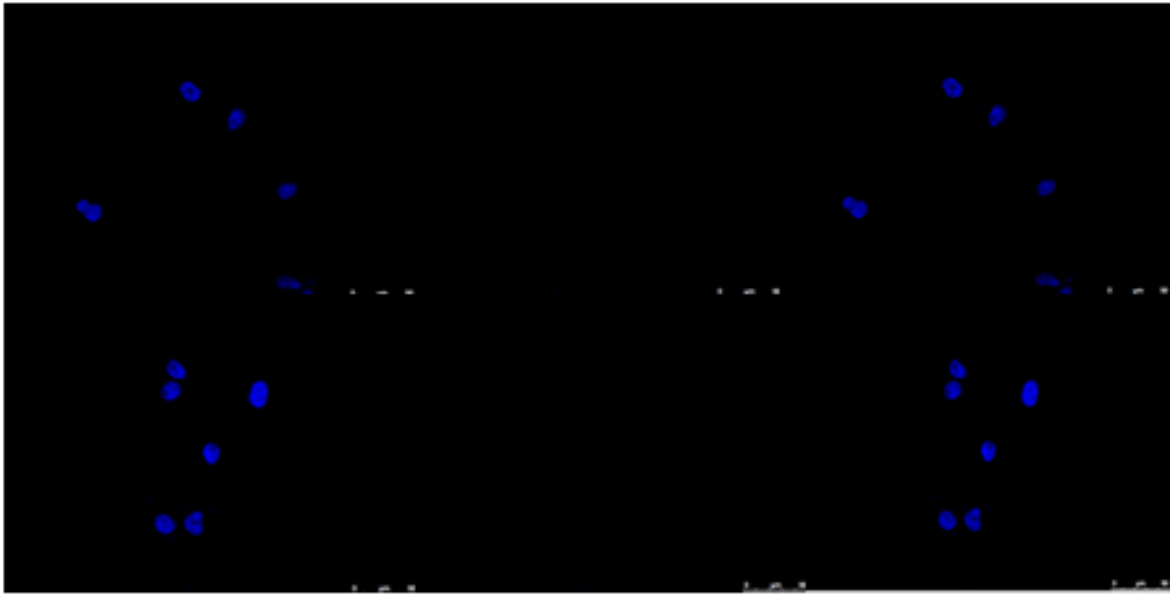
DAPI

FITC

merged

24 h no methanol

24 h no P-ab



D

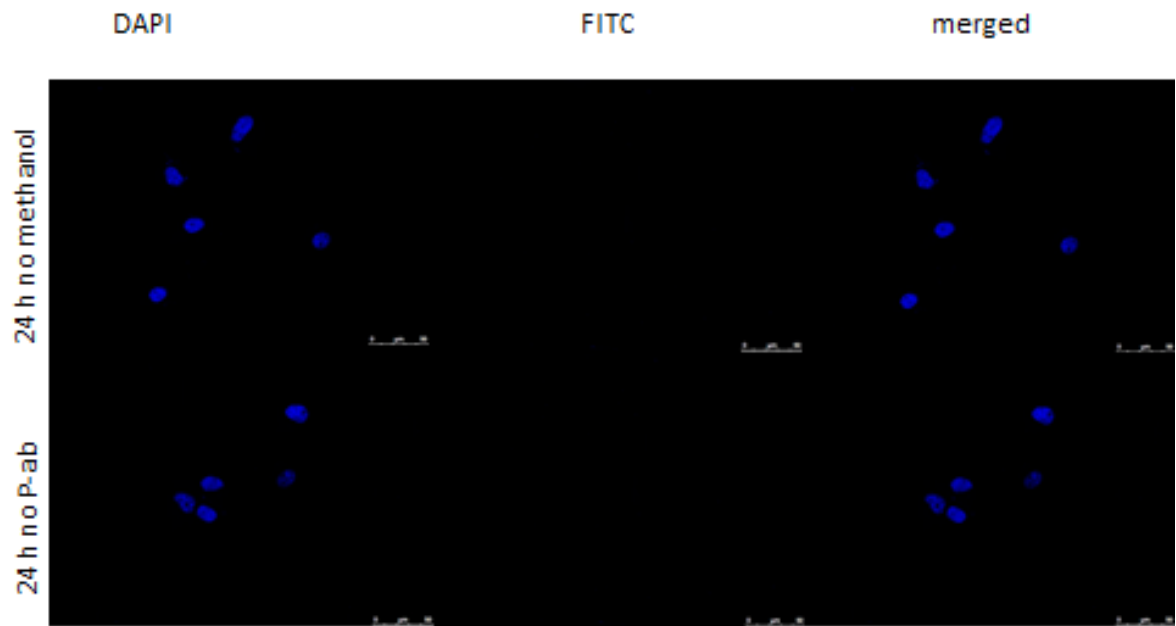


Fig 5.4. Detection of intracellular SP-D in U87 and B30 cells by immunofluorescent microscopy. U87 and B30 cells were grown in serum free media for 6 h, 12 h, 24 h, and 48 h at 37 °C with 5% CO₂. The cells were fixed with 4% paraformaldehyde and permeabilised with 100% methanol. 2% BSA was used to block the cells which were later probed with anti-SP-D and PA-FITC antibodies. A Leica fluorescent microscope was used to observe the presence of the fluorescence dyes at 20X magnification. A) U87 cell, B) B30 cells, C) U87 control, D) B30 control.

5.3.5. TNF- α and IL-6 gene expression is upregulated in U87 and B30

In order to investigate the gene expression of the pro-tumourigenic cytokines TNF- α and IL-6 an RT-qPCR was implemented for U87 and B30. The cells were grown in wells for 1 h, 6 h, 12 h, 24 h and 48 h at 37 °C with 5% CO₂. At each time point the pelleted cells were converted into RNA and then to cDNA. The cDNA was then subject to qPCR with the specific primer master mix. The results were normalised against the stably expressed 18S gene and calibrated against the 1 h time point. The data was expressed as RQ where the change in GBM gene expression is relative to the reference 1 h time point. A log₁₀ scale was used as results are highly skewed in a linear scale. An unpaired t-test was carried out to determine if the differences in the mean of gene expression of the 2 samples and their relative standard deviation was due to chance.

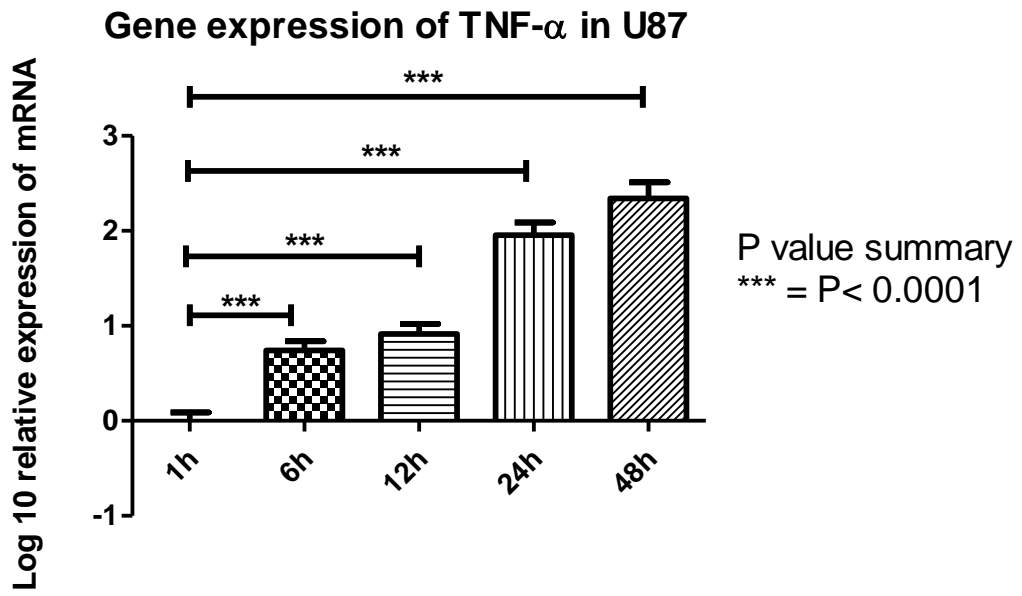
Over the 48 h incubation period of U87 cells it is clear that there was a time dependent increase in TNF- α gene expression. At each time point an unpaired T-test revealed that there was an extremely significant ($***=P<0.0001$) upregulation of TNF- α expression relative to the 1 h calibrator (Fig 5.5.A). Between 6 h and 12 h there was a slight upregulation in gene expression whereas a 2 fold increase was demonstrated between 12 h and 24 h. A considerable difference was also recorded between 24 h and 48 h. The gene expression of IL-6 revealed that there was an extremely significant upregulation at 6 h, 24 h, and 48 h ($***=P<0.0001$) after an unpaired T-test was carried out (Fig 5.5B). A very significant increase had taken place at 12 h represented by $**=P<0.001$. A biphasic trend was present between 6 h-24 h as at 12 h the gene expression was lower than the 6 h time point.

A time dependent upregulation of TNF- α gene expression similar to U87 was demonstrated in B30 cells. An unpaired T-test against the 1 h time point with the remaining 6 h-48 h was conducted individually. It was evident that at each time point the intensity of the significant difference increased in correlation (Fig 5.5 C). The unpaired T-test revealed that there was a significant difference at 6 h represented by $*=P<0.05$, a very significant increase at 12 h ($**=P<0.001$) and there was an extremely

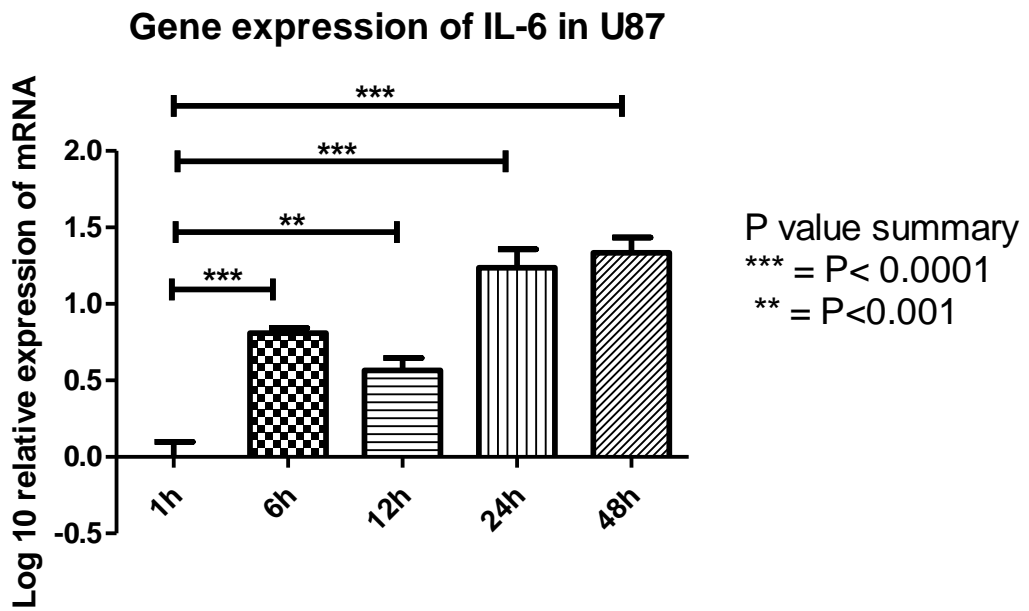
significant up-regulation at 24 h and 48 h ($***=P<0.0001$). A 2 fold increase was present between 6 h and 12 h as well as 24 h to 48 h with a slight increase recorded between 12 h to 24 h.

The gene expression of IL-6 in B30 over a 48 h growth period in serum free media showed that there was a time dependent increase. An unpaired T-test had shown that although there was an increase in IL-6 gene expression between 1 h and 6 h, the difference obtained was not significant which was indicated by $ns=P>0.05$. A very significant upregulation of gene expression had occurred at 12 h and 48 h ($**=P<0.001$) with an extremely significant increase recorded for 24 h revealed by $***=P<0.0001$ (Fig 5.5D). It must be noted that although the average gene expression of 48 h is greater than the expression for 24 h, the intensity of significance is greater at 24 h as the error bar is much smaller than 48 h. This is due to the fact that not only does the unpaired T-test take into account the mean difference but also the standard deviation between the replicates. There is also a 6 fold increase of IL-6 gene expression between 6 h to 12 h.

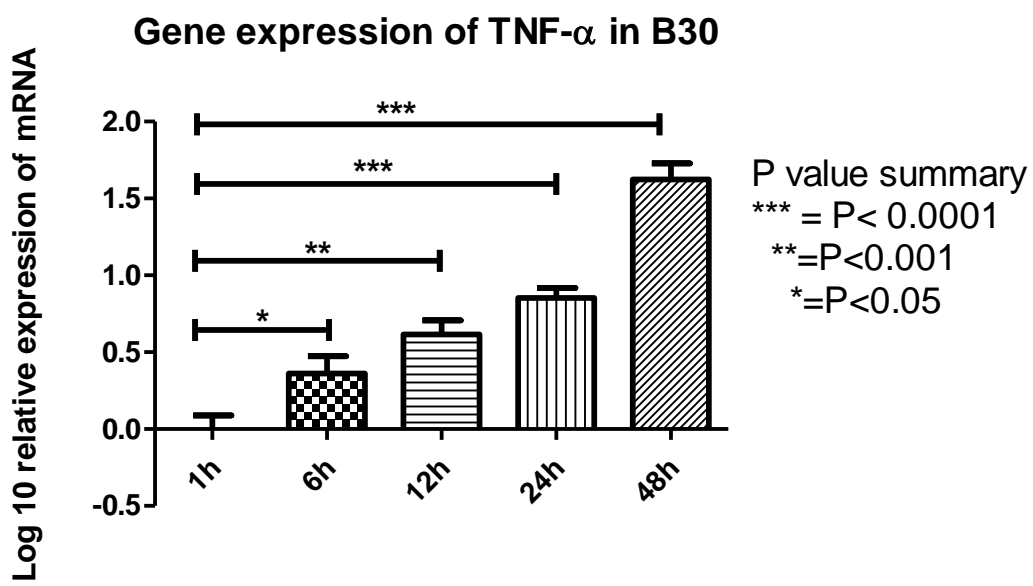
A



B



C



D

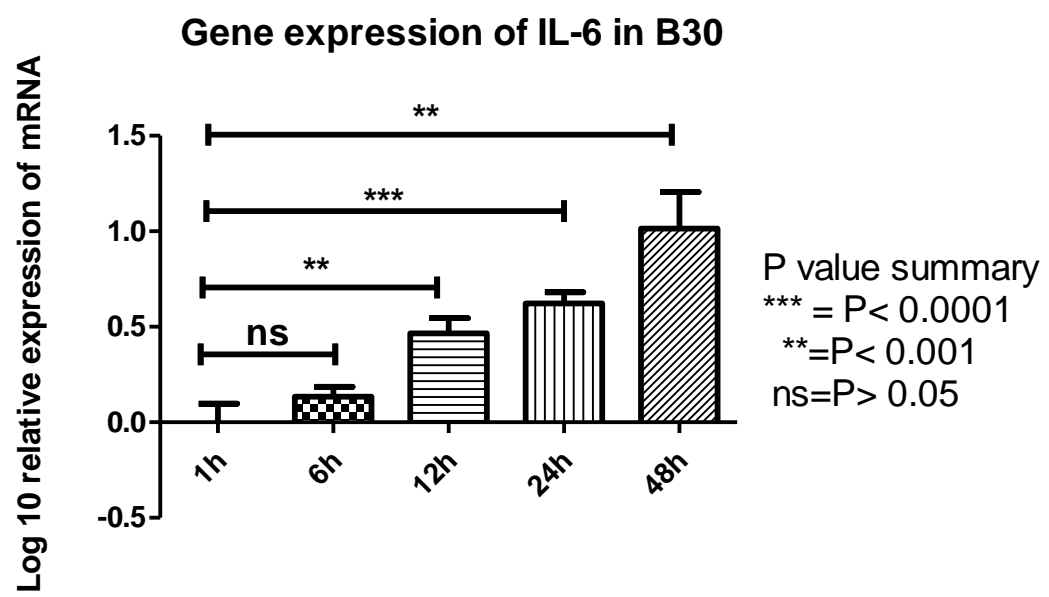


Fig 5.5. RT-qPCR analysis of cytokine gene expression in U87 and B30 cells. GBM cells were grown for 1 h, 6 h, 12 h, 24 h, and 48 h. RNA was extracted from U87 and B30 pellets and contaminating DNA was removed. cDNA was synthesised using 2X RT buffer and 20X enzyme mix in which the samples were heated to 37 °C for 1 h and 95 °C for 5 min. A master mix for qPCR was made with distilled water, SYBR green, forward and reverse IL-6, TNF- α or 18S primers. The master mix and cDNA were pipetted into a 96 well micro Amp plate and placed into a qPCR machine. The samples underwent

40 cycles of the plate heated to 95 °C, 55 °C, and 72 °C at each cycle. The data was normalised against 18S RNA endogenous control and calibrated against the reference of 1 h. Error bars represent $\log_{10} \pm$ standard deviation of the mean. The RQ value was calculated with the comparative Ct method using the formula: $RQ = 2^{-\Delta\Delta C_t}$. An unpaired 2-sided T-test were conducted. A) U87 TNF- α B) U87 IL-6 C) B30 TNF- α , D) B30 IL-6

5.4. Discussion

In the present study, the expression of SP-D was evaluated in the human cell line U87 and B30. We decided to investigate the expression of SP-D within GBM as the once known immune privileged site, has been revealed to host resident macrophages, microglia and innate immune cells. Pathogens can only enter the brain when the integrity of the BBB has been compromised (Carson *et al.*, 2006; Ransohoff and Brown, 2012; van Sorge and Doran, 2012). We already know that SP-D is a prominent innate immune cell of the lung capable of clearing pathogen and apoptotic cells which is a characteristic emulated in extrapulmonary regions such as the breast. Several cancers are known to produce SP-D such as prostate cancer and the presence of SP-D had also been detected in the brain but the source of the collectin remains unknown (Betz *et al.*, 1995; Schob *et al.*, 2013). Therefore, we decided to investigate if SP-D was also present in GBM. This finding would be of great interest as the brain is segregated from the lymphatic system therefore one would have to speculate where these cells would go. Astrocytes are known as key players to mediate innate immune response in the brain (Ransohoff and Brown, 2012) and with this in mind we hypothesised that not only may it be possible for SP-D to be produced in the brain but more specifically by GBM cells which are derived from astrocytes.

We wanted to investigate if SP-D was secreted by GBM cells through a western blot detection method. It was clear from the blot that after 48 h of GBM growth the cells had secreted SP-D into the supernatant. A single 43 kDa band produced which corresponds with SP-D revealed that no higher oligomers were present. This finding was ground breaking and of significant interest as no other publication has identified SP-D in GBM. Schob *et al.* had carried out experiments on the CNS and had detected SP-D but were unable to determine the source of the collectin. The western blot eludes that as GBM is able to secrete SP-D it is highly likely that normal astrocytes too have this ability. From the blot we can infer that SP-D is released from U87 and B30 cells and therefore will have an impact on GBM progression. It is interesting to find that SP-

D is secreted by GBM cells as many other expression sites, are within organs that are relatively prone to infection and do not have protection from the BBB which keeps entry of pathogens into the brain incredibly low (Pachter, de Vries and Fabry, 2003). In addition, the brain is known as a post mitotic region therefore clearance of dead cells that enter cell cycle arrest is not needed (Carson *et al.*, 2006). Bearing these 2 characteristics of the brain in mind, one would not put great emphasis on the potential secretion of the SP-D immune protein. This therefore suggests that the brain may be more susceptible to pathogen entry and cell cycle arrest leading to the formation of apoptotic bodies than previously believed. This would infer that under normal conditions SP-D would be expressed in order to maintain normal brain function.

Although the presence of SP-D has been detected in several adenocarcinomas, no one has yet identified the effect the protein has within cancer (Betz *et al.*, 1995). It could be suspected that the SP-D expressed would attempt to elicit a carefully executed innate immune response to destroy and clear altered self-cells. However, this trait would be more applicable to normal astrocytes surrounding the tumour. Instead it is likely that SP-D secreted by GBM cells have the ability to amplify tumour progression. One of the reasoning behind this proposed pro-tumourigenesis function of SP-D is that GBM is a highly aggressive tumour with many endogenous innate immune cells such as pro-inflammatory cytokines IL-6 and TNF- α contributing to the progression of the tumour. The second reason is that after U87 cells had been treated with rhSP-D, not only did the recombinant protein fail to induce apoptosis but resulted in an increased proliferation of GBM cells compared to untreated cells. This effect is therefore likely to be reflected within the endogenous expression of SP-D. Therefore the secretion of SP-D may be used as a mechanism through which GBM evade destruction from innate immunity.

The thick band produced on the western blot from U87 and B30 supernatant after 48 h of growth indicated that a considerable concentration of protein was secreted by the cells. We therefore decided to carry out an indirect ELISA method to establish the

concentration ($\mu\text{g/mL}$) of SP-D secreted by GBM at 6 h, 12 h, 24 h, and 48 h. Between 6 and 12 h the concentration of secreted SP-D increased steadily without a dramatic difference. This is likely to be due to the fact that within the first 12 h of cell growth the cells were transitioning between lag phase and early log phase as the cells pick up momentum and begin to adhere to the wells and divide. Despite this, the concentration increase from 0 h to 6 h and 12 h is extremely significant and should not be overlooked. Between 24 h and 48 h there was a large surge of secreted SP-D with a final concentration of 72 ($\mu\text{g/mL}$) for U87 and 56.5 ($\mu\text{g/mL}$) for B30. The continuous increase in concentration during cell proliferation is of significant interest as it is crucial for the protein to be secreted at a substantial concentration in order for the collectin to have an active role within the tumour. From these results we can infer that it is likely that as the tumour spreads in-vivo the concentration of SP-D will also increase and therefore continue to contribute to promoting a tumourigenic environment.

We then wanted to analyse the gene expression of the cells at the same time points used for ELISA to determine if the change in gene expression corresponded with the change in concentration of secreted SP-D. From the results, we were able to verify the presence of the gene within the nucleus of the cell and confirm that SP-D is an inherent protein of GBM. A time dependent expression level was also seen which was similar to the trend detected in the ELISA, and revealed that there is a correlation between gene expression and protein production to some extent. The increased SP-D gene expression at each time point suggests that there is a constant trigger of the innate immune protein system for increased production. The cells used are free from infection and are purely derived from GBM patients which indicate that the expression of SP-D is not controlled or regulated and is used by the tumour to create a pro-tumourigenic environment by inhibiting the destruction of abnormal cells.

The presence of SP-D within the cytoplasm of U87 and B30 was confirmed by indirect intracellular detection with fluorescent microscopy. It showed that SP-D was

successfully synthesised in the cytoplasm where it was later secreted into the micro-environment and therefore able to interact with other cells and influence their effect. The presence of cytoplasmic SP-D highlights that the innate immune protein has the ability to influence the cell it is in and therefore likely to inhibit cell cycle arrest.

Endogenous SP-D is known to influence the expression of cytokines (Schaub *et al.*, 2004). With this in mind we decided to investigate the change in gene expression of pro-inflammatory cytokines IL-6 and TNF- α which are known to have pro-tumourigenic effects in tumours (Chang *et al.*, 2005; Smyth *et al.*, 2004). The expected results were seen as there was an upregulation of both cytokines over a 48 h period. This trend mirrored the gene expression of SP-D and therefore suggested that the expression of the collectin enhanced the expression of the pro-tumourigenic cytokines TNF- α and IL-6 accordingly. It is known that expression of TNF- α triggers the expression of IL-6 and it is clear from the results that the gene expression levels of TNF- α in U87 and B30 is higher than the expression for IL-6 (Kurokouchi *et al.*, 1998). This suggests that it is possible that TNF- α expression induces the expression of IL-6 which is why TNF- α expression level is higher. The results have shown SP-D has the ability to promote the expression of pro-tumourigenic cytokines in order to promote tumour growth and infiltration whilst enabling GBM to avoid destruction.

In conclusion, the intrinsic and secreted form of SP-D from U87 and B30 is ground breaking and sheds new light on the previous immune privileged conception of the brain. It was also interesting to see that SP-D which would of likely had a pro-inflammatory innate immune response in normal astrocytes is likely to of had pro-tumourigenic effect in GBM. The ability of GBM to produce SP-D to favour tumour growth supports the notion that this highly invasive tumour is able to progress quickly by altering innate immune cells to support its growth.

Chapter 6: The effect of THP-1 in co-culture with U87

6.1. Abstract

In GBM, nearly 40% of the cellular component is constituted by microglia cells. We wanted to examine the effect of rhSP-D co-culturing a macrophage cell line THP-1 cells with GBM cells. THP-1 cells were induced into differentiation by rhSP-D on its own without requiring PMA. The adhesion of the cells to the surface was of a high affinity so much that trypsin-EDTA could not dissociate adherent THP-1 cells. The co-culturing altered the transcriptional levels of cytokines in a retrograde manner. Although THP-1 cells failed to uptake GBM cells, the viability and growth of GBM cells was considerably reduced in the co-culture system. In addition, the levels of secreted factor H and SP-D by GBM cells were also reduced in the THP-1-U87 co-culture system. These results suggest that macrophages/microglia can potentially be protective against GBM; however, their inability to engulf and process the GBM cells perhaps due to complement resistance can be the limiting factor in the fight against GBM.

6.2. Objectives

Previous reports indicate the ability of SP-D to opsonise cells for phagocytosis (Geunes-Boyer *et al.*, 2009). We hypothesised the rhSP-D would opsonise U87 cells in the presence of THP-1. The main objectives were:

- To study the ability of rhSP-D to differentiate THP-1
- To assess the change in cytokine gene expression of U87 cells in co-culture with THP-1
- To investigate the ability of rhSP-D to opsonise U87 cells
- To study the effect THP-1 co-culture has on the proliferation of U87
- To investigate the secretion of SP-D and factor H in a co-culture with U87 and THP-1

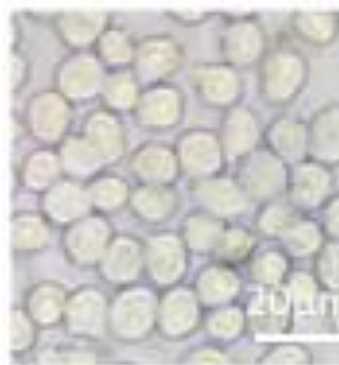
6.3 Results

6.3.1. THP-1 cells are differentiated by rhSP-D

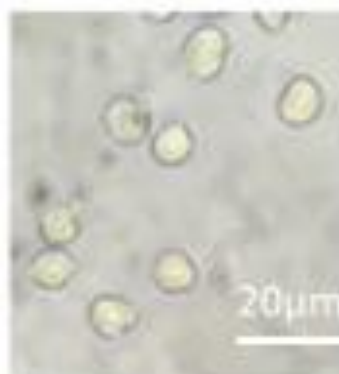
In order to analyse the ability of rhSP-D and PMA to differentiate THP-1 into macrophage a differentiation assay was implemented. THP-1 cells were incubated separately for 24 h with 25 ng/mL of PMA (Fig 6.1,A), 15 μ g/mL of rhSP-D and 5 mM of CaCl₂ (Fig 6.1,B) and THP-1 alone as a negative control (Fig 6.1,C). The number of adherent cells and cells in suspension were counted and the % of differentiation was calculated and a graph was produced (Fig 6.1,D).

After 24 h of growth an average of 98% of THP-1 cells had differentiated after treatment with 25 ng/mL of PMA . A paired T-test revealed that this % of differentiation had an extremely significant increase compared to the untreated sample (***)= $P < 0.0001$). Treatment with 15 μ g/mL of rhSP-D had an average of 20 % differentiated THP-1 cells. This percentage was a significant increase demonstrated by *= $P < 0.05$ when compared to the untreated sample of un-differentiated THP-1 cells.

A



B



C



D

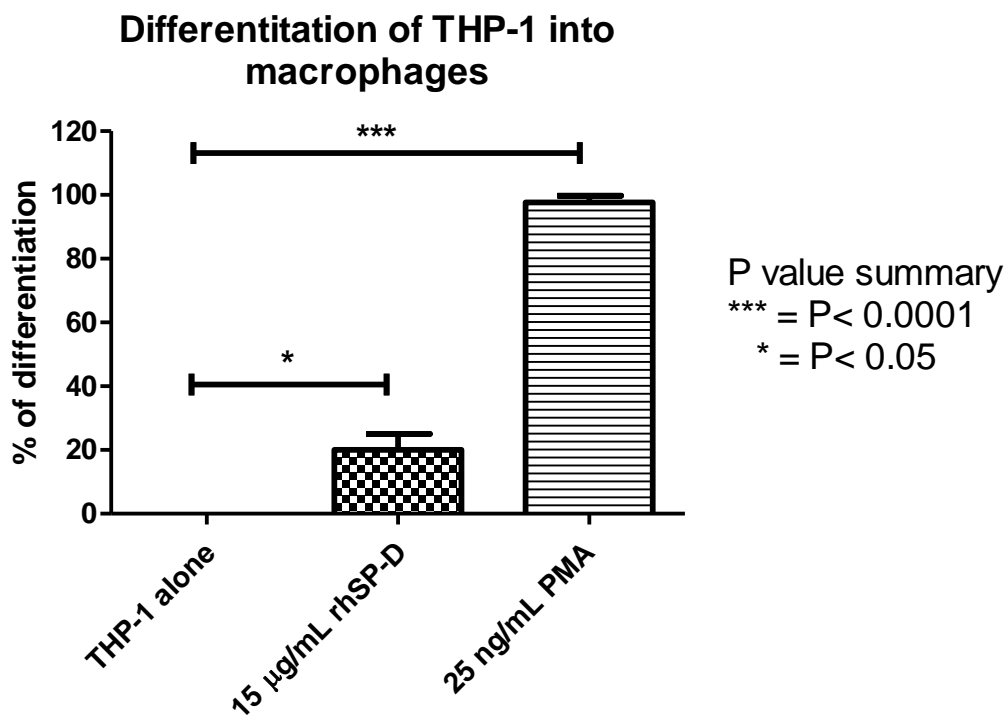


Fig 6.1. Differentiation of THP-1. 0.5×10^6 THP-1 cells were incubated in isolation or with A) 25 ng/mL of PMA, B) 15 µg/mL of rhSP-D with 5 mM of CaCl₂, or C) in isolation for 24 h in RPMI at 37 °C with 5% CO₂. The cells in suspension were collected and images of the adherent differentiated cell were taken. A cell count was taken of the differentiated and suspended cells. Formula: total cells/mL = ((Total cells counted/number of quadrants)/dilution factor) $\times 10^4$, (adherent cell count/total well cell count) $\times 100$ was used. D) A paired T-test in prism was carried out for the untreated and treated samples and a graph was formed.

6.3.2. Trypsin-EDTA does not dissociate THP-1

An experiment was carried out to determine if 1X trypsin-EDTA can cause adherent, differentiated THP-1 cells to go into suspension. The experiment was needed to assess whether 1X trypsin-EDTA can remove both THP-1 and U87 from the well surface or only U87 cells alone. THP-1 cells were incubated for 24 h with 25 ng/mL and were then left to rest for a further 24 h in RPMI. After the cells were treated with trypsin-EDTA and it was clear that no cells had been dissociated as the cell count was 0. This showed that trypsin-EDTA cannot dissociate THP-1 cells once they have been differentiated by PMA.

6.3.3. THP-1 co-culture alters U87 cytokine gene expression

To investigate the change in cytokine gene expression of U87 in a co-culture with THP-1 a RT-qPCR was performed. THP-1 cells were grown for 24 h in the presence of 25 ng/mL of PMA and left to rest for a further 24 h in RPMI alone. 15 µg/mL of rhSP-D was bound to the membrane of U87 cells and added to differentiated THP-1 cells along with untreated U87 cells for 1 h, 2 h, and 6 h. Only the U87 cells were removed and analysed by RT-qPCR.

The results are represented in a log₁₀ format as the data is heavily skewed in linear form. A 2-tailed paired t-test was carried out in order to analyse the significant change in gene expression at each time point between the U87 cells in co-culture and U87 cells alone. An extremely significant downregulation ($***=P<0.0001$) was observed for TNF- α gene expression of U87 cells that had been in co-culture with THP-1. A very significant decrease ($**=P<0.001$) in TNF- α gene expression of rhSP-D bound U87 cells in co-culture was also present. The down regulation of TNF- α expression was time dependent for both treated and untreated samples. It is evident that unbound U87 cells in co-culture had a greater overall decrease in cytokine expression (Fig 6.2.A).

The paired T-test analysis revealed that there was an extremely significant reduction in IL-6 gene expression in U87 co-culture during the time points 1 h, 2 h, and 6 h

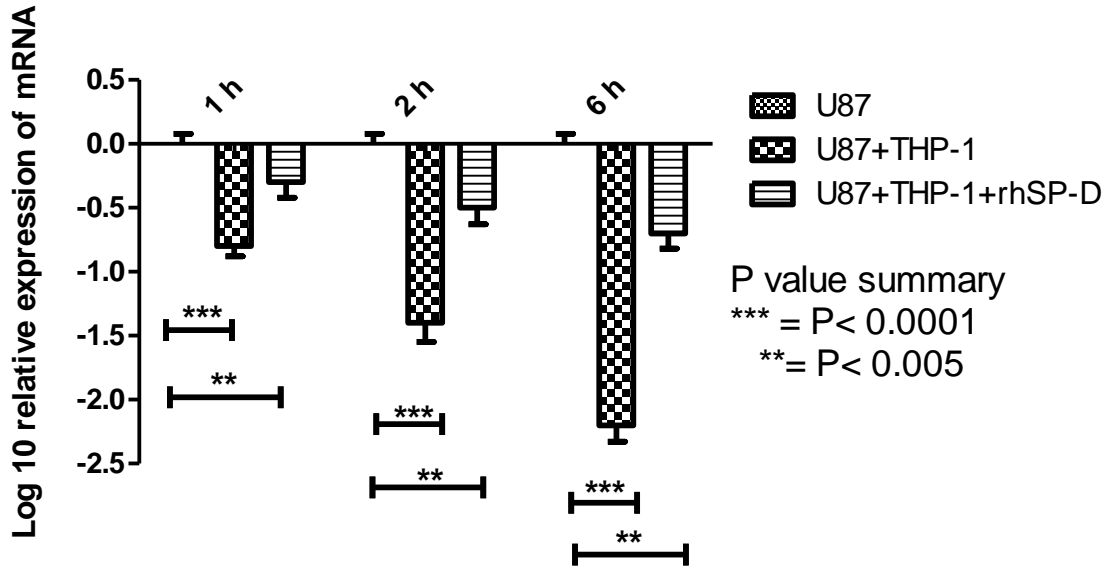
compared to U87 alone which was shown by $***=P<0.0001$. A biphasic trend was also observed as the 2 h time point expression was less than 1 h whereas the decline in gene expression at 6 h was greater than both 1 and 2 h. Despite the biphasic trend, all data points were extremely significant. After 1 h of rhSP-D bound U87 co-culture, there was a decline in IL-6 gene expression however this difference was not significant as the p value was greater than 0.05 (Fig 6.2.B). At 2 h there was a very significant decrease ($**=P<0.01$) in IL-6 gene expression of rhSP-D bound U87 cells in co-culture compared with U87 cells alone. An extremely significant downregulation in rhSP-D bound U87 cell was expressed at 6 h represented by $***=P<0.0001$. The decline in gene expression was time dependent.

The change in gene expression of TGF- β in U87 was analysed between co-culture cells and U87 alone. TGF- β gene expression in U87 cells that had been co-cultured with THP-1 for 1 h and 2 h was downregulated in a time dependent manner when compared to U87 alone. This difference was very significant ($**=P<0.001$). At 6 h the decline in TGF- β gene expression was extremely significant as the P value was greater than 0.0001. The U87 cells treated with rhSP-D at 1 h and 2 h also had a downregulated TGF- β expression when compared with U87 cells alone however this difference was not significant ($P>0.05$). At 6 h rhSP-D bound U87 cells had a very significant decrease in TGF- β expression, represented by $**=P<0.001$ when compared to U87 alone. Overall unbound U87 cells in co-culture with THP-1 had a greater downregulation in TGF- β gene expression than rhSP-D bound U87 cells (Fig 6.2.C).

At 1 h and 2 h for both U87 and rhSP-D bound U87 cells in co-culture, there was an increase in IL-12 gene expression however this increase was not significant and was shown by $ns=P>0.05$. At 6 h there was an extremely significant increase in IL-12 gene expression in U87 cells in co-culture with THP-1 shown by $***=P<0.0001$. There was also a very significant increase in IL-12 expression for rhSP-D bound U87 cells depicted by $**=P<0.001$ (Fig 6.2.D). The change in cytokine expression for rhSP-D bound U87 cells was time dependent.

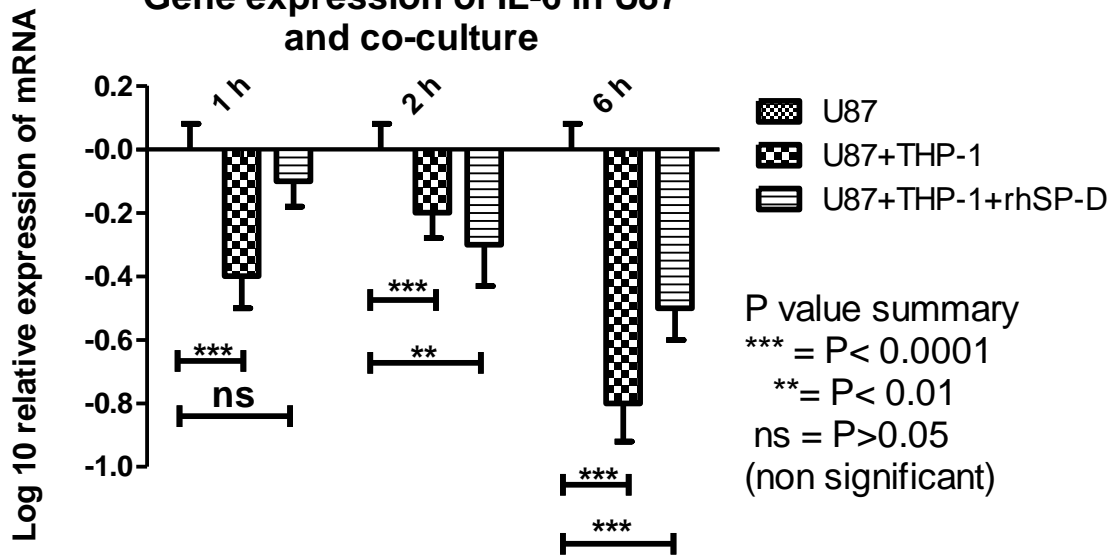
A

Gene expression of TNF- α in U87 and co-culture

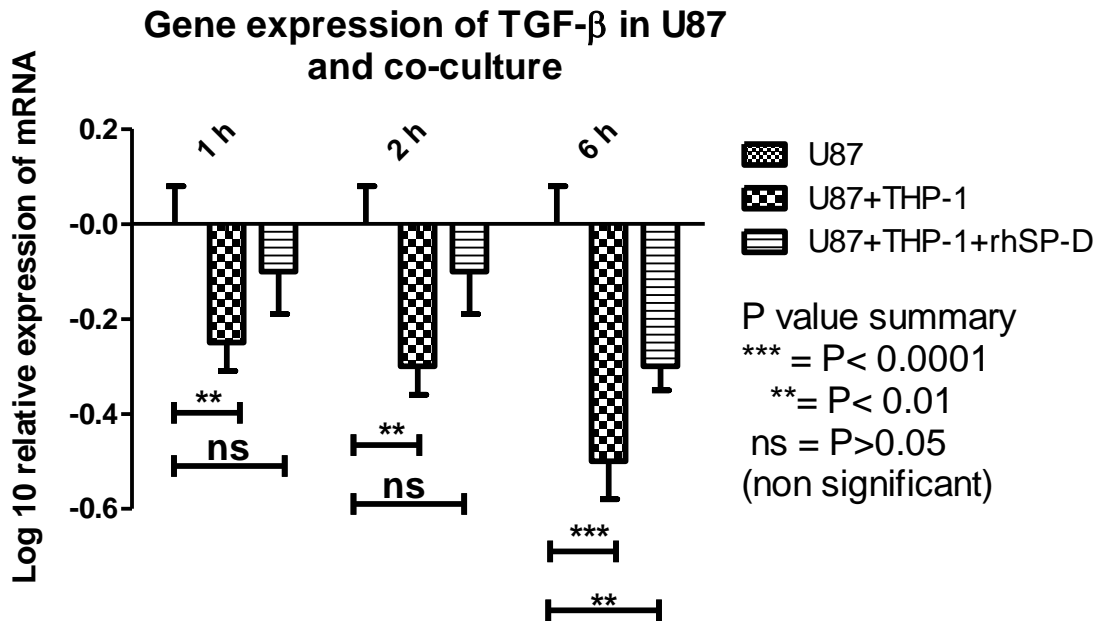


B

Gene expression of IL-6 in U87 and co-culture



C



D

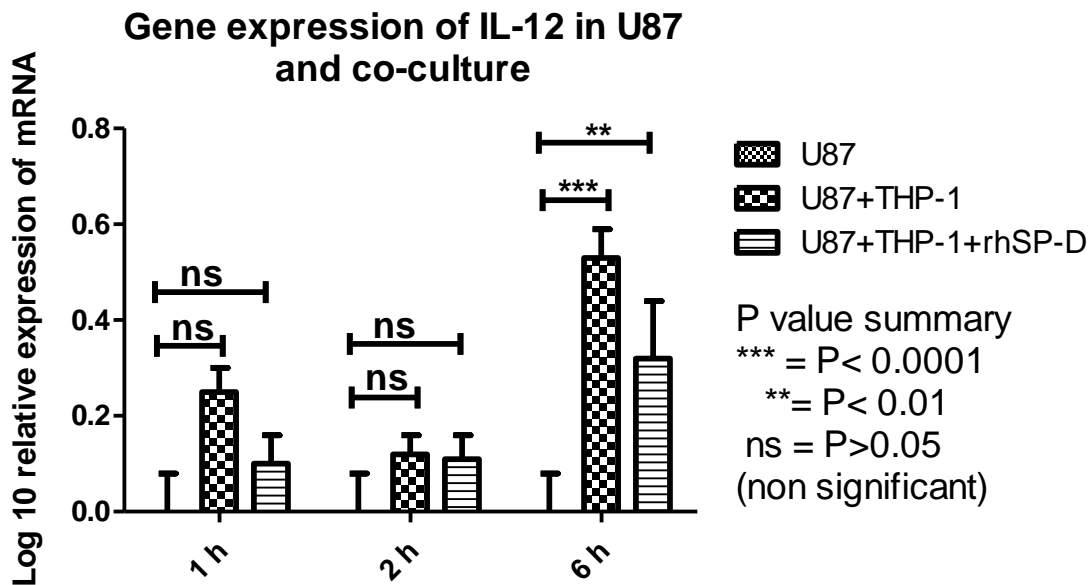


Fig 6.2. Analysis of cytokine gene expression in U87 and THP-1 co-culture. THP-1 cells were treated with 25 ng/mL of PMA for 24 h and left to rest overnight in RPMI alone. 15 μ g/mL of rhSP-D bound and unbound U87 cells were added to the THP-1 cells for 1 h, 2 h and 6 h. The cells were collected and RNA was extracted.

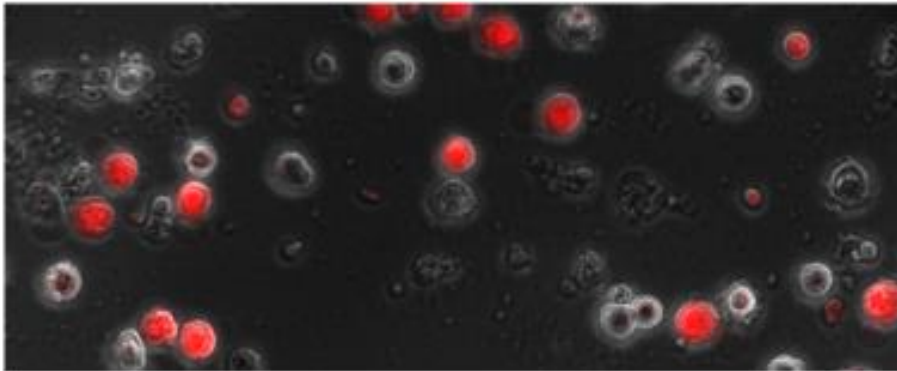
Contaminating DNA was then removed and RNA was converted into cDNA. A qPCR was run and data was analysed by RQ $2^{-\Delta\Delta C_t}$. A) TNF- α expression in U87, B) IL-6 expression in U87, C) TGF- β expression in U87, D) IL-12 expression in U87. Error bars represent standard deviation. A 2-tailed paired T-test was performed.

6.3.4. THP-1 do not engulf U87 cells.

In order to investigate whether rhSP-D had the ability to opsonise U87 cells for engulfment by THP-1 cells a live imaging fluorescent microscopy experiment was used. THP-1 cells were first differentiated with PMA into active macrophage and then left to rest overnight in serum free media. 15 µg/mL of rhSP-D was bound to the membrane of U87 cells in the presence of calcium. U87 cells were then probed with deep red dye cell tracker to distinguish between U87 and THP-1 in co-culture. A co-culture with THP-1 and U87 cells and another co-culture with THP-1 and rhSP-D bound U87 cells was set up. The cells were placed on a live cell imager under normal growth conditions at 37 °C with 5% CO₂ . An image was taken every 10 min for 6 h and were viewed as a merged image of phase contrast and Cy5.

After 6 h of co-culture both U87 and U87-rhSP-D came into close contact with THP-1 cells. The cells were consistently moving slightly throughout the incubation period and there was no obvious difference in the movement between U87 cells (Fig 6.3.A) and rhSP-D bound U87 cells (Fig 6.3. B). During the 6 h incubation there was no observation of temporary protrusion on the surface of the amoeboid THP-1 cells to attempt to grasp U87 and internalise them. No large vacuoles within THP-1 was present and no degradation of cells was seen.

A



B

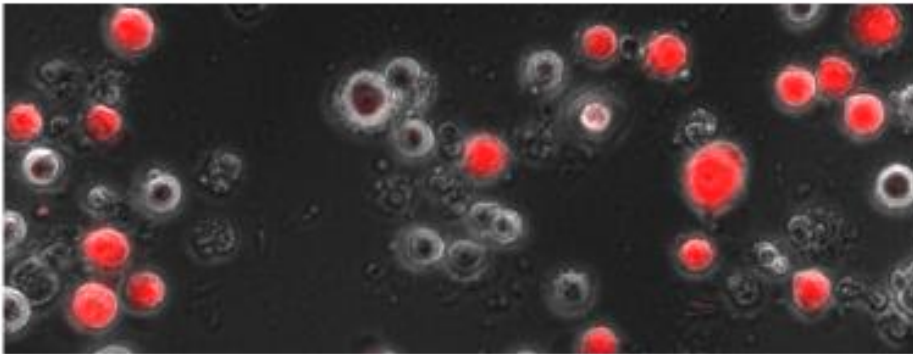


Fig 6.3. Co-culture of U87 and THP-1. 0.5×10^6 THP-1 cells were incubated with 25 ng/mL of PMA for 24 h, and then left to rest overnight in media. 1×10^6 U87 cells and 1×10^6 U87 cells bound to 15 $\mu\text{g}/\text{mL}$ of rhSP-D were treated with deep red dye and then added to the differentiated THP-1 cells for 1 h, 2 h, and 6 h. Live cell imaging was used to observe the co-culture at 37 °C with 5% CO_2 . Images were taken every 10 min for 6 h and were viewed as a merged image of phase contrast and cy5. A) U87 after 6 h of incubation with THP-1, B) rhSP-D bound U87 after 6 h of incubation with THP-1.

6.3.5. Reduced cell growth of U87 cells in co-culture

To analyse the change in cell proliferation between U87 alone and in co-culture with THP-1 a cell proliferation experiment was carried out. THP-1 cells were differentiated over 24 h of incubation with 25 ng/mL of PMA. The cells were left to rest for a further 24 h in RPMI. 15 µg/mL of rh-SPD was bound to the membrane of U87 cells and incubated with THP-1 in a 2:1 ratio. U87 cells with no protein bound were incubated alone and with THP-1 cells also in a 2:1 ratio. The co-culture and U87 were grown under normal growth conditions for up to 48 h and the U87 cells were collected. U87 cells were dissociated with trypsin-EDTA and a cell count was taken. A 2-tailed paired T-test was carried out to analyse the significance of change between the paired observation of U87 cells to the co-culture at each individual time point.

In the first 6 h of incubation the number of U87 cells had remained the same as the number of cells added at 0 h. No difference was observed between the number of U87 at the 6 h time point between U87 alone and U87 incubated with THP-1 or rhSP-D bound U87 incubated with THP-1. (Fig 6.4.). At 12 h the number of cells had increased by approximately 50,000 cells when compared to 0 h. There was an insignificant variation between the co-cultures and U87 with both having a P value >0.05. A significant difference (*=<P 0.05) in cell number was detected at 24 h between U87 and U87 derived from co-culture. The difference in cell number was 50,000 U87 cells less in co-culture compared to U87 grown in isolation. A difference of 30,000 cells was seen between U87 and U87-rhSP-D derived from co-culture, however this difference was not significant (*=>P 0.05). At 48 h a significant difference (*=>P 0.05) was present between U87 and U87 from co-culture. The difference in cell number was 70,000 cells less in U87 from co-culture compared to U87 alone. A significance difference (*=P<0.05) was also detected at 48 h between U87 alone and rhSP-D U87 from co-culture. rhSP-D bound U87 cells had 50,000 less cells present compared to U87 cells grown alone. At 24 h, and 48 h U87 cells from co-culture had less cell proliferation compared to rhSP-D U87 cells derived from co-culture.

Cell count of U87 cell alone and in co-culture

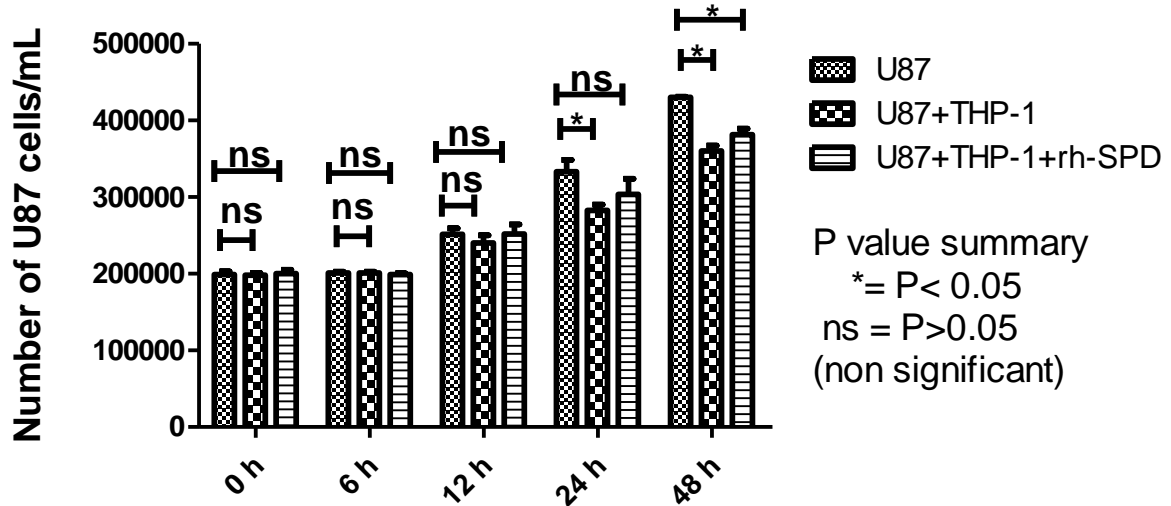


Fig 6.4. Co-culture reduced U87 proliferation. A co-culture with THP-1 cells with U87 and rhSP-D bound U87 cells were able to reduce the cell proliferation. 0.1×10^6 THP-1 cells were differentiated by PMA and left to rest for 24 h in serum free media. rhSP-D bound U87 cells and unbound U87 cells were incubated with THP-1 cells for 6 h, 12 h, 24 h and 48 h. At each time point U87 was dissociated and the cell count was taken. The number of cells in 4 quadrants was counted using a microscope at 10X magnification and a formula was used to calculate the cells per mL; Total cells/mL = ((Total cells counted/number of quadrants)/dilution factor) $\times 10^4$. A 2-tailed paired T-test was then carried out.

6.3.6. Co-culture reduces the secretion of factor H and SP-D

To study the effect a co-culture system with THP-1 and U87 cell would have on SP-D and factor H secretion a co-culture experiment was performed. This involved activating THP-1 cells for 24 h with 25 ng/mL of PMA. U87 cells were then added to the differentiated THP-1 cells in a 2:1 ratio and were also incubated alone (negative control). The cells were grown under normal conditions and at each time point of 6 h, 12 h, 24 h and 48 h. The supernatant was removed and used for ELISA in which the samples were probed with primary antibodies anti-factor H and anti-SP-D as well as secondary antibodies IgG-HRP and PA-HRP. A 2-tailed paired T-test was carried out between U87 and co-culture supernatant to analyse the significance between the two results at each time point.

The factor H linear graph depicts a steady upward trend. As the factor H concentration increased the absorbance reading at 450 nm increased as well. The majority of the data points fit the line of best fit (Fig 6.5 A) and is therefore reliable to deduce the concentration of secreted protein.

The graph illustrates a time dependent increase in the secretion of factor H from U87 cells and a co-culture composed of U87 and THP-1 (Fig 6.5 B). After 6 h of growth there was no significant difference between the concentration of factor H produced by U87 and co-culture as a paired t-test revealed a P value > 0.05. Both cell cultures had secreted an average of 10 µg/mL within the first 6 h of growth. At 12 h there was an increase in factor H secretion by 3 fold. However, the difference in concentration between co-culture and U87 was insignificant (>P 0.05) as both had produced an average of 30 µg/mL. It was clear that at 24 h there was a large surge of factor H secretion from U87 with a 5 fold increase from the 12 h time point. There was also an increase of protein production for co-culture with a 2 fold increase shown. The concentration of protein produced from co-culture was much less than the concentration obtained from U87. A paired t-test revealed that this difference was very significant (* = <P 0.001). An increase in Factor H secretion was also depicted at 48 h

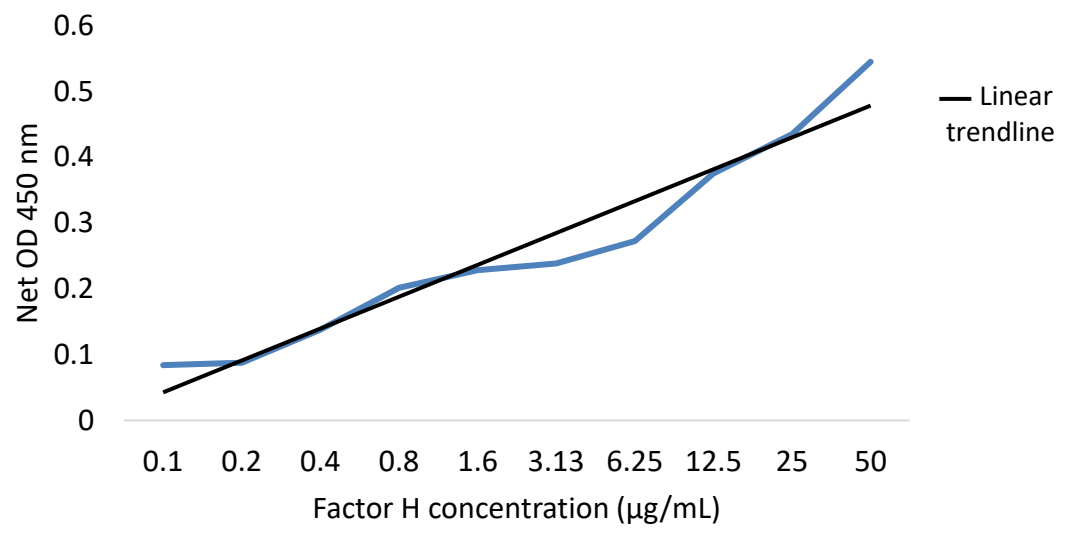
for both U87 and co-culture. Similarly, U87 secreted a greater concentration of factor H than the co-culture but the difference was not as dramatic as previously observed for 24 h. None the less the difference between the cell cultures were significant ($*=P<0.05$). It was clear that that the co-culture secreted less concentration of factor H than the U87 cells over the 48 h growth period

The upwards linear graph for the absorbance reading of the 2X serial dilution of rhSP-D increased gradually at each concentration. The majority of the data points fit closely to the line of best fit (Fig 6.5.C). This graph was deemed reliable to be used to deduce the concentration of SP-D secreted into the supernatant of U87 and co-cultures cells.

The graph shows that at 6 h an average of 3 $\mu\text{g/mL}$ of SP-D was secreted from both U87 and co-culture therefore no significant difference ($ns=P>0.05$) was seen between the 2 paired observations (Fig 6.5.D). There was little change between the concentration of SP-D secreted at 12 h compared to the concentration secreted at 6 h and no significant difference was present between the 2 groups. A high increase of SP-D secretion for both U87 and co-culture was displayed by the graph at 24 h with a 10 fold increase. It can be seen from the graph that the co-culture had produced less SP-D than U87, however the difference between both concentrations was not significant as a P value > 0.05 was present. Once again, an increase in SP-D secretion was depicted at 48 h with a 20 $\mu\text{g/mL}$ difference between U87 at 48 h compared to 24 h. A 10 $\mu\text{g/mL}$ difference was observed between co-culture at 48 h to the supernatant of 24 h. The difference in SP-D secretion between co-culture and U87 was significant ($*=P<0.05$). It was evident that during the 48 h growth period the concentration of SP-D had risen. It was also clear that overall the co-culture had secreted, less SP-D than U87 alone.

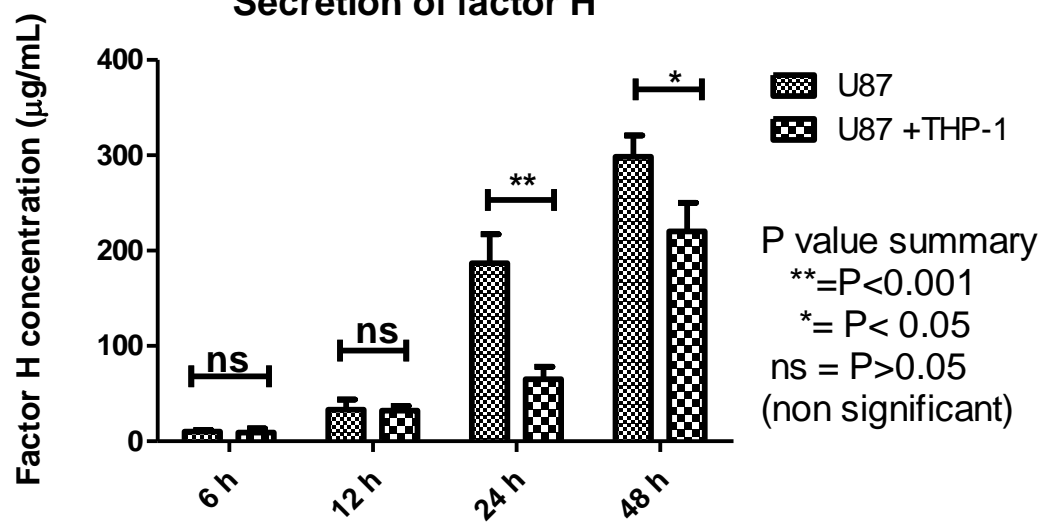
A

ELISA to detect factor H at different concentrations



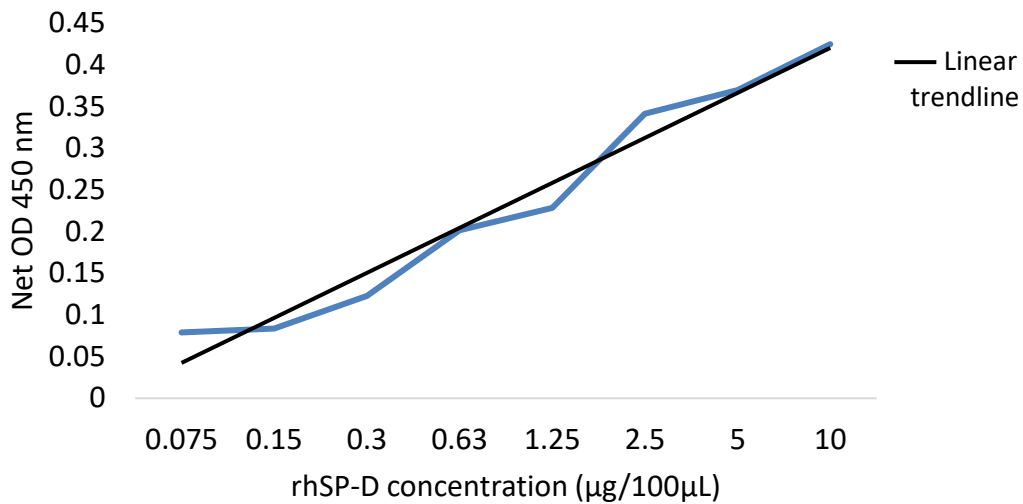
B

Secretion of factor H



C

ELISA to detect rhSP-D at different concentration



D

Secretion of SP-D

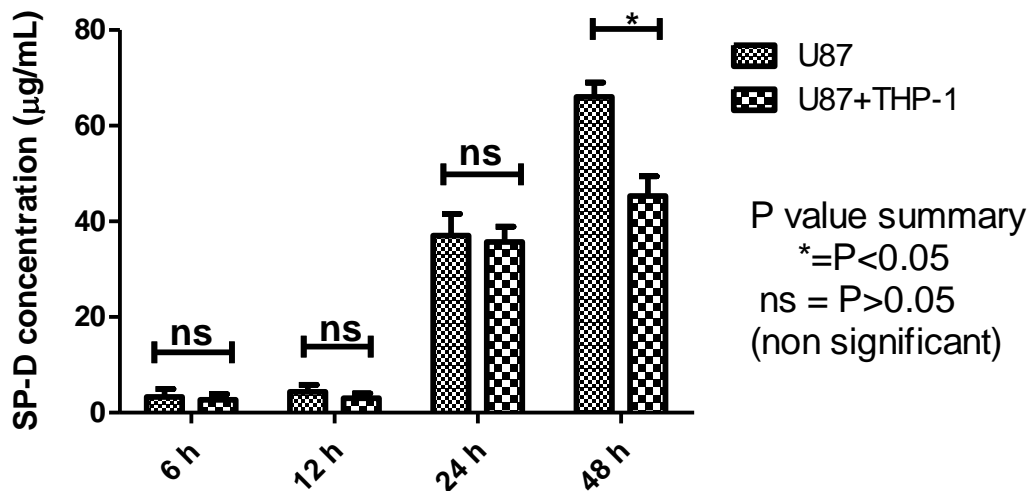


Fig 6.5.A co-culture of THP-1 and U87 cells reduced the production of SP-D and factor H. THP-1 cells were differentiated for 24 h with 25 ng/mL of PMA. U87 cells were incubated alone and with THP-1 cells for 6 h, 12 h, 24 h and 48 h. (B, D) At each time point the supernatant was removed and added to CBC. A 2 fold serial dilution was performed with factor H and rhSP-D. The proteins and supernatant were probed with primary antibodies anti- SP-D and anti-factor H as well as the secondary antibodies PA-HRP and IgG-HRP. OPD was added and the absorbance reading at 450

nm was measured. A graph was produced from the 2 fold protein serial dilution to deduce the concentration of supernatant. A) calibration curve for factor H, B) secretion of factor H, C) calibration curve for rhSP-D, D) secretion of SP-D. A 2- tailed paired t-test was carried out between co-culture and U87 at each time point.

6.4. Discussion

THP-1 are pre-monocytic cells that need to be differentiated into an activate macrophage in order to elicit its phagocytic function. PMA is commonly used to differentiate monocytes in-vitro. We tested different PMA concentrations between 25-100 ng/mL to deduce the most appropriate concentration for co-culture (Park *et al.*, 2007). 25 ng/ml was deemed sufficient for future experiments as after 24 h of incubation the cells had fully differentiated and were adherent to the surface of the wells with no cells in suspension observed. We later wanted to investigate whether purified rhSP-D was able to differentiate THP-1 into active macrophage as this would positively influence future co-culture experiments. It was interesting to see that this collectin was able to induce differentiation in THP-1 cells as it suggests that the presence of the innate immune cells promoted the activation of THP-1. This shows that the presence of rhSP-D is able to support the differentiation of THP-1 into active macrophage.

A vast amount of research surrounding macrophage and tumour relationship focus upon tumour associated macrophage. It is widely acknowledged that the majority of non-neoplastic cells are macrophage that have been recruited by GBM environment to facilitate tumour proliferation, survival and migration (Hambardzumyan, Gutmann and Kettenmann, 2016). Little attention has been given to the potential therapeutic effects of macrophage to phagocytose tumour cells. Monocytic THP-1 cells that had been differentiated by PMA had been shown to increase the engulfment of the bacteria *Listeria monocytogenes* (Van de Velde *et al.*, 2008). With this in mind we decided to assess the ability of differentiated THP-1 to phagocytose U87. It was evident that differentiated THP-1 cells were unable to phagocytose U87 cells over 6 h of incubation despite both cells coming into close contact. This insinuated that U87 cells were able to give off signals to prevent phagocytosis as not only did the cells fail to be phagocytosed but pseudopodia of THP-1 cells was also absent. The lack of pseudopodia infers that THP-1 made no attempt to engulf the cells.

Zhang et al had described 'don't eat me signals' on the surface of glioma membranes through the expression of CD47. Macrophage have signal regulatory protein alpha (SIRP- α) on their membrane which is known to bind to CD47 and prevent macrophage mediated tumour cell phagocytosis (Zhang *et al.*, 2016). We therefore wanted to prevent CD47 and SIRP- α from binding. Fournier et al had shown that SIRP- α and surfactant proteins including SP-D were able to bind together (Fournier *et al.*, 2012). We hypothesised that the ability of SP-D to prevent CD47 and SIRP- α from binding would allow mediated tumour phagocytosis to take place.

More importantly SP-D had been shown to opsonise a variety of pathogen. Geunes-Boyer et al, had revealed the ability of SP-D to enhance macrophage phagocytosis of the fungi *Cryptococcus neoformans* as part of its innate immune function. They were able to show that the ability of SP-D to bind to the pathogen facilitated phagocytosis by almost 4 fold in vitro (Geunes-Boyer *et al.*, 2009). As the recombinant protein rhSP-D has the same function as the full length collectin we decided to investigate whether rhSP-D bound to U87 would enhance the potential of THP-1 to engulf the cells. After 6 h of co-culture rhSP-D had not opsonised U87 and subsequently the cells were not engulfed despite the cells coming into close contact.

We suspect that rhSP-D failure to enhance phagocytosis of U87 by THP-1 was a result of the its inability to occupy all SIRP- α binding sites. Therefore it is likely that both SP-D and CD47 competed with each other for binding to SIRP- α on THP-1. The lack of phagocytosis suggests that there was not a substantial level of rhSP-D-SIRP- α binding over CD47-SIRP- α binding to override the inhibition of tumour mediated phagocytosis.

As THP-1 cells were unable to phagocytose U87 cells with or without membrane bound rhSP-D we decided to investigate the effect THP-1 had on the gene expression of cytokines in U87 cells. It is well known that within malignant glioma cells, the cytokines which are highly expressed contribute to the progressive invasion of tumour cells into tumour free environment within the brain. Under non-tumourigenic environments in which the brain is exposed to injury or pathogens the cytokine expressed induce a pro-

inflammatory response to eliminate the pathogen or repair the cells. In GBM a pro-inflammatory environment is also executed but instead contributes to the tumour progression. (Landskron *et al.*, 2014; Smyth *et al.*, 2004). We wanted to investigate whether despite THP-1 lack of ability to induce phagocytose of U87 cells if it was possible it could alter a change in U87 cytokine gene expression. Therefore we set-up a co-culture of differentiated THP-1 cells with U87 and rhSP-D bound U87 cells in a 1.2 ratio. Only the U87 cells were removed from the co-culture and the gene expression of pro- and anti- inflammatory cytokines within the cells were compared against U87 cells grown alone.

It was clear that there was an extremely significant down-regulation of TNF- α gene expression in U87 cells derived from co-culture when compared to U87 cells grown alone. It is likely that THP-1 induced an anti-inflammatory response in the co-culture which in turn reduced the expression of the pro-tumourigenic and pro-inflammatory cytokine TNF- α in U87. This reduced expression is of great interest as TNF- α is one of the most potent pro-tumourigenic cytokines in GBM invasion. The down regulated expression insinuates that the chronic inflammatory sites within GBM are reduced. Endogenous TNF- α is associated with the production of reactive oxygen species and activation of nuclear factor kappa B (NF- κ B) pathway to support tumour growth. Therefore, the reduced TNF- α expression is likely to decrease the generation of reactive oxygen species and the transcription regulator NF- κ B pathway. The reduced activation of this pathway would be beneficial to the inhibition of tumourigenesis as translocation of NF- κ B to the nucleus induces gene expression of anti-apoptotic genes (Balkwill, 2006; Gupta *et al.*, 2005; Woo *et al.*, 2000).

The gene expression of TNF- α from a co-culture with rhSP-D bound U87 cells was also investigated. We wanted to determine whether rhSP-D would enhance the effect THP-1 would have on U87 cells. Bound rhSP-D also demonstrated a reduced expression of TNF- α however the significance in decreased expression was less. This may be due to the fact that our previous studies had identified this protein to enhance U87

proliferation and may be the reason why the down-regulated expression was not as significant as U87 without rhSP-D. Although previous experiments had shown that bound rhSP-D contributed to tumour enhancement, we wanted to determine the influence rhSP-D would have on the outcome of results in the presence of another innate immune cell. It is evident that rhSP-D did not promote the effect of THP-1 and instead dampened its downregulating effect on TNF- α expression.

TNF- α expression and activation of NF-KB promote the expression of the pro-inflammatory cytokine IL-6 (Suarez-Cuervo *et al.*, 2003). This cytokine promotes tumourigenesis in GBM which contributes to the dismal prognosis of patients. From our earlier results it was demonstrated that U87 cells in co-culture with macrophage THP-1 had a reduced TNF- α expression. We therefore wanted to investigate whether the down-regulation observed for TNF- α was also present in IL-6 expression from U87 in co-culture. It was clear that the expression of IL-6 was also significantly reduced in U87 cells. It is likely that the reduced IL-6 expression is due to decreased TNF- α levels of GBM in co-culture as TNF- α can mediate IL-6 expression. The down-regulated expression of the pro-tumourigenic cytokine suggests that as a result there would be less IL-6 present to bind to their receptors including IL-6R which would lead to a reduction of the JAK/STAT pathway that promotes tumourigenesis (Landskron *et al.*, 2014). It is possible that the reduced activation of the JAK/STAT pathway would promote an anti-tumourigenic environment.

TGF- β is a known anti-inflammatory cytokine, which is highly expressed within GBM and promotes tumourigenesis. We wanted to investigate the expression the anti-inflammatory cytokine would have in response to the anti-inflammatory effect induced by THP-1 cells. Over the 6 h incubation period of U87 and THP-1 the gene expression of TGF- β was significantly reduced in U87 cells. The reduced expression is likely to have an anti-tumourigenic effect as less TGF- β is expressed. This cytokine promotes a tumourigenic environment through inducing epithelial mesenchymal transition (EMT) in-vivo. Therefore, reduced activity of epithelial transition will support anti-tumour

effects (Bryukhovetskiy and Shevchenko, 2016). The addition of rhSP-D to the membrane of U87 cells reduced the downregulated effect of THP-1 cells. This may be due to rhSP-D enhancing GBM invasion as was shown in earlier studies.

IL-12 is a cytokine that has a reduced expression in GBM. It is believed that this cytokine contributes to the prevention of glioma growth and is the reason why IL-12 is not highly expressed in the tumour. In addition, there have been therapeutic breakthroughs with the administration of IL-12 leading to reduced tumour growth (Liu *et al.*, 2002; Vom Berg *et al.*, 2013). Interestingly gene expression analysis revealed a significant upregulation of IL-12 expression after 6 h of growth. This result suggested that IL-12 expression was enhanced in co-culture as an attempt by THP-1 to prevent tumourigenesis.

The presence of THP-1 with U87 over a 48 h incubation period led to a significant down regulation of U87 cells at 24 h and 48 h compared to U87 cells that were not in co-culture. This finding supported the notion that THP-1 promoted an anti-inflammatory response in U87 cells which reduced the expression of over expressed cytokines. As a result, this effected the proliferation of cells and led to a reduced cell count of U87 cells. This depicts that the expression of cytokines from U87 has a direct effect on the proliferation of U87 cells. Therefore it is likely that cytokine overexpression is a key component of GBM proliferation. It also indicates that differentiated THP-1 cells has the potential to have therapeutic effects on GBM cells.

In correlation with assessing the cell number of U87 cells we also assessed whether any cells had stained blue and ultimately died. However it was clear that neither U87 derived from co-culture or grown alone had died and all the cells were viable. This showed that THP-1 did not induce destruction of U87 but alternatively reduced the proliferation of the cells.

From our previous studies we had found that GBM cells secrete factor H and SP-D which is believed to also promote tumour growth. Considering the down regulation of cytokine expression and reduced cell proliferation THP-1 had on U87 we decided to

investigate the effect it had on factor H and SP-D secretion. It was evident that between 24 h and 48 h of incubation with U87 and THP-1 cells that the secretion of factor H was significantly less compared to the concentration of factor H secreted from U87 alone. This shows that THP-1 presence is able to reduce the concentration of factor H thereby relinquishing its ability to inhibit cell lysis through preventing activation of the alternative pathway. Similarly after 48 h of co-culture the concentration of SP-D was significantly less at 48 h of growth. This shows that THP-1 is able to reduce the secretion of SP-D and potentially contribute to the reduced proliferation of cells.

7. General discussion

Why is this research into GBM important?

GBM is the most common malignant brain tumour that has a dismal prognosis. Despite aggressive treatment including surgical resection, radiation, and chemotherapy, patients on average survive for 14.6 months (Furnari *et al.*, 2007). Immunotherapy in which the immune system is stimulated to attack tumour cells may provide promising treatment for GBM. Understanding the immunobiology of GBM is central to designing successful immunotherapies (Parney, 2012). Although a number of studies have examined various innate immune cells in GBM, the detection and importance of CFHR5 and SP-D had yet to be investigated.

Why is the finding of CFHR5 significant into our understanding of GBM?

CFHR5 is a member of the factor H family composed of 9 SCRs, making it the longest CFHR protein. The gene is located on the RCA down stream of factor H gene. CFHR5 is unique as unlike CFHR 1-4 not only does it share homology with SCR 6-7 and 19-20 of factor H but also 10-14 (Skerka *et al.*, 2013). It is known that this protein is mainly secreted by the liver, and recently, McRae identified that similar to factor H, CFHR5 was able to inhibit C3 convertase and act as a co-factor for factor I but could not induce decay acceleration activity (McRae *et al.*, 2005). In this study, for the first time, we detected the presence of CFHR5 in primary GBM cells. This was of significant interest as previous reports had only showed the presence of factor H (Junnikkala *et al.*, 2000). We demonstrated that CFHR5 derived from GBM was functionally active as it was able to inhibit the alternative pathway, act as a co-factor for factor I, and also established that it had decay acceleration activity.

These findings provided significant understanding about the involvement of the alternative pathway in primary GBM and its potential contribution to GBM progression. It is extremely likely that the secretion of functionally active CFHR5 by GBM is a mechanism used by the tumour cells to evade cell lysis by preventing induction of the

alternative pathway. The results suggest that for meaningful development towards the inhibition or reduced cell growth of GBM cells, the expression of CFHR5 would need to be taken into consideration. The ability of GBM cells to produce functionally active CFHR5 sheds new light on the current conception that the functional ability of factor H is restricted to SCR 1-4 and suggests that SCR 10-14 may also provide functional activity.

Having identified that primary GBM cells produce complement proteins capable of inhibiting activation of the alternative pathway, we hypothesise that silencing the expression of CFHR5 in primary GBM may render tumour cells susceptible to complement attack.

We also analysed the gene expression of pro-inflammatory cytokine TNF- α , IL-6 and IL-12 as well as the anti-inflammatory cytokine TGF- β . It was clear that TNF- α , IL-6 and TGF- β were upregulated in a time-dependent manner as the gene expression continued to increase the longer the cells were incubated for. This upregulation inferred that these cytokines promoted tumour growth in GBM. It is likely that IL-12 suppresses tumour growth, hence, the reason for its down regulated expression over 48 h. It is known that the expression of complement also influences gene expression. Therefore, we hypothesise that inhibition of factor H will reduce cytokine expression of IL-6 TNF- α and TGF- β .

Why was the study of rhSP-D interaction with GBM important?

SP-D acts as a PRR which binds to pathogens via its CRD region. The protein is commonly associated with providing an innate immune response in the lungs through agglutination, opsonisation and promoting clearance of bacteria, fungi and virus (Hartl and Griese, 2006). Therefore, recombinant SP-D had been proposed as having potential therapeutic effects, not only in the lung but other organs.

Mahajan et al had shown that rhSP-D has the ability to bind to eosinophils and in doing so were able to induce apoptosis (Mahajan *et al.*, 2008). In order to establish

whether this effect could be demonstrated in GBM, we first needed to express and purify rhSP-D. The expression of plasmid pUK-D1 containing rhSP-D was successful under the bacteriophage T7 promoter as the protein was successfully expressed in insoluble inclusion bodies. We were then able to denature the protein and refold it into its active form and purify the protein on a maltose agarose column. We were then able to show through immuno-fluorescent microscopy that purified rhSP-D was able to bind to GBM cells. However, rhSP-D was unable to induce apoptosis. It is known that in primary GBM that make up over 90% of all GBM cases, the p53 tumour suppressor is not mutated or over-expressed. Therefore, the ability of rhSP-D to down-regulate the expression of this gene further did not contribute to the inhibition of tumour growth and instead promoted tumour growth.

Although the treatment of GBM cells with rhSP-D did not have the anticipated effect, we can gain a deeper understanding of the role p53 and cytokines TNF- α and IL-6 play in GBM. Our study has shown that rhSP-D decreased the gene expression of p53 but enhanced the expression of TNF- α and IL-6. Due to these changes, the proliferation of U87 cells increased. This infers that TNF- α and IL-6 promote tumour growth and that the suppression of the p53 gave way to a pro-tumour microenvironment.

Why is the detection of SP-D in GBM significant?

The function of SP-D in extrapulmonary tissue is poorly understood. Although in many pulmonary and few extrapulmonary studies including pancreatic and uterus cells, SP-D is known to contribute to host defence and regulating inflammation (Sotiriadis *et al.*, 2015; Liu *et al.*, 2015). However, there is currently no data available regarding the effect SP-D has in tumour cells.

Why was the study of opsonisation of GBM important?

As rhSP-D was unable to induce apoptosis, the next step was to assess its ability to opsonise GBM cells for uptake by THP-1 cells, as it is known that SP-D promotes phagocytosis of cells (Carreto-Binaghi, Aliouat el and Taylor, 2016). However, our

results showed that opsonisation did not occur and THP-1 cells did not engulf U87, or rhSP-D bound U87 cells. The ability to avoid phagocytic uptake despite coming into close contact with THP-1 highlights the successful ability of GBM cells to evade opsonophagocytosis. The results obtained coincide with the lack of development of new therapy for GBM in over a decade. It is likely that as this grade IV tumour is extremely aggressive and patients have a median survival of 14.6 months, the production of new therapeutic treatments will be challenging.

Future work

- Gene silencing of CFHR5 of B30, B31 and B33 cells to assess susceptibility to complement mediated attack. The experiment would involve designing oligonucleotides for small interference (si) RNA of CFHR5 mRNA. The siRNA would then be cloned into a vector such as PSHH using a gene silencer system. Primary GBM cells would be grown till 80% confluent under normal growth conditions. Transfection would then be performed with siRNA plasmid and lipofectamine 2000 in α MEM. Cells would then be incubated at 37 °C with 5% CO₂ for 4 h and stable clones would then be selected. Results for successful inhibition could be confirmed by ELISA and western blot. Proliferation and complement assays could then be implemented to assess the effect of silencing CFHR5.
- Future experiments would involve silencing CFHR5 and assessing the difference in cytokine gene expression between silenced and unsilenced cells. This would also provide greater understanding into the effect the alternative pathway has on cytokine gene expression.
- To further confirm the presence of CFHR5 in B30, B31 and B33 cells a mass spectrometry analysis would be used. This would involve measuring the mass to charge ratio of ions to identify CFHR5 from the mass of its peptide fragments. The relative or absolute quantity of CFHR5 could also be deduced by using mass spectrometry.

- To gain a greater understanding of the role SP-D plays in GBM, future experiments could involve silencing SP-D gene expression and analyse the effect this has on cell proliferation, cytokine and p53 expression. This further work would enable us to determine whether SP-D has a pro- or anti- tumour effect in GBM. It would also be interesting to investigate the ability of rhSP-D to induce apoptosis in GBM cells in which SP-D expression is silenced.
- Future work would also involve using microglia cells from patients that have GBM and from patients that do not/normal microglia, in order to assess the interaction with GBM cells in co-culture. qPCR would then be used to analyse cytokine gene expression and the phagocytic ability of the microglia would be observed using live microscopy.

8. References

1. Akira, S., Uematsu, S. and Takeuchi, O. (2006) 'Pathogen recognition and innate immunity', *Cell*, 124(4), pp. 783-801.
2. Akiyama, J., Hoffman, A., Brown, C., Allen, L., Edmondson, J., Poulain, F. and Hawgood, S. (2002) 'Tissue distribution of surfactant proteins A and D in the mouse', *The journal of histochemistry and cytochemistry : official journal of the Histochemistry Society*, 50(7), pp. 993-996
3. Alarcon, R., Fuenzalida, C., Santibanez, M. and von Bernhardi, R. (2005) 'Expression of scavenger receptors in glial cells. Comparing the adhesion of astrocytes and microglia from neonatal rats to surface-bound beta-amyloid', *The Journal of biological chemistry*, 280(34), pp. 30406-30415.
4. Ali, Y.M., Lynch, N.J., Haleem, K.S., Fujita, T., Endo, Y., Hansen, S., Holmskov, U., Takahashi, K., Stahl, G.L., Dudler, T., Girija, U.V., Wallis, R., Kadioglu, A., Stover, C.M., Andrew, P.W. and Schwaeble, W.J. (2012) 'The lectin pathway of complement activation is a critical component of the innate immune response to pneumococcal infection', *PLoS pathogens*, 8(7), pp. e1002793.
5. Anspach, F.B. and Hilbeck, O. (1995) 'Removal of endotoxins by affinity sorbents', *Journal of chromatography.A*, 711(1), pp. 81-92.
6. Anzil, A.P. (1970) 'Glioblastoma multiforme with extracranial metastases in the absence of previous craniotomy. Case report', *Journal of neurosurgery*, 33(1), pp. 88-94.
7. Appel, G.B., Cook, H.T., Hageman, G., Jennette, J.C., Kashgarian, M., Kirschfink, M., Lambris, J.D., Lanning, L., Lutz, H.U., Meri, S., Rose, N.R., Salant, D.J., Sethi, S., Smith, R.J., Smoyer, W., Tully, H.F., Tully, S.P., Walker, P., Welsh, M., Wurzner, R. and Zipfel, P.F. (2005) 'Membranoproliferative glomerulonephritis type II (dense deposit disease): an update', *Journal of the American Society of Nephrology : JASN*, 16(5), pp. 1392-1403.
8. Barcellos-Hoff, M.H., Newcomb, E.W., Zagzag, D. and Narayana, A. (2009) 'Therapeutic targets in malignant glioblastoma microenvironment', *Seminars in radiation oncology*, 19(3), pp. 163-170.
9. Balkwill, F. (2006) 'TNF-alpha in promotion and progression of cancer', *Cancer metastasis reviews*, 25(3), pp. 409-416.
10. Bergers, G. and Benjamin, L.E. (2003) 'Tumorigenesis and the angiogenic switch', *Nature reviews.Cancer*, 3, pp. 401-410
11. Benveniste, E.N. (1997) 'Role of macrophages/microglia in multiple sclerosis and experimental allergic encephalomyelitis', *Journal of Molecular Medicine (Berlin, Germany)*, 75(3), pp. 165-173.
12. Betz, C., Papadopoulos, T., Buchwald, J., Dammrich, J. and Muller-Hermelink, H.K. (1995) 'Surfactant protein gene expression in metastatic and micrometastatic pulmonary adenocarcinomas and other non-small cell lung carcinomas: detection by

- reverse transcriptase-polymerase chain reaction', *Cancer research*, 55(19), pp. 4283-4286
13. Bickel, M. (1993) 'The role of interleukin-8 in inflammation and mechanisms of regulation', *Journal of periodontology*, 64(5 Suppl), pp. 456-460.
 14. Boche, D., Cunningham, C., Docagne, F., Scott, H. and Perry, V.H. (2006) 'TGFbeta1 regulates the inflammatory response during chronic neurodegeneration', *Neurobiology of disease*, 22(3), pp. 638-650.
 15. Bowman, C.C., Rasley, A., Tranguch, S.L. and Marriott, I. (2003) 'Cultured astrocytes express toll-like receptors for bacterial products', *Glia*, 43(3), pp. 281-291.
 16. Brat, D.J., Bellail, A.C. and Van Meir, E.G. (2005) 'The role of interleukin-8 and its receptors in gliomagenesis and tumoral angiogenesis', *Neuro-oncology*, 7(2), pp. 122-133.
 17. Brauer, L., Kindler, C., Jager, K., Sel, S., Nolle, B., Pleyer, U., Ochs, M. and Paulsen, F.P. (2007) 'Detection of surfactant proteins A and D in human tear fluid and the human lacrimal system', *Investigative ophthalmology & visual science*, 48(9), pp. 3945-3953.
 18. Brown-Augsburger, P., Hartshorn, K., Chang, D., Rust, K., Fliszar, C., Welgus, H.G. and Crouch, E.C. (1996) 'Site-directed mutagenesis of Cys-15 and Cys-20 of pulmonary surfactant protein D. Expression of a trimeric protein with altered anti-viral properties', *The Journal of biological chemistry*, 271(23), pp. 13724-13730.
 19. Bryukhovetskiy, I. and Shevchenko, V. (2016) 'Molecular mechanisms of the effect of TGF-beta1 on U87 human glioblastoma cells', *Oncology letters*, 12(2), pp. 1581-1590.
 20. Bsibsi, M., Ravid, R., Gveric, D. and van Noort, J.M. (2002) 'Broad expression of Toll-like receptors in the human central nervous system', *Journal of neuropathology and experimental neurology*, 61(11), pp. 1013-1021.
 21. Bunz, F., Dutriaux, A., Lengauer, C., Waldman, T., Zhou, S., Brown, J.P., Sedivy, J.M., Kinzler, K.W. and Vogelstein, B. (1998) 'Requirement for p53 and p21 to sustain G2 arrest after DNA damage', *Science (New York, N.Y.)*, 282(5393), pp. 1497-1501.
 22. Burnet, M. (1957) 'Cancer: a biological approach. III. Viruses associated with neoplastic conditions. IV. Practical applications', *British medical journal*, 1(5023), pp. 841-847.
 23. Burudi, E.M., Riese, S., Stahl, P.D. and Regnier-Vigouroux, A. (1999) 'Identification and functional characterization of the mannose receptor in astrocytes', *Glia*, 25(1), pp. 44-55.
 24. Byrne, A.M., Bouchier-Hayes, D.J., and Harmey, J.H. (2005) 'Angiogenic and cell survival functions of Vascular Endothelial Growth Factor (VEGF)', *Journal of Cellular and Molecular Medicine*, 9, pp. 777-794
 25. Carpentier, P.A., Begolka, W.S., Olson, J.K., Elhofy, A., Karpus, W.J. and Miller, S.D. (2005) 'Differential activation of astrocytes by innate and adaptive immune stimuli', *Glia*, 49(3), pp. 360-374.
 26. Carreto-Binaghi, L.E., Aliouat el, M. and Taylor, M.L. (2016) 'Surfactant proteins, SP-A and SP-D, in respiratory fungal infections: their role in the inflammatory response', *Respiratory research*, 17(1), pp. 66-016-0385-9.

27. Carson, M.J., Doose, J.M., Melchior, B., Schmid, C.D. and Ploix, C.C. (2006) 'CNS immune privilege: hiding in plain sight', *Immunological reviews*, 213, pp. 48-65.
28. Cavaillon, J.M. and Haeffner-Cavaillon, N. (1986) 'Polymyxin-B inhibition of LPS-induced interleukin-1 secretion by human monocytes is dependent upon the LPS origin', *Molecular immunology*, 23(9), pp. 965-969.
29. Celik, I., Stover, C., Botto, M., Thiel, S., Tzima, S., Kunkel, D., Walport, M., Lorenz, W. and Schwaeble, W. (2001) 'Role of the classical pathway of complement activation in experimentally induced polymicrobial peritonitis', *Infection and immunity*, 69(12), pp. 7304-7309.
30. Chan, W.Y., Kohsaka, S. and Rezaie, P. (2007) 'The origin and cell lineage of microglia: new concepts', *Brain Research Reviews*, 53(2), pp. 344-354.
31. Chan, C.L., Renia, L. and Tan, K.S. (2012) 'A simplified, sensitive phagocytic assay for malaria cultures facilitated by flow cytometry of differentially-stained cell populations', *PloS one*, 7(6), pp. e38523.
32. Chang, C.Y., Li, M.C., Liao, S.L., Huang, Y.L., Shen, C.C. and Pan, H.C. (2005) 'Prognostic and clinical implication of IL-6 expression in glioblastoma multiforme', *Journal of clinical neuroscience : official journal of the Neurosurgical Society of Australasia*, 12(8), pp. 930-933.
33. Chaitanya, G.V., Steven, A.J. and Babu, P.P. (2010) 'PARP-1 cleavage fragments: signatures of cell-death proteases in neurodegeneration', *Cell communication and signaling : CCS*, 8, pp. 31-811X-8-31.
34. Charles, N. A., Holland, E. C., Gilbertson, R., Glass, R., and Kettenmann, H. (2011) 'The brain tumor microenvironment', *Glia*, 59(8), pp. 1169-1180.
35. Chen, T.C., Hinton, D.R., Apuzzo, M.L. and Hofman, F.M. (1993) 'Differential effects of tumor necrosis factor-alpha on proliferation, cell surface antigen expression, and cytokine interactions in malignant gliomas', *Neurosurgery*, 32(1), pp. 85-94.
36. Clark, R. and Kupper, T. (2005) 'Old meets new: the interaction between innate and adaptive immunity', *The Journal of investigative dermatology*, 125(4), pp. 629-637.
37. Coniglio, S.J. and Segall, J.E. (2013) 'Review: molecular mechanism of microglia stimulated glioblastoma invasion', *Matrix biology : journal of the International Society for Matrix Biology*, 32(7-8), pp. 372-380.
38. Corn, P.G., El-Deiry, W.S. (2002) 'Derangement of growth and differentiation control in oncogenesis', *BioEssays*, 24, pp. 83-90
39. Cosacak, M.I., Papadimitriou, C. and Kizil, C. (2015) 'Regeneration, Plasticity, and Induced Molecular Programs in Adult Zebrafish Brain', *BioMed research international*, 2015, pp. 769763.
40. Crouch, E.C. (2000) 'Surfactant protein-D and pulmonary host defense', *Respiratory research*, 1(2), pp. 93-108.
41. Crouch, E., Persson, A., Chang, D. and Heuser, J. (1994) 'Molecular structure of pulmonary surfactant protein D (SP-D)', *The Journal of biological chemistry*, 269(25), pp. 17311-17319.

- 42.Cui, W., Fowles, D.J., Bryson, S., Duffie, E., Ireland, H., Balmain, A. and Akhurst, R.J. (1996) 'TGFbeta1 inhibits the formation of benign skin tumors, but enhances progression to invasive spindle carcinomas in transgenic mice', *Cell*, 86(4), pp. 531-542.
- 43.Curtin, J.F., King, G.D., Candolfi, M., Greeno, R.B., Kroeger, K.M., Lowenstein, P.R. and Castro, M.G. (2005) 'Combining cytotoxic and immune-mediated gene therapy to treat brain tumors', *Current topics in medicinal chemistry*, 5(12), pp. 1151-1170.
- 44.Diaz-Guillen, M.A., Rodriguez de Cordoba, S. and Heine-Suner, D. (1999) 'A radiation hybrid map of complement factor H and factor H-related genes', *Immunogenetics*, 49(6), pp. 549-552.
- 45.Dunn, G.P., Old, L.J. and Schreiber, R.D. (2004) 'The immunobiology of cancer immunosurveillance and immunoediting', *Immunity*, 21(2), pp. 137-148.
- 46.Dunkelberger, J.R. and Song, W.C. (2010) 'Complement and its role in innate and adaptive immune responses', *Cell research*, 20(1), pp. 34-50.
- 47.Ehrlich P. (1909) 'Ueber den jetzigen stand der Karzinomforschung', *Ned Tijdschr Geneeskde*, 5, PP. 273-290.
- 48.in a living cell', *Science (New York, N.Y.)*, 316(5828), pp. 1191-1194.
- 49.Elmore, S. (2007) 'Apoptosis: a review of programmed cell death', *Toxicologic pathology*, 35(4), pp. 495-516.
- 50.Erta, M., Quintana, A. and Hidalgo, J. (2012) 'Interleukin-6, a major cytokine in the central nervous system', *International journal of biological sciences*, 8(9), pp. 1254-1266.
- 51.Fabry, Z., Raine, C.S. and Hart, M.N. (1994) 'Nervous tissue as an immune compartment: the dialect of the immune response in the CNS', *Immunology today*, 15(5), pp. 218-224.
- 52.Fajardo, L.F., Kwan, H.H., Kowalski, J., Prionas, S.D. and Allison, A.C. (1992) 'Dual role of tumor necrosis factor-alpha in angiogenesis', *The American journal of pathology*, 140(3), pp. 539-544.
- 53.Farina, C., Krumbholz, M., Giese, T., Hartmann, G., Aloisi, F. and Meinl, E. (2005) 'Preferential expression and function of Toll-like receptor 3 in human astrocytes', *Journal of neuroimmunology*, 159(1-2), pp. 12-19.
- 54.Fedi, P., Tronick, S.R., and Aaronson, S.A. (1997) 'Growth Factors', *Cancer Medicine*, pp.41-54
- 55.Ferreira, V.P., Pangburn, M.K. and Cortes, C. (2010) 'Complement control protein factor H: the good, the bad, and the inadequate', *Molecular immunology*, 47(13), pp. 2187-2197.
- 56.Fenstermaker, R.A. and Ciesielski, M.J. (2004) 'Immunotherapeutic strategies for malignant glioma', *Cancer control : journal of the Moffitt Cancer Center*, 11(3), pp. 181-191
- 57.Ferluga, J., Kouser, L., Murugaiah, V., Sim, R.B. and Kishore, U. (2017) 'Potential influences of complement factor H in autoimmune inflammatory and thrombotic disorders', *Molecular immunology*, .

58. Fialkow, P.J. (1979) 'Clonal origin of human tumors', *Annual Review of Medicine*, 30, pp. 135-143.
59. Fidler, I.J. (1975) 'Biological behaviour of malignant melanoma cells correlated to their survival in vivo', *Cancer Research*, 35, pp. 218-244
60. Fidler, I.J. (2003) 'The pathogenesis of cancer metastasis: the 'seed and soil' hypothesis revisited', *Nature reviews.Cancer*, 3(6), pp. 453-458.
61. Fischer, H.G. and Reichmann, G. (2001) 'Brain dendritic cells and macrophages/microglia in central nervous system inflammation', *Journal of immunology (Baltimore, Md.: 1950)*, 166(4), pp. 2717-2726.
62. Forbes, L.R. and Haczku, A. (2010) 'SP-D and regulation of the pulmonary innate immune system in allergic airway changes', *Clinical and experimental allergy : journal of the British Society for Allergy and Clinical Immunology*, 40(4), pp. 547-562.
63. Fournier, B., Andargachew, R., Robin, A.Z., Laur, O., Voelker, D.R., Lee, W.Y., Weber, D. and Parkos, C.A. (2012) 'Surfactant protein D (Sp-D) binds to membrane-proximal domain (D3) of signal regulatory protein alpha (SIRPalpha), a site distant from binding domain of CD47, while also binding to analogous region on signal regulatory protein beta (SIRPbeta)', *The Journal of biological chemistry*, 287(23), pp. 19386-19398.
64. Friese, M.A., Steinle, A. and Weller, M. (2004) 'The innate immune response in the central nervous system and its role in glioma immune surveillance', *Onkologie*, 27(5), pp. 487-491.
65. Frigault, M.M., Lacoste, J., Swift, J.L. and Brown, C.M. (2009) 'Live-cell microscopy - tips and tools', *Journal of cell science*, 122(Pt 6), pp. 753-767.
66. Fujisawa, H., Reis, R.M., Nakamura, M., Colella, S., Yonekawa, Y., Kleihues, P. and Ohgaki, H. (2000) 'Loss of heterozygosity on chromosome 10 is more extensive in primary (de novo) than in secondary glioblastomas', *Laboratory investigation; a journal of technical methods and pathology*, 80(1), pp. 65-72.
67. Furnari, F.B., Fenton, T., Bachoo, R.M., Mukasa, A., Stommel, J.M., Stegh, A., Hahn, W.C., Ligon, K.L., Louis, D.N., Brennan, C., Chin, L., DePinho, R.A. and Cavenee, W.K. (2007) 'Malignant astrocytic glioma: genetics, biology, and paths to treatment', *Genes & development*, 21(21), pp. 2683-2710
68. Gabrusiewicz, K., Ellert-Miklaszewska, A., Lipko, M., Sielska, M., Frankowska, M. and Kaminska, B. (2011) 'Characteristics of the alternative phenotype of microglia/macrophages and its modulation in experimental gliomas', *PLoS one*, 6(8), pp. e23902.
69. Gabrusiewicz, K., Liu, D., Cortes-Santiago, N., Hossain, M.B., Conrad, C.A., Aldape, K.D., Fuller, G.N., Marini, F.C., Alonso, M.M., Idoate, M.A., Gilbert, M.R., Fueyo, J. and Gomez-Manzano, C. (2014) 'Anti-vascular endothelial growth factor therapy-induced glioma invasion is associated with accumulation of Tie2-expressing monocytes', *Oncotarget*, 5(8), pp. 2208-2220.
70. Gasque, P., Dean, Y.D., McGreal, E.P., VanBeek, J. and Morgan, B.P. (2000) 'Complement components of the innate immune system in health and disease in the CNS', *Immunopharmacology*, 49(1-2), pp. 171-186.

71. Getz, G.S. (2005) 'Thematic review series: the immune system and atherogenesis. Bridging the innate and adaptive immune systems', *Journal of lipid research*, 46(4), pp. 619-622.
72. Giancotti, F.G. and Ruoslahti, E. (1999) 'Integrin signaling', *Science (New York, N.Y.)*, 285(5430), pp. 1028-1032.
73. Giembycz, M.A. and Lindsay, M.A. (1999) 'Pharmacology of the eosinophil', *Pharmacological reviews*, 51(2), pp. 213-340.
74. Goswami, S., Gupta, A. and Sharma, S.K. (1998) 'Interleukin-6-mediated autocrine growth promotion in human glioblastoma multiforme cell line U87MG', *Journal of neurochemistry*, 71(5), pp. 1837-1845.
75. Gotlieb, W.H., Watson, J.M., Rezai, A., Johnson, M., Martinez-Maza, O. and Berek, J.S. (1994) 'Cytokine-induced modulation of tumor suppressor gene expression in ovarian cancer cells: up-regulation of p53 gene expression and induction of apoptosis by tumor necrosis factor-alpha', *American Journal of Obstetrics and Gynecology*, 170(4), pp. 1121-8; discussion 1128-30.
76. Granger, M.P., Wright, W.E., and Shay, J. W. (2002) 'Telomerase in cancer and aging', *Oncology Hematology*, 41, pp. 29-40
77. Grauer, O., Poschl, P., Lohmeier, A., Adema, G.J. and Bogdahn, U. (2007) 'Toll-like receptor triggered dendritic cell maturation and IL-12 secretion are necessary to overcome T-cell inhibition by glioma-associated TGF-beta2', *Journal of neuro-oncology*, 82(2), pp. 151-161.
78. Greter, M., Lelios, I. and Croxford, A.L. (2015) 'Microglia Versus Myeloid Cell Nomenclature during Brain Inflammation', *Frontiers in immunology*, 6, pp. 249.
79. Grivennikov, S.I., Greten, F.R. and Karin, M. (2010) 'Immunity, inflammation, and cancer', *Cell*, 140(6), pp. 883-899.
80. Geunes-Boyer, S., Oliver, T.N., Janbon, G., Lodge, J.K., Heitman, J., Perfect, J.R. and Wright, J.R. (2009) 'Surfactant protein D increases phagocytosis of cryptococcal neoformans by murine macrophages and enhances fungal survival', *Infection and immunity*, 77(7), pp. 2783-2794.
81. Gupta, S., Bi, R., Kim, C., Chiplunkar, S., Yel, L. and Gollapudi, S. (2005) 'Role of NF-kappaB signaling pathway in increased tumor necrosis factor-alpha-induced apoptosis of lymphocytes in aged humans', *Cell death and differentiation*, 12(2), pp. 177-183.
82. Haczku, A. (2008) 'Protective role of the lung collectins surfactant protein A and surfactant protein D in airway inflammation', *The Journal of allergy and clinical immunology*, 122(5), pp. 861-79; quiz 880-1
83. Hagberg, H., Mallard, C., Ferriero, D.M., Vannucci, S.J., Levison, S.W., Vexler, Z.S. and Gressens, P. (2015) 'The role of inflammation in perinatal brain injury', *Nature reviews. Neurology*, 11(4), pp. 192-208.
84. Hambardzumyan, D., Gutmann, D.H. and Kettenmann, H. (2016) 'The role of microglia and macrophages in glioma maintenance and progression', *Nature neuroscience*, 19(1), pp. 20-27.
85. Hamburger, A. and Salmon, S.E. (1977) 'Primary bioassay of human myeloma stem cells', *The Journal of clinical investigation*, 60, pp. 846-854.

- 86.Hanahan, D. and Weinberg, R.A. (2000) 'The hallmarks of cancer', *Cell*, 100(1), pp. 57-70.
- 87.Hanahan, D. and Weinberg, R.A. (2011) 'Hallmarks of cancer: the next generation', *Cell*, 144(5), pp. 646-674.
- 88.Hansson, G.K., Libby, P., Schonbeck, U. and Yan, Z.Q. (2002) 'Innate and adaptive immunity in the pathogenesis of atherosclerosis', *Circulation research*, 91(4), pp. 281-291.
- 89.Harris, C.C. (1996) 'p53 tumor suppressor gene: from the basic research laboratory to the clinic- unabridged historical perspective', *Carcinogenesis*, 17, pp. 1187-1198
- 90.Harris, C.L., Pettigrew, D.M., Lea, S.M. and Morgan, B.P. (2007) 'Decay-accelerating factor must bind both components of the complement alternative pathway C3 convertase to mediate efficient decay', *Journal of immunology (Baltimore, Md.: 1950)*, 178(1), pp. 352-359.
- 91.Hartl, D. and Griese, M. (2006) 'Surfactant protein D in human lung diseases', *European journal of clinical investigation*, 36(6), pp. 423-435.
- 92.Hartshorn, K.L., Crouch, E., White, M.R., Colamussi, M.L., Kakkanatt, A., Tauber, B., Shepherd, V. and Sastry, K.N. (1998) 'Pulmonary surfactant proteins A and D enhance neutrophil uptake of bacteria', *The American Journal of Physiology*, 274(6 Pt 1), pp. L958-69.
- 93.Hartshorn, K.L., Crouch, E.C., White, M.R., Eggleton, P., Tauber, A.I., Chang, D. and Sastry, K. (1994) 'Evidence for a protective role of pulmonary surfactant protein D (SP-D) against influenza A viruses', *The Journal of clinical investigation*, 94(1), pp. 311-319.
- 94.Herias, M.V., Hogenkamp, A., van Asten, A.J., Tersteeg, M.H., van Eijk, M. and Haagsman, H.P. (2007) 'Expression sites of the collectin SP-D suggest its importance in first line host defence: power of combining in situ hybridisation, RT-PCR and immunohistochemistry', *Molecular immunology*, 44(13), pp. 3324-3332.
- 95.Herx, L.M., Rivest, S. and Yong, V.W. (2000) 'Central nervous system-initiated inflammation and neurotrophism in trauma: IL-1 beta is required for the production of ciliary neurotrophic factor', *Journal of immunology (Baltimore, Md.: 1950)*, 165(4), pp. 2232-2239.
- 96.Hickling, T.P., Bright, H., Wing, K., Gower, D., Martin, S.L., Sim, R.B. and Malhotra, R. (1999) 'A recombinant trimeric surfactant protein D carbohydrate recognition domain inhibits respiratory syncytial virus infection in vitro and in vivo', *European journal of immunology*, 29(11), pp. 3478-3484.
- 97.Hoesel, B. and Schmid, J.A. (2013) 'The complexity of NF-kappaB signaling in inflammation and cancer', *Molecular cancer*, 12, pp. 86-4598-12-86.

- 98.Hoh, J., Jin, S., Parrado, T., Edington, J., Levine, A.J. and Ott, J. (2002) 'The p53MH algorithm and its application in detecting p53-responsive genes', *Proceedings of the National Academy of Sciences of the United States of America*, 99(13), pp. 8467-8472.
- 99.Holland, E.C.(2000) 'Glioblastoma multiforme:The terminator', *Proceedings of the national academy of science of the United States of America*, 97(12), pp. 6242-6244
- 100.Holmskov, U., Thiel, S. and Jensenius, J.C. (2003) 'Collections and ficolins: humoral lectins of the innate immune defense', *Annual Review of Immunology*, 21, pp. 547-578.
- 101.Hong, S. and Van Kaer, L. (1999) 'Immune privilege: keeping an eye on natural killer T cells', *The Journal of experimental medicine*, 190(9), pp. 1197-1200.
- 102.Hourcade, D.E. (2006) 'The role of properdin in the assembly of the alternative pathway C3 convertases of complement', *The Journal of biological chemistry*, 281(4), pp. 2128-2132.
- 103.Hourcade, D.E. and Mitchell, L.M. (2011) 'Access to the complement factor B scissile bond is facilitated by association of factor B with C3b protein', *The Journal of biological chemistry*, 286(41), pp. 35725-35732.
- 104.Huettner, C., Czub, S., Kerkau, S., Roggendorf, W. and Tonn, J.C. (1997) 'Interleukin 10 is expressed in human gliomas in vivo and increases glioma cell proliferation and motility in vitro', *Anticancer Research*, 17(5A), pp. 3217-3224.
- 105.Husain, S.R. and Puri, R.K. (2003) 'Interleukin-13 receptor-directed cytotoxin for malignant glioma therapy: from bench to bedside', *Journal of neuro-oncology*, 65(1), pp. 37-48.
- 106.Huse, J. T., Phillips, H. S., and Brennan, C. W. (2011)'Molecular subclassification of diffuse gliomas: Seeing order in the chaos', *Glia*, 59(8), 1190-1199
- 107.Husemann, J., Loike, J.D., Anankov, R., Febbraio, M. and Silverstein, S.C. (2002) 'Scavenger receptors in neurobiology and neuropathology: their role on microglia and other cells of the nervous system', *Glia*, 40(2), pp. 195-205.
- 108.Husemann, J. and Silverstein, S.C. (2001) 'Expression of scavenger receptor class B, type I, by astrocytes and vascular smooth muscle cells in normal adult mouse and human brain and in Alzheimer's disease brain', *The American journal of pathology*, 158(3), pp. 825-832.
- 109.Ignatova, T.N., Kukekov, V.G., Laywell, E.D., Suslov, O.N., Vrionis, F.D. and Steindler, D.A. (2002) 'Human cortical glial tumors contain neural stem-like cells expressing astroglial and neuronal markers in vitro', *Glia*, 39, pp. 193-206.
- 110.Jack, C.S., Arbour, N., Manusow, J., Montgrain, V., Blain, M., McCrea, E., Shapiro, A. and Antel, J.P. (2005) 'TLR signaling tailors innate immune responses in human microglia and astrocytes', *Journal of immunology (Baltimore, Md.: 1950)*, 175(7), pp. 4320-4330.
- 111.Jackson, R. J., Fuller, G. N., Abi-Said, D., Lang, F. F., Gokaslan, Z. L., Shi, W. M., et al. (2001). Limitations of stereotactic biopsy in the initial management of gliomas. *Neuro-Oncology*, 3(3), 193-200.

112. Jefford, C.E., and Finger, I.I. (2006) 'Mechanisms of chromosome instability in cancers', *Oncology Hematology*, 59, pp. 1-14
113. Jones, D.T.W., Gronych, J., Lichter, P., Witt, O., and Pfister, S.M. (2012) 'MAPK pathway activation in pilocytic astrocytoma', *Cellular and Molecular Life Sciences*, 69, pp. 1799-1811
114. Jordan, T.C., Guzman, M.L., Noble, M. (2006) 'Cancer Stem Cells', *The new England journal of medicine*, 355, pp. 1253-1261
115. Joseph, J.V., Balasubramaniyan, V., Walenkamp, A. and Kruyt, F.A. (2013) 'TGF-beta as a therapeutic target in high grade gliomas - promises and challenges', *Biochemical pharmacology*, 85(4), pp. 478-485.
116. Jounblat, R., Kadioglu, A., Iannelli, F., Pozzi, G., Eggleton, P. and Andrew, P.W. (2004) 'Binding and agglutination of Streptococcus pneumoniae by human surfactant protein D (SP-D) vary between strains, but SP-D fails to enhance killing by neutrophils', *Infection and immunity*, 72(2), pp. 709-716.
117. Jozsi, M., Heinen, S., Hartmann, A., Ostrowicz, C.W., Halbich, S., Richter, H., Kunert, A., Licht, C., Saunders, R.E., Perkins, S.J., Zipfel, P.F. and Skerka, C. (2006) 'Factor H and atypical hemolytic uremic syndrome: mutations in the C-terminus cause structural changes and defective recognition functions', *Journal of the American Society of Nephrology : JASN*, 17(1), pp. 170-177.
118. Junnikkala, S., Jokiranta, T.S., Friese, M.A., Jarva, H., Zipfel, P.F. and Meri, S. (2000) 'Exceptional resistance of human H2 glioblastoma cells to complement-mediated killing by expression and utilization of factor H and factor H-like protein 1', *Journal of immunology (Baltimore, Md.: 1950)*, 164(11), pp. 6075-6081.
119. Kaltschmidt, B., Kaltschmidt, C., Hofmann, T.G., Hehner, S.P., Droge, W. and Schmitz, M.L. (2000) 'The pro- or anti-apoptotic function of NF-kappaB is determined by the nature of the apoptotic stimulus', *European journal of biochemistry*, 267(12), pp. 3828-3835.
120. Kankavi, O., Baykara, M., Eren Karanis, M.I., Bassorgun, C.I., Ergin, H. and Ciftcioglu, M.A. (2014) 'Evidence of surfactant protein A and D expression decrement and their localizations in human prostate adenocarcinomas', *Renal failure*, 36(2), pp. 258-265.
121. Kanu, O. O., Mehta, A., Di, C., Lin, N., Bortoff, K., Bigner, D. D., Yan, H. and Adamson, D.C. (2009) 'Glioblastoma multiforme: a review of therapeutic targets', *Expert opinion on therapeutic targets*, 13(6), pp. 701-718.
122. Kimelberg, H.K. and Nedergaard, M. (2010) 'Functions of astrocytes and their potential as therapeutic targets', *Neurotherapeutics : the journal of the American Society for Experimental NeuroTherapeutics*, 7(4), pp. 338-353.

123. Kishore, U., Wang, J.Y., Hoppe, H.J. and Reid, K.B. (1996) 'The alpha-helical neck region of human lung surfactant protein D is essential for the binding of the carbohydrate recognition domains to lipopolysaccharides and phospholipids', *The Biochemical journal*, 318 (Pt 2)(Pt 2), pp. 505-511.
124. Kishore, U., Gaboriaud, C., Waters, P., Shrive, A.K., Greenhough, T.J., Reid, K.B., Sim, R.B. and Arlaud, G.J. (2004) 'C1q and tumor necrosis factor superfamily: modularity and versatility', *Trends in immunology*, 25(10), pp. 551-561.
125. Kishore, U., Greenhough, T.J., Waters, P., Shrive, A.K., Ghai, R., Kamran, M.F., Bernal, A.L., Reid, K.B., Madan, T. and Chakraborty, T. (2006) 'Surfactant proteins SP-A and SP-D: structure, function and receptors', *Molecular immunology*, 43(9), pp. 1293-1315
126. Klein, R.J., Zeiss, C., Chew, E.Y., Tsai, J.Y., Sackler, R.S., Haynes, C., Henning, A.K., SanGiovanni, J.P., Mane, S.M., Mayne, S.T., Bracken, M.B., Ferris, F.L., Ott, J., Barnstable, C. and Hoh, J. (2005) 'Complement factor H polymorphism in age-related macular degeneration', *Science (New York, N.Y.)*, 308(5720), pp. 385-389.
127. Knobbe, C.B., Merlo, A. and Reifemberger, G. (2002) 'Pten signaling in gliomas', *Neuro-oncology*, 4(3), pp. 196-211.
128. Koenderman, L., van der Bruggen, T., Schweizer, R.C., Warringa, R.A., Coffey, P., Caldenhoven, E., Lammers, J.W. and Raaijmakers, J.A. (1996) 'Eosinophil priming by cytokines: from cellular signal to in vivo modulation', *The European respiratory journal. Supplement*, 22, pp. 119s-125s.
129. Kolble, K., Lu, J., Mole, S.E., Kaluz, S. and Reid, K.B. (1993) 'Assignment of the human pulmonary surfactant protein D gene (SFTP4) to 10q22-q23 close to the surfactant protein A gene cluster', *Genomics*, 17(2), pp. 294-298.
130. Kominsky, S., Johnson, H.M., Bryan, G., Tanabe, T., Hobeika, A.C., Subramaniam, P.S. and Torres, B. (1998) 'IFN γ inhibition of cell growth in glioblastomas correlates with increased levels of the cyclin dependent kinase inhibitor p21WAF1/CIP1', *Oncogene*, 17(23), pp. 2973-2979.
131. Kopp, A., Hebecker, M., Svobodova, E. and Jozsi, M. (2012) 'Factor h: a complement regulator in health and disease, and a mediator of cellular interactions', *Biomolecules*, 2(1), pp. 46-75.
132. Kovacs, H., O'Donoghue, S.I., Hoppe, H.J., Comfort, D., Reid, K.B., Campbell, I. and Nilges, M. (2002) 'Solution structure of the coiled-coil trimerization domain from lung surfactant protein D', *Journal of Biomolecular NMR*, 24(2), pp. 89-102.#
133. Krakstad, C. and Chekenya, M. (2010) 'Survival signalling and apoptosis resistance in glioblastomas: opportunities for targeted therapeutics', *Molecular cancer*, 9, pp. 135-4598-9-13
134. Kuan, S.F., Rust, K. and Crouch, E. (1992) 'Interactions of surfactant protein D with bacterial lipopolysaccharides. Surfactant protein D is an Escherichia coli-binding protein in bronchoalveolar lavage', *The Journal of clinical investigation*, 90(1), pp. 97-106.
135. Kudo, K., Sano, H., Takahashi, H., Kuronuma, K., Yokota, S., Fujii, N., Shimada, K., Yano, I., Kumazawa, Y., Voelker, D.R., Abe, S. and Kuroki, Y. (2004) 'Pulmonary collectins enhance phagocytosis of Mycobacterium avium through increased activity

- of mannose receptor', *Journal of immunology (Baltimore, Md.: 1950)*, 172(12), pp. 7592-7602.
- 136.Kumar, H., Kawai, T. and Akira, S. (2011) 'Pathogen recognition by the innate immune system', *International reviews of immunology*, 30(1), pp. 16-34.
- 137.Kuroki, Y., Takahashi, H., Chiba, H. and Akino, T. (1998) 'Surfactant proteins A and D: disease markers', *Biochimica et biophysica acta*, 1408(2-3), pp. 334-345.
- 138.Kurokouchi, K., Kambe, F., Yasukawa, K., Izumi, R., Ishiguro, N., Iwata, H. and Seo, H. (1998) 'TNF-alpha increases expression of IL-6 and ICAM-1 genes through activation of NF-kappaB in osteoblast-like ROS17/2.8 cells', *Journal of bone and mineral research : the official journal of the American Society for Bone and Mineral Research*, 13(8), pp. 1290-1299.
- 139.Kwon, H.J., Breese, E.H., Vig-Varga, E., Luo, Y., Lee, Y., Goebel, M.G. and Harrington, M.A. (2004) 'Tumor necrosis factor alpha induction of NF-kappaB requires the novel coactivator SIMPL', *Molecular and cellular biology*, 24(21), pp. 9317-9326.
- 140.Landskron, G., De la Fuente, M., Thuwajit, P., Thuwajit, C. and Hermoso, M.A. (2014) 'Chronic inflammation and cytokines in the tumor microenvironment', *Journal of immunology research*, 2014, pp. 149185.
- 141.Lawson, L.J., Perry, V.H. and Gordon, S. (1992) 'Turnover of resident microglia in the normal adult mouse brain', *Neuroscience*, 48(2), pp. 405-415.
- 142.Lee, S.H., Meng, X.W., Flatten, K.S., Loegering, D.A. and Kaufmann, S.H. (2013) 'Phosphatidylserine exposure during apoptosis reflects bidirectional trafficking between plasma membrane and cytoplasm', *Cell death and differentiation*, 20(1), pp. 64-76.
- 143.Lee, Y.B., Nagai, A. and Kim, S.U. (2002) 'Cytokines, chemokines, and cytokine receptors in human microglia', *Journal of neuroscience research*, 69(1), pp. 94-103.
- 144.Lemos, M.P., McKinney, J. and Rhee, K.Y. (2011) 'Dispensability of surfactant proteins A and D in immune control of Mycobacterium tuberculosis infection following aerosol challenge of mice', *Infection and immunity*, 79(3), pp. 1077-1085.
- 145.Leth-Larsen, R., Floridon, C., Nielsen, O. and Holmskov, U. (2004) 'Surfactant protein D in the female genital tract', *Molecular human reproduction*, 10(3), pp. 149-154.
- 146.Li, S., Crothers, J., Haqq, C.M., and Blackburn, E.H., (2005) 'Cellular and Gene Expression Responses Involved in the Rapid Growth Inhibition of Human Cancer Cells by RNA Interference-mediated depletion of Telomerase RNA', *The journal of Biological Chemistry*, 280 pp. 23709-23717
- 147.Li, R., Li, G., Deng, L., Liu, Q., Dai, J., Shen, J. and Zhang, J. (2010) 'IL-6 augments the invasiveness of U87MG human glioblastoma multiforme cells via up-regulation of MMP-2 and fascin-1', *Oncology reports*, 23(6), pp. 1553-1559.
- 148.Lim, B.L., Wang, J.Y., Holmskov, U., Hoppe, H.J. and Reid, K.B. (1994) 'Expression of the carbohydrate recognition domain of lung surfactant protein D and

- demonstration of its binding to lipopolysaccharides of gram-negative bacteria', *Biochemical and biophysical research communications*, 202(3), pp. 1674-1680.
- 149.Lin, Z., Thomas, N.J., Bibikova, M., Seifart, C., Wang, Y., Guo, X., Wang, G., Vollmer, E., Goldmann, T., Garcia, E.W., Zhou, L., Fan, J.B. and Floros, J. (2007) 'DNA methylation markers of surfactant proteins in lung cancer', *International journal of oncology*, 31(1), pp. 181-191.
- 150.Liu, Y., Ehtesham, M., Samoto, K., Wheeler, C.J., Thompson, R.C., Villarreal, L.P., Black, K.L. and Yu, J.S. (2002) 'In situ adenoviral interleukin 12 gene transfer confers potent and long-lasting cytotoxic immunity in glioma', *Cancer gene therapy*, 9(1), pp. 9-15.
- 151.Liu, Q., Li, G., Li, R., Shen, J., He, Q., Deng, L., Zhang, C. and Zhang, J. (2010) 'IL-6 promotion of glioblastoma cell invasion and angiogenesis in U251 and T98G cell lines', *Journal of neuro-oncology*, 100(2), pp. 165-176.
- 152.Liu, K.Q., Liu, Z.P., Hao, J.K., Chen, L. and Zhao, X.M. (2012) 'Identifying dysregulated pathways in cancers from pathway interaction networks', *BMC bioinformatics*, 13, pp. 126-2105-13-126.
- 153.Liu, Y., Liu, H., Kim, B.O., Gattone, V.H., Li, J., Nath, A., Blum, J. and He, J.J. (2004) 'CD4-independent infection of astrocytes by human immunodeficiency virus type 1: requirement for the human mannose receptor', *Journal of virology*, 78(8), pp. 4120-4133.
- 154.Liu, Z., Shi, Q., Liu, J., Abdel-Razek, O., Xu, Y., Cooney, R.N. and Wang, G. (2015) 'Innate Immune Molecule Surfactant Protein D Attenuates Sepsis-induced Acute Pancreatic Injury through Modulating Apoptosis and NF-kappaB-mediated Inflammation', *Scientific reports*, 5, pp. 17798.
- 155.Llopiz, D., Dotor, J., Casares, N., Bezunartea, J., Diaz-Valdes, N., Ruiz, M., Aranda, F., Berraondo, P., Prieto, J., Lasarte, J.J., Borrás-Cuesta, F. and Sarobe, P. (2009) 'Peptide inhibitors of transforming growth factor-beta enhance the efficacy of antitumor immunotherapy', *International journal of cancer. Journal international du cancer*, 125(11), pp. 2614-2623.
- 156.Lote, K., Egeland, T., Hager, B., Stenwig, B., Skullerud, K., Berg-Johnsen, J., Storm-Mathisen, I. and Hirschberg, H. (1997) 'Survival, prognostic factors, and therapeutic efficacy in low-grade glioma: a retrospective study in 379 patients', *Journal of clinical oncology : official journal of the American Society of Clinical Oncology*, 15, pp. 3129-3140.
- 157.Louis, D.N., Ohgaki, H., Wiestler, O.D., Cavenee, W.K., Burger, P.C., Jouvett, A., Scheithauer, B.W., and Kleihues, P. (2007) 'The 2007 WHO classification of tumours of the central nervous system', *Acta Neuropathologica*, 114, pp. 97-109
- 158.Lu, Y., Jiang, F., Zheng, X., Katakowski, M., Buller, B., To, S.S. and Chopp, M. (2011) 'TGF-beta1 promotes motility and invasiveness of glioma cells through activation of ADAM17', *Oncology reports*, 25(5), pp. 1329-1335.
- 159.Lukashev, M.E. and Werb, Z. (1998) 'ECM signalling: orchestrating cell behaviour and misbehaviour', *Trends in cell biology*, 8(11), pp. 437-441.

160. Lull, M.E. and Block, M.L. (2010) 'Microglial activation and chronic neurodegeneration', *Neurotherapeutics : the journal of the American Society for Experimental NeuroTherapeutics*, 7(4), pp. 354-365.
161. Madan, T., Eggleton, P., Kishore, U., Strong, P., Aggrawal, S.S., Sarma, P.U. and Reid, K.B. (1997) 'Binding of pulmonary surfactant proteins A and D to *Aspergillus fumigatus* conidia enhances phagocytosis and killing by human neutrophils and alveolar macrophages', *Infection and immunity*, 65(8), pp. 3171-3179.
162. Madan, T., Kishore, U., Shah, A., Eggleton, P., Strong, P., Wang, J.Y., Aggrawal, S.S., Sarma, P.U. and Reid, K.B. (1997) 'Lung surfactant proteins A and D can inhibit specific IgE binding to the allergens of *Aspergillus fumigatus* and block allergen-induced histamine release from human basophils', *Clinical and experimental immunology*, 110(2), pp. 241-249.
163. Madan, T., Reid, K.B., Singh, M., Sarma, P.U. and Kishore, U. (2005) 'Susceptibility of mice genetically deficient in the surfactant protein (SP)-A or SP-D gene to pulmonary hypersensitivity induced by antigens and allergens of *Aspergillus fumigatus*', *Journal of immunology (Baltimore, Md.: 1950)*, 174(11), pp. 6943-6954.
164. Madsen, J., Kliem, A., Tornøe, I., Skjodt, K., Koch, C. and Holmskov, U. (2000) 'Localization of lung surfactant protein D on mucosal surfaces in human tissues', *Journal of immunology (Baltimore, Md.: 1950)*, 164(11), pp. 5866-5870.
165. Maher, E.A., Brennan, C., Wen, P.Y., Durso, L., Ligon, K.L., Richardson, A., Khatry, D., Feng, B., Sinha, R., Louis, D.N., Quackenbush, J., Black, P.M., Chin, L. and DePinho, R.A. (2006) 'Marked genomic differences characterize primary and secondary glioblastoma subtypes and identify two distinct molecular and clinical secondary glioblastoma entities', *Cancer research*, 66(23), pp. 11502-11513.
166. Maitland, N.J. and Collins, A.T. (2008) 'Prostate cancer stem cells: a new target for therapy', *Journal of clinical oncology : official journal of the American Society of Clinical Oncology*, 26(17), pp. 2862-2870.
167. Mahajan, L., Madan, T., Kamal, N., Singh, V.K., Sim, R.B., Telang, S.D., Ramchand, C.N., Waters, P., Kishore, U. and Sarma, P.U. (2008) 'Recombinant surfactant protein-D selectively increases apoptosis in eosinophils of allergic asthmatics and enhances uptake of apoptotic eosinophils by macrophages', *International immunology*, 20(8), pp. 993-1007.
168. Mahajan, L., Pandit, H., Madan, T., Gautam, P., Yadav, A.K., Warke, H., Sundaram, C.S., Sirdeshmukh, R., Sarma, P.U., Kishore, U. and Surolia, A. (2013) 'Human surfactant protein D alters oxidative stress and HMGA1 expression to induce p53 apoptotic pathway in eosinophil leukemic cell line', *PLoS one*, 8(12), pp. e85046.
169. Male, D.A., Ormsby, R.J., Ranganathan, S., Giannakis, E. and Gordon, D.L. (2000) 'Complement factor H: sequence analysis of 221 kb of human genomic DNA containing the entire fH, fHR-1 and fHR-3 genes', *Molecular immunology*, 37(1-2), pp. 41-52.

- 170.Mao, H., Lebrun, D.G., Yang, J., Zhu, V.F. and Li, M. (2012) 'Deregulated signaling pathways in glioblastoma multiforme: molecular mechanisms and therapeutic targets', *Cancer investigation*, 30(1), pp. 48-56.
- 171.Markiewicz, I. and Lukomska, B. (2006) 'The role of astrocytes in the physiology and pathology of the central nervous system', *Acta Neurobiologiae Experimentalis*, 66(4), pp. 343-358.
- 172.Markovic, D.S., Vinnakota, K., Chirasani, S., Synowitz, M., Raguet, H., Stock, K., Sliwa, M., Lehmann, S., Kalin, R., van Rooijen, N., Holmbeck, K., Heppner, F.L., Kiwit, J., Matyash, V., Lehnardt, S., Kaminska, B., Glass, R. and Kettenmann, H. (2009) 'Gliomas induce and exploit microglial MT1-MMP expression for tumor expansion', *Proceedings of the National Academy of Sciences of the United States of America*, 106(30), pp. 12530-12535.
- 173.Mathon, N.F. and Lloyd, A.C. (2001) 'Cell senescence and cancer', *Nature reviews.Cancer*, 1(3), pp. 203-213.
- 174.McRae, J.L., Cowan, P.J., Power, D.A., Mitchelhill, K.I., Kemp, B.E., Morgan, B.P. and Murphy, B.F. (2001) 'Human factor H-related protein 5 (FHR-5). A new complement-associated protein', *The Journal of biological chemistry*, 276(9), pp. 6747-6754.
- 175.McRae, J.L., Murphy, B.E., Eyre, H.J., Sutherland, G.R., Crawford, J. and Cowan, P.J. (2002) 'Location and structure of the human FHR-5 gene', *Genetica*, 114(2), pp. 157-161.
- 176.McRae, J.L., Duthy, T.G., Griggs, K.M., Ormsby, R.J., Cowan, P.J., Cromer, B.A., McKinstry, W.J., Parker, M.W., Murphy, B.F. and Gordon, D.L. (2005) 'Human factor H-related protein 5 has cofactor activity, inhibits C3 convertase activity, binds heparin and C-reactive protein, and associates with lipoprotein', *Journal of immunology (Baltimore, Md.: 1950)*, 174(10), pp. 6250-6256.
- 177.Medzhitov, R. and Janeway, C.A., Jr (1997) 'Innate immunity: the virtues of a nonclonal system of recognition', *Cell*, 91(3), pp. 295-298.
- 178.Medzhitov, R. and Janeway, C., A. (1998) 'Innate immune recognition and control of adaptive immune responses', *Seminars in Immunology*, 10(5), pp. 351-353
- 179.Meschi, J., Crouch, E.C., Skolnik, P., Yahya, K., Holmskov, U., Leth-Larsen, R., Tornøe, I., Teclé, T., White, M.R. and Hartshorn, K.L. (2005) 'Surfactant protein D binds to human immunodeficiency virus (HIV) envelope protein gp120 and inhibits HIV replication', *The Journal of general virology*, 86(Pt 11), pp. 3097-3107
- 180.Miller, R.H. and Raff, M.C. (1984) 'Fibrous and protoplasmic astrocytes are biochemically and developmentally distinct', *The Journal of neuroscience : the official journal of the Society for Neuroscience*, 4(2), pp. 585-592.

181. Miller, B.E., Miller, F.R., Leith, J. and Heppner, G.H. (1980) 'Growth interaction in vivo between tumor subpopulations derived from a single mouse mammary tumor', *Cancer research*, 40(11), pp. 3977-3981.
182. Mittal, D., Gubin, M.M., Schreiber, R.D. and Smyth, M.J. (2014) 'New insights into cancer immunoediting and its three component phases--elimination, equilibrium and escape', *Current opinion in immunology*, 27, pp. 16-25.
183. Miyamura, K., Malhotra, R., Hoppe, H.J., Reid, K.B., Phizackerley, P.J., Macpherson, P. and Lopez Bernal, A. (1994) 'Surfactant proteins A (SP-A) and D (SP-D): levels in human amniotic fluid and localization in the fetal membranes', *Biochimica et biophysica acta*, 1210(3), pp. 303-307.
184. Mogensen, T.H. (2009) 'Pathogen recognition and inflammatory signaling in innate immune defenses', *Clinical microbiology reviews*, 22(2), pp. 240-73, Table of Contents.
185. Mori, S., Maher, P. and Conti, B. (2016) 'Neuroimmunology of the Interleukins 13 and 4', *Brain sciences*, 6(2), pp. 10.3390/brainsci6020018.
186. Morse, M.A., Lyerly, H.K., Clay, T.M., Abdel-Wahab, O., Chui, S.Y., Garst, J., Gollob, J., Grossi, P.M., Kalady, M., Mosca, P.J., Onaitis, M., Sampson, J.H., Seigler, H.F., Toloza, E.M., Tyler, D., Vieweg, J. and Yang, Y. (2004) 'Immunotherapy of surgical malignancies', *Current problems in surgery*, 41(1), pp. 15-132.
187. Moses, H., Yang, E.Y., and Pietsenpol, J. A. (1990) 'TGF- β stimulation and inhibition of cell proliferation: new mechanistic insight', *Cell*, 63, pp. 245-247
188. Muller, P.A. and Vousden, K.H. (2013) 'P53 Mutations in Cancer', *Nature cell biology*, 15(1), pp. 2-8.
189. Nagane, M., Coufal, F., Lin, H., Bogler, O., Cavenee, W.K. and Huang, H.J. (1996) 'A common mutant epidermal growth factor receptor confers enhanced tumorigenicity on human glioblastoma cells by increasing proliferation and reducing apoptosis', *Cancer research*, 56(21), pp. 5079-5086.
190. Nagpal, J., Jamoona, A., Gulati, N.D., Mohan, A., Braun, A., Murali, R. and Jhanwar-Uniyal, M. (2006) 'Revisiting the role of p53 in primary and secondary glioblastomas', *Anticancer Research*, 26(6C), pp. 4633-4639.
191. Nair, A., Frederick, T.J. and Miller, S.D. (2008) 'Astrocytes in multiple sclerosis: a product of their environment', *Cellular and molecular life sciences : CMLS*, 65(17), pp. 2702-2720.
192. Nakamura, K., Ohya, W., Funakoshi, H., Sakaguchi, G., Kato, A., Takeda, M., Kudo, T. and Nakamura, T. (2006) 'Possible role of scavenger receptor SRCL in the clearance of amyloid-beta in Alzheimer's disease', *Journal of neuroscience research*, 84(4), pp. 874-890.
193. Natsume, A., Tsujimura, K., Mizuno, M., Takahashi, T. and Yoshida, J. (2000) 'IFN-beta gene therapy induces systemic antitumor immunity against malignant glioma', *Journal of neuro-oncology*, 47(2), pp. 117-124

194. Nayak, A., Dodagatta-Marri, E., Tsolaki, A.G. and Kishore, U. (2012) 'An Insight into the Diverse Roles of Surfactant Proteins, SP-A and SP-D in Innate and Adaptive Immunity', *Frontiers in immunology*, 3, pp. 131.
195. Newton, H.B., Rosenblum, M.K. and Walker, R.W. (1992) 'Extraneural metastases of infratentorial glioblastoma multiforme to the peritoneal cavity', *Cancer*, 69(8), pp. 2149-2153.
196. Oberndorfer, S., Lindeck-Pozza, E., Lahrmann, H., Struhal, W., Hitzemberger, P. and Grisold, W. (2008) 'The end-of-life hospital setting in patients with glioblastoma', *Journal of palliative medicine*, 11(1), pp. 26-30.
197. O'Brien, A.C., Pollett, A., Gallinger, S., and Dick, J.E. (2006) 'A human colon cancer cell capable of initiating tumour growth in immunodeficient mice', *Nature*, 445, pp. 106-110.
198. Ogasawara, Y. and Voelker, D.R. (1995) 'The role of the amino-terminal domain and the collagenous region in the structure and the function of rat surfactant protein D', *The Journal of biological chemistry*, 270(32), pp. 19052-19058.
199. Ohgaki, H., Dessen, P., Jourde, B., Horstmann, S., Nishikawa, T., Di Patre, P. L., Burkhard, C., Schuler, D., Probst-Hensch, N.M., Maiorka, P.C., Baeza, N., Pisani, P., Yonekawa, Y., Yasargil, M.G., Lutolf, U.M. and Kleihues, P. (2004) 'Genetic pathways to glioblastoma: A population-based study' *Cancer Research*, 64(19), pp. 6892-6899.
200. Ohgaki, H., and Kleihues P. (2005) 'Population-based studies on incidence, survival rates and genetic alterations in astrocytic and oligodendroglial gliomas', *Journal of neuropathology and experimental neurology*, 64, pp. 479-489
201. Ohgaki, H. and Kleihues, P. (2007) 'Genetic pathways to primary and secondary glioblastoma' *The American Journal of Pathology*, 175(5), pp. 1445-1453
202. Ohka, F., Natsume, A. and Wakabayashi, T. (2012) 'Current trends in targeted therapies for glioblastoma multiforme', *Neurology research international*, 2012, pp. 878-885.
203. Ohlsson, M., Bellander, B.M., Langmoen, I.A. and Svensson, M. (2003) 'Complement activation following optic nerve crush in the adult rat', *Journal of neurotrauma*, 20(9), pp. 895-904.
204. Okada, H., Lieberman, F.S., Walter, K.A., Lunsford, L.D., Kondziolka, D.S., Bejjani, G.K., Hamilton, R.L., Torres-Trejo, A., Kalinski, P., Cai, Q., Mabold, J.L., Edington, H.D., Butterfield, L.H., Whiteside, T.L., Potter, D.M., Schold, S.C., Jr and Pollack, I.F. (2007) 'Autologous glioma cell vaccine admixed with interleukin-4 gene transfected fibroblasts in the treatment of patients with malignant gliomas', *Journal of translational medicine*, 5, pp. 67.
205. Olivier, M., Hollstein, M. and Hainaut, P. (2010) 'TP53 mutations in human cancers: origins, consequences, and clinical use', *Cold Spring Harbor perspectives in biology*, 2(1), pp. a001008.

- 206.Olofsson, A., Miyazono, K., Kanzaki, T., Colosetti, P., Engstrom, U. and Heldin, C.H. (1992) 'Transforming growth factor-beta 1, -beta 2, and -beta 3 secreted by a human glioblastoma cell line. Identification of small and different forms of large latent complexes', *The Journal of biological chemistry*, 267(27), pp. 19482-19488.
- 207.Pace, A., Di Lorenzo, C., Guariglia, L., Jandolo, B., Carapella, C.M. and Pompili, A. (2009) 'End of life issues in brain tumor patients', *Journal of neuro-oncology*, 91(1), pp. 39-43.
- 208.Pachter, J.S., de Vries, H.E. and Fabry, Z. (2003) 'The blood-brain barrier and its role in immune privilege in the central nervous system', *Journal of neuropathology and experimental neurology*, 62(6), pp. 593-604.
- 209.Pangburn, M.K. and Muller-Eberhard, H.J. (1984) 'The alternative pathway of complement', *Springer seminars in immunopathology*, 7(2-3), pp. 163-192.
- 210.Pangburn, M.K., Pangburn, K.L., Koistinen, V., Meri, S. and Sharma, A.K. (2000) 'Molecular mechanisms of target recognition in an innate immune system: interactions among factor H, C3b, and target in the alternative pathway of human complement', *Journal of immunology (Baltimore, Md.: 1950)*, 164(9), pp. 4742-4751.
- 211.Parameswaran, N. and Patial, S. (2010) 'Tumor necrosis factor-alpha signaling in macrophages', *Critical reviews in eukaryotic gene expression*, 20(2), pp. 87-103.
- 212.Park, C.H., Bergsagel, D.E., and McCulloch. (1971) 'Mouse Myeloma Tumor Stem Cells: A Primary Cell Culture Assay', *Journal of the national cancer institute*, 46, pp. 411-422
- 213.Park, E.K., Jung, H.S., Yang, H.I., Yoo, M.C., Kim, C. and Kim, K.S. (2007) 'Optimized THP-1 differentiation is required for the detection of responses to weak stimuli', *Inflammation research : official journal of the European Histamine Research Society ...[et al.]*, 56(1), pp. 45-50.
- 214.Park, C., Lee, S., Cho, I.H., Lee, H.K., Kim, D., Choi, S.Y., Oh, S.B., Park, K., Kim, J.S. and Lee, S.J. (2006) 'TLR3-mediated signal induces proinflammatory cytokine and chemokine gene expression in astrocytes: differential signaling mechanisms of TLR3-induced IP-10 and IL-8 gene expression', *Glia*, 53(3), pp. 248-256.
- 215.Pastor, D.M., Irby, R.B. and Poritz, L.S. (2010) 'Tumor necrosis factor alpha induces p53 up-regulated modulator of apoptosis expression in colorectal cancer cell lines', *Diseases of the colon and rectum*, 53(3), pp. 257-263.
- 216.Pachter, J.S., de Vries, H.E. and Fabry, Z. (2003) 'The blood-brain barrier and its role in immune privilege in the central nervous system', *Journal of neuropathology and experimental neurology*, 62(6), pp. 593-604.
- 217.Parney, I.F. (2012) 'Basic concepts in glioma immunology', *Advances in Experimental Medicine and Biology*, 746, pp. 42-52.
- 218.Pellegatta, S., Cuppini, L. and Finocchiaro, G. (2011) 'Brain cancer immunoediting: novel examples provided by immunotherapy of malignant gliomas', *Expert review of anticancer therapy*, 11(11), pp. 1759-1774.

219. Petersen, S.V., Thiel, S. and Jensenius, J.C. (2001) 'The mannan-binding lectin pathway of complement activation: biology and disease association', *Molecular immunology*, 38(2-3), pp. 133-149.
220. Pfister, S. and Witt, O. (2009) 'Pediatric gliomas', *Recent results in cancer research. Fortschritte der Krebsforschung. Progres dans les recherches sur le cancer*, 171, pp. 67-81.
221. Pierantoni, G.M., Rinaldo, C., Esposito, F., Mottolese, M., Soddu, S. and Fusco, A. (2006) 'High Mobility Group A1 (HMGA1) proteins interact with p53 and inhibit its apoptotic activity', *Cell death and differentiation*, 13(9), pp. 1554-1563.
222. Pivneva, T.A. (2008) 'Microglia in normal condition and pathology', *Fiziologichnyi zhurnal (Kiev, Ukraine : 1994)*, 54(5), pp. 81-89.
223. Ransohoff, R.M., Kivisakk, P. and Kidd, G. (2003) 'Three or more routes for leukocyte migration into the central nervous system', *Nature reviews. Immunology*, 3(7), pp. 569-581.
224. Ransohoff, R.M. and Brown, M.A. (2012) 'Innate immunity in the central nervous system', *The Journal of clinical investigation*, 122(4), pp. 1164-1171.
225. Rasper, M., Schafer, A., Piontek, G., Teufel, J., Brockhoff, G., Ringel, F., Heindl, S., Zimmer, C. and Schlegel, J. (2010) 'Aldehyde dehydrogenase 1 positive glioblastoma cells show brain tumor stem cell capacity', *Neuro-oncology*, 12(10), pp. 1024-1033.
226. Reddy, A.L. and Fialkow, P.J. (1979) 'Multicellular origin of fibrosarcomas in mice induced by the chemical carcinogen 3-methylcholanthrene', *The Journal of experimental medicine*, 150, pp. 878-887.
227. Reid, K.B. (1998) 'Interactions of surfactant protein D with pathogens, allergens and phagocytes', *Biochimica et biophysica acta*, 1408(2-3), pp. 290-295.
228. Reya, T., Morrison, S.J., Clarke, and M.F., Weissman, I.L. (2001) 'Stem cells, cancer, and cancer stem cells', *Nature*, 414, pp. 105-111
229. Ricklin, D., Hajishengallis, G., Yang, K. and Lambris, J.D. (2010) 'Complement: a key system for immune surveillance and homeostasis', *Nature immunology*, 11(9), pp. 785-797.
230. Ripoché, J., Day, A.J., Harris, T.J. and Sim, R.B. (1988) 'The complete amino acid sequence of human complement factor H', *The Biochemical journal*, 249(2), pp. 593-602.
231. Rivest, S. (2009) 'Regulation of innate immune responses in the brain', *Nature reviews. Immunology*, 9(6), pp. 429-439.
232. Robert, M. and Wastie, M. (2008) 'Glioblastoma multiforme: a rare manifestation of extensive liver and bone metastases', *Biomedical imaging and intervention journal*, 4(1), pp. e3.
233. Rock, R.B., Gekker, G., Hu, S., Sheng, W.S., Cheeran, M., Lokensgard, J.R. and Peterson, P.K. (2004) 'Role of microglia in central nervous system infections', *Clinical microbiology reviews*, 17(4), pp. 942-64, table of contents.
234. Rodriguez de Cordoba, S., Esparza-Gordillo, J., Goicoechea de Jorge, E., Lopez-Trascasa, M. and Sanchez-Corral, P. (2004) 'The human complement factor H: functional roles, genetic variations and disease associations', *Molecular immunology*, 41(4), pp. 355-367.

- 235.Roth, W. and Weller, M. (1999) 'Chemotherapy and immunotherapy of malignant glioma: molecular mechanisms and clinical perspectives', *Cellular and molecular life sciences : CMLS*, 56(5-6), pp. 481-506.
- 236.Roy, E.J., Gawlick, U., Orr, B.A., Rund, L.A., Webb, A.G. and Kranz, D.M. (2000) 'IL-12 treatment of endogenously arising murine brain tumors', *Journal of immunology (Baltimore, Md.: 1950)*, 165(12), pp. 7293-7299.
- 237.Rus, H., Cudrici, C. and Niculescu, F. (2005) 'The role of the complement system in innate immunity', *Immunologic research*, 33(2), pp. 103-112.
- 238.Saijo, K. and Glass, C.K. (2011) 'Microglial cell origin and phenotypes in health and disease', *Nature reviews.Immunology*, 11(11), pp. 775-787.
- 239.Salazar-Ramiro, A., Ramirez-Ortega, D., Perez de la Cruz, V., Hernandez-Pedro, N.Y., Gonzalez-Esquivel, D.F., Sotelo, J. and Pineda, B. (2016) 'Role of Redox Status in Development of Glioblastoma', *Frontiers in immunology*, 7, pp. 156.
- 240.Samaras, V., Piperi, C., Korkolopoulou, P., Zisakis, A., Levidou, G., Themistocleous, M.S., Boviatsis, E.I., Sakas, D.E., Lea, R.W., Kalofoutis, A. and Patsouris, E. (2007) 'Application of the ELISPOT method for comparative analysis of interleukin (IL)-6 and IL-10 secretion in peripheral blood of patients with astroglial tumors', *Molecular and cellular biochemistry*, 304(1-2), pp. 343-351.
- 241.Sansone, P. and Bromberg, J. (2012) 'Targeting the interleukin-6/Jak/stat pathway in human malignancies', *Journal of clinical oncology : official journal of the American Society of Clinical Oncology*, 30(9), pp. 1005-1014.
- 242.Santambrogio, L., Belyanskaya, S.L., Fischer, F.R., Cipriani, B., Brosnan, C.F., Ricciardi-Castagnoli, P., Stern, L.J., Strominger, J.L. and Riese, R. (2001) 'Developmental plasticity of CNS microglia', *Proceedings of the National Academy of Sciences of the United States of America*, 98(11), pp. 6295-6300.
- 243.Sarma, J.V. and Ward, P.A. (2011) 'The complement system', *Cell and tissue research*, 343(1), pp. 227-235.
- 244.Sasaki, N., Toki, S., Chowei, H., Saito, T., Nakano, N., Hayashi, Y., Takeuchi, M. and Makita, Z. (2001) 'Immunohistochemical distribution of the receptor for advanced glycation end products in neurons and astrocytes in Alzheimer's disease', *Brain research*, 888(2), pp. 256-262.
- 245.Sawada, K., Arika, S., Kojima, T., Saito, A., Yamazoe, M., Nishitani, C., Shimizu, T., Takahashi, M., Mitsuzawa, H., Yokota, S., Sawada, N., Fujii, N., Takahashi, H. and Kuroki, Y. (2010) 'Pulmonary collectins protect macrophages against pore-forming activity of Legionella pneumophila and suppress its intracellular growth', *The Journal of biological chemistry*, 285(11), pp. 8434-8443.
- 246.Sawada, M., Suzumura, A. and Marunouchi, T. (1992) 'TNF alpha induces IL-6 production by astrocytes but not by microglia', *Brain research*, 583(1-2), pp. 296-299.
- 247.Schaub, B., Westlake, R.M., He, H., Arestides, R., Haley, K.J., Campo, M., Velasco, G., Bellou, A., Hawgood, S., Poulain, F.R., Perkins, D.L. and Finn, P.W. (2004) 'Surfactant protein D deficiency influences allergic immune responses', *Clinical and experimental*

- allergy : journal of the British Society for Allergy and Clinical Immunology*, 34(12), pp. 1819-1826.
- 248.Schelenz, S., Malhotra, R., Sim, R.B., Holmskov, U. and Bancroft, G.J. (1995) 'Binding of host collectins to the pathogenic yeast *Cryptococcus neoformans*: human surfactant protein D acts as an agglutinin for acapsular yeast cells', *Infection and immunity*, 63(9), pp. 3360-3366.
- 249.Shrestha, R., Millington, O., Brewer, J. and Bushell, T. (2013) 'Is central nervous system an immune-privileged site?', *Kathmandu University medical journal (KUMJ)*, 11(41), pp. 102-107.
- 250.Scheurer, M.E., Amirian, E., Cao, Y., Gilbert, M.R., Aldape, K.D., Kornguth, D.G., El-Zein, R. and Bondy, M.L. (2008) 'Polymorphisms in the interleukin-4 receptor gene are associated with better survival in patients with glioblastoma', *Clinical cancer research : an official journal of the American Association for Cancer Research*, 14(20), pp. 6640-6646.
- 251.Schob, S., Schicht, M., Sel, S., Stiller, D., Kekule, A.S., Paulsen, F., Maronde, E. and Brauer, L. (2013) 'The detection of surfactant proteins A, B, C and D in the human brain and their regulation in cerebral infarction, autoimmune conditions and infections of the CNS', *PloS one*, 8(9), pp. e74412.
- 252.Shah, S.N., Cope, L., Poh, W., Belton, A., Roy, S., Talbot, C.C., Jr, Sukumar, S., Huso, D.L. and Resar, L.M. (2013) 'HMGA1: a master regulator of tumor progression in triple-negative breast cancer cells', *PloS one*, 8(5), pp. e63419.
- 253.Shan, Y., He, X., Song, W., Han, D., Niu, J. and Wang, J. (2015) 'Role of IL-6 in the invasiveness and prognosis of glioma', *International journal of clinical and experimental medicine*, 8(6), pp. 9114-9120.
- 254.Shaw, E.G., Dumas-Duport, C., Scheithauer, B.W., Gilbertson, D.T., O'Fallon, J.R., Earle, J.D., Laws, E.R., Jr and Okazaki, H. (1989) 'Radiation therapy in the management of low-grade supratentorial astrocytomas', *Journal of neurosurgery*, 70, pp. 853-861.
- 255.Shinojima, N., Tada, K., Shiraishi, S., Kamiryo, T., Kochi, M., Nakamura, H., Makino, K., Saya, H., Hirano, H., Kuratsu, J., Oka, K., Ishimaru, Y. and Ushio, Y. (2003) 'Prognostic value of epidermal growth factor receptor in patients with glioblastoma multiforme', *Cancer research*, 63(20), pp. 6962-6970.
- 256.Sidransky, D., Mikkelsen, T., Schwachheimer, K., Rosenblum, M.L., Cavanee, W. and Vogelstein, B. (1992) 'Clonal expansion of p53 mutant cells is associated with brain tumour progression', *Nature*, 355(6363), pp. 846-847.
- 257.Siebzehnrubl, F. A., Reynolds, B. A., Vescovi, A., Steindler, D. A., and Deleyrolle, L. P. (2011)'The origins of glioma: E pluribus unum?', *Glia*, 59(8), pp.1135-1147.
- 258.Sikora, J.P., Chlebna-Sokol, D. and Krzyzanska-Oberbek, A. (2001) 'Proinflammatory cytokines (IL-6, IL-8), cytokine inhibitors (IL-6sR, sTNFRII) and anti-inflammatory cytokines (IL-10, IL-13) in the pathogenesis of sepsis in newborns and infants', *Archivum Immunologiae et Therapiae Experimentalis*, 49(5), pp. 399-404.

259. Silhavy, T.J., Kahne, D. and Walker, S. (2010) 'The bacterial cell envelope', *Cold Spring Harbor perspectives in biology*, 2(5), pp. a000414.
260. Singh, S.K., Clarke, I.D., Terasaki, M., Bonn, V.E., Hawkins, C., Squire, J. and Dirks, P.B. (2003) 'Identification of a cancer stem cell in human brain tumors', *Cancer research*, 63, pp. 5821-5828.
261. Singh, S.K., Hawkins, C., Clarke, I.D., Squire, J.A., Bayani, J., Hide, T., Henkelman, R.M., Cusimano, M.D. and Dirks, P.B. (2004) 'Identification of human brain tumour initiating cells', *Nature*, 432, pp. 396-401.
262. Singh, M., Madan, T., Waters, P., Parida, S.K., Sarma, P.U. and Kishore, U. (2003) 'Protective effects of a recombinant fragment of human surfactant protein D in a murine model of pulmonary hypersensitivity induced by dust mite allergens', *Immunology letters*, 86(3), pp. 299-307.
263. Skerka, C., Chen, Q., Fremeaux-Bacchi, V. and Roumenina, L.T. (2013) 'Complement factor H related proteins (CFHRs)', *Molecular immunology*, 56(3), pp. 170-180.
264. Smyth, M.J., Cretney, E., Kershaw, M.H. and Hayakawa, Y. (2004) 'Cytokines in cancer immunity and immunotherapy', *Immunological reviews*, 202, pp. 275-293.
265. Sofroniew, M.V. and Vinters, H.V. (2010) 'Astrocytes: biology and pathology', *Acta Neuropathologica*, 119(1), pp. 7-35.
266. Sotiriadis, G., Dodagatta-Marri, E., Kouser, L., Alhamlan, F.S., Kishore, U. and Karteris, E. (2015) 'Surfactant Proteins SP-A and SP-D Modulate Uterine Contractile Events in ULTR Myometrial Cell Line', *PloS one*, 10(12), pp. e0143379.
267. Stupp, R., Reni, M., Gatta, G., Mazza, E. and Vecht, C. (2007) 'Anaplastic astrocytoma in adults', *Critical reviews in oncology/hematology*, 63, pp. 72-80.
268. Sterka, D., Jr, Rati, D.M. and Marriott, I. (2006) 'Functional expression of NOD2, a novel pattern recognition receptor for bacterial motifs, in primary murine astrocytes', *Glia*, 53(3), pp. 322-330.
269. Suarez-Cuervo, C., Harris, K.W., Kallman, L., Vaananen, H.K. and Selander, K.S. (2003) 'Tumor necrosis factor-alpha induces interleukin-6 production via extracellular-regulated kinase 1 activation in breast cancer cells', *Breast cancer research and treatment*, 80(1), pp. 71-78.
270. Swartz, K.R., Liu, F., Sewell, D., Schochet, T., Campbell, I., Sandor, M. and Fabry, Z. (2001) 'Interleukin-6 promotes post-traumatic healing in the central nervous system', *Brain research*, 896(1-2), pp. 86-95.
271. Takeda, K., Kaisho, T. and Akira, S. (2003) 'Toll-like receptors', *Annual Review of Immunology*, 21, pp. 335-376.
272. Talmadge, J.E., and Fidler, I.J. (2010) 'AACR Centennial Series: The biology of cancer metastasis: Historical perspective', *American Association for Cancer Research*, 70(14), pp. 5649-5669
273. Tanabe, K., Matsushima-Nishiwaki, R., Yamaguchi, S., Iida, H., Dohi, S. and Kozawa, O. (2010) 'Mechanisms of tumor necrosis factor-alpha-induced interleukin-6 synthesis in glioma cells', *Journal of neuroinflammation*, 7, pp. 16-2094-7-16.

274. Taylor, W.R. and Stark, G.R. (2001) 'Regulation of the G2/M transition by p53', *Oncogene*, 20(15), pp. 1803-1815.
275. Tchirkov, A., Rolhion, C., Bertrand, S., Dore, J.F., Dubost, J.J. and Verrelle, P. (2001) 'IL-6 gene amplification and expression in human glioblastomas', *British journal of cancer*, 85(4), pp. 518-522.
276. Thurman, J.M. and Holers, V.M. (2006) 'The central role of the alternative complement pathway in human disease', *Journal of immunology (Baltimore, Md.: 1950)*, 176(3), pp. 1305-1310.
277. Thomas L. (1959) 'Cellular and humoral aspects of the hypersensitive states', *New York: Hoeber-Harper*, pp. 529-532.
278. Tohma, Y., Gratas, C., Biernat, W., Peraud, A., Fukuda, M., Yonekawa, Y., Kleihues, P. and Ohgaki, H. (1998) 'PTEN (MMAC1) mutations are frequent in primary glioblastomas (de novo) but not in secondary glioblastomas', *Journal of neuropathology and experimental neurology*, 57(7), pp. 684-689
279. Tran Thang, N.N., Derouazi, M., Philippin, G., Arcidiaco, S., Di Bernardino-Besson, W., Masson, F., Hoepner, S., Riccadonna, C., Burkhardt, K., Guha, A., Dietrich, P.Y. and Walker, P.R. (2010) 'Immune infiltration of spontaneous mouse astrocytomas is dominated by immunosuppressive cells from early stages of tumor development', *Cancer research*, 70(12), pp. 4829-4839.
280. Tran, P.B. and Miller, R.J. (2003) 'Chemokine receptors: signposts to brain development and disease', *Nature reviews. Neuroscience*, 4(6), pp. 444-455.
281. Tu, S.M., Lin, S-H., and Logothetis, C.J., (2002) 'Stem-cell origin of metastasis and heterogeneity in solid tumours', *The lancet oncology*, 3, pp. 508-513
282. Tugues, S., Burkhard, S.H., Ohs, I., Vrohling, M., Nussbaum, K., Vom Berg, J., Kulig, P. and Becher, B. (2015) 'New insights into IL-12-mediated tumor suppression', *Cell death and differentiation*, 22(2), pp. 237-246.
283. Uchida, N., Buck, D.W., He, D., Reitsma, M.J., Masek, M., Phan, T.V., Tsukamoto, A.S., Gage, F.H. and Weissman, I.L. (2000) 'Direct isolation of human central nervous system stem cells', *Proceedings of the National Academy of Sciences of the United States of America*, 97(26), pp. 14720-14725.
284. Van de Velde, S., Nguyen, H.A., Van Bambeke, F., Tulkens, P.M., Grellet, J., Dubois, V., Quentin, C. and Saux, M.C. (2008) 'Contrasting effects of human THP-1 cell differentiation on levofloxacin and moxifloxacin intracellular accumulation and activity against Staphylococcus aureus and Listeria monocytogenes', *The Journal of antimicrobial chemotherapy*, 62(3), pp. 518-521.
285. van der Sanden, G.A.C., Schouten, L.J., van Dijck, J.A.A.M., van Andel, J.P., and Coebergh, J.W.W. (1998) 'Incidence of primary central nervous system cancers in South and East Netherlands in 1989-1994', *Neuroepidemiology*, 17, pp. 247-57
286. van Rozendaal, B.A., van Spriel, A.B., van De Winkel, J.G. and Haagsman, H.P. (2000) 'Role of pulmonary surfactant protein D in innate defense against Candida albicans', *The Journal of infectious diseases*, 182(3), pp. 917-922.
287. van Sorge, N.M. and Doran, K.S. (2012) 'Defense at the border: the blood-brain barrier versus bacterial foreigners', *Future microbiology*, 7(3), pp. 383-394.

- 288.Vaupel, P. (2004) 'Tumor microenvironment physiology and its implications for radiation oncology', *Seminars in Radiation Oncology*, 14, pp.198-206.
- 289.Vom Berg, J., Vrohling, M., Haller, S., Haimovici, A., Kulig, P., Sledzinska, A., Weller, M. and Becher, B. (2013) 'Intratumoral IL-12 combined with CTLA-4 blockade elicits T cell-mediated glioma rejection', *The Journal of experimental medicine*, 210(13), pp. 2803-2811.
- 290.Voorhout, W.F., Veenendaal, T., Kuroki, Y., Ogasawara, Y., van Golde, L.M. and Geuze, H.J. (1992) 'Immunocytochemical localization of surfactant protein D (SP-D) in type II cells, Clara cells, and alveolar macrophages of rat lung', *The journal of histochemistry and cytochemistry : official journal of the Histochemistry Society*, 40(10), pp. 1589-1597.
- 291.Vousden, K.H. and Lu, X. (2002) 'Live or let die: the cell's response to p53', *Nature reviews.Cancer*, 2(8), pp. 594-604.
- 292.Wang, H., Lathia, J.D., Wu, Q., Wang, J., Li, Z., Heddleston, J.M., Eyler, C.E., Elderbroom, J., Gallagher, J., Schusch, J., MacSwords, J., Cao, Y., McLendon, R.E., Wang, X.F., Hjelmeland, A.B. and Rich, J.N. (2009) 'Targeting interleukin 6 signaling suppresses glioma stem cell survival and tumor growth', *Stem cells (Dayton, Ohio)*, 27(10), pp. 2393-2404.
- 293.Watanabe, K., Tachibana, O., Sata, K., Yonekawa, Y., Kleihues, P. and Ohgaki, H. (1996) 'Overexpression of the EGF receptor and p53 mutations are mutually exclusive in the evolution of primary and secondary glioblastomas', *Brain pathology (Zurich, Switzerland)*, 6(3), pp. 217-23; discussion 23-4.
- 294.Watanabe, K., Sato, K., Biernat, W., Tachibana, O., von Ammon, K., Ogata, N., Yonekawa, Y., Kleihues, P. and Ohgaki, H. (1997) 'Incidence and timing of p53 mutations during astrocytoma progression in patients with multiple biopsies', *Clinical cancer research : an official journal of the American Association for Cancer Research*, 3(4), pp. 523-530.
- 295.Watters, J.J., Schartner, J.M. and Badie, B. (2005) 'Microglia function in brain tumors', *Journal of neuroscience research*, 81(3), pp. 447-455.
- 296.Weinberg, R.A. (1995) 'The retinoblastoma protein and cell cycle control', *Cell*, 81(3), pp.323-30
- 297.Weissenberger, J., Loeffler, S., Kappeler, A., Kopf, M., Lukes, A., Afanasieva, T.A., Aguzzi, A. and Weis, J. (2004) 'IL-6 is required for glioma development in a mouse model', *Oncogene*, 23(19), pp. 3308-3316.
- 298.Weller, M. and Fontana, A. (1995) 'The failure of current immunotherapy for malignant glioma. Tumor-derived TGF-beta, T-cell apoptosis, and the immune privilege of the brain', *Brain research.Brain research reviews*, 21(2), pp. 128-151.
- 299.Wright, J.R. (2005) 'Immunoregulatory functions of surfactant proteins', *Nature reviews.Immunology*, 5(1), pp. 58-68.
- 300.Wong, C.J., Akiyama, J., Allen, L. and Hawgood, S. (1996) 'Localization and developmental expression of surfactant proteins D and A in the respiratory tract of the mouse', *Pediatric research*, 39(6), pp. 930-937.

301. Woo, C.H., Eom, Y.W., Yoo, M.H., You, H.J., Han, H.J., Song, W.K., Yoo, Y.J., Chun, J.S. and Kim, J.H. (2000) 'Tumor necrosis factor- α generates reactive oxygen species via a cytosolic phospholipase A2-linked cascade', *The Journal of biological chemistry*, 275(41), pp. 32357-32362.
302. Wu, H., Kuzmenko, A., Wan, S., Schaffer, L., Weiss, A., Fisher, J.H., Kim, K.S. and McCormack, F.X. (2003) 'Surfactant proteins A and D inhibit the growth of Gram-negative bacteria by increasing membrane permeability', *The Journal of clinical investigation*, 111(10), pp. 1589-1602
303. Wu, A., Wei, J., Kong, L.Y., Wang, Y., Priebe, W., Qiao, W., Sawaya, R. and Heimberger, A.B. (2010) 'Glioma cancer stem cells induce immunosuppressive macrophages/microglia', *Neuro-oncology*, 12(11), pp. 1113-1125.
304. Yarlagadda, A., Alfson, E. and Clayton, A.H. (2009) 'The blood brain barrier and the role of cytokines in neuropsychiatry', *Psychiatry (Edgmont (Pa.: Township))*, 6(11), pp. 18-22.
305. Yoshida, S., Ono, M., Shono, T., Izumi, H., Ishibashi, T., Suzuki, H. and Kuwano, M. (1997) 'Involvement of interleukin-8, vascular endothelial growth factor, and basic fibroblast growth factor in tumor necrosis factor α -dependent angiogenesis', *Molecular and cellular biology*, 17(7), pp. 4015-4023.
306. Yu, J.S., Wei, M.X., Chiocca, E.A., Martuza, R.L. and Tepper, R.I. (1993) 'Treatment of glioma by engineered interleukin 4-secreting cells', *Cancer research*, 53(13), pp. 3125-3128.
307. Zhang, M., Hutter, G., Kahn, S.A., Azad, T.D., Gholamin, S., Xu, C.Y., Liu, J., Achrol, A.S., Richard, C., Sommerkamp, P., Schoen, M.K., McCracken, M.N., Majeti, R., Weissman, I., Mitra, S.S. and Cheshier, S.H. (2016) 'Anti-CD47 Treatment Stimulates Phagocytosis of Glioblastoma by M1 and M2 Polarized Macrophages and Promotes M1 Polarized Macrophages In Vivo', *PloS one*, 11(4), pp. e0153550.
308. Zhang, P., McAlinden, A., Li, S., Schumacher, T., Wang, H., Hu, S., Sandell, L. and Crouch, E. (2001) 'The amino-terminal heptad repeats of the coiled-coil neck domain of pulmonary surfactant protein d are necessary for the assembly of trimeric subunits and dodecamers', *The Journal of biological chemistry*, 276(23), pp. 19862-19870.
309. Zhang, F., Pao, W., Umphress, S.M., Jakowlew, S.B., Meyer, A.M., Dwyer-Nield, L.D., Nielsen, L.D., Takeda, K., Gelfand, E.W., Fisher, J.H., Zhang, L., Malkinson, A.M. and Mason, R.J. (2003) 'Serum levels of surfactant protein D are increased in mice with lung tumors', *Cancer research*, 63(18), pp. 5889-5894.
310. Zilfou, J.T. and Lowe, S.W. (2009) 'Tumor suppressive functions of p53', *Cold Spring Harbor perspectives in biology*, 1(5), pp. a001883.
311. Zipfel, P.F., Skerka, C., Hellwage, J., Jokiranta, S.T., Meri, S., Brade, V., Kraiczy, P., Noris, M. and Remuzzi, G. (2002) 'Factor H family proteins: on complement, microbes and human diseases', *Biochemical Society transactions*, 30(Pt 6), pp. 971-978.
312. Zipfel, P.F. and Skerka, C. (2009) 'Complement regulators and inhibitory proteins', *Nature reviews.Immunology*, 9(10), pp. 729-740.

